Jet DRA

UNION CARBIDE

FINAL REPORT

SECONDARY ZINC-OXYGEN CELL FOR SPACECRAFT APPLICATIONS

(23 June 1966 – 1 September 1968)

CONTRACT NO. NAS-5-10247

for

NATIONAL AERONAUTICS AND SPACE ADMINISTRATION
GODDARD SPACE FLIGHT CENTER
GREENBELT, MARYLAND

April 1971

UNION CARBIDE CORPORATION
CONSUMER PRODUCTS DIVISION
RESEARCH LABORATORY - PARMA, OHIO

FINAL REPORT

SECONDARY ZINC-OXYGEN CELL FOR SPACECRAFT APPLICATIONS

(23 June 1966 — 1 September 1968)

CONTRACT NO. NAS-5-10247
for
NATIONAL AERONAUTICS AND SPACE ADMINISTRATION
GODDARD SPACE FLIGHT CENTER
GREENBELT, MARYLAND

APRIL 1971

APPROVED BY:

R. A. Powers, Director

CONSUMER PRODUCTS DIVISION
RESEARCH LABORATORY
PARMA, OHIO

TABLE OF CONTENTS

Table of Contents (Cont.)

Table of Contents (Cont.)

Table of Contents (Cont.)

Table of Contents (Cont.)

APPENDIX

Table of Contents-Appendix (Cont.)

LIST OF ILLUSTRATIONS

List of Illustrations (Cont.)

List of Illustrations (Cont.)

List of Illustrations (Cont.)

List of Illustrations (Cont.)

APPENDIX

LIST OF TABLES

ABSTRACT

Th zinc-oxygen system was found to be capable of producing up to 350 discharge-charge cycles above the 1.0 volt end-point at 25° C on the 2-hour discharge/2-hour charge regime at a discharge current density of 11-12 mA/cm^2. Unit cell performance was further determined at various current densities over the temperature range of 0° to 40° C. Test cycle regimes included the 2-hour discharge/2-hour charge; 2-hour discharge/4-hour charge; 2-hour discharge/22-hour charge; and the 24-hour discharge/24-hour charge. Cycle life was limited by configurational changes in the anode and in some instances by the oxygen electrode.

Two types of zinc anodes were tested: (a) the zinc powder-carboxy methyl cellulose (CMC) gel suspended anode, and (b) the zinc oxide formulated anode. Both types were mechanically supported by silver expanded grids. Of the two types of zinc anodes, the zinc powder-CMC gel electrodes gave the longest cycle life with the limiting factor being degradation of the CMC gel and subsequent shape change.

Two types of oxygen cathodes were also tested. The first was purchased from the American Cyanamid Company under the designation of "LAB-40." This was used as the oxygen electrode on discharge and as the charging electrode (at which oxygen was evolved) during charge. Cycle life was limited by an electrolyte wetting problem and the solution of noble metal catalyst into the KOH with subsequent deposition upon the zinc electrode and consequent formation of a hydrogen gassing couple.

The second type of cathode was the Union Carbide "fixed-zone" electrode in which the catalytically active carbon layer is bonded upon a thin but strong porous metal backing. A nickel charging electrode was used for charging the zinc in order to protect the catalytic carbon layer from oxidation. Resulting unit cells, therefore, were of a 3-electrode design.

Data developed from the experimental unit cell work were used as a basis for a paper design study of a 28-volt, 3 KWH rechargeable zinc-oxygen battery. The two-electrode structure, employing American Cyanamid "LAB-40" oxygen cathodes, was selected for this study. An important consideration which led to the selection of the American Cyanamid cathode was the simplicity and weight reduction of the 2-electrode charge-discharge circuit as opposed to that required for cycling a 3-electrode cell system. The energy density of the design battery including tankage and auxiliary equipment is directly related to discharge time and the size of the battery. For a 2-hour discharge, this value is 22 watt-hours per pound. If the discharge time is increased to 8 hours, the energy density rises to 35 watt-hours per pound.

Fifteen rechargeable zinc-oxygen unit cells and two 6-volt-10 ampere-hour batteries complete with tankage and auxiliary equipment were delivered to NASA.

INTRODUCTION

The zinc-oxygen system was selected for development as a rechargeable battery system for spacecraft applications because of its energy density advantage over the other common rechargeable systems. With a theoretical energy density of 541 watt-hours per pound, the energy density of the zinc-oxygen system exceeds the best of other rechargeable systems, such as, silver-zinc, nickel-cadmium and lead acid by a factor of over four. A comparison of the calculated maximum theoretical watt-hours per pound figures for these systems is presented in Table I.

TABLE I.

MAXIMUM THEORETICAL ENERGY DENSITY OF RECHARGEABLE BATTERY SYSTEMS

(from thermodynamic data or the working voltage)

System	Characteristic Cell Reaction	Open Circuit Voltage	Watt-Hours per pound
Lead-Acid	$Pb + PbO_2 + 2H_2SO_4 \rightleftarrows 2PbSO_4 + 2H_2O$	2.1	76
Nickel-Cadmium	$Cd + 2NiOOH + 2H_2O \rightleftarrows Cd(OH)_2 + 2Ni(OH)_2$	1.35	100
Silver-Zinc	$Zn + Ag_2O \rightleftarrows ZnO + 2Ag$	1.5	118
Zinc-Oxygen	$2Zn + O_2 \rightleftarrows 2ZnO$	1.65	541

The technical approach was based upon Union Carbide's background experience in fuel cell technology, in the "Air Cell" and in various primary alkaline and rechargeable battery systems.

Two types of oxygen electrodes were employed in the present work; (a) the thin "fixed zone" plastic-bonded carbon electrodes developed by Union Carbide(1-7) and, (b) fuel cell electrodes developed by the American Cyanamid Company designated as "LAB-40". Two general types of zinc electrodes were used: (i) a zinc powder suspension in a carboxy methyl cellulose gel developed by Union Carbide for use in alkaline batteries and, (ii) zinc oxide powder formulations of the general type used in silver oxide-zinc batteries.

All materials used in making the cells and batteries are readily available from domestic suppliers.

The feasibility of recharging the zinc-oxygen system was demonstrated by the program of work conducted. Work was done on parallel programs exploring a two electrode and a three electrode experimental cell construction. The two electrode cell used the American Cyanamid Company "LAB-40" oxygen electrodes while the three electrode cell employed Union Carbide "fixed zone" plastic-bonded carbon oxygen electrodes in conjunction with an expanded nickel "charging electrode". The greater stability and longer cycle life was realized from cells in which Union Carbide "fixed zone" oxygen electrodes were used.

Cell performance was determined at various current densities and over a temperature range of 0° to 40° C. Most of the unit cell testing was carried out on cycling schedules of 2-hour discharge - 2-hour charge, 2-hour discharge - 4-hour charge, 2-hour discharge - 22-hour charge and 24-hour discharge - 24-hour charge.

The zinc electrodes used for most of the work were zinc gel type anodes from which over 350 cycles were delivered when cycled at current density of 11-12 mA/cm^2 and 176 cycles when cycled at a current density of 20-25 mA/cm^2. Anodes molded from formulations of zinc oxide with admixtures also showed promise of extended cycle life.

Data developed from the experimental unit cell work was used as the basis for a paper design study whose object was to determine the optimum weight and volume of a 28 volt - 3 KWH rechargeable zinc-oxygen battery. Unit cell performance data was likewise used as the basis for constructing the batteries delivered to NASA. Two 6 volt - 10 ampere-hour battery systems were built and delivered to NASA in accordance with the terms of Contract No. NAS-5-10247. One was made with American Cyanamid oxygen electrodes while the other employed Union Carbide "fixed zone" oxygen electrodes.

DISCUSSION

A. Description of Electrodes

1. Oxygen Electrodes

Two different types of oxygen electrodes were used in constructing the experimental cell made under this contract. These are:

(a) Union Carbide Thin "Fixed-Zone" Oxygen Electrodes

The Union Carbide "fixed-zone" electrode consists of an electrochemically active carbon layer applied to a porous metal backing. These electrodes were originally developed for use in fuel cell batteries. A cross section of such an oxygen electrode is shown in Figure 1. Since catalyzed carbon is used in this electrode in place of platinum metal catalysts, the electrode is relatively inexpensive. Bonding this catalyzed carbon layer to a thin but strong porous nickel structure, however, results in a mechanically strong electrode. Oxygen easily reaches the reaction site by flowing through the porous nickel backing of the electrode. Permeation of electrolyte through the porous electrode is prevented by a wetproofing treatment. This wetproofing treatment results in a hydrophobic electrode that has a stable interface which does not rely upon a sensitive pressure balance with its attendant sensor problem to maintain the gas-liquid interface at an appropriate level in the structure.

Since the thin "fixed-zone" oxygen electrode is susceptible to damage from oxygen evolution which would occur during charging, it is necessary to use a separate nickel charging electrode. If oxygen were evolved directly upon the catalyzed carbon surface of the oxygen electrode during charge, anodic oxidation of this surface would occur. Surface oxides would be formed that can be

viewed as intermediates in the combustion of carbon (8). Efforts to characterize the surface oxides of carbon have been reviewed by Garten and Weiss (9). Functional groups, such as hydroxyl, carbonyl, and carboxyl have been inferred by Lygin et al (10) from chemical and IR studies. The polarographic identification of quinone and hydroquinone has been reported by Hallum and Drushel (11).

FIGURE 1.

CROSS-SECTION OF THIN "FIXED-ZONE" ELECTRODES

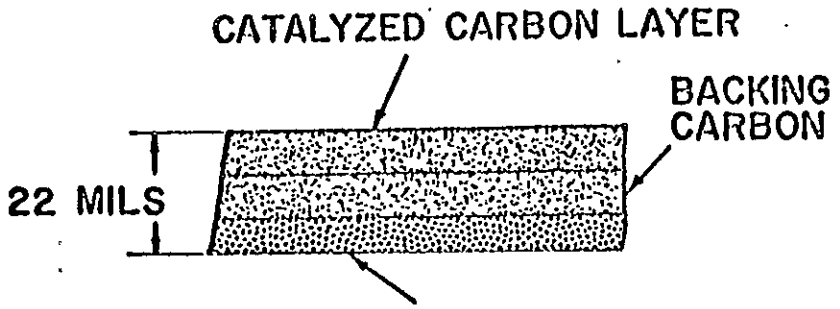

(b) American Cyanamid "LAB-40" Oxygen Electrodes

The second type of oxygen electrode used was obtained from American Cyanamid. This electrode is composed of a catalyzed, electrochemically active layer bonded with TEFLON, molded onto a gold-plated nickel screen collector and backed with a porous hydrophobic material. The particular electrode used was labeled "LAB-40". The "LAB-40" electrodes investigated had a backing designated as BII4. No further information beyond the notation that the backing was porous and hydrophobic was available from the supplier. Since the "LAB-40" oxygen electrodes had been reported previously to be resistant to oxygen, they were used directly (as oxygen evolving anodes) for cell charging.

(c) Oxygen Electrode Reaction

The most probable reaction for oxygen consumption during discharge at either of the two types of oxygen electrodes described above would be in accordance with the reaction:

$$O_2 + H_2O + 2e = HO_2^- + OH^-$$

Since the peroxide is unstable in the presence of the catalyzed active layers of both types of oxygen electrodes, it would be expected to decompose. The rate of peroxide decomposition increases with higher temperatures thereby resulting in reduced polarization and higher electrode potential. Reduction in current density also results in reduced polarization and higher electrode potential.

2. Zinc Electrodes

(a) Zinc Gel-Type Anodes

The zinc gel-type anodes used in the present work are those developed within Union Carbide for use in primary and rechargeable alkaline battery systems. Work done prior to initiation of this contract effort had indicated that such an electrode was capable of performing at current drains at least as high as those represented by the two-hour discharge rate of the present spacecraft application.

The zinc anode mass is contained within an expanded amalgamated silver metal basket. A silver backing sheet is spot welded within this basket to provide a rigid positive contact to the silver basket. The silver basket serves primarily as the anode mass restraining member in this electrode while the silver backing sheet serves as a strong current collector. The zinc gel-type anodes are assembled in the charged condition.

(b) Anodes Fabricated from Zinc-Oxide Formulations

The second type of zinc anode used in building the experimental cells of the present contact effort was one in which the electrode was

fabricated in the discharged condition using "formulations" of zinc oxide. This was done in an attempt to minimize anode slump due to shape change (discussed in detail in another section of this report). The zinc oxide anode "formulations" are listed in Table II. Anode plates were constructed from each by doctor-blading a weight of "formulation" equivalent to 7.5 ampere hours of zinc on each side (15 A-h total) of a 3" x 3" expanded silver grid (5 Ag 12-3/0) to which a 4-5/8" long silver wire of .032" diameter previously had been spot welded as a lead. The plate was then completed by being surrounded with an envelope of expanded silver (5 Ag 5-6/0) and pressed to a 3" x 3" anode.

TABLE II

ZINC OXIDE FABRICATED ANODES

Component	Electrode Formulation ZnO-1	ZnO-19
ZnO	83.1	83.1
HgO	4.0	4.4
Asbestos fibers	5.2	5.2
Distilled H_2O	7.7	——
35% KOH + 5% ZnO	——	7.3
Total	100.0	100.0

The expanded silver used for both the grids and the restraining envelopes for both the zinc gel-type anodes and the zinc oxide formulation anodes was obtained from the Exmet Corporation. Their designations for these are 5 Ag12-3/0 and 5 Ag5-6/0, respectively.

(c) Zinc Anode Reaction

The oxidation of zinc during discharge may be written by the following series of reactions:

$$Zn + OH^{-1} \rightleftharpoons ZnOH^{-1}$$
$$ZnOH^{-1} \rightleftharpoons ZnOH + e^{-}$$
$$ZnOH + OH^{-1} \rightleftharpoons Zn(OH)_2 + e^{-}$$
$$Zn(OH)_2 + 2OH^{-} \rightleftharpoons Zn(OH)_4^{--}$$
$$Zn(OH)_4^{--} \rightleftharpoons ZnO + H_2O + 2OH^{-}$$

Obviously the final product of the reaction will be dependent upon the hydroxyl ion concentration. A discussion of this is given by Farr and Hampson (12).

During charging of the zinc electrode, the zinc that is first deposited comes directly from the zincate ion in solution in the immediate vicinity of the anode plate. This results in a drop of zincate concentration at the face of the electrode plate and within the pores of the plate. With the depletion or

serious reduction of the concentration of zincate ion in the immediate vicinity of the positive electrode, additional zincate ion diffuses towards the electrode. However, the rate of the latter is so low that solid zinc oxide at the anode plate now becomes the principal source of zinc that is reduced to metal during charge.

3. Charging Electrode

An expanded nickel grid was used as the charging electrode for zinc cells made with Union Carbide "fixed-zone" oxygen electrodes. This consisted of Exmet Corporation 5 Ni 15-2/0 material of 3" x 3" x 0.020". The nickel electrode was used as the positive electrode versus the zinc negative during charging and, of course, was not in the circuit during discharge.

An experiment was performed to compare the theoretical ampere-hour equivalent of oxygen evolved (209 cm^3 per ampere hour) with the actual amount of oxygen leaving the charging electrode compartment during charge. Two cells were charged at a constant current following a 3 A-h discharge. The oxygen leaving the charging electrode compartment during charge was collected in an inverted graduated cylinder filled with oil. This was possible

because of the effectiveness of the membrane separator in confining the evolved oxygen to its respective chambers and preventing it from entering the anode compartment of the cell. The mouth of the graduated cylinder was immersed in a pool of oil 2" to 3" deep which was contained in a 2000 cm^3 beaker. Experimental data recorded were time, current and oil displacement readings. A comparison between the theoretical and actual oxygen gas evolution for the ampere hours of charge is shown in Figure 2. These data indicate that within the limits of experimental error the actual and theoretical oxygen gas evolution are the same.

B. Spacers

The configurational design of the spacers used between the charging electrode and the other two electrodes of the unit cell was found to be critical because oxygen entrapment occurred during charging of the cell in a flooded static system. As oxygen is evolved at the nickel grid charging electrode, it must rise as bubbles which break at the surface. An obstruction-free path is therefore essential as entrapped oxygen pushes electrolyte out of its designated compartment.

The early unit cells were constructed by using two woven polypropylene spacers, one on either side of the nickel grid charging electrode and each 3" x 3" in size. No problem was encountered with respect to oxygen entrapment or expansion of electrolyte so long as the charging current density did not exceed 12 mA/cm^2. When current densities higher than this were used

FIGURE 2

O_2 EVOLVED FROM A SEPARATE CHARGING ELECTRODE AS A FUNCTION OF AMPERE-HOUR INPUT
(Theoretical 209 cc/Amp-Hr)

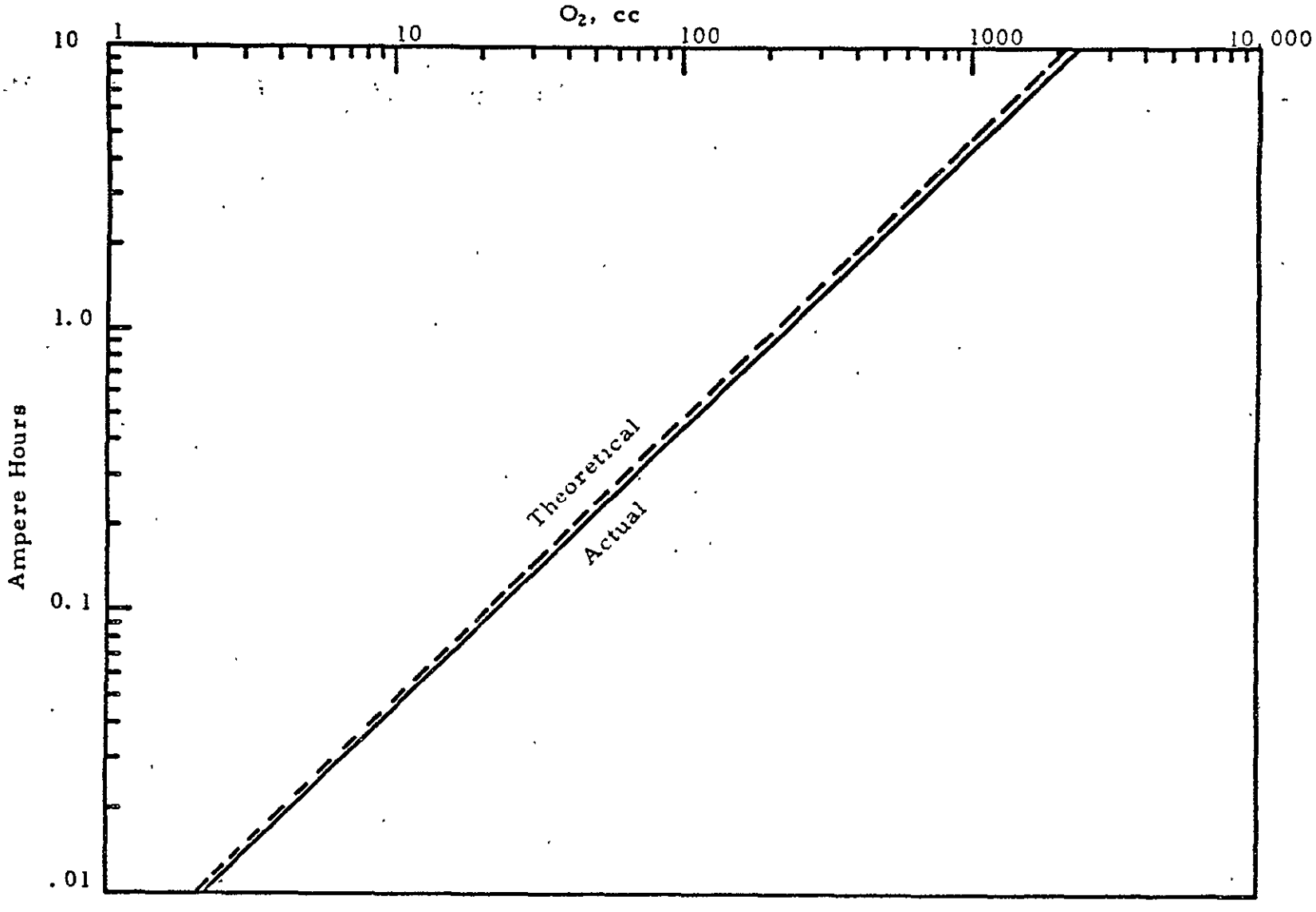

C-4148

for charging, a problem was encountered with gas entrapment and expansion of the electrolyte-gas mixture above the electrolyte chamber. The woven polypropylene spacers were accordingly replaced with eight vertically positioned vinyl strips spaced equidistant from one another. Each of these was 3 inches in length by 0.020-and 0.020-inch. This redesign of the spacer system enabled the charging rate to be increased from 12 mA/cm^2 to 24 mA per cm^2. Above 24 mA/cm^2, however, a new problem was encountered. This was simply that oxygen was not evolved at a faster rate than it could conveniently travel up through the electrolyte and break at the surface without pushing a portion of the electrolyte above the electrolyte container. An additional modification was made to the charging electrode spacer cell arrangement for the purpose of further improving the charge rate capability of the cell. The spacing on the zinc side of the charging electrode was eliminated while the spacing on the oxygen side was doubled. With this change, while the total volume of the charging electrode space remains the same, a considerably larger passageway now existed for the movement of oxygen to the top of the cell. This change also resulted in more uniform support for the zinc electrode which was achieved by putting the charge electrode immediately adjacent to the separator system of the zinc electrode. The use of equispaced vertically positioned vinyl strips was retained but, of course, the thickness of these was now doubled. With this additional change, cells demonstrated the capability of accepting charge at current densities in excess of 85 mA/cm^2. Before this modification was introduced, charging current densities of only 24 mA/cm^2 could be handled by the cell.

C. Separator System

The basic requirements of a good separator system for the zinc-oxygen rechargeable cell include the following:

1. Resistance to penetration by zinc dendrites
2. Low resistivity
3. Impermeability to oxygen
4. Resistance to oxidation
5. Inertness in the cell environment over the temperature range of 0 to 40° C.

The two separator membranes which almost satisfied these requirements were the Borden C-3 membrane and the RAI PERMION membranes (110, 116, and 1770C).

1. Borden C-3 Membrane

The C-3 membrane was produced by the Borden Chemical Company under a NASA contract. It is reported to be a composition of 30 percent poly(vinyl methyl ether/maleic anhydride) in a methyl cellulose base. The use of even a single layer of C-3 membrane separator resulted in shelf life extension from 15 to 20 cycles, delivered by sausage-casing cells, to 50 cycles delivered by the C-3 membrane cells. This performance was obtained in spite of an abusive 50 percent overcharge (less than the amount of overcharge required to compensate for chemical shorting of the zinc electrode in cells employing sausage-casing type separators) used in the cycling regime. Cell operation during this time was essentially unattended.

The C-3 membrane effectively separates the anolyte from the catholyte, and is quite resistant to zinc dendrite growth. It is also an effective separating member for preventing oxygen, generated at the charging electrode during charge, from reaching the zinc electrodes and thereby chemically "discharging" the zinc electrode.

A double layer of C-3 separator was effective to the extent that 168, 356, and 252 cycles were delivered from unit cells at 0°, 25°, and 40°C, respectively. These cells were cycled on a 2-hour discharge/2-hour charge schedule. Thirty cycles to 100% of rated cell capacity (5 ampere-hours) were obtained at 25°C on a 24-hour discharge/24-hour charge schedule. Cycling current densities on the 2-hour discharge/2-hour charge schedule and the 24-hour discharge/24-hour charge schedule correspond to 11.5 mA per cm^2 and 3.6 mA/cm^2, respectively. Unfortunately, the C-3 separator is subject to the following two limitations: 1) foaming of the electrolyte at charge current densities greater than 12 mA/cm^2, and 2) degradation of the separator with time to the extent that it loses its ability to keep the oxygen evolved on charge confined to the charging electrode cavity. Chemical shorting of the zinc inevitably occurred when the separator degraded to this extent.

It was observed that discoloration and apparent degradation of the C-3 separator had occurred in the cells removed from test because of foaming of the electrolyte. Since it was known that the C-3 separator dissolved in water, an examination of the C-3 and other similar materials for foaming as a function of KOH concentration was conducted. The examination was designed to determine: a) if the C-3 was definitely causing the foaming problem; b) if so, was there a KOH concentration where foaming occurred at a minimum tolerable

level; and c) if there were a separator material suitable for use in the zinc-oxygen rechargeable unit cell among other similar materials received from the Borden Chemical Company.

To simulate actual cell conditions in terms of separator and electrolyte volume, two 9-inch^2 pieces of each of several separator materials received from the Borden Chemical Company were immersed in 40 cc portions of each of eight KOH concentrations. Oxygen was bubbled in at the rate of 5 cc/min. This corresponded to the rate at which oxygen was evolved from the charging electrode in cells that were removed from test because of electrolyte foaming. The KOH concentrations tried were: 31, 33, 36, 39, 41, 43, 45, and 49 percent. These samples were observed for discoloration of the separator and electrolyte foaming. A blank (a sample of each of the KOH concentrations mentioned with no separator immersed therein) was observed along with samples containing separator materials.

Green discoloration of the separators tested was observed at KOH concentrations below 39 percent. No discoloration was observed at 41 percent. The 41 percent level also seemed to be the optimum concentration in terms of foaming. KOH concentrations above 41 percent did not seem to further retard foaming. Although foaming was observed in the samples containing separators at all KOH concentrations tried, no foaming was observed in any of the samples of KOH that did not contain separators.

a) Surfactants as a Means of Controlling Electrolyte Foaming

Next a study of surface active agents as possible means of controlling the electrolyte foaming was conducted. Since 41 percent KOH was established as the optimum electrolyte concentration, this was selected as the basic electrolyte for the study.

The surface active agents tried were meta-cresol, octyl alcohol, dibutyl phthalate and G. E. ANTIFOAM-10. The latter was recommended and supplied by the Borden Chemical Company. Each of these materials was tried at concentrations of 0. 1 ppm, 1. 0 ppm, 5 ppm, and 10 ppm. Tests were conducted in the same manner as those used to determine the optimum KOH concentration. The results were as follows:

(1) G. E. ANTIFOAM-10 and meta-cresol did not reduce foaming at any concentration tried.

(2) A marked reduction in foaming was observed in samples containing 5 ppm of octyl alcohol.

(3) A reduction in foaming was observed in samples containing 1 ppm of dibutyl phthalate. No foam was observed at the higher concentrations of dibutyl phthalate tried.

Based on these findings, four cells were activated with electrolytes containing the surface active agents in concentrations that seemed to control foaming, namely, 5 ppm and 10 ppm of octyl alcohol and 1 ppm and 5 ppm of dibutyl phthalate. Attempts to cycle these cells at a current density of 24 mA/cm^2 resulted with the following:

(1) With 5 ppm of octyl alcohol, foaming to an intolerable level occurred during the first charge.

(2) With 10 ppm of octyl alcohol, foaming occurred near the end of the first charge and to an intolerable level during the second charge.

(3) With 1 ppm and 5 ppm of dibutyl phthalate, there was no foaming during the first charge; however, foaming to an intolerable level occurred during the second charge.

Only temporary relief was gained through the use of the surface active agents tried. In addition, electrolyte flooding to the back side of the oxygen electrode was observed in every cell to which a surfactant had been added. For these two reasons, further studies of surfactants were abandoned.

b) Cell Reaction Mechanism Vs. C-3 Separator

The Borden C-3 separator is reported to be a composition of 30 percent poly(vinyl methyl ether/maleic anhydride) in a methyl cellulose base. In the present zinc-oxygen unit cell, foaming of the electrolyte could be caused by decomposition of the methyl cellulose to lower molecular weight materials which would tend to reduce the surface tension of the electrolyte.

During discharge both the anodic and cathodic reaction mechanisms could contribute to the formation of an environment favorable to degradation of the C-3 separator. The reactions are as follows:

$$\text{Anodic:} \quad Zn + 4OH^- = ZnO_2^{--} + 2H_2O + 2e^-$$

Since hydroxyl ions are consumed and water is produced in the reaction, the anolyte becomes weaker in concentration. With this condition more pronounced at the electrolyte layer between the C-3 separator and the zinc anode, conditions favorable to degradation of the C-3 could occur. The C-3 separator dissolves in water and tends to degrade faster and foam more in electrolytes weak in caustic.

$$\text{Cathodic:} \quad O_2 + H_2O + 2e^- = HO_2^- + OH^-$$

It is known that methyl cellulose is attacked by peroxides. Since the cathodic reaction mechanism involves peroxide formation, possible C-3 degradation from this source cannot be ignored.

During the charge mode of unit cell operation, oxygen is evolved from a third charging electrode. The rate at which oxygen is evolved is a function of the charge current density. C-3 degradation could occur in the rich oxygen environment to which it is subjected during this mode of cell operation, particularly during higher current density charges.

2. PERMION-110-and 116 Separators

These separators are reported to be radiation-crosslinked low density polyethylene-acrylic acid copolymers. One layer of each of these films was first introduced into each of two cells as a second film-type separator situation between the C-3 and the charging source to protect the C-3 membrane from the effects of the oxygen evolved from the charging electrode. The foaming was inhibited to some extent but not to a tolerable level.

Investigation of both PERMION-110-and 116 used as single membrane separators for the zinc-oxygen rechargeable system was very encouraging. These materials possessed the ability both to resist dendrite penetration and oxygen permeation. In addition, they possess comparatively low electrical resistivity. Cells employing these separators were charged at current densities up to 24 mA/cm^2 and absolutely no foaming of the electrolyte was observed. PERMION-110 seems to be more resistant to dendrite penetration than the 116 type. Whereas, not a single case of dendrite penetration was observed in cells employing the former membrane, dendrite penetration was observed in three cells employing the latter. Multiple layers of PERMION 110 were not necessary to prevent dendritic shorting.

3. PERMION 1770C Separator

This separator is also a product of RAI Research Corporation and is reported to be a chemically grafted polyethylene-acrylic acid film.

This material was investigated as a replacement for PERMION-110 and found to be its apparent equivalent. The 1770C material performs equally as well as the 110, both in terms of its resistance to dendrite penetration and oxygen permeation as well as comparatively low electrical resistance. This investigation was made necessary because the 110 film was no longer available.

D. Electrolytes

The electrolytes used in rechargeable zinc oxygen experimental unit cells consisted of aqueous solutions of potassium hydroxide with or without dissolved zinc oxide. The major portion of the work was done with potassium hydroxide solutions within the range of 31% to 42% by weight. The weight percent of zinc oxide varied from 0% to 7%. Examples of the solutions used are 31% KOH plus 5.4% ZnO, 36% KOH plus 2.6% ZnO, 38% KOH plus 2% ZnO, 38% KOH plus 3.5% ZnO, 41% KOH plus 7% ZnO, 42% KOH plus 2% ZnO, and 42% KOH plus 3.5% ZnO. In general, the zincate dissolved in the potassium hydroxide electrolyte was found to be desirable in the anolyte and undesirable in the catholyte.

The presence of zincate in the anolyte is particularly desirable when the zinc electrodes used are of the type fabricated from zinc oxide formulations. Excess zincate in the electrolyte prevents the solution of zinc oxide from the electrode and thereby preserves the mechanical integrity of the electrode. Two additional advantages are derived from the presence of zincate in the anolyte: i.e., the tendency for dendrite formation during charging and the likelihood of hydrogen evolution is reduced. These latter two advantages apply equally

to cells made with zinc gel-type anodes as well as to cells made with anodes fabricated from zinc oxide formulations. The presence of high concentrations of zincate in the catholyte were found to be undesirable because they have the effect of depressing the potential of the oxygen electrode and thereby reducing the over-all cell voltage.

Potassium hydroxide concentrations of 41% were found to be the more desirable ones within the range of concentrations studied. This was found to be quite important in cells in which Borden C-3 separator membranes were used. Lower potassium hydroxide concentrations lead to greater likelihood of dissolution of the membrane. The 41% potassium hydroxide solutions were found to minimize the electrolyte leakage through the cathode while still providing adequate wetting to its active layer. Leakage of electrolyte through the cathode occurs when electrolytes of lower potassium hydroxide concentration are used.

E. Unit Cell Construction

The structural material used for building the experimental unit zinc oxygen cells was LUCITE. The initial test cell was an assembly that was designed for reuse as well as to allow possible changes in the components that would result in alterations of the over-all cell thickness. The test cell was composed of two LUCITE endplates that were machined to slip-fit into a rectangular shaped box. Cell components were housed in the box between the two plastic plates. The LUCITE plates were originally sealed in place with a silicone-type adhesive (a material that could be cut away with a scalpel after a test was completed, so that the enclosure could be re-used and the

cell parts could be examined). The original silicone adhesives used were not totally satisfactory as evidenced by a leakage problem. This problem was solved by substituting epoxy resins to accomplish the seal in the place of the silicones. A detached view of this early cell assembly can be seen in Figure 3.

Significant changes and modifications that were made to the unit cell enclosure as work progressed during the period of this contract included the following:

1. A LUCITE frame assembly was designed to compartmentize the anode behind a membrane separator away from the oxygen-rich environment of the compartment housing both the charging electrode and the oxygen electrode. The membrane was sealed into a 3" x 3" opening of the frame. The zinc electrode was subsequently sealed into its own compartment behind this separator assembly.
2. Reservoirs were provided to accommodate electrolyte expansion above both the negative and positive cell compartments.
3. A connecting channel was introduced between the reservoirs above the positive and negative compartments to allow electrolyte flow from one compartment into the other when the level of the channel was reached. This maintained a balance in the electrolyte levels of the respective compartments thus compensating for the fluctuation of electrolyte level with cycling at the sacrifice of contamination of the catholyte with some zincate.

FIGURE 3

DETACHED VIEW OF ZINC-OXYGEN UNIT CELL

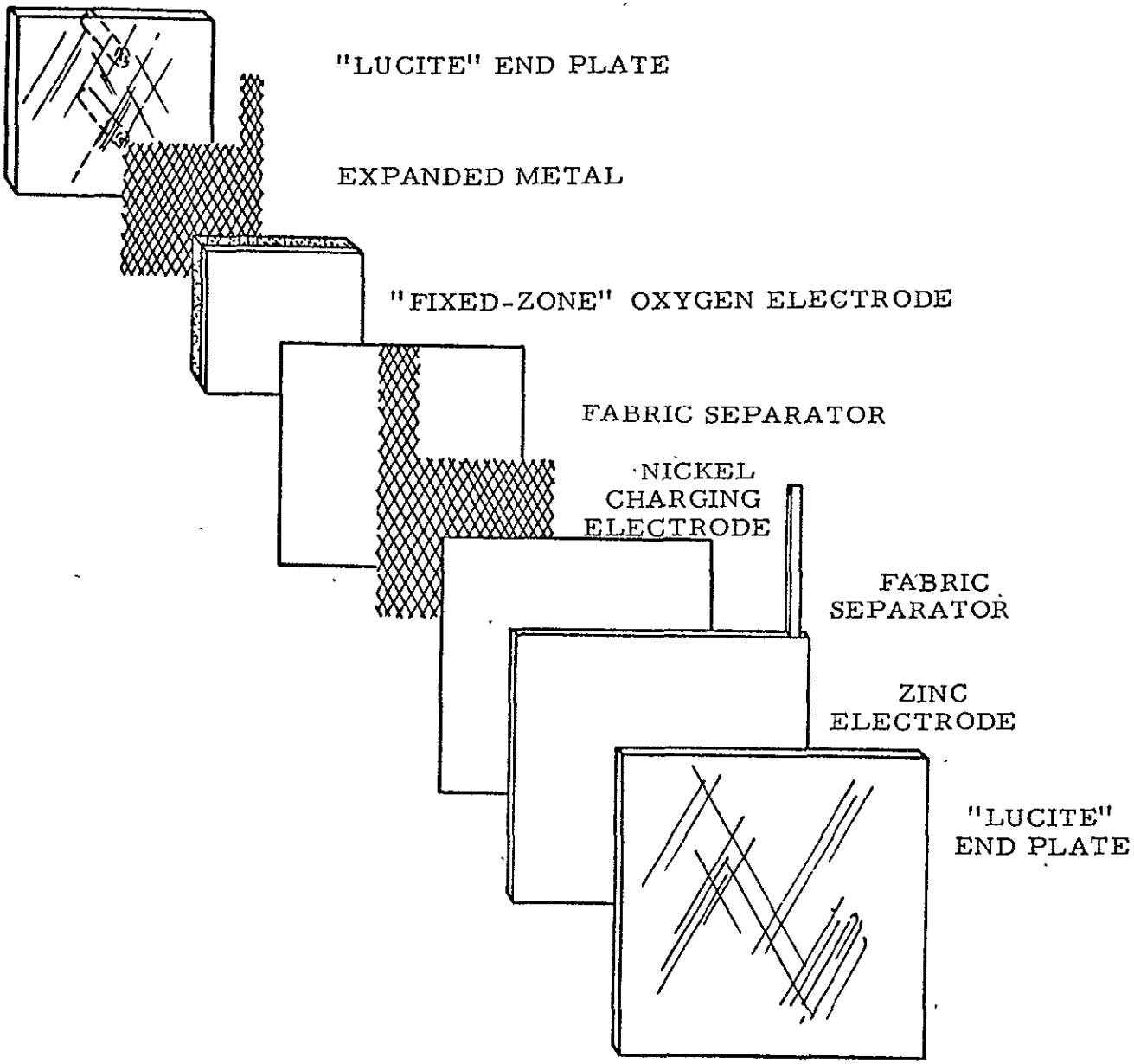

C-3180

A comparison of the size of the original zinc oxygen rechargeable experimental unit cell with that of the final unit cell is shown photographically in Figure 4. The reduction resulting from the smaller cell construction amounted to 25% without any decrease in cell capacity. The area of the respective electrodes remained unchanged. The components of the larger experimental unit cell are described in Table III. Cutaway and cross section views are shown in Figure 5.

TABLE III

COMPONENTS OF EXPERIMENTAL UNIT CELL

Component	Dimensions	Weight (g)
"Fixed-Zone" oxygen electrode[a]	3" x 3" x 0.022"	10.0
Polypropylene screen[b]	3" x 3" x 0.030"	1.5
Expanded nickel metal[c] charging electrode	3" x 3" x 0.020"	2.6
Polypropylene screen[b]	3" x 3" x 0.030"	1.5
C-3 membrane separator (dry)[d]	3" x 3" x 0.0015"	0.3
Zinc gel-type anode[a]	3" x 3" x 0.100"	12.2
Electrolyte (44% KOH + 2% ZnO dissolved therein)		25.0
Oxygen source[e]	oxygen cylinder	

[a] UCC Type-2 electrode

[b] Lamport

[c] Exmet

[d] Borden

[e] Linde

FIGURE 4

SIZE REDUCTION ACHIEVED IN UNIT $Zn-O_2$ CELL DESIGN

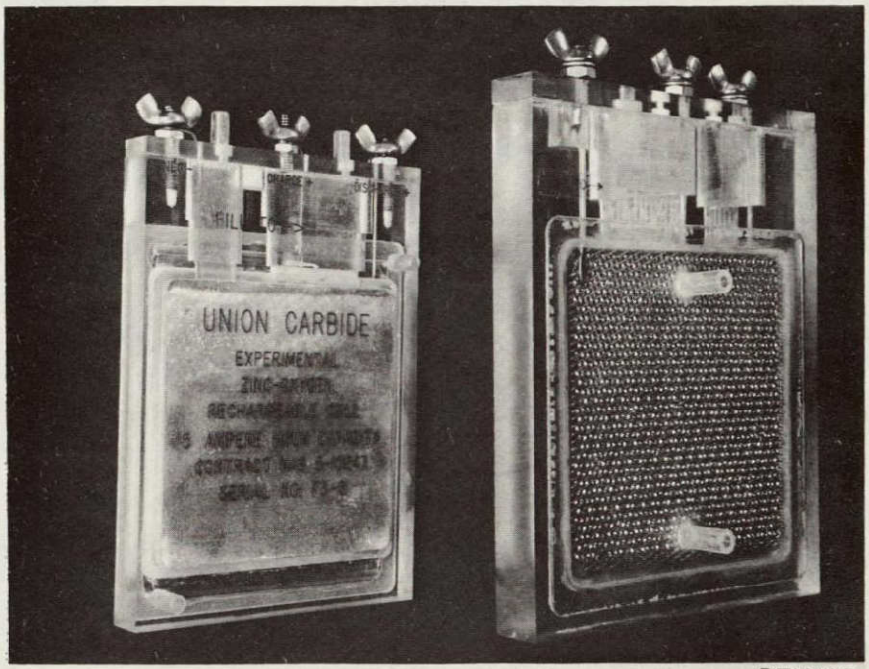

P710185

C-5941

FIGURE 5

CUTAWAY AND CROSS SECTION VIEWS OF EXPERIMENTAL ZINC-OXYGEN RECHARGEABLE UNIT CELL

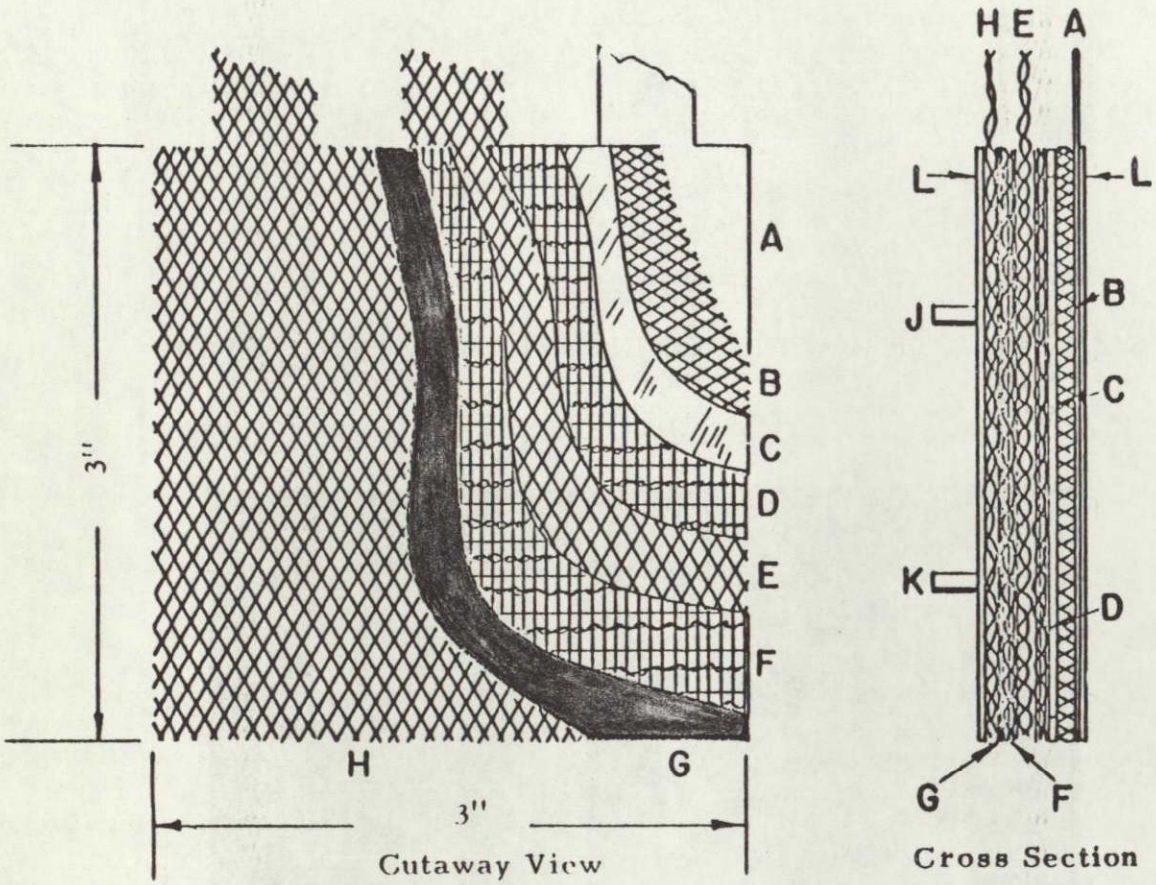

A Silver sheet anode collector

B Zinc anode restrained in a silver screen envelope

C Separator system

D Polypropylene screen

E Nickel Screen (Charging Electrode)

F Polypropylene screen

G "Fixed-Zone" oxygen electrode

H Nickel spacers and cathode current collector

J Gas inlet

K Gas Outlet

L "Lucite" backing plates

C-3308(revised)

The zinc-oxygen rechargeable unit cell shown in Figure 5 and described in Table III has demonstrated its ability to deliver over 350 cycles at a current density of 11.5 mA/cm^2 at room temperature.

With increased discharge rates the objective, cells of the aforementioned construction (PERMION separators substituted for C-3 separators) were discharged across a fixed resistance of 0.75 ohm. Although cycle life was obtainable in cells of this construction at the increased rate of discharge, the findings indicated the need for further constructional changes to improve the overall electrical performance. The discharge voltage at this higher rate of discharge was comparatively low.

A series of cells, each with a modification in the cell design to improve the discharge voltage characteristics, were built. The cell construction, the details of which are described in Table III, provided a base against which these modifications of cell elements could be compared.

The modifications were as follows:

1. Decrease in separator resistance by using one layer of PERMION 110 and 116 instead of two layers. It was established that one layer of these separator materials was effective for successful cycling of the cell. PERMION 1770C proved to be just as effective as the 110 and 116 membranes.

2. Increased anode collector contact. Zinc equivalent to 10 ampere-hours of theoretical capacity was applied to both sides of an expanded silver collector. The silver collector was cut to size 3-1/8 in. x 3 in. so as to leave 1/8 in. of exposed expanded silver across the top of the 3 in. x 3 in. area that comprised the zinc mass. The expanded silver envelope that tightly restrains the zinc was spot welded across the top to the centrally situated

expanded silver grid. This arrangement provides bilateral symmetrical collector contact to the zinc mass as opposed to only bilateral contact made by the expanded silver restraining envelope in the construction shown in Figure 6. The expanded silver used as the center grid was designated 10 Ag 20-4/o. The expanded silver used for the restraining envelope was 5 Ag 5-6/o. Both materials were products of the Exmet Corporation.

3. Electrolyte resistance was decreased by reducing the electrolyte gap by 25 percent. This was accomplished by replacing the polypropylene spacers on each side of the charging electrode with 8 equispaced 1/8 in. wide x 0. 02 in. thick x 3 in. long vertically positioned vinyl strips. This change also provided an obstruction-free path for oxygen to leave the cell during charge, thus decreasing the possibility of oxygen entrapment that was a problem with the woven polypropylene spacers.

4. The use of the American Cyanamid oxygen electrode eliminates the need for a separate charging electrode as the cell is charged directly off the charging electrode. Elimination of the charging electrode further reduces the electrolyte gap by another 50 percent. Reduction of the amount of electrolyte through reduction of the electrolyte gap also improves the watt-hours per pound ratio.

Two cells were constructed, each with a combination of the features that individually improved the electrical performance of the sequence of aforementioned cells. However, one cell employed a thin "fixed-zone" oxygen electrode that required a separate charging electrode for charging the zinc, while the other cell employed an American Cyanamid "LAB 40" oxygen electrode. PERMION 110 was the separator used in both constructions.

FIGURE 6

RECHARGEABLE ZINC-OXYGEN UNIT CELL WITH THIN "FIXED-ZONE" OXYGEN ELECTRODES

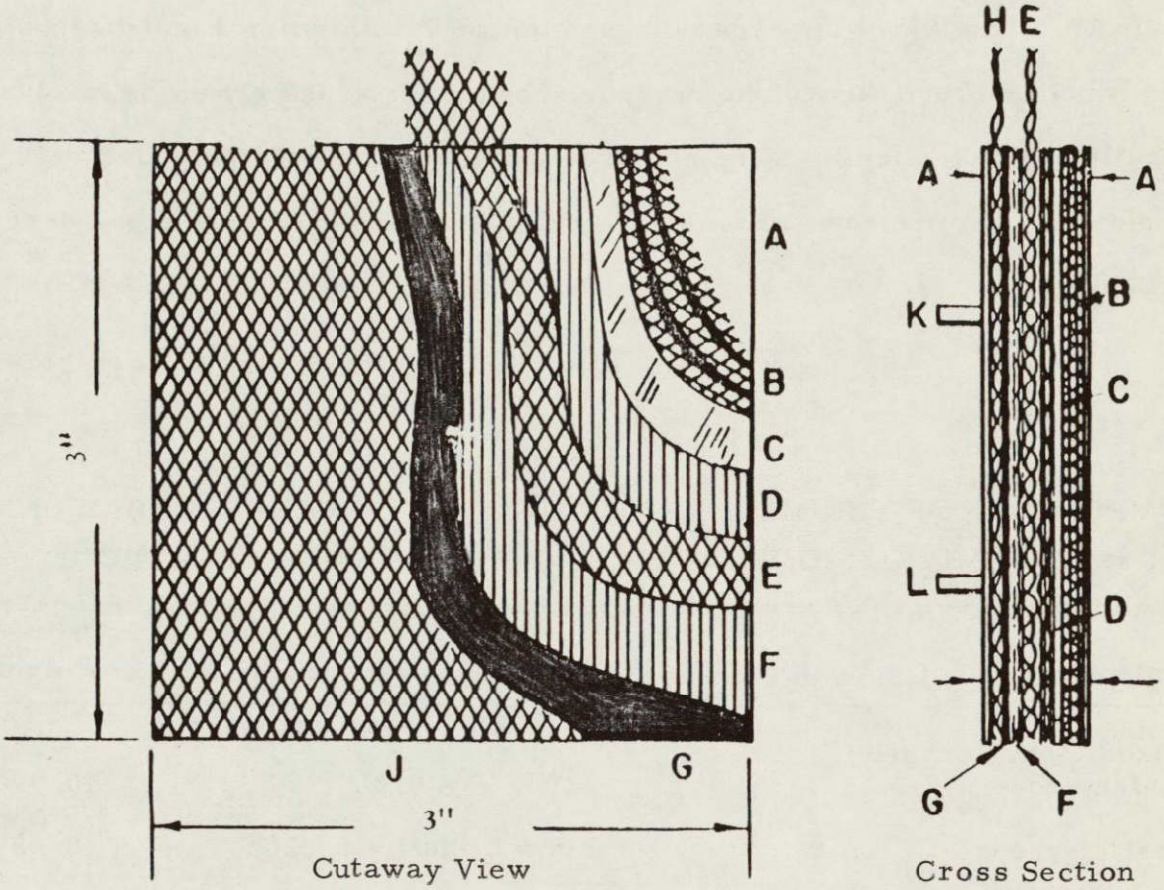

C-4146

A - LUCITE backing plates

B - Zinc anode bilaterally disposed on an expanded silver grid and restrained in an expanded silver envelope.

C - Separator system:

a) VISKON vinyon (electrolyte cushion absorber and retainer)

b) PERMION membrane separator

c) PELLON cushion

D* - Equispaced vertically positioned vinyl strips

E - Nickel screen (charging electrode)

F - Equispaced vertically-positioned vinyl strips

G - "Fixed-Zone" oxygen electrode

H - Expanded Ni cathode collector

J - Woven polypropylene spacer provides space for oxygen passage

K - Gas inlet

L - Gas outlet

*Removed from final unit cell.

Construction of the modified three electrode unit cell employing a thin "fixed-zone" oxygen electrode is shown schematically in Figure 7 and described in Table IV. The travel of oxygen through the cell is shown in Figure 7a while Figures 7b through 7e are photographs showing the assembly steps involved in building the test cell. The construction of the two-electrode unit cell employing an American Cyanamid electrode is shown in Figure 8 and described in Table V.

TABLE IV

COMPONENTS OF THE MODIFIED ZINC-OXYGEN RECHARGEABLE UNIT CELL EMPLOYING THIN "FIXED-ZONE" OXYGEN ELECTRODE

Components	Dimensions	Weight (g)
"Fixed-Zone" oxygen electrode	3" x 3" x 0.22"	10.09
Plastic spacers	3" x 0.060" x 0.020"	0.58
Expanded Ni charging electrode	3" x 3" x 0.020"	2.6
Plastic spacers - 8 equispaced vertical strips	3" x 0.060" x 0.020"	.58
PELLON No. 10194C	3" x 3" x 0.010"	.4
PERMION separator	3" x 3" x 0.0015" (wet)	.33
VISKON vinyon*	3" x 3" x 0.007"	.28
Zinc gel type anode	3" x 3" x 0.075"	31.0
Electrolyte: 41% KOH containing 7% ZnO	20-25 cc	27-34

*VISKON vinyon is a nonwoven synthetic fabric whose composition is reported to be rayon, vinyon and wood floc by the supplier, Chicopee Mills, Inc., Nonwoven Fabric Division, 47th & Worth Street, New York, N. Y.

FIGURE 7

CUTAWAY AND CROSS SECTIONAL VIEWS OF
ZINC-OXYGEN RECHARGEABLE UNIT CELL

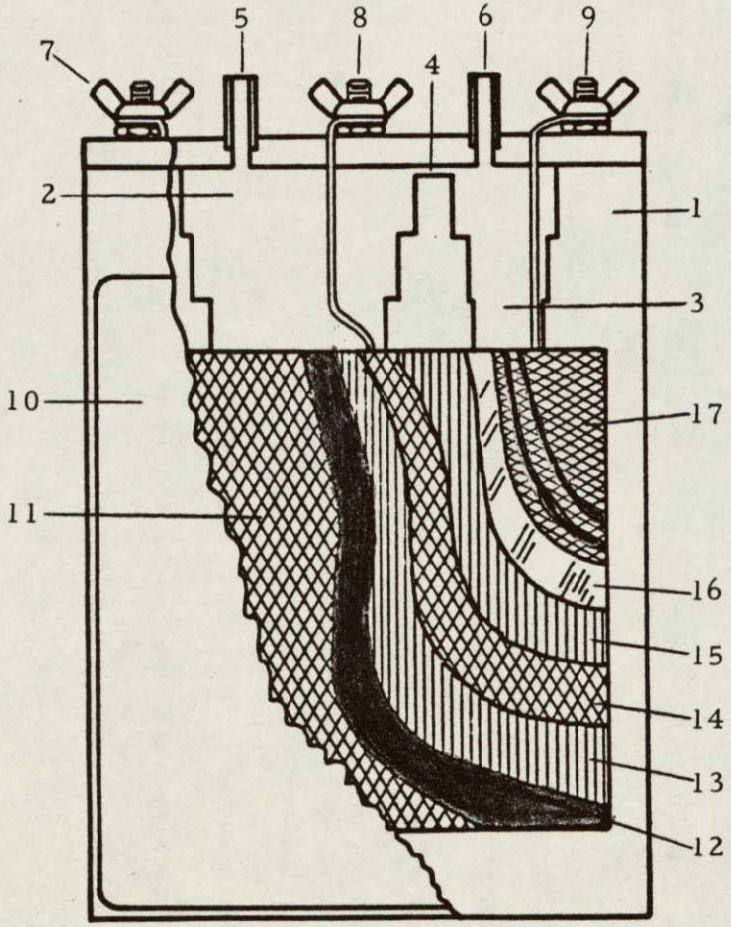

Cutaway View

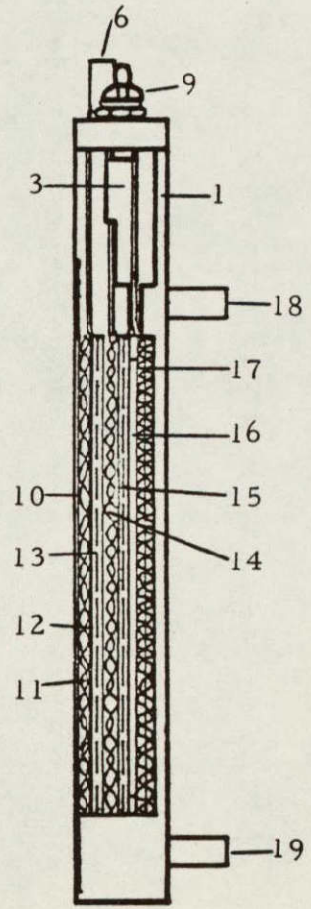

Cross Sectional View

See page 30 for legend

C-4517

LEGEND FOR FIGURE 7

1. LUCITE case.
2. Electrolyte reservoir above the positive compartment. (Positive compartment houses both the oxygen electrode and the charging electrode.)
3. Electrolyte reservoir above the negative compartment. (Negative compartment houses the zinc electrode.)
4. Channel connecting the electrolyte reservoirs above the positive compartment and the negative compartment. (Allows electrolyte to flow from one compartment to the other when levels rise due to electroosmosis.)
5. Gas exit tube above positive compartment.
6. Gas exit tube above negative compartment.
7. External lead to oxygen electrode (only in the electrical circuit during discharge).
8. External lead to charging electrode (only in the electrical circuit during charge).
9. External lead to zinc electrode (in the electrical circuit during both charge and discharge).
10. LUCITE backing plate.
11. Gas spacer.
12. Oxygen electrode (2.7" x 2.7" x 0.022").
13. Vertically positioned vinyl spacers.
14. Charging electrode (2.7" x 2.7" x 0.020").
15. Vertically positioned vinyl spacers.
16. Separator system: (a) PERMION 1770C, (b) VISKON vinyon, (c) PELLON.
17. Zinc electrode (3" x 3" x 0.120").
18. Oxygen inlet tube.
19. Oxygen outlet tube.

FIGURE 7a

TRAVEL OF OXYGEN THROUGH ZINC-OXYGEN RECHARGEABLE UNIT CELL

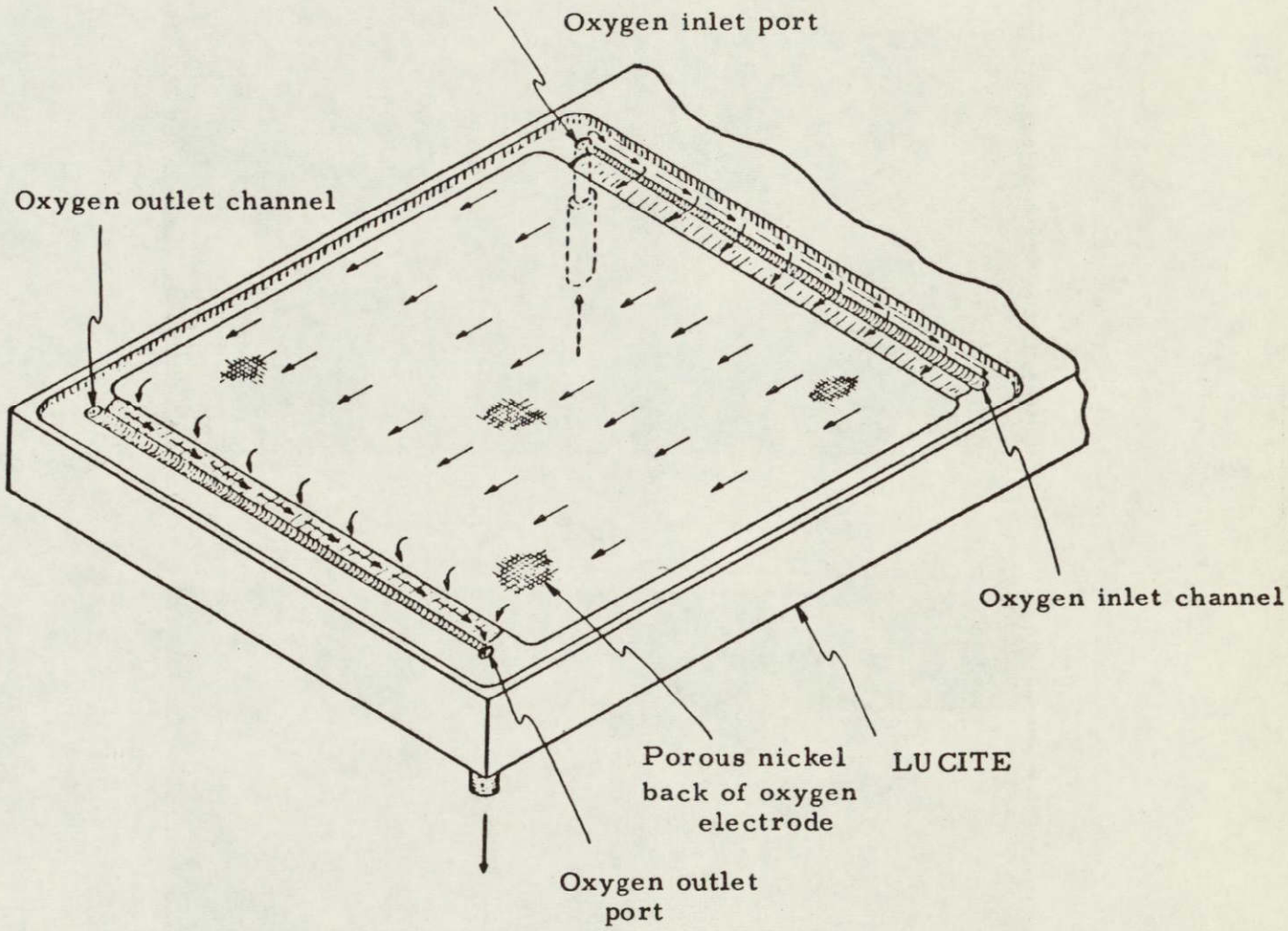

C-6336

Both inlet and outlet ports terminate into channels of increasing diameter with increasing distance from the ports in order to provide more uniform oxygen feed. Arrows show oxygen paths through the cell.

FIGURE 7b

ASSEMBLY OF $Zn-O_2$ CELL

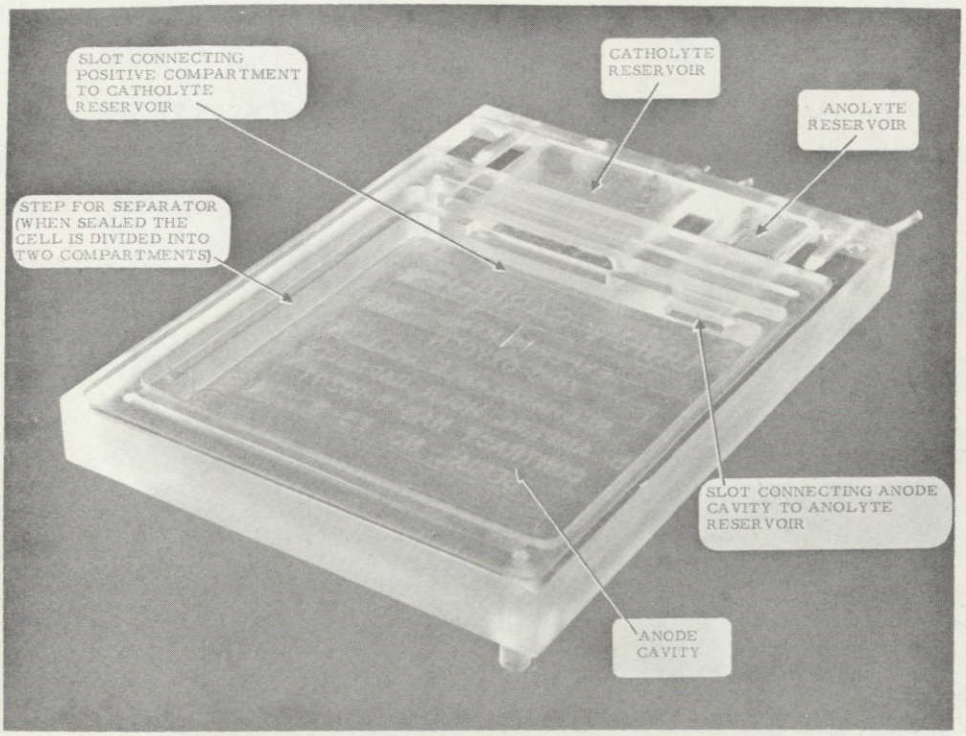

C-6342

Step 1

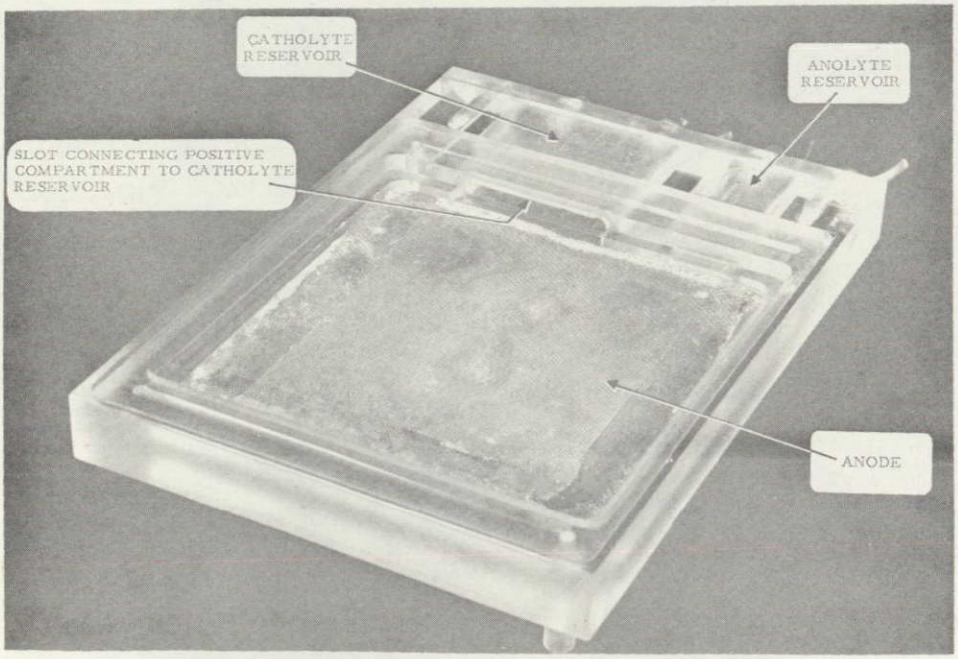

Step 2

C-6343

FIGURE 7 c

ASSEMBLY OF $Zn-O_2$ CELL

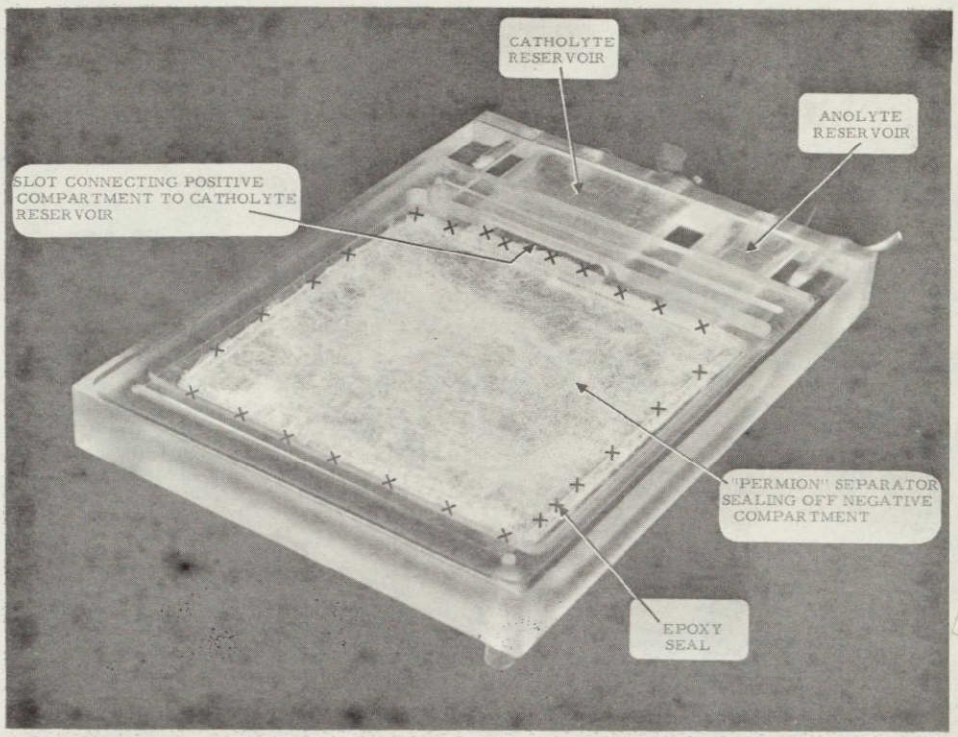

C-6344

Step 3

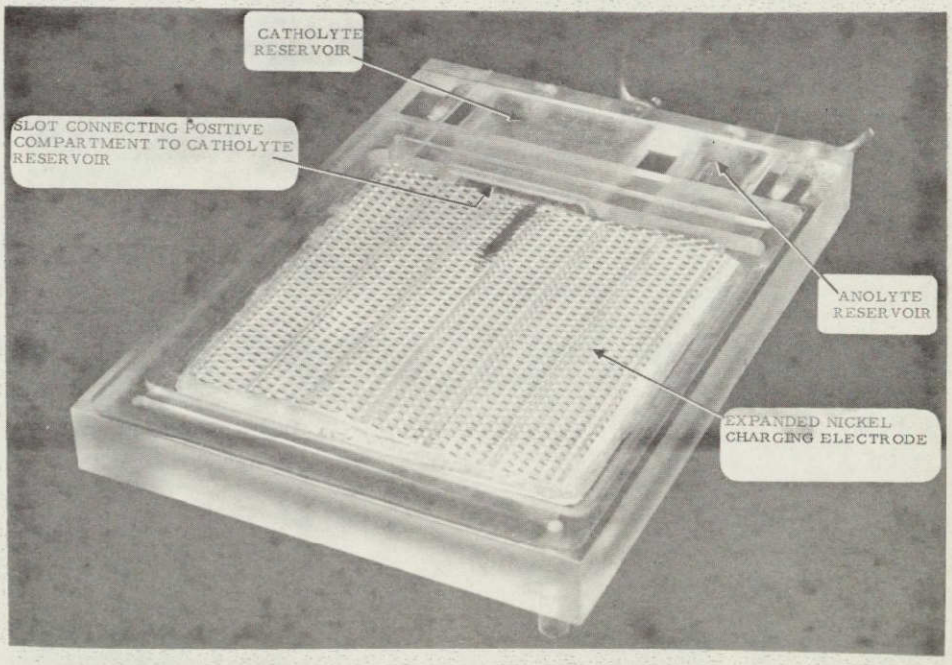

Step 4

C-6347

FIGURE 7d
ASSEMBLY OF $Zn-O_2$ CELL

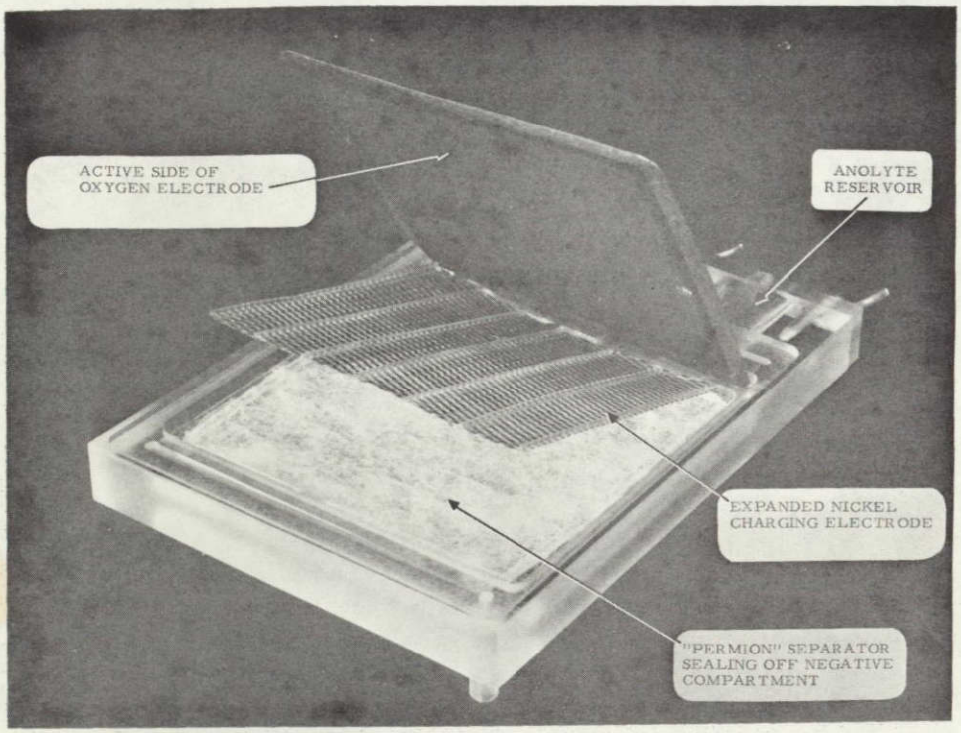

C-6346

Step 5

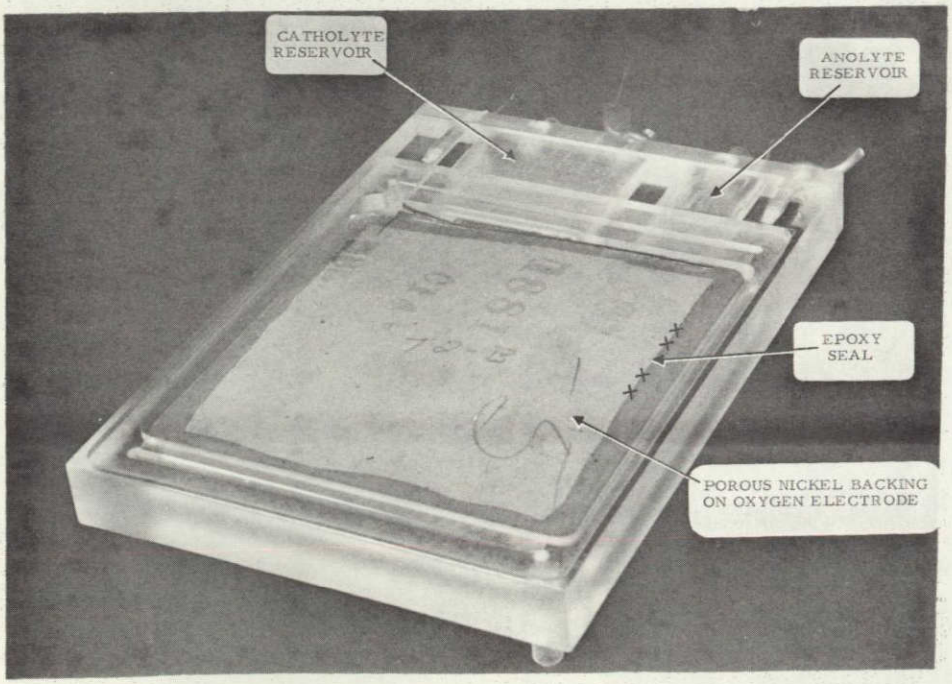

C-6345

Step 6

FIGURE 7e

COMPLETED RECHARGEABLE $Zn-O_2$ CELL

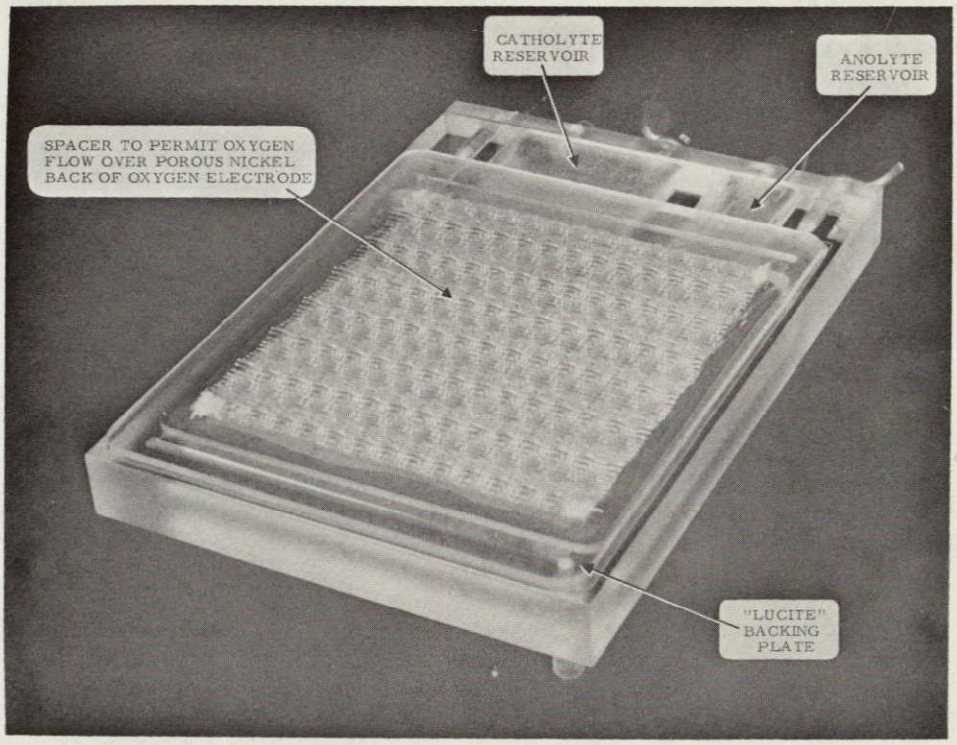

C-6348

FIGURE 8

Rechargeable Zinc Oxygen Unit Cell Using American Cyanamid Oxygen Electrode "LAB 40"

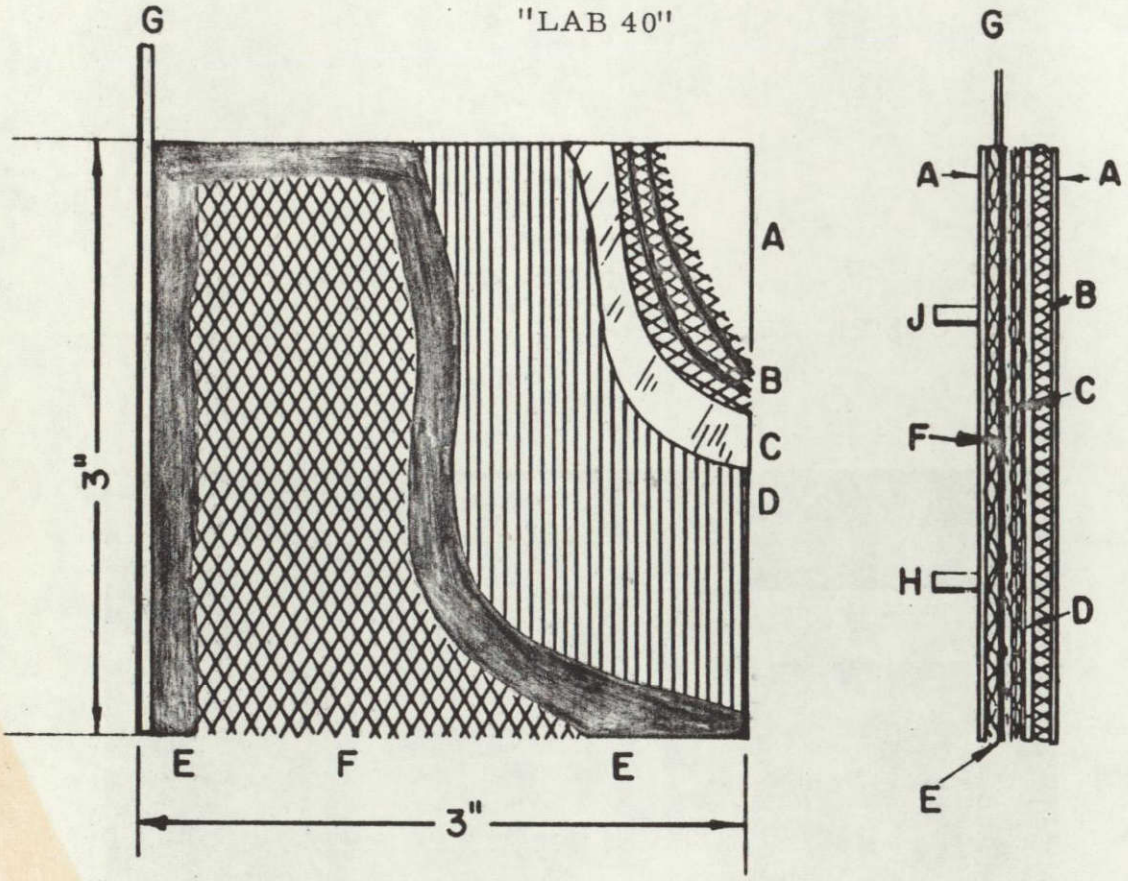

C-4147

A LUCITE backing plates

B Zinc anode bilaterally disposed on an expanded silver grid and restrained in an expanded silver envelope.

C Separator system:

a) VISKON vinyon (electrolyte absorber and retainer)

b) PERMION membrane separator

D Equispaced vertically positioned vinyl strips

E American Cyanamid LAB-40 oxygen cathode

F Expanded nickel (gas spacer)

G Ag strip cathode collector spot welded to edge of cathode

H Gas inlet

J Gas outlet

TABLE V

COMPONENTS OF THE MODIFIED ZINC-OXYGEN RECHARGEABLE EXPERIMENTAL UNIT CELL EMPLOYING AN AMERICAN CYANAMID "LAB-40" OXYGEN ELECTRODE

Components	Dimensions	Weight (g)
American Cyanamid oxygen electrode (LAB-40)	3" x 3" x 0.028"	15.09
Plastic spacers (8 vertically positioned)	3" x 1/8" x 0.020"	0.58
PERMION separator	3" x 3" x 0.0015"	0.33
VISKON vinyon	3" x 3" x 0.007"	0.28
Zinc electrode	3" x 3" x 0.075"	31
Electrolyte: 41% KOH + 7% ZnO	15-17 cc	21-23

F. Zinc Dendrite Penetration and Electrical Resistance Testing of Several Separator Materials

Separator materials were evaluated for resistance to zinc dendrite penetration and for electrical resistance in alkali media. The separator materials tested were the Borden C-3, VISKON vinyon, PERMION 110 and 1770C. Testing of the separators was conducted at 25°C. The Borden C-3 separator was tested in 41 percent KOH because of its tendency to degrade faster in lower KOH concentrations. The other materials were tested in 31 percent KOH. These tests provided a means for comparing separator materials in two areas that most significantly influence electrical performance. The test procedures were as follows:

1. Zinc Dendrite Penetration

The test equipment consisted of a two-chamber cell with the separator (1" diameter) being tested held between the chambers. A zinc microcathode (0.0049 sq. cm) was placed with its face up against one side of the separator while a zinc macroanode (5 sq. cm) was placed 1/16" away from the cathode on the opposite side of the separator. The two electrodes were so positioned that the microcathode was parallel and centered with respect to the macroanode. Current was allowed to flow at a cathode current density of 250 mA/cm^2 and the time required to grow a zinc dendrite through the separator to the anode was measured. The maximum electrolysis time used was 2 hours. This zinc dendrite penetration test is a somewhat modified form of the test described by Dalin and Solomon (13). Table VI shows that when no separator is used a shorting dendrite is grown after only 25 minutes of electrolysis. The use of VISKON vinyon as the separator only slightly retards the growth of dendrites. Borden C-3, PERMION 110 and PERMION 1770C films, however, do not allow zinc dendrite penetration even after 2 hours of electrolysis. For this reason these separator films were chosen for more exhaustive evaluation in test cells.

TABLE VI

ZINC DENDRITE–SEPARATOR TEST

Separator	Time required to grow dendrites through separator to the anode
No separator	25 minutes
VISKON vinyon	35 minutes
Borden C-3	Did not grow dendrite through separator
PERMION 110	" " " " " "
PERMION 1770C	" " " " " "

2. Separator Resistance

An alternating current method (14) was used to measure the separator resistance. The test cell was designed in such a way that the area of exposed separator surface was 0. 15 square inch. The test consisted of measuring the cell resistance (without any separator) then measuring the resistance with the separator in place. Samples were kept in the "as received" condition until the test was started. Thirty-one percent KOH was added to the test cell and resistance measurements were taken across the fixed platinized platinum electrodes. An Industrial Electronics bridge was used to measure resistance. Polarization-free measurements are determined by this method. Table VII shows typical data on several separator materials.

TABLE VII

RESISTANCE–SEPARATOR TESTS

(A) 24-Hour Typical Values

Separator	Measured Resistance	Dry Thickness	Wet Thickness
Borden C-3	1. 52Ω	0. 0013"	0. 0022"
PERMION 110	0. 2Ω	0. 001"	0. 0015"
PERMION 1770C	0. 3Ω	0. 0015"	0. 002"

(B) Specific Resistances

Separator	Ω/cm 5 min	Ω/cm 10 min	Ω/cm 1 hr	Ω/cm 24 hr
Borden C-3	——	——	130	130
PERMION 110	41	41	41	41
PERMION 1770C	37	37	37	37

G. Problem Areas Encountered in Cycling Unit Cells

1. Electroosmosis and Cycling of the Unit Cell

Electroosmosis hindered cycling of zinc-oxygen cells on a 2-hour discharge/4-hour charge schedule to a theoretical output/input balance of 2.5-3.0 ampere-hours. This was not a problem when cells were cycled on a 2-hour discharge/2-hour charge schedule to a theoretical output/input balance of 1.2-1.4 ampere-hours.

As cycling progressed, the electrolyte level in the anode compartment would rise during charge and was accompanied by a corresponding lowering of the electrolyte level in the cathode compartment during charge. This electrolyte would not return to the cathode compartment during discharge. This was not a simple problem of electrolyte level fluctuation in the respective electrode compartment during cycling, which is normal in cells employing a membrane separator.

A carboxymethyl cellulose gel-zinc powder anode was used in the cells in which this problem occurred, thus the viscosity of the anolyte increased after overnight contact with the gelled anode. The viscosity of the catholyte was not affected by this gel, since the anode was sealed off in a separate compartment on the other side of the PERMION 110 membrane separator. During discharge the more viscous anolyte would not move to the cathode compartment as would normally be expected. However, the catholyte would move to the anode compartment during charge and mix with the more viscous anolyte. The catholyte involved, which was now also viscous, would not return to the cathode compartment. The net effect was overflowing of electrolyte from the anode compartment and ultimate evacuation of the cathode compartment.

The problem was the reverse in cells employing anodes fabricated from zinc oxide mixtures in which no CMC gel was present. The rise in the electrolyte level now occurred in the cathode compartment. As the electrolyte level of the cathode compartment rose with cycling, the electrolyte level of the anode compartment dropped. Electrolyte return to the anode compartment could now be achieved only with a slow-low current density charge. No problem was encountered when 2-hour discharges were followed by the slow 22-hour charges, nor was it a problem when cells were cycled on a 24-hour discharge/24-hour charge schedule.

A solution to the problem was provided simply by designing an interconnecting channel between the positive and negative electrolyte reservoirs. With such a channel electrolyte levels can easily equilibrate with cycling.

2. Zinc Anode Shape Change

It was demonstrated that the zinc-oxygen unit cell is capable of rechargeability and continuous operation after occasional very deep discharge. Performance of a cell that was completely discharged and returned to the normal cycling schedule is shown in the Experimental Unit Cell Performance section of this report.

Repeated deep discharges caused severe anode shape change and associated problems. Impaired anode mass-collector contact and a loss of capacity associated with the continually diminished geometric surface area was the primary mode of failure of all cells consistently discharged at a current density of 25 mA/cm^2 to 25 percent theoretical depth in two hours.

The active anode area of dissected cells had decreased by as much as 70-80 percent. As a result, the current density imposed on both the anode

and the cathode was continually increased as cycling progressed. An initial current density of 25 mA/cm^2 on a fresh cell becomes over 100 mA/cm^2 after 75 percent zinc reorientation has occurred.

Over 300 cycles were delivered from a unit cell employing a 10-ampere-hour zinc anode. This cell was discharged at a current density of 11-12 mA/cm^2 to 12-14 percent zinc depth in two hours. Low discharge voltages associated with 22-25 mA/cm^2 discharging of this cell necessitated modifications to improve the anode-collector contact and to decrease the cell internal resistance. These modifications improved the discharge performance to the extent that a discharge current density of 22-25 mA/cm^2 could be attained at essentially the same voltage level as the 11-12 mA/cm^2 discharge current density in the cell from which over 300 cycles were delivered.

Doubling the rate of discharge, while maintaining the discharge time constant, correspondingly doubled the discharge depth (12-14 percent to 25-30 percent depth of a 10 ampere-hour anode). Severe anode shape change occurred early in the cycle life of cells discharged to this depth. Failures due to problems associated with 70-80 percent zinc slump (estimated visually) were not uncommon after 50-60 cycles.

Over 300 cycles could be obtained from a 10 ampere-hour cell subjected to 12-14 percent depth of discharge in two hours, while only 50-60 cycles could be expected from a cell consistently subjected to 25-30 percent depth of discharge. This observation suggested the feasibility of retarding anode slump and correspondingly increasing cycle life by limiting the discharge depth to a value comparable with that at which the previous cell delivered over 300 cycles. Two cells were built, both employing anode structures identical to the aforementioned 10 ampere-hour cells, but with increased zinc capacity.

One of these cells contained a 20 ampere-hour anode and the other a 15 ampere-hour anode. Both of the cells were discharged across a fixed load of 0.75 ohm at an average current density of 23 mA/cm^2. The theoretical zinc depth per discharge on the 20 ampere-hour cell and the 15 ampere-hour cell was 13 and 17 percent, respectively. Both of these cells delivered 176 cycles before failure due to anode slump and associated problems. Approximately 50% slump had occurred when cycling was terminated.

3. Problems Associated with the Cathode

a) The Union Carbide thin "fixed-zone" oxygen electrode demonstrated far better stability of performance than did the American Cyanamid "LAB 40" oxygen electrode. Performance of the thin "fixed-zone" electrode usually improved with cycle life due to improved wetting of the electrode active layer as cycling progressed.

A small amount of water transpiration through the "fixed-zone" electrode to its gas side that usually appeared as moisture across the bottom part of the electrode was observed after 40-50% anode slump had occurred. Severe flooding of the thin "fixed-zone" electrode occurred only when cycling was continued after anode slump reached the 50-65% level. Zinc electrode failure preceded flooding in most cases.

Unit cell operation was not affected by small amounts of water transpiration to the gas side of the thin "fixed-zone" oxygen electrode. The cathode vs. zinc reference potential was usually higher after a small amount of transpiration than before.

The problem of water transpiration can at least partially be attributed to a higher current density imposed on the cathode as a result of anode slump

(overloading of that part of the cathode facing the reduced zinc area). However, very little increase in cathode polarization was observed at cathodes operating under this imposition.

b) Problems associated with cycling of the American Cyanamid "LAB 40" oxygen electrode involved both the oxygen electrode itself and the zinc electrode. Severe cathode flooding and/or serious cathode polarization limited cycle life of cells employing this electrode. The result of polarization at the "LAB 40" oxygen electrode was a continuously declining discharge voltage as well as a progressively higher charge voltage as cycling progressed. This problem occurred regardless of whether the zinc electrode was charged against the "LAB 40" oxygen electrode or against a separate charging electrode. However, it was retarded to some extent (about 10%) when the zinc was not charged against the oxygen electrode. "LAB 40" oxygen electrode vs. zinc reference measurements as low as 0.09V have been observed due to cathode polarization while the "LAB 40" was operating under a moderate discharge load of 1.3 amperes (a current density of 27 mA/cm^2).

Severe flooding of the "LAB 40" oxygen electrode cannot be attributed to high current density operation resulting from anode slumping. Very early flooding of this electrode always preceded significant anode shape change. As a matter of fact flooding of these electrodes in cells that were activated with electrolyte and left to soak over night occurred when no back pressure was applied during the soak period. Subsequent cells employing this electrode were activated only after applying back pressure equivalent to 2 inches of water. This applied back pressure was sustained during cell operation. Although leakage through the electrode was retarded, it still occurred shortly after cycling began.

Serious gassing at the zinc electrode was also a problem with cells employing the "LAB 40" oxygen electrode, thereby contributing to anode slumping. Gas build-up within the anode mass occurred during both charge and discharge. The problem was more severe in cells employing the "LAB 40" electrode when the zinc was charged directly against the oxygen electrode itself than in cells utilizing a separate charging electrode to charge the zinc. A probable explanation for the anode gassing is the dissolution and migration of noble metal from the oxygen electrode over to the zinc electrode to form a gas couple. Actual plating of noble metal on the anode is also a possibility particularly when the anode is charged directly against the oxygen electrode. The presence of both platinum and palladium on zinc anodes removed from spent cells was substantiated by x-ray fluoresence examination.

4. Possible Explanations for Drop-Off in Performance of the Zinc-Oxygen Unit Cell at 0° C

Zinc-oxygen experimental unit cells suffered a drop-off in discharge voltage when they were cycled at 0° C. Factors thought to contribute to this include:

1. Increased ohmic resistance resulting from the increased viscosity of the electrolyte at low temperatures.
2. Because of the increased viscosity, diffusion of the electrolyte through the electrolyte film (which is continuously built up during discharge) is hindered.
3. Decreased wetting of the active layer of the oxygen electrode resulting from increased electrolyte viscosity.
4. Shaw and Remanick (15) proposed that the drop-off in performance at 0° C could be caused by localized freezing resulting from changes in the electrolyte concentration in cells employing membrane separators.

H. Charging Techniques

Cells employing the Union Carbide thin "fixed-zone" oxygen electrodes were charged by using an expanded nickel charging electrode. Thus, the oxygen electrode is not in the circuit during the charging process. Cells employing American Cyanamid "LAB 40" oxygen electrode were charged directly against the oxygen electrode. A detailed discussion of the various charging techniques investigated follows:

1. Constant Current Method

Constant current charging for a fixed time was the method employed for most of the work. Charge input was the same as discharge output for zinc-gel type anode cells. Overcharge, however, was necessary to properly charge anodes fabricated from zinc oxide compositions. Cycling was carried out on schedules of 2-hour discharge followed by 2, 4, 6, and 22 hours of constant current charge. Twenty-four hour discharging followed by 24-hour constant current charging was also studied.

2. Constant Current-Voltage Limited and Constant Current-Voltage Limited Trickle Charging of Unit Cells

Constant current-voltage limited and constant current-voltage limited trickle charging was investigated to: (1) prevent serious overcharge; (2) control dendrite growth, and (3) minimize hydrogen evolution. The constant current-voltage limited and the constant current-voltage limited trickle charging are essentially the same. These are described below:

a) Constant Current-Voltage Limited Charge

The current was preset at a constant value such that the input was balanced with the output in the required time (depending on the cycling schedule) to a preset voltage (below hydrogen evolution).

When the preset voltage was reached, the charge was switched to open circuit and remained on open circuit until the required time (depending on the cycling schedule) had elapsed.

b) Constant Current-Voltage Limited Trickle Charge

The current was preset at a constant value such that the input was balanced with the output in the required time in the same manner as was employed with the constant current-voltage limited method. The difference being that when the preset voltage was reached, the charge was switched to constant voltage trickle charge instead of open circuit. The charge is then voltage limited and decreases from the initial constant current limit to some significantly smaller current value. This value would depend upon the ability of the cell to accept charge at that voltage value.

The feasibility of charging zinc by means of this type of charge was not established because of the unstable end-of-charge voltage associated with shape change of the zinc anode structures evaluated. During the constant current portion of the charge the cells reached the voltage limit before being fully charged. Decrease in zinc mass-collector contact and polarization of the zinc anode, both associated with anode shape change, were the main

causes of the end-of-charge voltage increase that prohibited full utilization of a constant current charge with a voltage limit, or a voltage limiting trickle charge unless the charge time was sufficiently extended.

3. Modulated Current Charging Methods

Modulated current charging has been used in electroplating to control the character of electrodeposits. This method of charging was also investigated for charging the experimental zinc-oxygen unit cells. It has been suggested that a decay of the concentration gradient at an electrode occurs when the current is shut off. This has the effect of equilibrating the metal ion at the electrode surface to that of the bulk solution. Metal ions thus diffuse to the surface of the electrode where the plating occurs. When the current is on, these ions are available for deposition. The net effect is a more uniform electrodeposition.

Three methods of modulated current charging were investigated during the course of the contract effort. The methods investigated were:

a) Asymmetrical Alternating Current Method

This technique was first investigated by Ernest Beer of the Netherlands and described by R. W. Hallows (16). Maurice Baddour of the Lewis Research Center constructed a charging system based on this work and used it successfully to charge Leclanché cells. The circuitry used to charge zinc-oxygen experimental unit cells was a duplication of the circuit used by Baddour and later by Donald Vargo (17) in his evaluation of the technique.

The charging technique utilized a 5.4 ampere peak current during the forward component. The reverse component was approximately 10% of

the forward component. The net current during the charge was 1. 32 amperes. Charging was carried out over a 2-hour period against a separate charging electrode. Figure 9 is an oscillogram of the current trace used together with a quantitative description of the cycle used. Cell cycling performance is described in Section I, 2h and is graphed on Figure 53.

b) Periodic Open Circuit and Periodic Reversal Methods

A constant current D-C power supply was used in conjunction with a pulse generator to provide variable pulse lengths and frequencies. Essentially the same circuitry was used for both periodic open circuit and periodic current reversal methods of charging. A fixed resistance of proper value to produce the desired reverse current was across the cell during the OFF (deplating) time in the case of the periodic current reversal method. During the OFF (deplating) time in the case of the periodic current reversal method zinc metal was actually being removed.

Charging by means of periodic open circuit and periodic current reversal methods was carried out over a period of 6 hours and 22 hours, respectively. The periodic open circuit cycle was 22. 5 seconds with an ON (plating) time of 7. 5 seconds and an OFF (open circuit) time of 15 seconds. The plating current density was 24 mA/cm^2. The periodic reversal cycle was 60 seconds with an ON (plating) time of 54 seconds and an OFF (deplating) time of 6 seconds. The current density during both plating and deplating times was approximately 4 mA/cm^2. Figure 10 shows typical periodic open circuit and periodic reverse current cycles as they were applied to charging zinc-oxygen experimental unit cells.

FIGURE 9

OSCILLOGRAM AND DESCRIPTION OF

ASYMMETRICAL A.C. CELL CHARGING METHOD

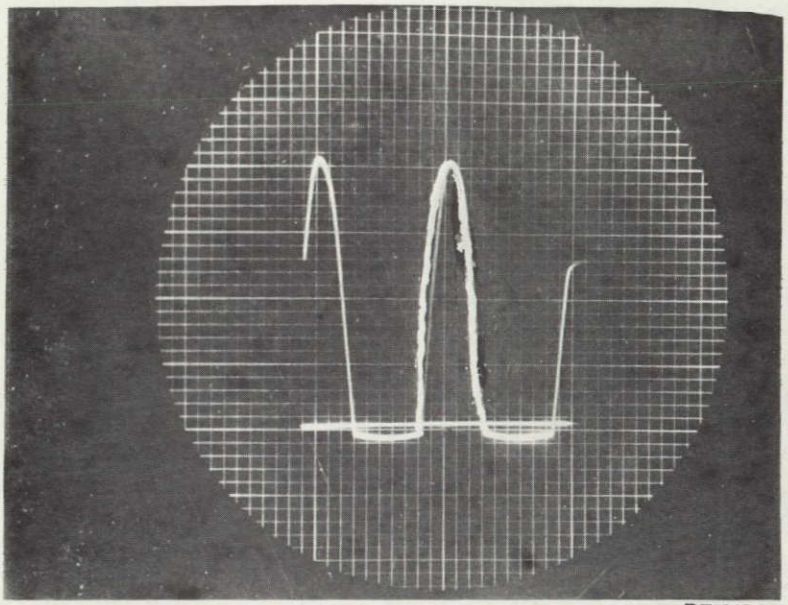

P710186

C-7008

Description of Current Trace

Peak current	5.4 amperes
Average current	3.3 "
Cycle efficiency	40%
Net charging current	1.32 amperes
Ampere hour charge	(2 hrs) (1.32 amps) = 2.64 amp-hrs (this includes 1.5% overcharge)
Net charging current density	28 mA/cm^2
Reverse component	10% of forward component

FIGURE 10

INTERRUPTED D. C. CHARGING CYCLES

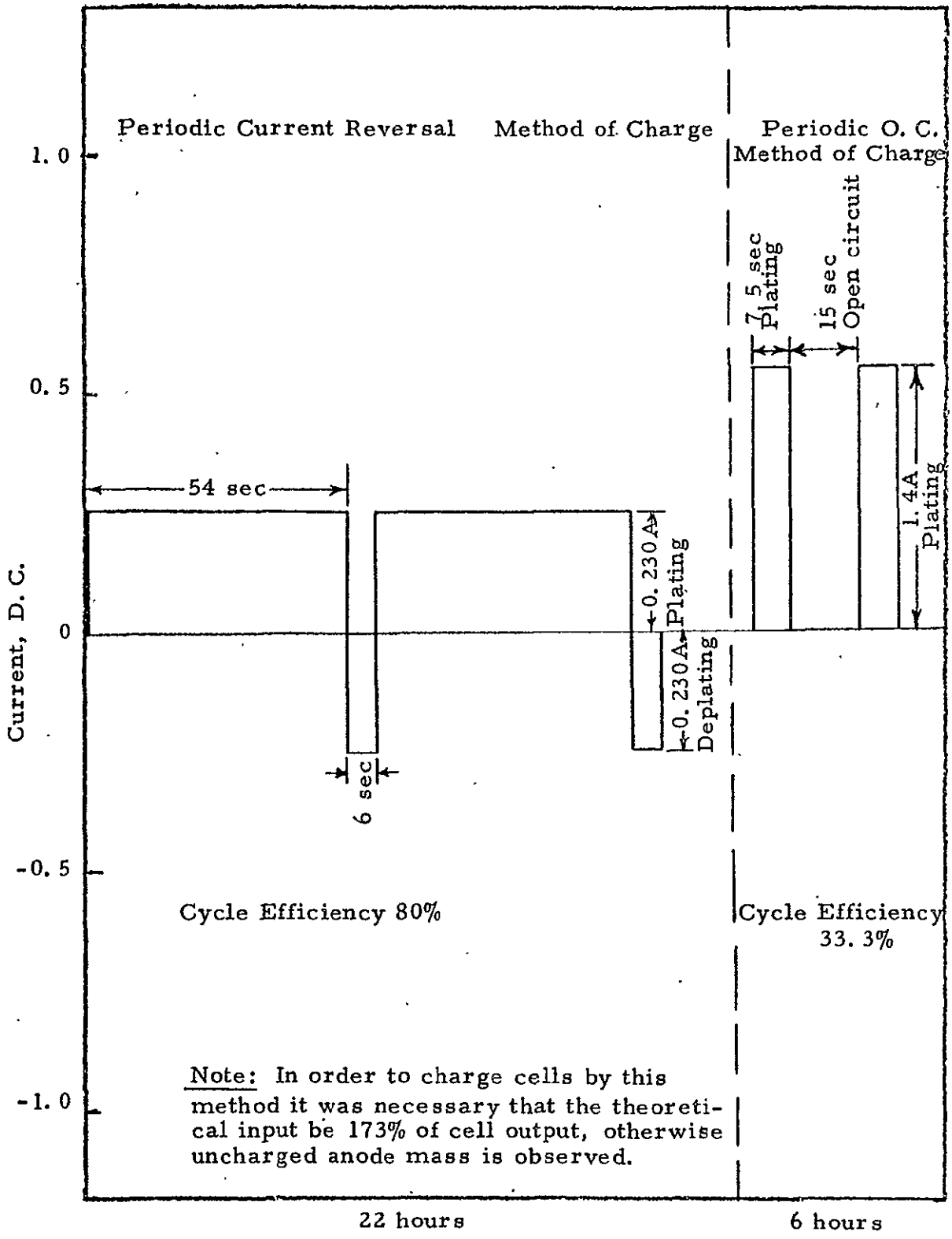

C-5834

I. Zinc-Oxygen Rechargeable Unit Cell Performance

Performance data of zinc-oxygen unit cells are divided into two sections based upon the type of zinc anode structures used. Cycling is shown to termination of tests. The number of cycles obtained from a cell by the time the end of discharge voltage declined to 0.8 volt was noted. Figures 11 through 57 placed immediately following Section I in this report describe the various cycling tests performed. Cycle life summaries are given in Tables VIII and IX.

1. Zinc Gel-Type Anodes

a) Performance of Unit Cells at 0°, 25°, and 40°C with Thin "Fixed-Zone" Oxygen Electrodes and Double Layers of C-3 Membranes

Cells tested on a 2-hour discharge/2-hour charge schedule at 0°, 25°, and 40°C delivered 168, 356, and 256 cycles, respectively. Discharge was through a fixed resistor of 1.75 ohms. This represented the 14% depth level based upon the actual ampere-hour equivalents of zinc present at an average current density of 11.5 mA/cm^2. A balanced constant current charge was used. All of the energy was delivered above 1.0 volt on the 25° and 40°C tests. Cells were operated at 0°C at a somewhat reduced capacity. These data are presented in Figure 11 to 16.

Rechargeability after complete discharge of the zinc was also demonstrated with an experimental unit cell operated at 25°C. This is graphed in Figure 17. Figure 17 shows a period from the 156th through the 172nd cycle when the cell was discharged for 2 hours, followed by 2 hours on open circuit, for a total of 16 discharges. Following the 172nd discharge the cell was charged until the theoretical ampere-hour input was equal to the total output of the discharges. The rate at which the cell was

TABLE VIII

SUMMARY OF CYCLE LIFE OF ZINC-OXYGEN RECHARGEABLE EXPERIMENTAL UNIT CELLS EMPLOYING UNION CARBIDE PROPRIETARY ZINC GEL-TYPE ANODES AND THEIR THIN "FIXED-ZONE" OXYGEN ELECTRODES

Actual anode capacity, ampere-hours, zinc metal	10									15		
Discharge-charge schedule, hours	2-2			2-4			24-24			2-4		
Temperature, degrees, Centigrade	0°	25°	40°	0°	25°	40°	0°	25°	40°	0°	25°	40°
Average discharge current density, mA/cm^2	10.4	11.8	11.8	22.5	24	24.6	—		—	22	25	24
Average charge current density, mA/cm^2	10.4	11.8	11.8	11.3	12	12.3	—		—	11	12.5	12
Output per discharge, ampere-hours	1.18	1.3	1.3	2.6	2.8	2.86	—		—	2.54	2.90	2.78
Input per charge, ampere-hours	1.12	1.3	1.3	2.6	2.8	2.86	—		—	2.54	2.90	2.78
Number of cycles to 0.8 volt	168	356	256	50-60	50-60	50-60	—	30	—	100	176	100
Performance shown in Figure No.	11&12	13&14	15&16	26	24	25		18&19		31	28	32

TABLE IX

SUMMARY OF CYCLE LIFE OF ZINC-OXYGEN RECHARGEABLE EXPERIMENTAL UNIT CELLS EMPLOYING UNION CARBIDE'S THIN "FIXED-ZONE" OXYGEN ELECTRODES AND ANODES FABRICATED FROM ZINC-OXIDE FORMULATIONS

Anode mix designation	ZnO#1		ZnO #10	ZnO#19														
Rated anode capacity, ampere-hours	5		5	10														
Method of charge	Constant Current																AC/DC	PR
Discharge-charge schedule, hours	2-2	2-4	2-4	2-2			2-4			2-22			24-24			2-2	2-22	
Temperature, degrees, Centigrade	25°	25°	25°	0°	25°	40°	0°	25°	40°	0°	25°	40°	0°	25°	40°	25°	25°	
Average discharge, current density mA/cm²	24	31	31	27	27	27	27	27	27	27	27	27	6.45	6.45	6.45	27	27	
Average charge, current density, mA/cm²	30	15.3	17.35	30	30	30	15	15	15	2.75	2.75	2.75	8.54	8.54	8.54	2.7		
Output per discharge, ampere-hours	2.74	3.0	3.0	2.6	2.6	2.6	2.6	2.6	2.6	2.6	2.6	2.6	7.44	7.44	7.44	2.6	2.0	
Input per charge, ampere-hours	3.00	3.0	3.36	2.8	2.8	2.8	2.8	2.8	2.8	2.86	2.86	2.86	9.85	9.85	9.85	2.65	3.85	
Number of cycles to 0.8 volt	100	124	108	60	128	116	72	165	115	60	130	114	17	60	24	134		
Performance shown in Figure No.	38	39	40	49	41	45	50	42	46	51	43	47	52	44	48	53	54	

recharged after complete discharge of the zinc was identical to the routine 2-hour rate of charge. The unit cell was returned to the original 2-hour discharged/2-hour charge schedule and continued to cycle out to 356 cycles. The discharge performance after recharging the zinc from complete discharge was essentially unchanged.

Cycle life at 25°C on a 24-hour discharge/24-hour charge schedule is shown in Figures18 and 19. Discharges were across a fixed resistor of 6 ohms. This represented the 50% zinc depth based upon the theoretical ampere-hour equivalents of the actual weight of zinc present in the anodes. The average discharge current density was 3.7 mA/cm^2. Balanced constant current charging was used.

With higher current density operation as a major objective, cycling current densities on a 2-hour discharge/2-hour charge schedule commensurate to 25% zinc depth were attempted on cells employing C-3 as the separator. Continued cycling of these cells was prohibitive due to foaming of the electrolyte during charge. The foaming problem was found to be associated with the C-3 separator as was previously described.

b) Performance of Unit Cells at 25°C with Thin "Fixed-Zone" Oxygen Electrodes and Double Layers of PERMION Membranes

PERMION 110- and 116 obtained from RAI Research Corp. (formerly Radiation Applications, Inc.) were tested as separators after foaming problems were found to be associated with the C-3 separator. Both of these materials appeared to meet the requirements for successful operation. PERMION 110 was somewhat more resistant to dendrite penetration than the 116 film. Cycle life obtained with cells using these two separator membranes is shown in Figures 20 and 21. Even a single layer of the 110 membrane was sufficient for successful cycling as shown in Figure 22.

c.) Typical 25°C Cycling of Cells Designed to have Improved High-Rate Discharge Capability

The low discharge voltage associated with 0.75 ohm discharging of the unit cell (see Figures 21 and 22) necessitated the need for modifications of the unit cell element to improve its high-rate discharge capability. Improvement in this regard was achieved by making the following modifications in the unit cell element arrangement.

1. Improved anode-collector contact.
2. Decreased cell internal resistance obtained by reducing the electrolyte gap and by the use of only one layer of PERMION 110 membrane.

Further improvement in discharge performance could have been obtained by the use of the American Cyanamid oxygen electrode if this electrode had demonstrated capability of stable operating performance. However, problems with this electrode, as was described in section G, prohibits its use. Figure 23 shows typical cycles delivered by unit cells constructed as described below:

1. A unit cell incorporating the changes designed to improve the high-rate discharge capability and employing a T-2 oxygen electrode*.
2. A unit cell incorporating the changes designed to improve the high-rate discharge capability and employing an American Cyanamid oxygen electrode.
3. A unit cell employing a T-2 oxygen electrode with no other changes in cell construction.

These cells were discharged across a fixed resistance of 0.75 ohm. Constant current charging was balanced so the input was equal to the output. Cycling was on a 2-hour discharge/4-hour charge schedule.

---

* See pages 3 and 4 for a description of this Union Carbide "fixed-zone" oxygen electrode which is designated here as the T-2 electrode.

d) Performance of a Unit Cell at 25°C Employing a Thin "Fixed-Zone" Oxygen Electrode with a 10-Amp-Hour Zinc Gel-Type Anode Discharged to 2.5-3.0 Amp-Hours Output

The continually declining discharge voltage level of the cell described in Figure 24 was the result of anode slump due to shape change. Testing was terminated when the end-of-discharge voltage reached 0.8 volt, which value was associated with 70-80% anode slump in practically every cell repeatedly discharged to 25-30% depth in 2 hours. Fifty to sixty cycles were generally delivered by cells repeatedly discharged to this depth in 2 hours. However, 108 cycles were delivered by the cell shown in Figure 24.

e) Performance of a Unit Cell at 40°C Employing a Thin "Fixed-Zone" Oxygen Electrode with a 10-Amp-Hour Zinc Gel-Type Anode

Figure 25 shows the 1st, 12th, 24th, 36th, 48th, and 56th cycles of a cell discharged across a fixed resistance of 0.75 ohm at a current density of 22 mA/cm^2 to 26% depth. Cycling was on a 2-hour discharge/4-hour charge schedule. This cell employed a 10 ampere-hour anode and was susceptible to the same problem of anode slump as the cell cycled at 25°C.

f) Performance of a Unit Cell at 0°C Employing a Thin "Fixed-Zone" Oxygen Electrode with a 10-Amp-Hour Zinc Gel-Type Anode

Figure 26 shows the 1st, 12th, 24th, 36th, 48th, and 56th cycles of a cell cycled at 0°C on a 2-hour discharge/4-hour charge schedule. Discharges were across a fixed resistance of 0.75 ohm. The discharge current density was approximately 21 mA/cm^2. The same anode problem limited the life of this cell.

g) Performance of a Unit Cell at 25°C Employing a Single Layer of PERMION 110 Before, During and After Complete Discharge of a 10-Amp-Hour Zinc Gel-Type Anode

Figure 27 shows the discharge performance of a cell that was cycled on a 2-hour discharge/4-hour charge schedule. The first two discharges were followed by charges. The zinc was not recharged following discharges 3 through 12. The cell was on open circuit during the 4-hour periods scheduled for charge. At the end of the 12th discharge the zinc was charged so that the theoretical ampere-hour input was 9.6 ampere-hours. The charged current was 800 mA; this is equivalent to a current density of 14 mA/cm^2 or the normal charge current for a 4-hour charge of this cell on a 2-hour discharge/4-hour charge schedule. The cell was returned to the original cycle with no change in discharge performance.

h) Performance of Unit Cells at 25°C " Employing Thin "Fixed-Zone" Oxygen Electrodes with 15 and 20 Amp-Hour Zinc Gel-Type Anodes

Over 350 cycles were delivered by a unit cell that was discharged to 1.2-1.4 ampere-hours output (12-14% zinc depth) in 2 hours. The discharge current density was 11-12 mA/cm^2. Discharges were across a fixed resistance of 1.75 ohms.

The unit cells that were modified to improve the high-rate discharge capability are capable of discharges at double the current density (22-25 mA/cm^2) with good voltage regulation. However, repeated 2-hour discharges across a fixed resistance of 0.75 ohm to 2.5-3.0 ampere-hours output (equivalent to 25-30% zinc depth on a 10 ampere-hour anode) drastically reduced cycle life. Anode slump of 70-80% as was explained above was the

cause of failure after 50-60 cycles. The fact that cycle life was so drastically reduced when identical anode structures were discharged to 2.5-3.0 ampere-hours output (25-30% zinc depth), suggested the possibility of minimizing anode shape change, and extending cycle life by employing anodes of such capacity that a 2.5-3.0 ampere-hour output was to a depth comparable to that of the 350 cycle cell.

Two cells, one with a 15 ampere-hour anode, and one with a 20 ampere-hour anode were cycled. The charge-discharge current densities and the cycling schedule was identical to that of the 10-ampere-hour cells from which only 50-60 cycles were delivered. However, discharges across a fixed resistance of 0.75 ohm to 2.5-3.0 ampere-hours output were equivalent to 13% and 17% zinc depth, respectively, on a 20-ampere-hour and a 15-ampere-hour anode, compared to 25-30% depth on the 10-ampere-hour anodes. One hundred and seventy-six cycles with good voltage regulation were delivered from both the 20 ampere-hour and the 15 ampere-hour cell. A threefold extension of cycle life was realized from a 50% increase in zinc capacity. These data are shown in Figures 28 through 30.

i) Performance of Unit Cells at 0° and 40°C Employing Thin "Fixed-Zone" Oxygen Electrodes and 15-Amp-Hour Zinc Gel-Type Anodes

Cycle life of 100 and 120 was obtained from these cells at 0°and 40°C, respectively. Performance data are plotted in Figures 31 and 32.

j) Performance of Unit Cells at 25°C Employing American Cyanamid "LAB 40" Oxygen Electrodes

The feasibility of using American Cyanamid "LAB 40" oxygen electrodes for recharging was demonstrated. However, apparent deterioration

of the active layer and flooding of this electrode limited cycle life. Migration and deposition of noble metal upon the zinc electrode thereby forming a serious gassing couple was another problem. X-ray fluorescence examination of zinc electrodes removed from spent cells employing the "LAB 40" electrode substantiated the presence of noble metals. The problems associated with the use of the "LAB 40" oxygen electrode seem to be less severe when the electrode was not used for charging the zinc, i. e., when a separate charging electrode was used for charging. However, under all conditions of open cell operation in which cells employing "LAB 40" oxygen electrodes were tested, the ultimate cause of failure was associated with the oxygen electrode.

Cycling of cells employing "LAB 40" oxygen electrodes was carried out on schedules of 2-hour discharge/4-hour charge, 2-hour discharge/22-hour charge, and 24-hour discharge/24-hour charge. One or more of the aforementioned problems associated with the use of this electrode was the cause of failure of every cell tested. The problems were not eliminated when the electrodes were only subjected to very low current density 22-hour charging, nor were they eliminated when the electrodes were only subjected to very low current density 24-hour discharge/24-hour charge cycling.

Generally, failure associated with the use of the "LAB 40" oxygen electrode occurred very early in the life of the cell. However, 52 cycles were delivered from one cell before failure due to cathode polarization occurred. Another cell delivered 36 cycles before failure due to electrolyte flooding of the electrode was observed. In contrast, 129 cycles were delivered from a cell built with a separate charging electrode for charging the zinc after the first 31 cycles.

Figure 33 shows 52 cycles delivered by a unit cell employing a "LAB 40" oxygen electrode and a 20 ampere-hour zinc gel-type anode. Failure was due to cathode polarization.

Figure 34 shows 36 cycles delivered by a unit cell employing a "LAB 40" oxygen electrode. Failure was due to cathode flooding.

Figure 35 shows 129 cycles delivered by a unit cell employing a "LAB 40" oxygen electrode and a separate charging electrode. The cell was charged over the first 31 cycles against the "LAB 40" oxygen electrode.

k) Comparison of the Polarization Characteristics of the Thin "Fixed-Zone" Oxygen Electrode with that of the American Cyanamid "LAB-40" Oxygen Electrode

Figure 36 shows a comparison of the polarization characteristics of the Union Carbide thin "fixed-zone" oxygen electrode and the American Cyanamid "LAB-40" oxygen electrode as cycling progressed.

Performance of the Union Carbide thin "fixed-zone" electrode actually improved over 56 cycles whereas the "LAB-40" electrode started to polarize badly after 36 cycles. The improvement seen in the performance of the Union Carbide thin "fixed-zone" electrode was due to improved wetting of the electrode active layer as cycling progressed. Although the voltage of the "LAB-40" oxygen electrode versus a zinc reference electrode was higher than that of a "fixed-zone" electrode on a fresh cell, the "LAB-40" electrode flooded and suffered apparent degradation of its activity as cycling progressed. The "LAB-40" electrode was used to recharge the zinc. The zinc electrode in the cell employing a thin "fixed-zone" oxygen electrode was charged by a separate charging electrode.

2. Anodes Fabricated from Zinc Oxide Formulations

An investigation of anode structures other than zinc gel-type anodes undertaken in an effort to determine if additional cycle life and deeper discharge were possible. The work was aimed toward extending cycle life by minimizing shape change of the anodes when subjected to repeated deep discharging and higher discharge current densities. This investigation involved the testing of anode plates fabricated from zinc oxide formulations. The formulations were designated ZnO#1, ZnO#10 and ZnO#19*.

In addition, cells employing anode plates fabricated from the formulation designated ZnO#19 were made with 0. 15-inch edge overlap (negative plate larger than positive plate) to investigate the effect of this concept on minimizing edge effect and subsequent shape change. This concept was suggested in the literature by McBreen et al(18) who reported that preferential plating toward the higher zincate center of the anode face resulted in a thicker more dense mass toward the center and depletion at the edges. Based on these findings, they suggested that the negative plate be made slightly larger than the positive plate.

Performance of zinc oxygen experimental unit cells employing anodes fabricated from zinc oxide formulations was as follows:

a) Formation Cycling of Unit Cells Employing Anodes Fabricated from Zinc Oxide Formulations

Cells employing anodes fabricated from zinc oxide formulations were assembled while the anodes were in the discharged state. Formation cycling was required before cell operation. The objective of formation cycling was to ensure the availability of the desired ampere-hour equivalents of actual zinc (100% availability as ampere-hour output).

*See p. 6 for description of ZnO #1 and ZnO #19. ZnO #10 consists of 43g ZnO, 1. 5g asbestos fibers, 21. 5g Cu powder, 21..5g Zn powder, 3. 4g Hg, and 9. 1g 0. 1N KOH. The resulting amalgamated copper serves as a matrix collector for the zinc electrode.

This was accomplished by subjecting the unit cells employing these anodes to three formation cycles before cell operation. Typically, the anodes fabricated from the formulation designated ZnO#19 were cycled to ensure a 10-ampere-hour output by subjecting them to three cycles consisting of 72 hours charge at 210 mA, followed by discharging at 400 mA constant current to 0.30 volt. Figure 37 shows the result of formation cycling of a ZnO#19 anode.

b) Performance of a Unit Cell at 25°C Employing a Thin "Fixed-Zone" Oxygen Electrode and a 5 Amp-Hour ZnO#1 Anode Cycled on a 2-Hour Discharge/2-Hour Charge Schedule

A cell employing an anode fabricated from the zinc oxide formulation designated ZnO#1 was formation cycled to provide 5 ampere-hours zinc capacity. Cycling was carried out on a 2-hour discharge/2-hour charge schedule. Discharges were across a fixed resistance of 0.750 ohm. The discharge current density was 24 mA/cm^2. The charge current density was 30 mA/cm^2. Total output per discharge was 2.75 ampere-hour (55% zinc depth). The required 3.0 ampere-hour input was equivalent to 8.7% overcharge. Figure 38 shows 100 cycles to 0.8 volt delivered from such a cell.

c) Performance of a Unit Cell at 25°C Employing a Thin "Fixed-Zone" Oxygen Electrode and a 5 Amp-Hour ZnO#1 Anode Cycled on a 2-Hour Discharge/4-Hour Charge Schedule

Electroformation of zinc was to the 5 ampere-hour level. Cycling was on a 2-hour discharge/4-hour charge schedule. The discharge current density was 26 mA/cm^2 to a 3.0 ampere-hour output. Discharges were to 60% zinc depth. The charge current density was 15.6 mA/cm^2 to

a 3.25 ampere-hour input. The 3.25 ampere-hour input was equivalent to 8.2% overcharge. Both charging and discharging was done with constant current. Figure 39 shows 144 cycles delivered from such a cell.

d) Performance of a Unit Cell at 25°C Employing a Thin "Fixed-Zone" Oxygen Electrode and a 5 Amp-Hour ZnO#10 Anode

This ZnO#10 anode was formation cycled to 5.0 ampere-hours capacity. Routine cycling was on a 2-hour discharge-4-hour charge schedule. Cycling current density, output per discharge, and input per charge were identical to that of the 5 ampere-hour ZnO#1 anode described above. Figure 40 shows 120 cycles to 0.8 volt delivered from such a cell

e) Performance of a Unit Cell at 25°C Employing Thin "Fixed-Zone" Oxygen Electrode and ZnO#19 Anodes

Anodes fabricated from the zinc oxide formulation ZnO#19 were formation cycled to ensure an input of 10 ampere-hours zinc capacity (the capacity of zinc gel-type anodes). Routine cycling was carried out on schedules of 2-hour discharge/2-hour charge, 2-hour discharge/4-hour charge, 2-hour discharge/22-hour charge, and 24-hour discharge/24-hour charge. Both discharging and charging was constant current. Discharge current densities were 27 mA/cm^2 and 6.45 mA/cm^2 for 2-hour discharges and 24-hour discharges, respectively. The charge current densities were 30 mA/cm^2 during a 2-hour charge, 15 mA/cm^2 during a 4-hour charge, and 2.75 mA/cm^2 for a 22-hour charge of cells discharged for 2 hour to a 2.6 amp-hour output (26% zinc depth). The charge current density was 8.5 mA/cm^2 for 24 hours for cells discharged for 24 hours to a 7.5 ampere-hour output (75% zinc depth). Figures 41 to 44 show these data.

f) Performance of Unit Cells at 40°C Employing Thin "Fixed-Zone" Oxygen Electrodes and ZnO#19 Anodes

Cycling at 40°C of unit cells employing ZnO#19 anodes was identical (cycling current density, output, input, etc.) to 25°C cycling. Figure 45 shows 40°C performance of a cell cycled on a 2-hour discharge/2-hour charge schedule. Figure 46 shows 40°C performance of a cell cycled on a 2-hour discharge/4-hour charge schedule. Figure 47 shows 40°C performance of a cell cycled on a 2-hour discharge/22-hour charge schedule. Figure 48 shows 40°C performance of a cell cycled on a 24-hour discharge/24-hour charge schedule.

g) Performance of Unit Cells at 0°C Employing Thin "Fixed-Zone" Oxygen Electrodes and ZnO#19 Anodes

The operating parameters (cycling current density, output, etc.) were identical to those of the 25°C cycling tests. Figure 49 indicates the 0°C performance of a cell cycled on a 2-hour discharge/2-hour charge schedule. Figure 50 shows 0°C performance of a cell cycled on a 2-hour discharge/4-hour charge schedule. Figure 51 gives 0°C performance of a cell cycled on a 2-hour discharge-22-hour charge schedule. Figure 52 shows 0°C performance of a cell cycled on a 24-hour discharge/24-hour charge schedule.

h) Performance of a Unit Cell at 25°C Employing a Thin "Fixed-Zone" Oxygen Electrode and a ZnO#19 Anode Charged by Asymmetrical A-C Method of Charge

Cycling of a unit cell at 25°C to determine the effect of asymmetrical alternating current on recharging the anode was carried out on a 2-hour discharge/2-hour charge schedule. Charging was against a separate charging electrode.

The peak charging current density was approximately 112 mA/cm^2. The average current density was 69 mA/cm^2. Since the cycle efficiency was 40% as a result of a 10% reverse (deplating) component, the net charge current density was approximately 27.5 mA/cm^2. The discharge current density was 27 mA/cm^2. Discharges were at 1.3 amperes with constant current. The mode of failure after 134 cycles was due to a break in the seal around the oxygen electrode. Approximately 25% slump had occurred by this time as compared to failures due to 50-60% slump of anodes in cells charged by conventional 2-hour constant current charging. Figure 53 shows the 25° C performance of a cell charged by asymmetrical alternating current.

j) Performance of Unit Cells at 25° C Employing Thin "Fixed-Zone" Oxygen Electrodes and ZnO #19 Anodes charged by Periodic Reverse and Periodic Open Circuit Methods of Charge

Figure 54 presents the performance of a cell charged by the periodic reverse method of charge. The periodic reverse cycle was 60 seconds with a plating time of 54 seconds and a deplating time of 6 seconds. The current density during both plating and deplating was 4.7 mA/cm^2. Cycling was carried out on a 2-hour discharge/22-hour charge schedule. Discharging was constant current at a current density of 27 mA/cm^2.

Figure 55 plots the performance of two cells charged by periodic open circuit methods. The periodic open circuit cycle on one of the cells was 22.5 seconds with a plating or charge time of 7.5 seconds and an open

circuit time of 15 seconds. The plating current density was 33 mA/cm^2. The periodic open circuit cycle on the other cell was 28 seconds with a charge time of 7 seconds and an open circuit time of 21 seconds. The plating current density was 17.7 mA/cm^2.

k) Comparison of a Typical 2-Hour Discharge at 25°C Following a 2-Hour Asymmetrical A-C Charging with a 2-Hour Discharge Following 2-Hour Constant Current Charging

Figure 56 shows a comparison of typical 2-hour discharge performance of a cell following 2-hour asymmetrical alternating current charging with that of a cell charged with constant current for 2 hours. Both cells were discharged at a current density of 27 mA/cm^2.

l) Comparison of a Typical 2-Hour Discharge at 25°C Following 22-Hour Periodic Reverse Charging with a 2-Hour Discharge Following 22-Hour Constant Current Charging

Figure 57 presents a comparison of typical 2-hour discharge performance of a cell following 22-hour periodic reverse charging with that of a cell charged with constant current for 22 hours. Both cells were discharged at a current density of 27 mA/cm^2.

m) Summary of Cycle Life of Zinc-Oxygen Rechargeable Experimental Unit Cells Employing Union Carbide's Proprietary Zinc Gel-Type Anodes and their Thin "Fixed-Zone" Oxygen Electrodes

Table VIII summarizes the cycle life obtained from experimental unit cells employing Union Carbide's proprietary zinc gel-type anodes and thin "fixed-zone" oxygen electrodes.

n) Summary of Cycle Life of Zinc-Oxygen Rechargeable Experimental Unit Cells Employing Union Carbide's Thin "Fixed-Zone" Oxygen Electrodes and Anodes Fabricated from Zinc Oxide Formulations

Table IX summarizes cycle life obtained from experimental unit cells employing anodes fabricated from zinc oxide mixtures and thin "fixed-zone" oxygen electrodes.

FIGURE 11

0°C DISCHARGE-CHARGE PERFORMANCE OF A UNIT CELL EMPLOYING A THIN "FIXED-ZONE" OXYGEN ELECTRODE, 10 AMPERE-HOUR ZINC GEL TYPE ANODE AND A DOUBLE LAYER OF C-3 SEPARATOR

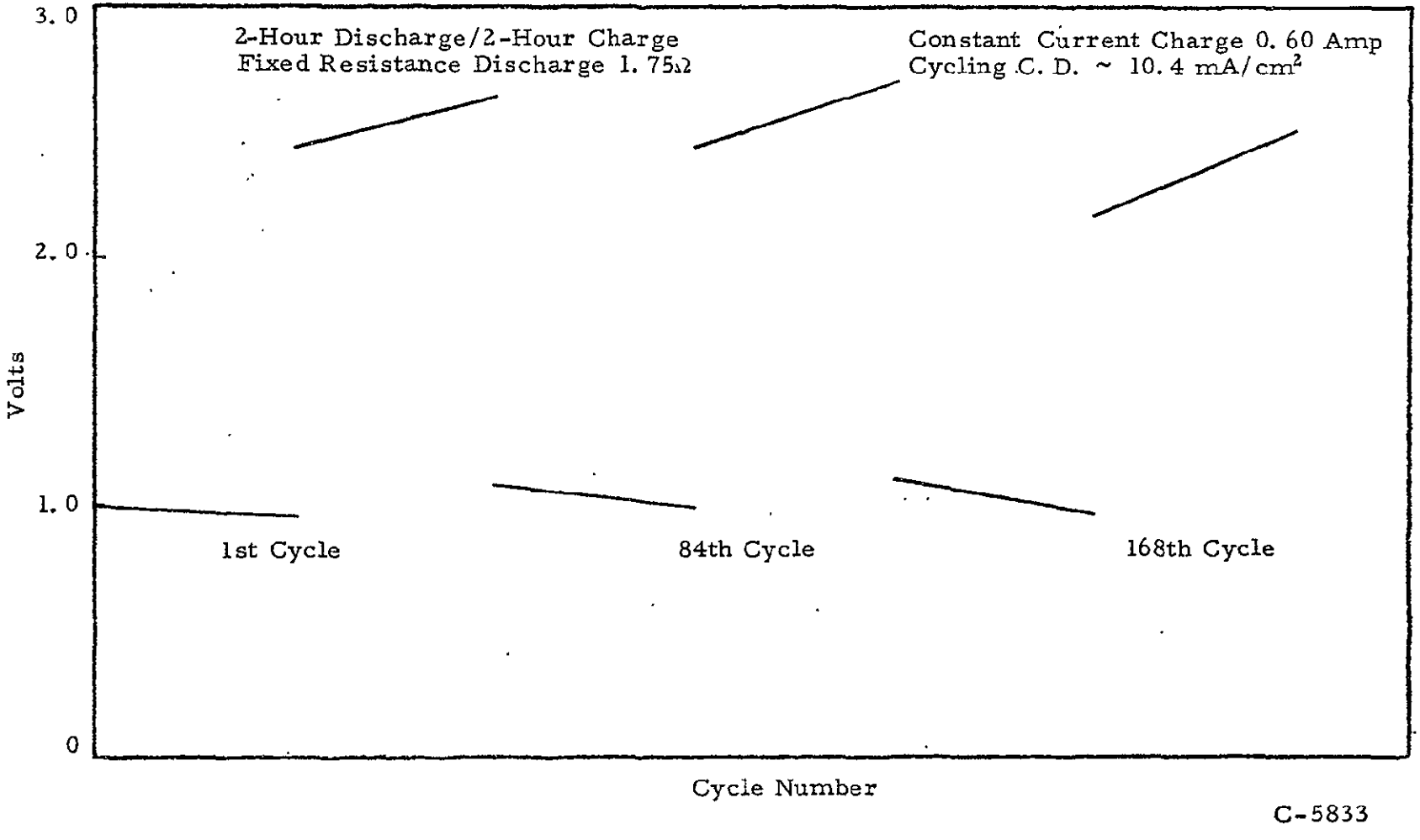

FIGURE 12

DISCHARGE OF RECHARGEABLE UNIT CELL MADE WITH BORDEN C-3 SEPARATOR FOR 168 CYCLES

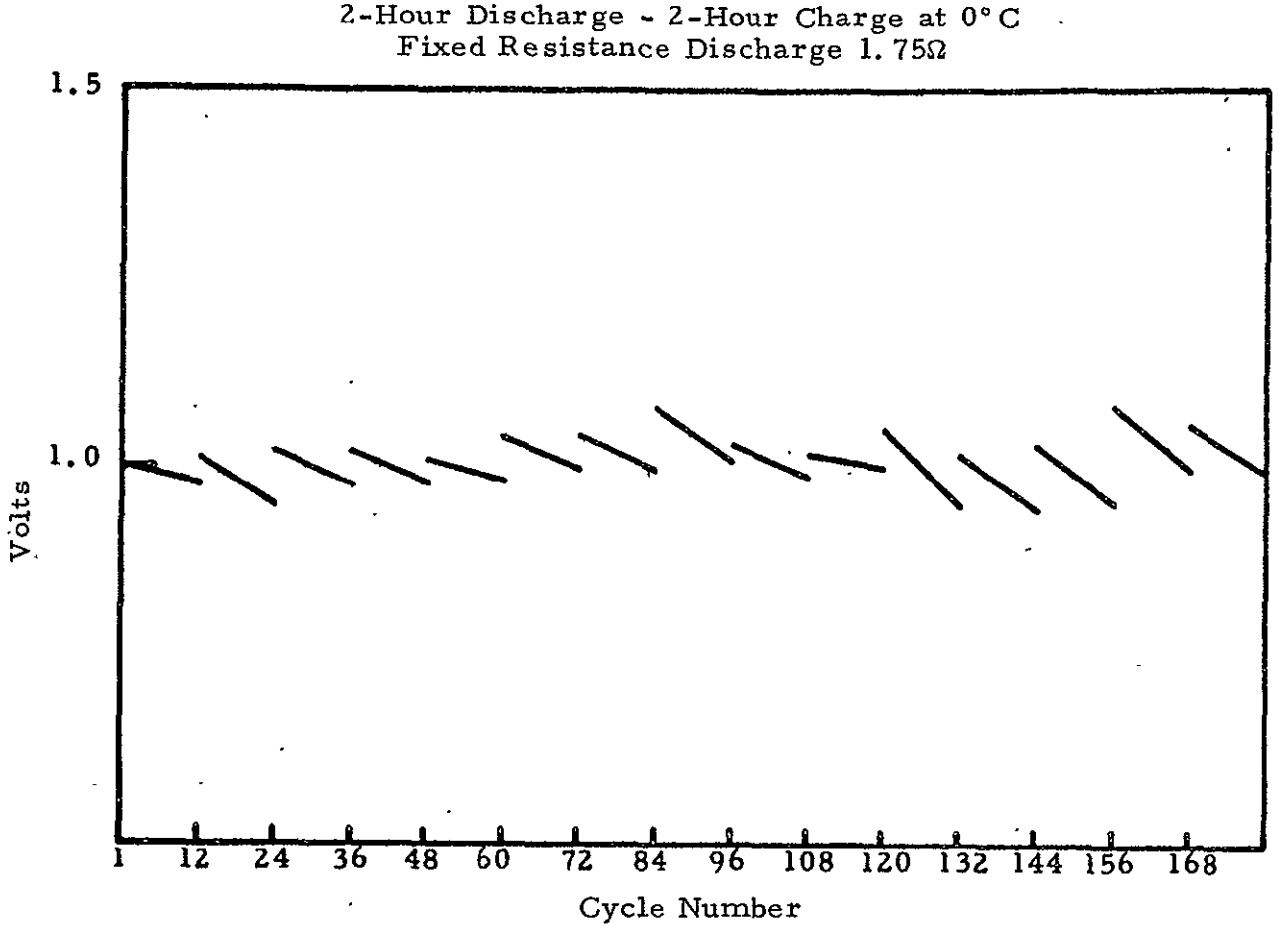

C-4150

FIGURE 13

25°C DISCHARGE-CHARGE PERFORMANCE OF A UNIT CELL EMPLOYING A THIN "FIXED-ZONE" OXYGEN ELECTRODE, 10 AMPERE-HOUR ZINC GEL TYPE ANODE AND A DOUBLE LAYER OF BORDEN C-3 SEPARATOR - 1ST, 178TH, AND 354TH CYCLES ARE SHOWN

2-Hour Discharge/2-Hour Charge at 25°C
Fixed Resistance Discharge 1.75 Ω
Constant Current Charge 0.65 Amperes
Cycling C.D. ~ 11.8 ma/cm²

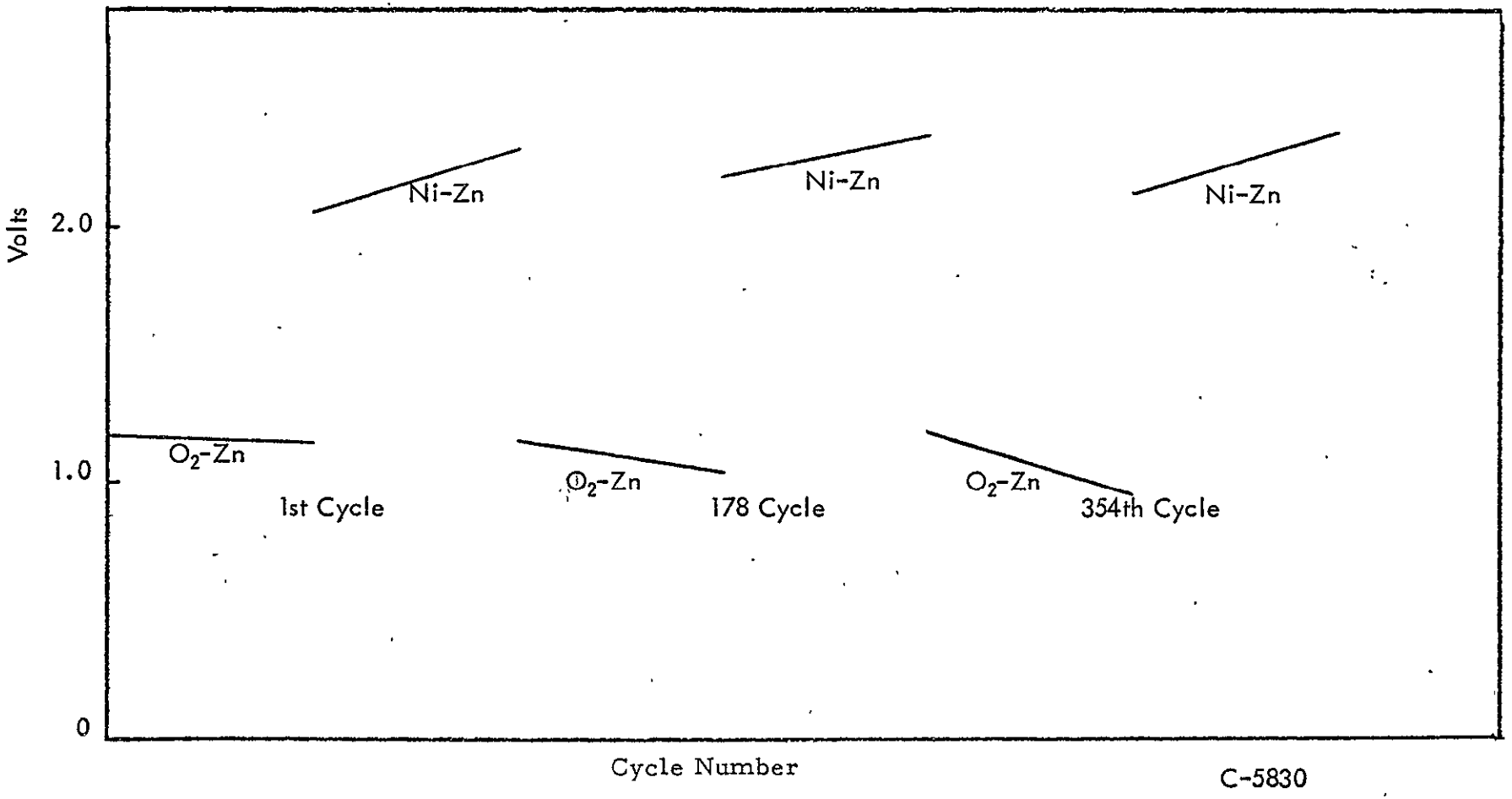

FIGURE 14

DISCHARGE OF RECHARGEABLE ZINC-OXYGEN UNIT CELL MADE WITH BORDEN C-3 SEPARATOR FOR 356 CYCLES

2-Hour Discharge - 2-Hour Charge at 25°C
Fixed Resistance Discharge 1.75Ω
Average Zn Discharge Depth 13%

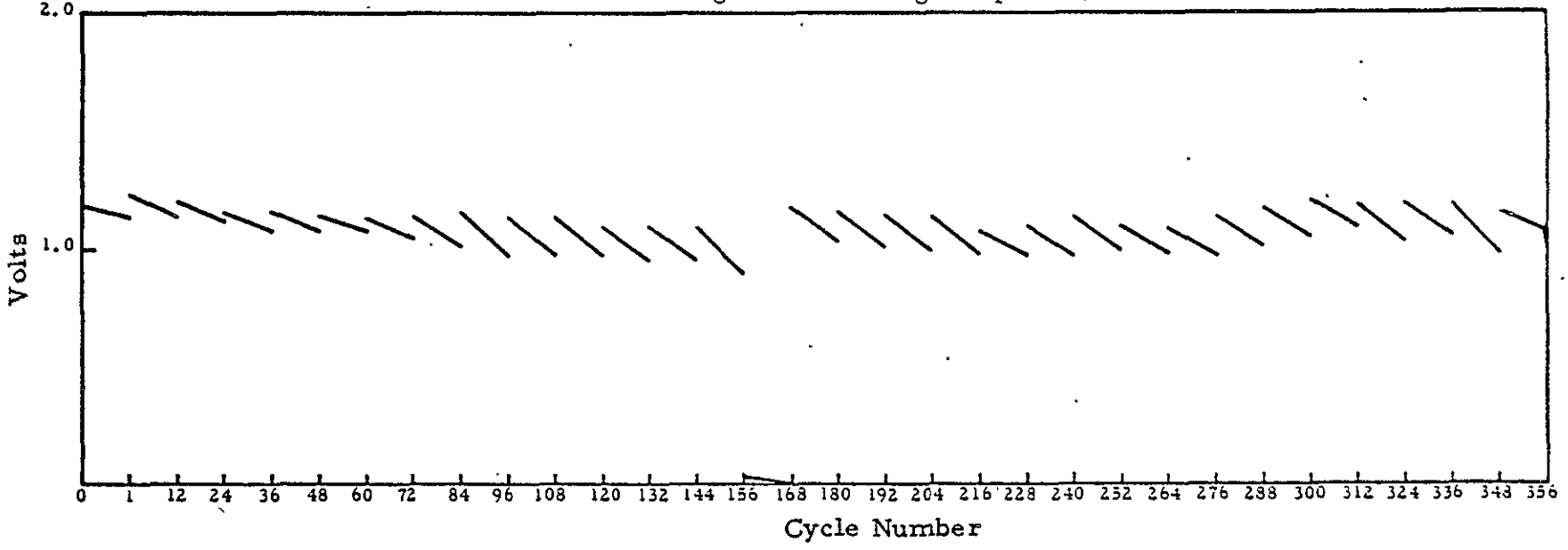

C-4151

FIGURE 15

40°C DISCHARGE-CHARGE PERFORMANCE OF A UNIT CELL EMPLOYING BORDEN C-3 SEPARATOR AND A 10 AMPERE-HOUR ZINC GEL TYPE ANODE

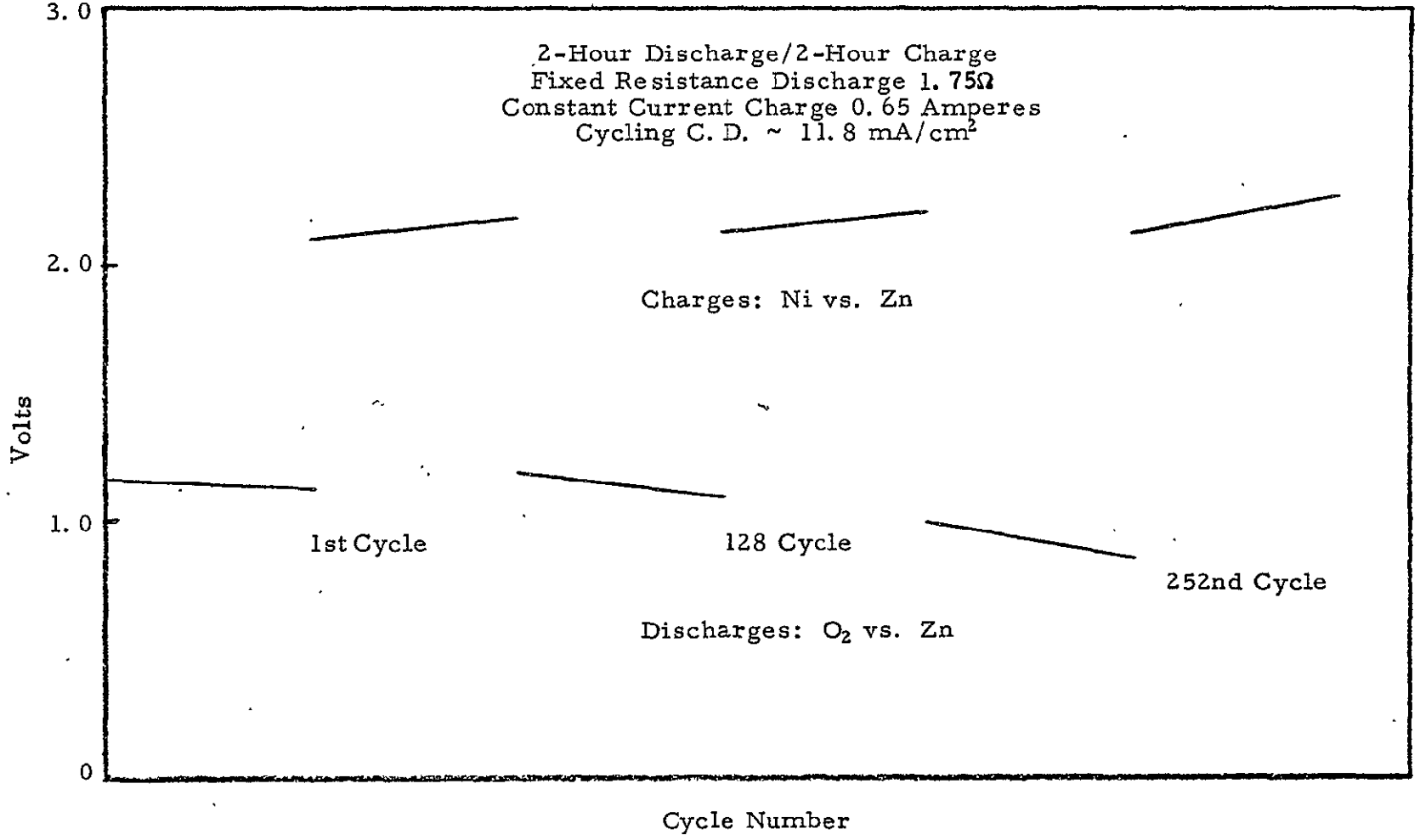

C-5832

FIGURE 16

DISCHARGE OF RECHARGEABLE UNIT CELL MADE WITH BORDEN SEPARATOR FOR 256 CYCLES

2 Hour Discharge - 2 Hour Charge at 40°C
Fixed Resistance Discharge 1.75 Ω

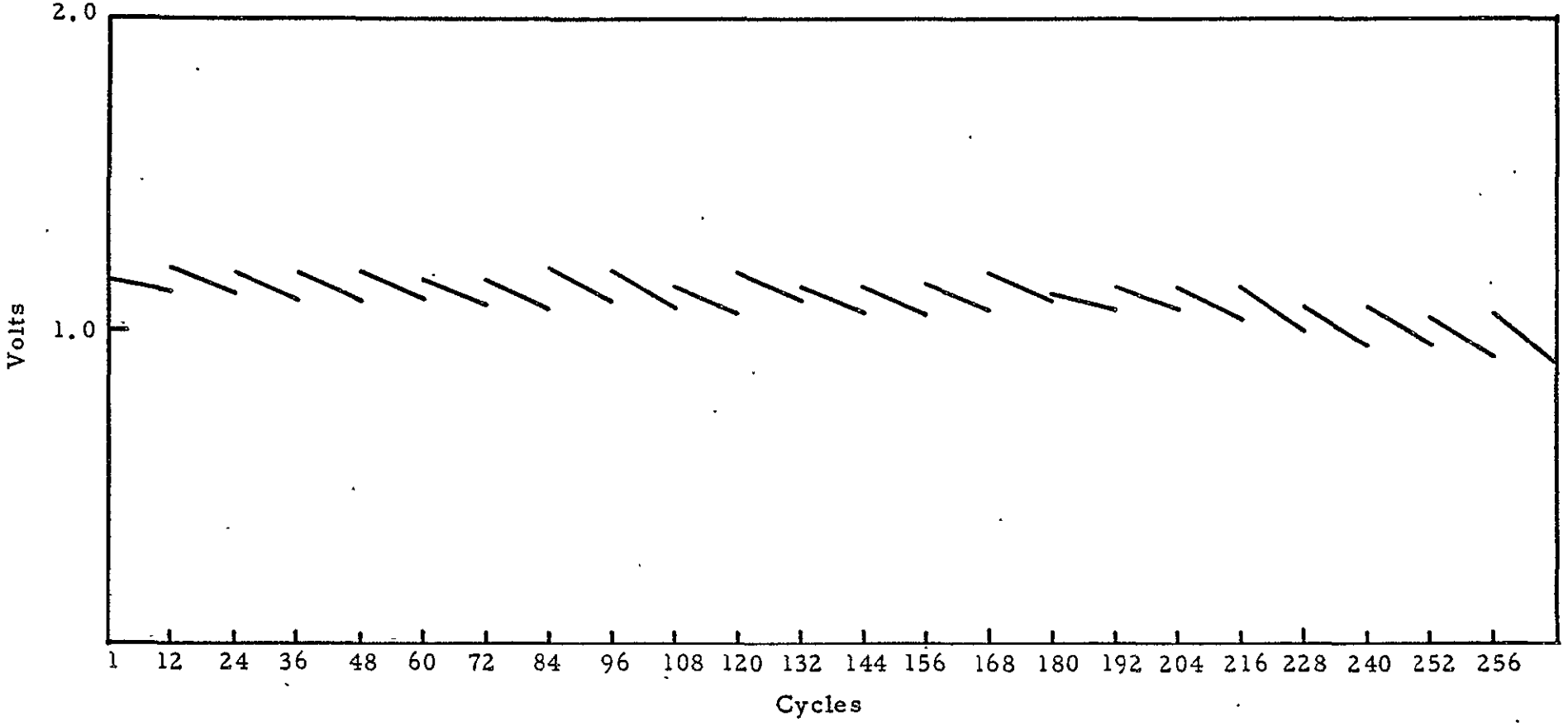

C-4152

FIGURE 17

RECHARGEABILITY AFTER COMPLETE DISCHARGE OF ZINC
IN UNIT CELL SHOWN IN FIGURE 2

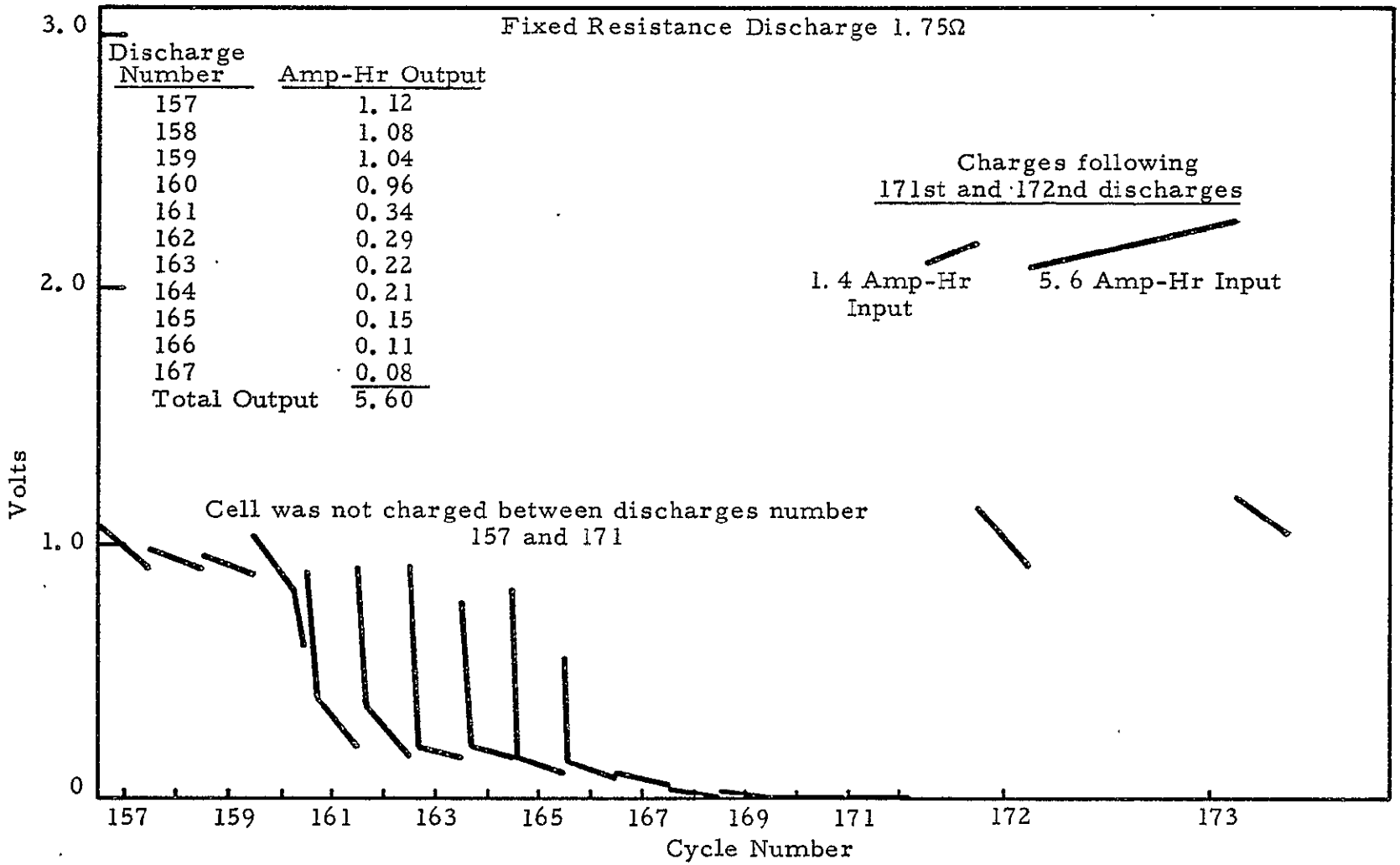

C-3884

FIGURE 18

1ST, 6TH, 12TH CYCLE OF ZINC-OXYGEN UNIT CELL CONTAINING A DOUBLE LAYER OF C-3 SEPARATOR

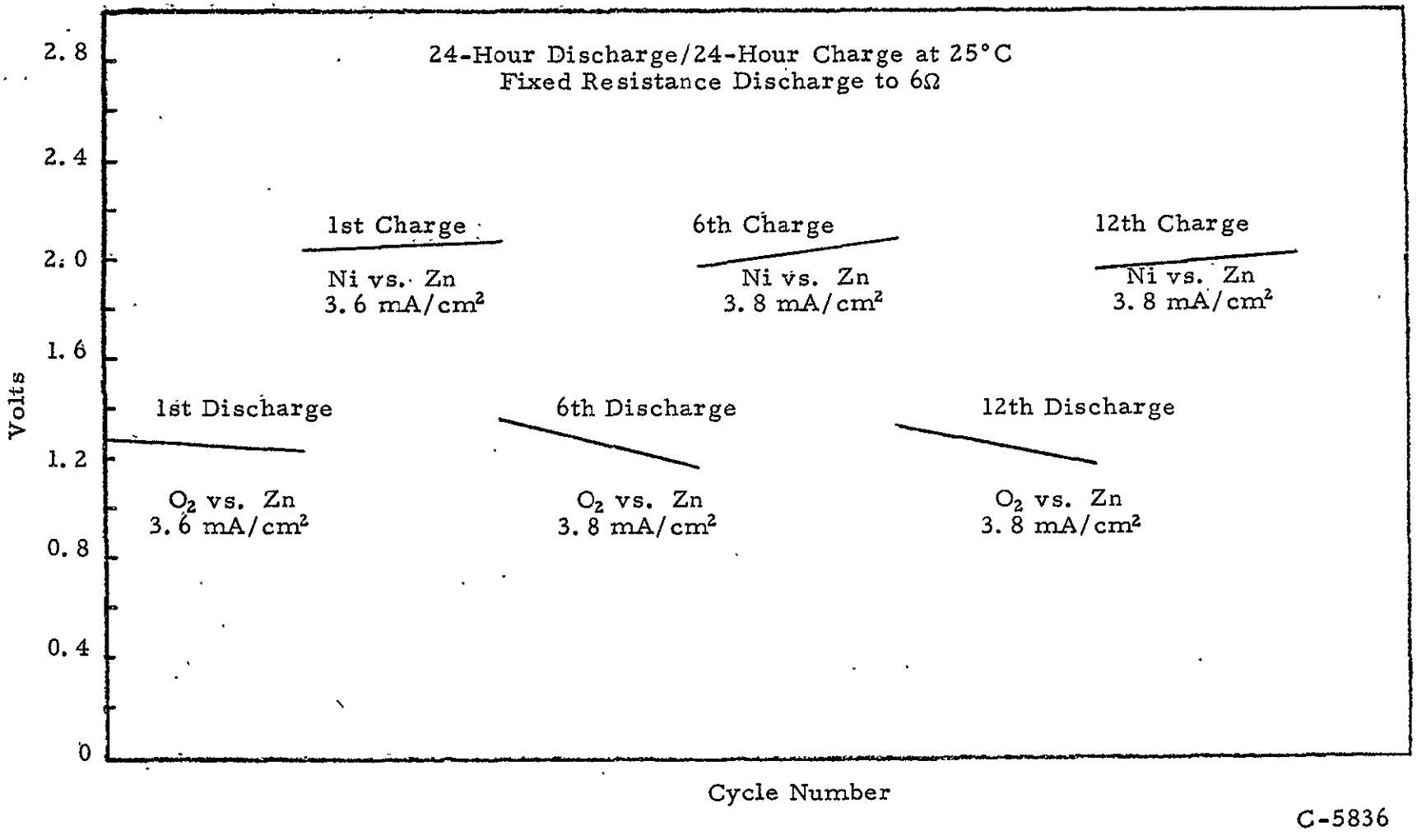

C-5836

FIGURE 19

18th, 24th, and 30th CYCLE OF ZINC-OXYGEN UNIT CELL CONTAINING A DOUBLE LAYER OF C-3 SEPARATOR

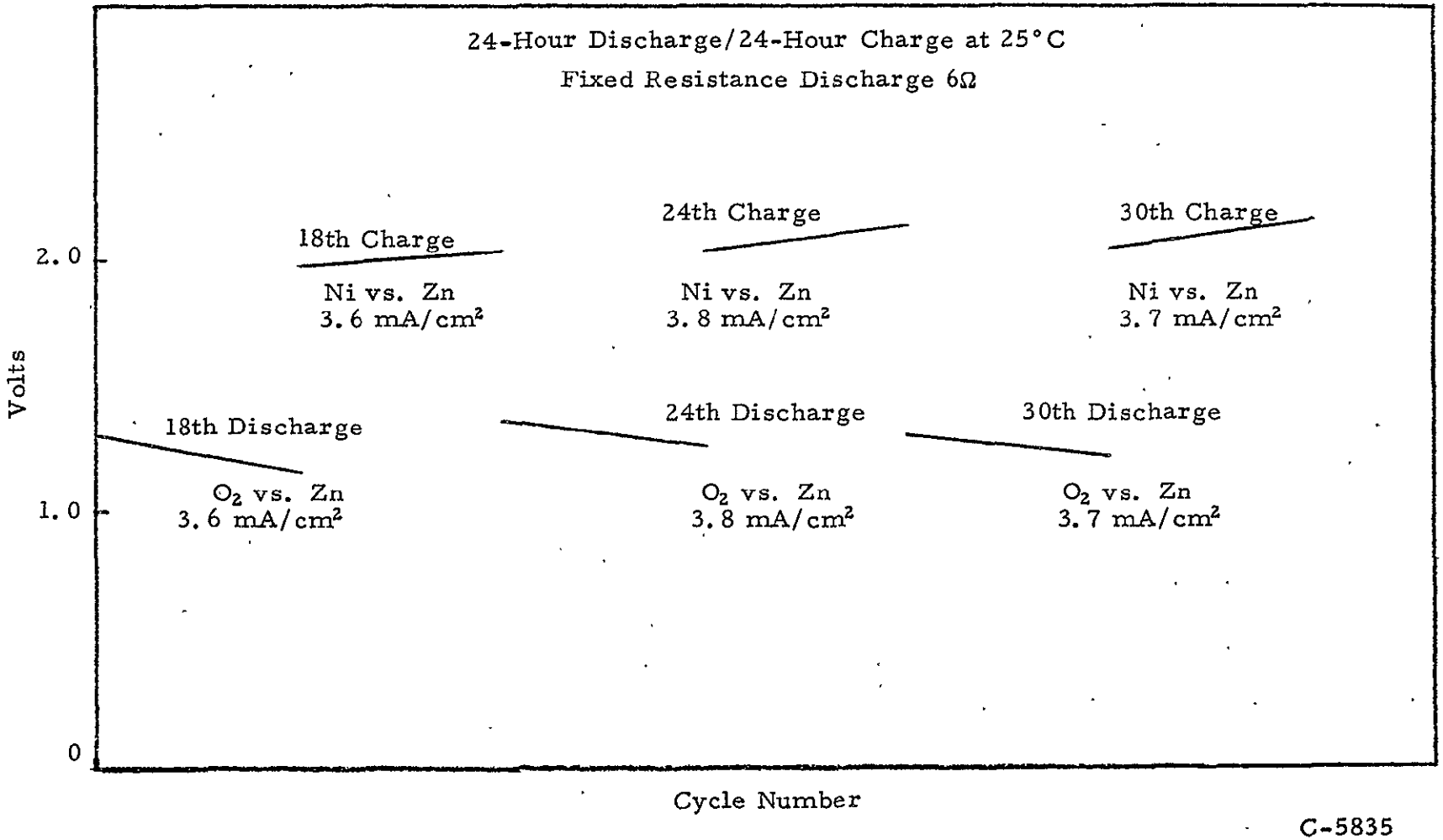

FIGURE 20

DISCHARGE OF RECHARGEABLE UNIT CELL AT 25°C CONTAINING A DOUBLE-LAYER OF PERMION 110 SEPARATOR

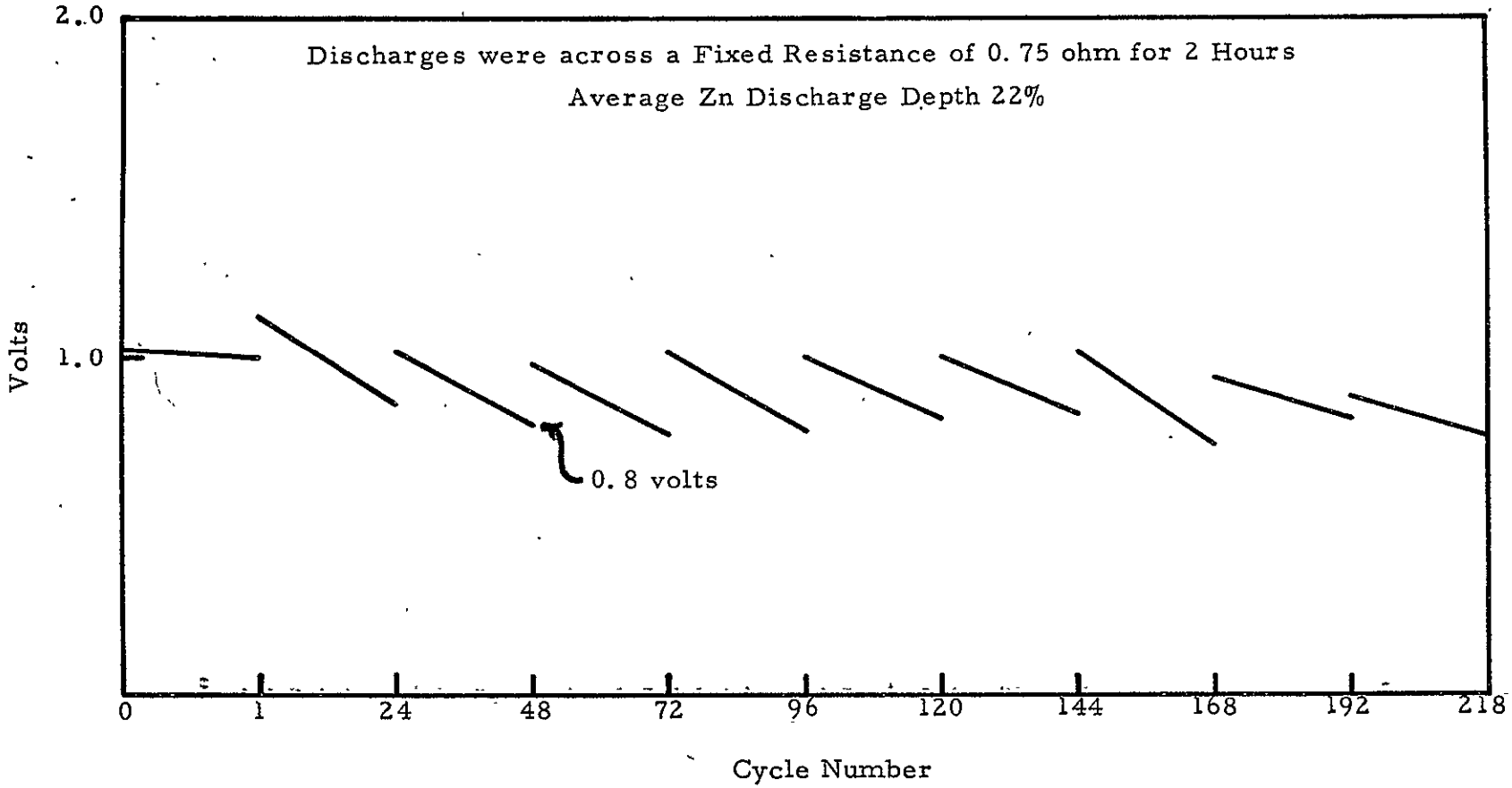

C-4153

FIGURE 21

25° C DISCHARGE OF RECHARGEABLE UNIT CELL CONTAINING A DOUBLE LAYER OF PERMION 116 SEPARATOR

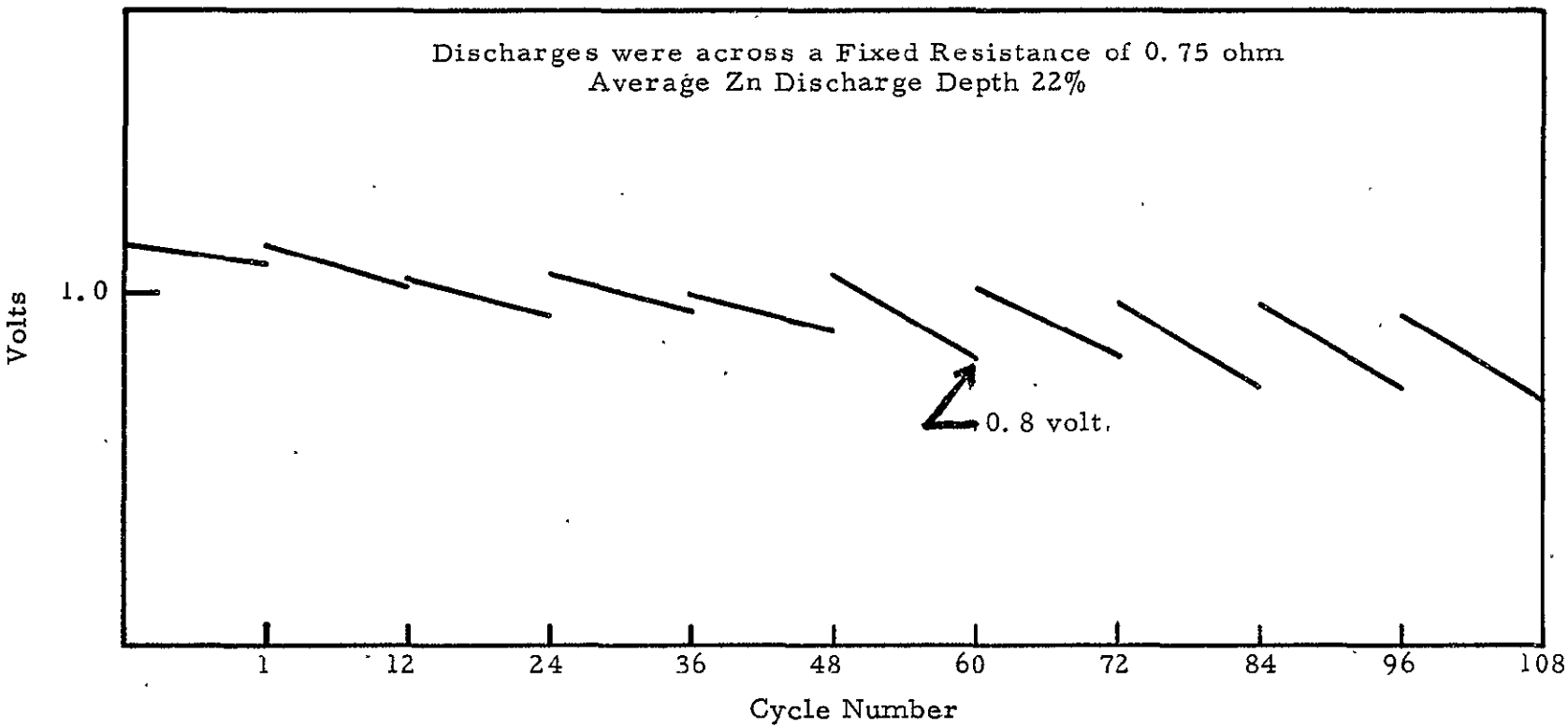

C-4154

FIGURE 22

PERFORMANCE OF RECHARGEABLE UNIT CELL AT 25°C CONTAINING A SINGLE
A SINGLE LAYER OF PERMION 110

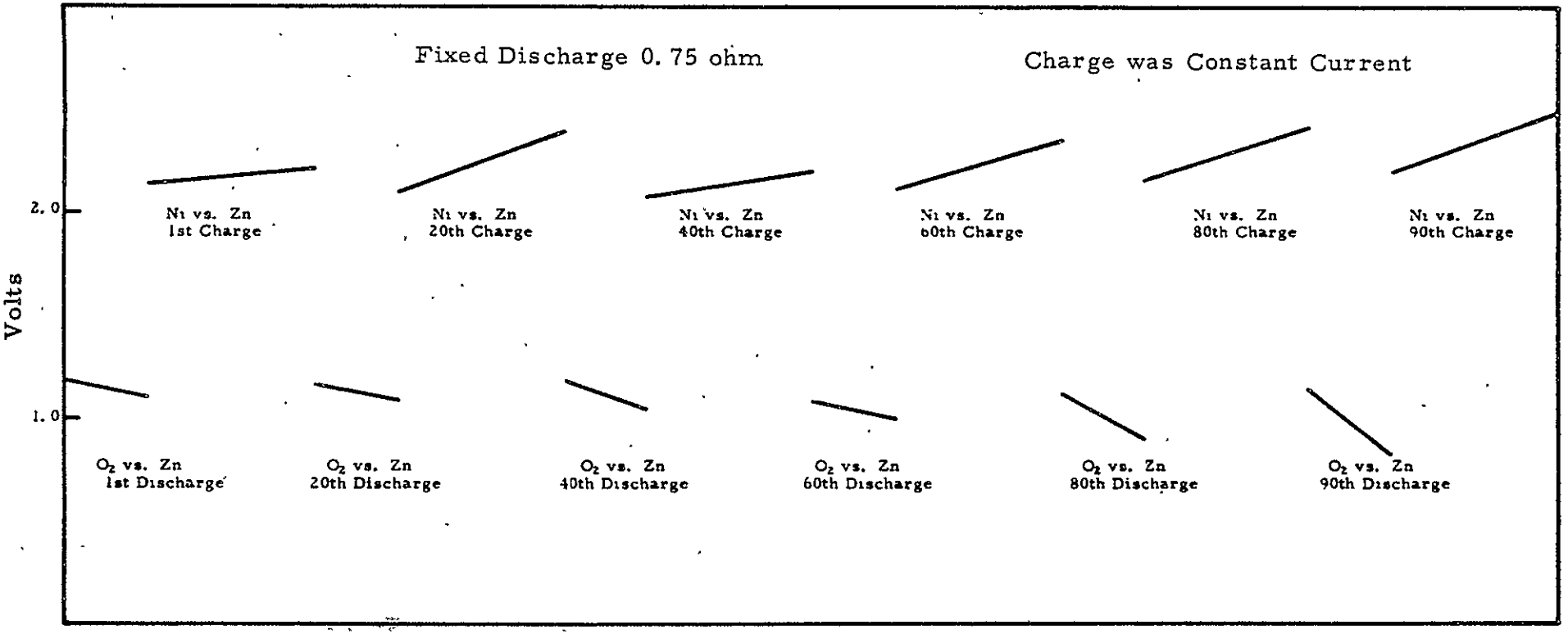

C-4155

FIGURE 23

TYPICAL CYCLE AT 25°C OF CELLS INCORPORATING DESIGN MODIFICATIONS AIMED AT IMPROVING THE HIGH-RATE CAPABILITY OF THE UNIT CELL

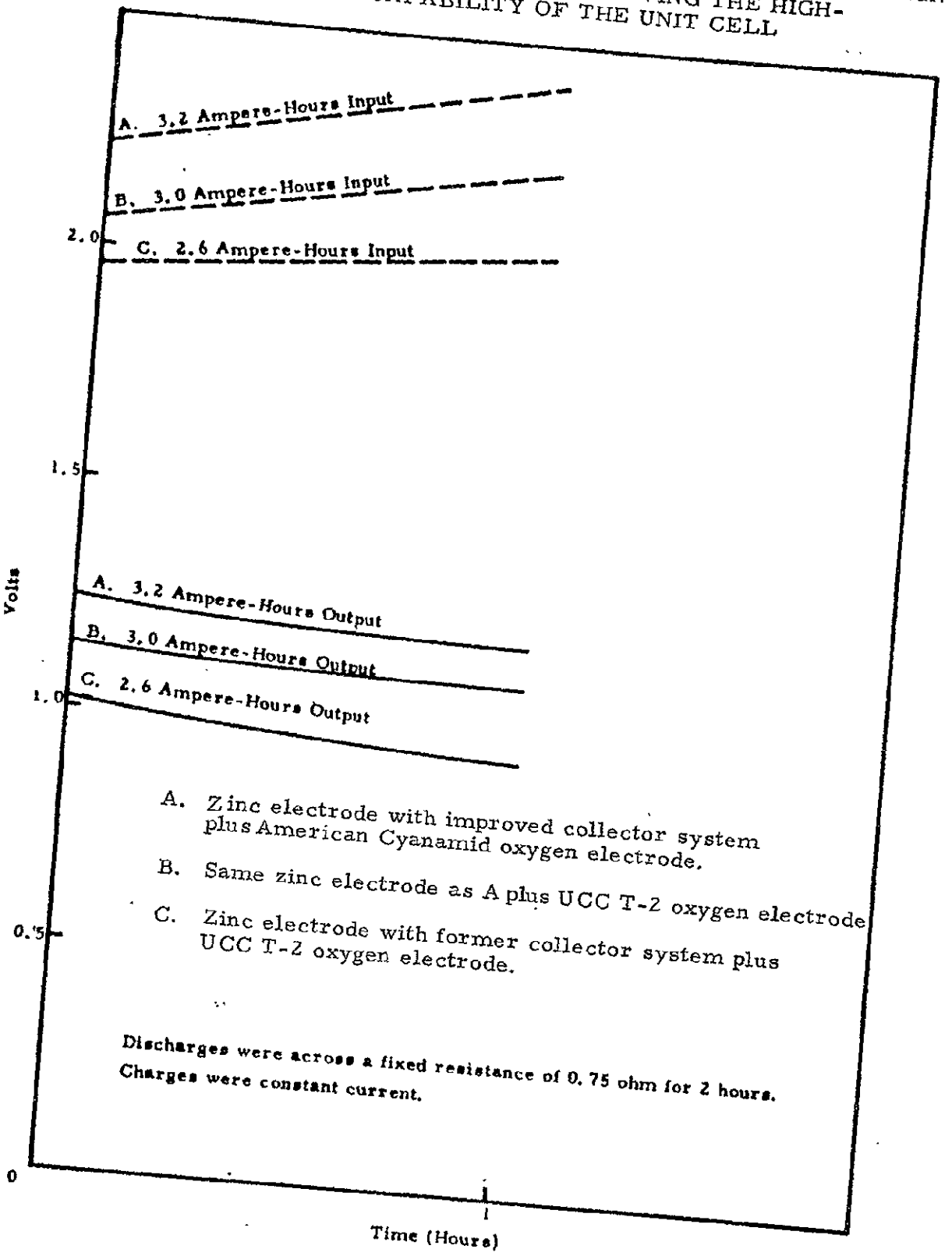

A. Zinc electrode with improved collector system plus American Cyanamid oxygen electrode.

B. Same zinc electrode as A plus UCC T-2 oxygen electrode

C. Zinc electrode with former collector system plus UCC T-2 oxygen electrode.

Discharges were across a fixed resistance of 0.75 ohm for 2 hours.
Charges were constant current.

C-4156

FIGURE 24

PERFORMANCE OF CELL AT 25°C WITH "FIXED-ZONE" OXYGEN ELECTRODE AND 10 AMP-HR ZINC GEL ANODE DISCHARGED TO 2.5 - 3.5 AMP-HR OUTPUT

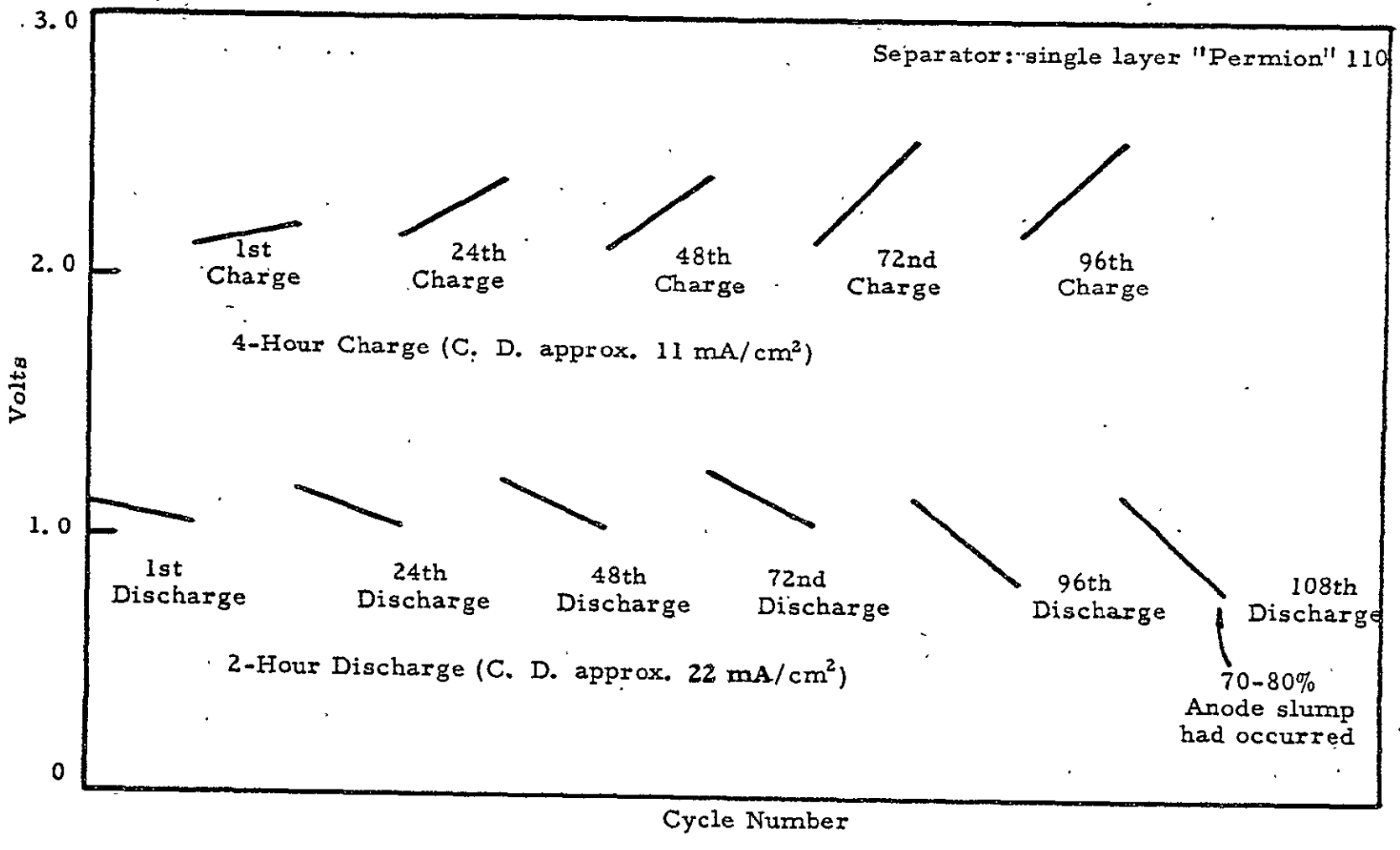

C-4203

FIGURE 25

40°C PERFORMANCE OF 10 AMPERE HOUR CELL DISCHARGED TO 2.5 - 3.0 AMPERE HOUR OUTPUT

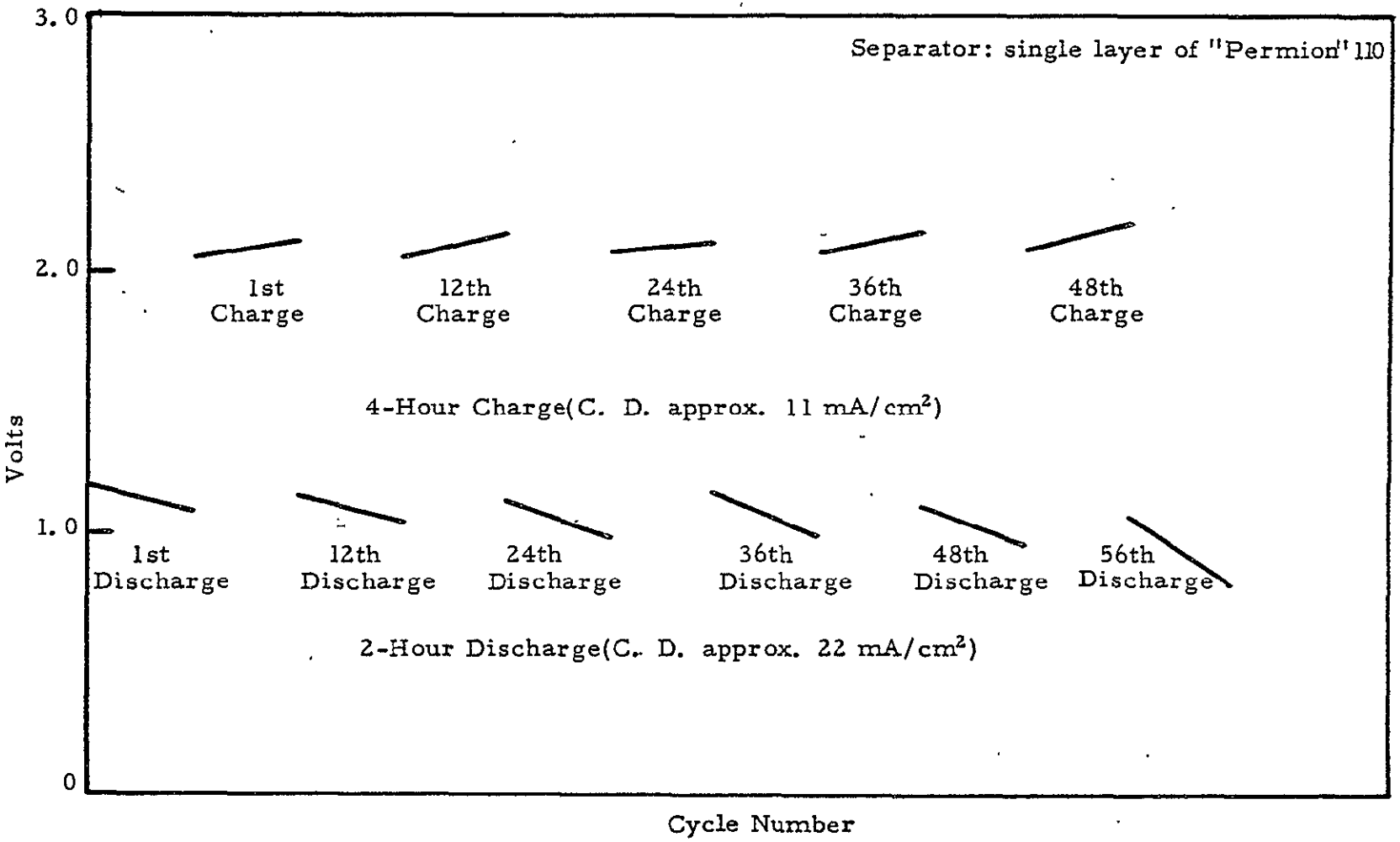

C-4209

FIGURE 26

0°C PERFORMANCE OF 10 AMPERE-HOUR CELL DISCHARGE AT 25% ZINC DEPTH

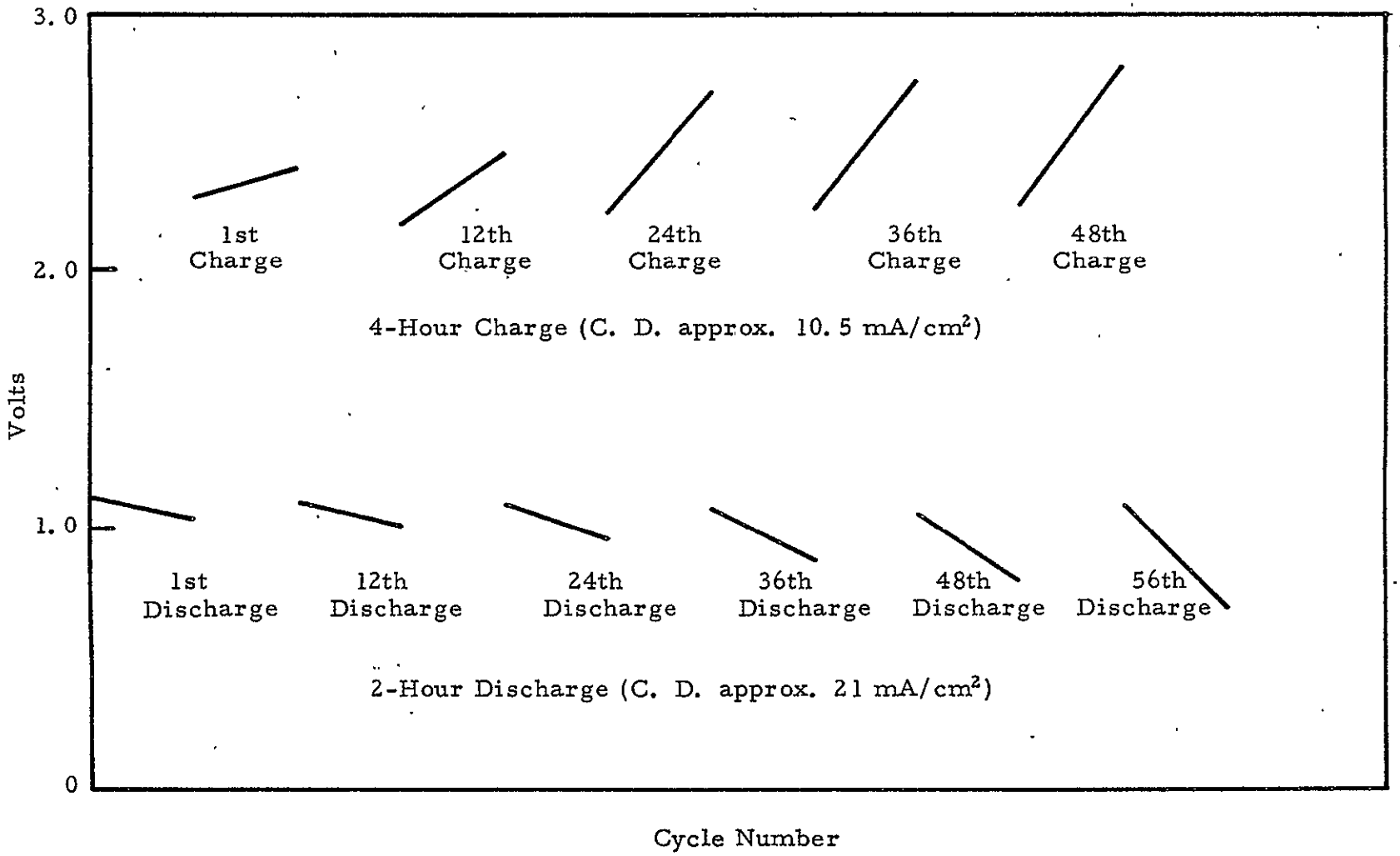

C-4210

FIGURE 27

DISCHARGE PERFORMANCE BEFORE, DURING, AND AFTER COMPLETE DISCHARGE OF ZINC-OXYGEN UNIT CELL

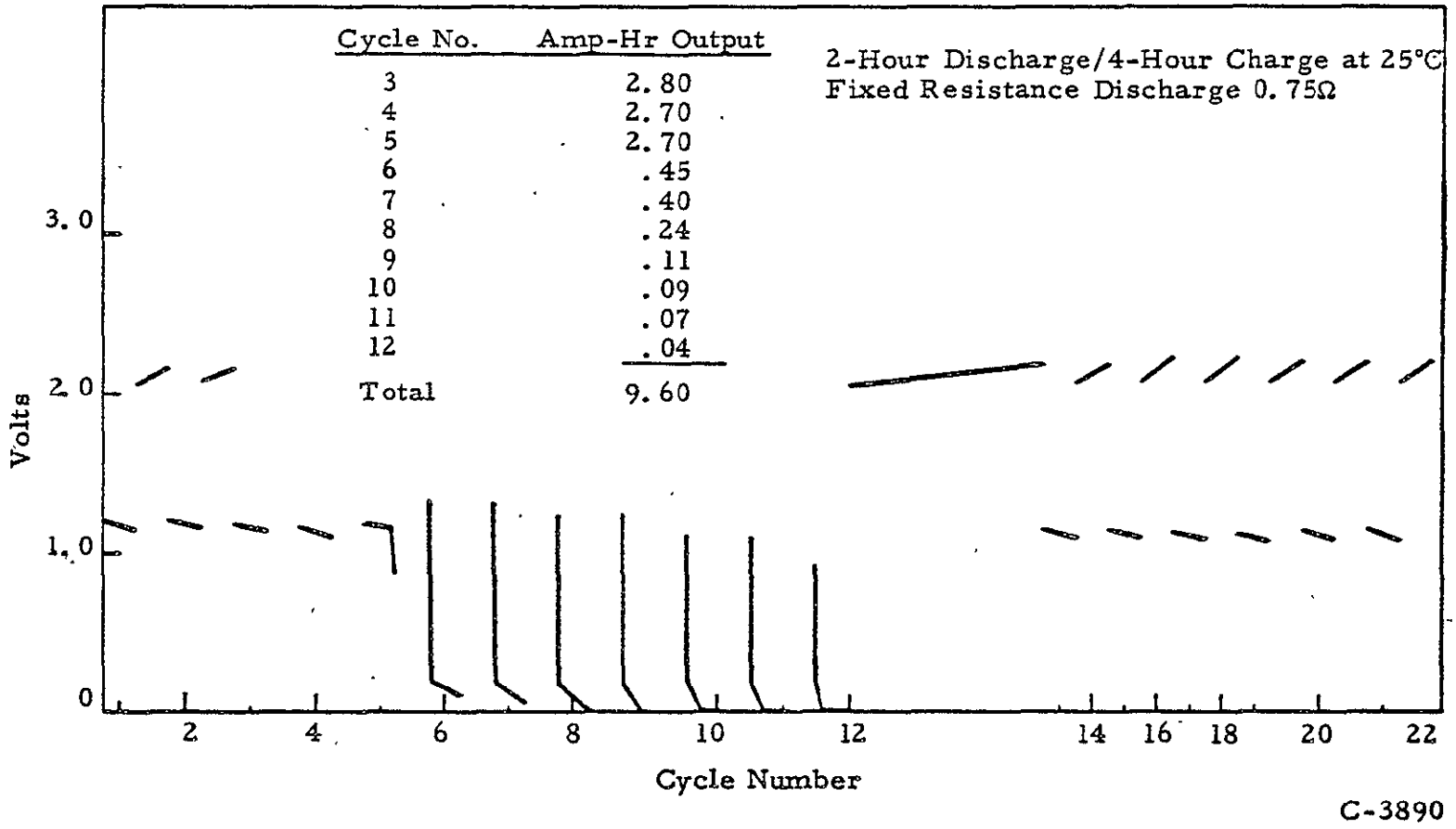

FIGURE 28

PERFORMANCE OF A UNIT CELL EMPLOYING A THIN "FIXED-ZONE" OXYGEN ELECTRODE AND A 15-AMPERE-HOUR ZINC GEL TYPE ANODE

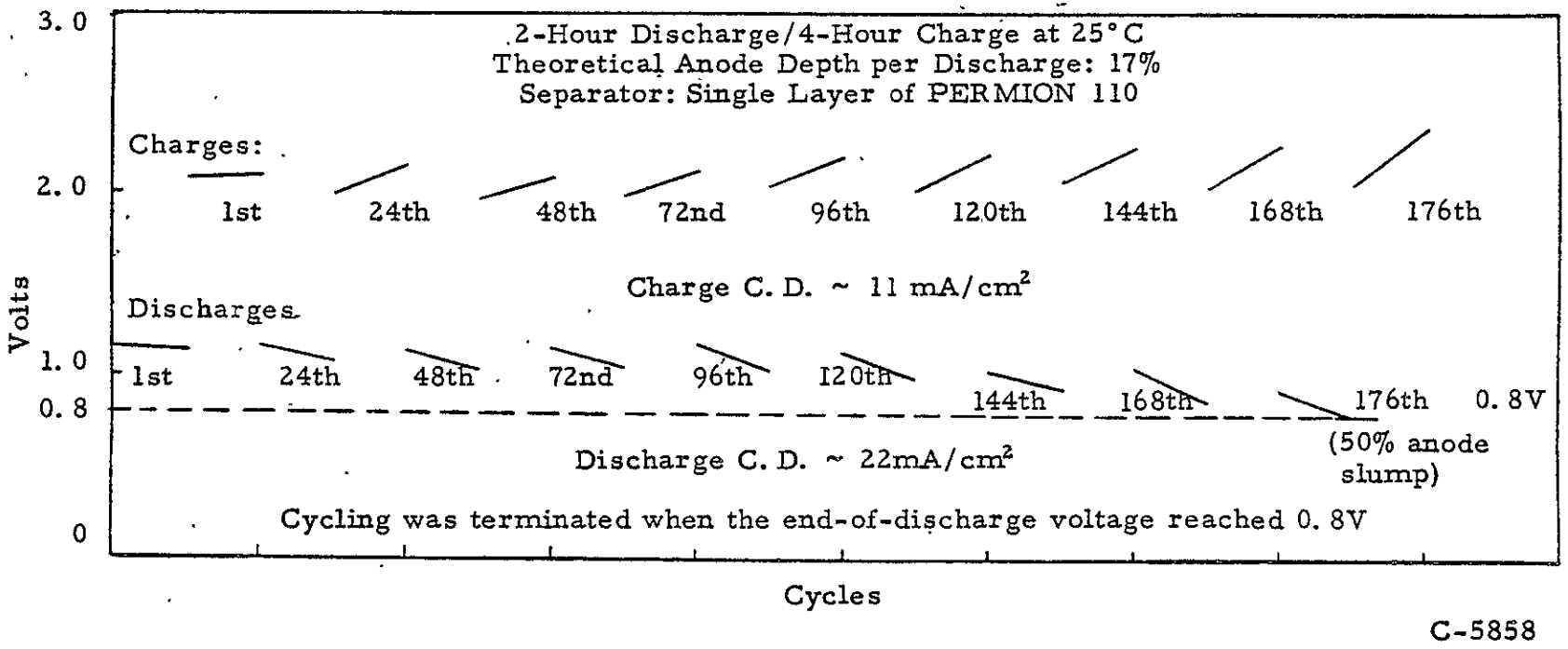

C-5858

FIGURE 29

PERFORMANCE OF A UNIT CELL EMPLOYING A THIN "FIXED-ZONE" OXYGEN ELECTRODE AND A 20 AMPERE-HOUR ZINC GEL TYPE ANODE

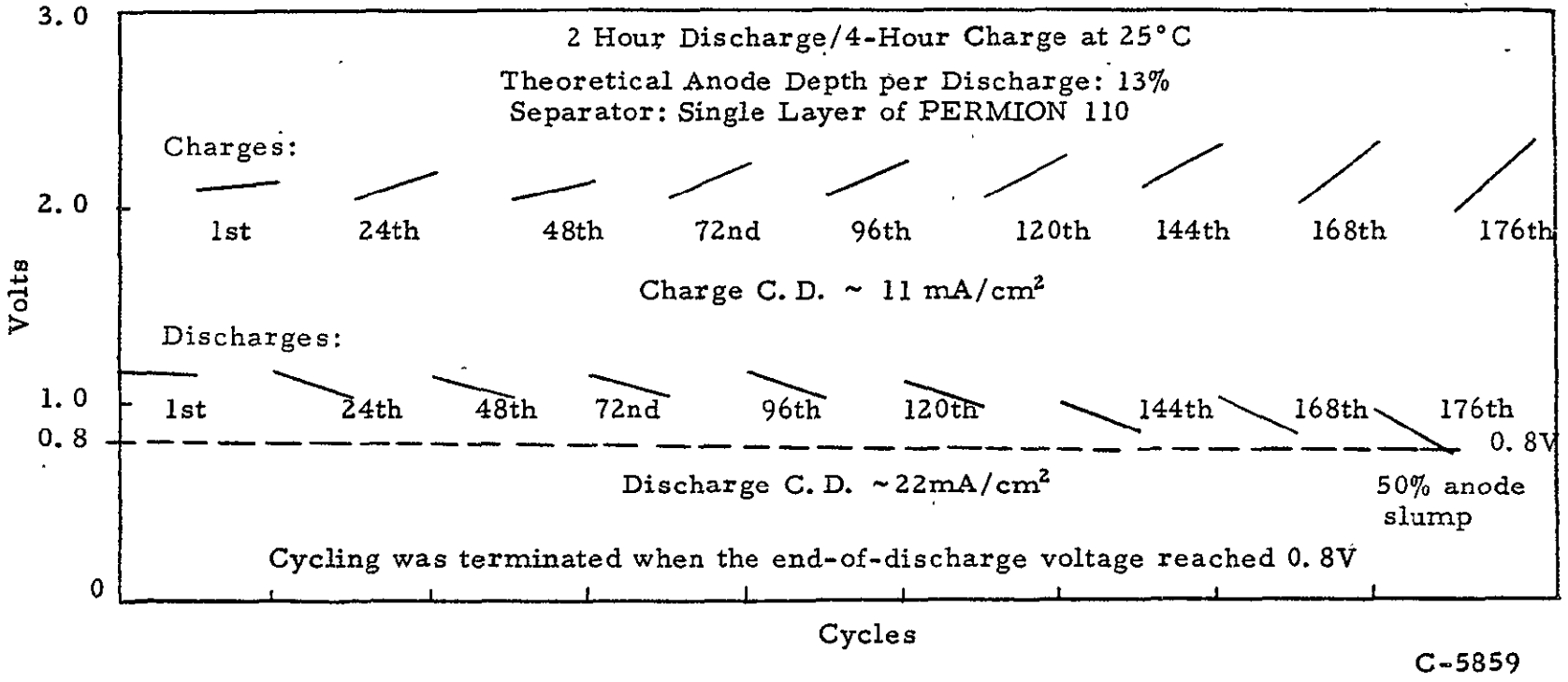

C-5859

FIGURE 30

COMPARISON OF 10, 15, and 20 AMPERE-HOUR ZINC GEL TYPE ANODES
DISCHARGED TO 26%, 17% and 13% DEPTH

Cell No.	Capacity	Discharged	Discharge C. D.	Output	No. Cycles to 0.8V	Separator
1	15 A-h	2 hours	22 mA/cm²	2.6 A-h	176	Single layer
2	20 A-h	2 hours	22 mA/cm²	2.6 A-h	176	Permion 110
3	10 A-h	2 hours	22 mA/cm²	2.6 A-h	108 (1 cell)	
4	10 A-h	2 hours	22 mA/cm²	2.6 A-h	50-60 Avg. of 10 cells	

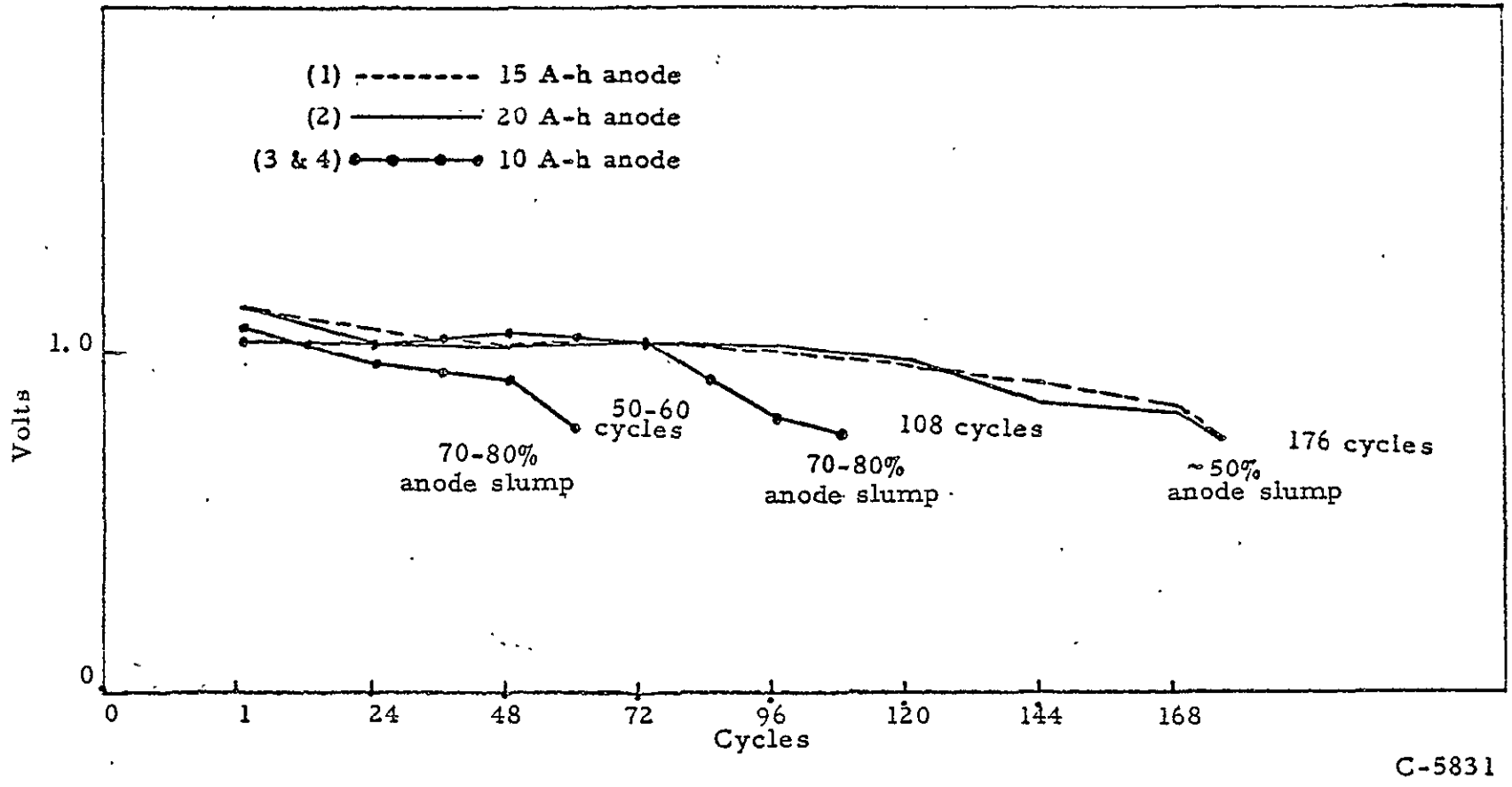

C-5831

FIGURE 31

PERFORMANCE OF A UNIT CELL EMPLOYING A THIN "FIXED-ZONE" OXYGEN ELECTRODE, AND A 15 AMPERE-HOUR ZINC GEL TYPE ANODE

2-Hour Discharge/4-Hour Charge at 0°C

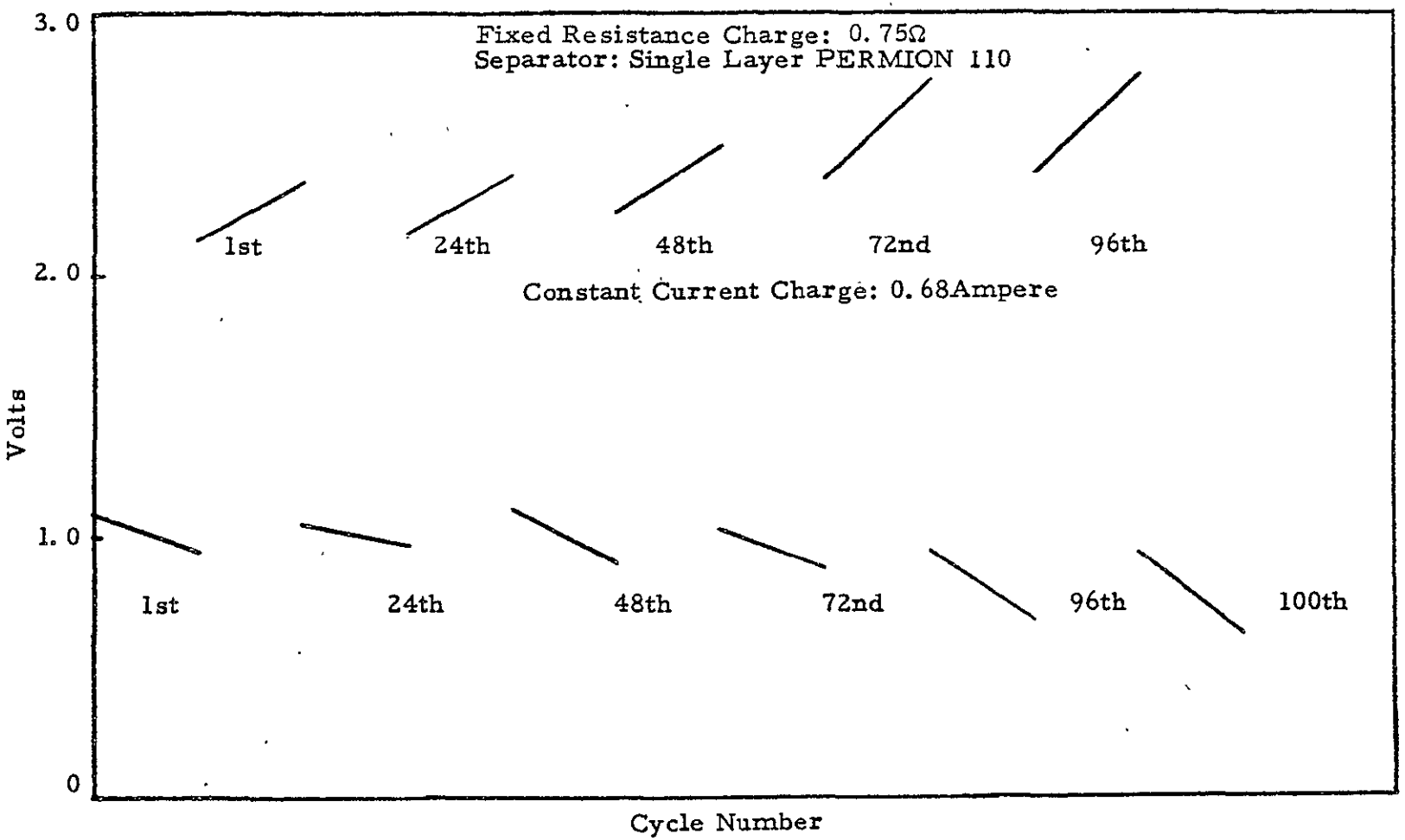

C-5837

FIGURE 32

40°C PERFORMANCE OF A UNIT CELL EMPLOYING A THIN "FIXED-ZONE" OXYGEN ELECTRODE AND A 15 AMPERE-HOUR ZINC GEL TYPE ANODE

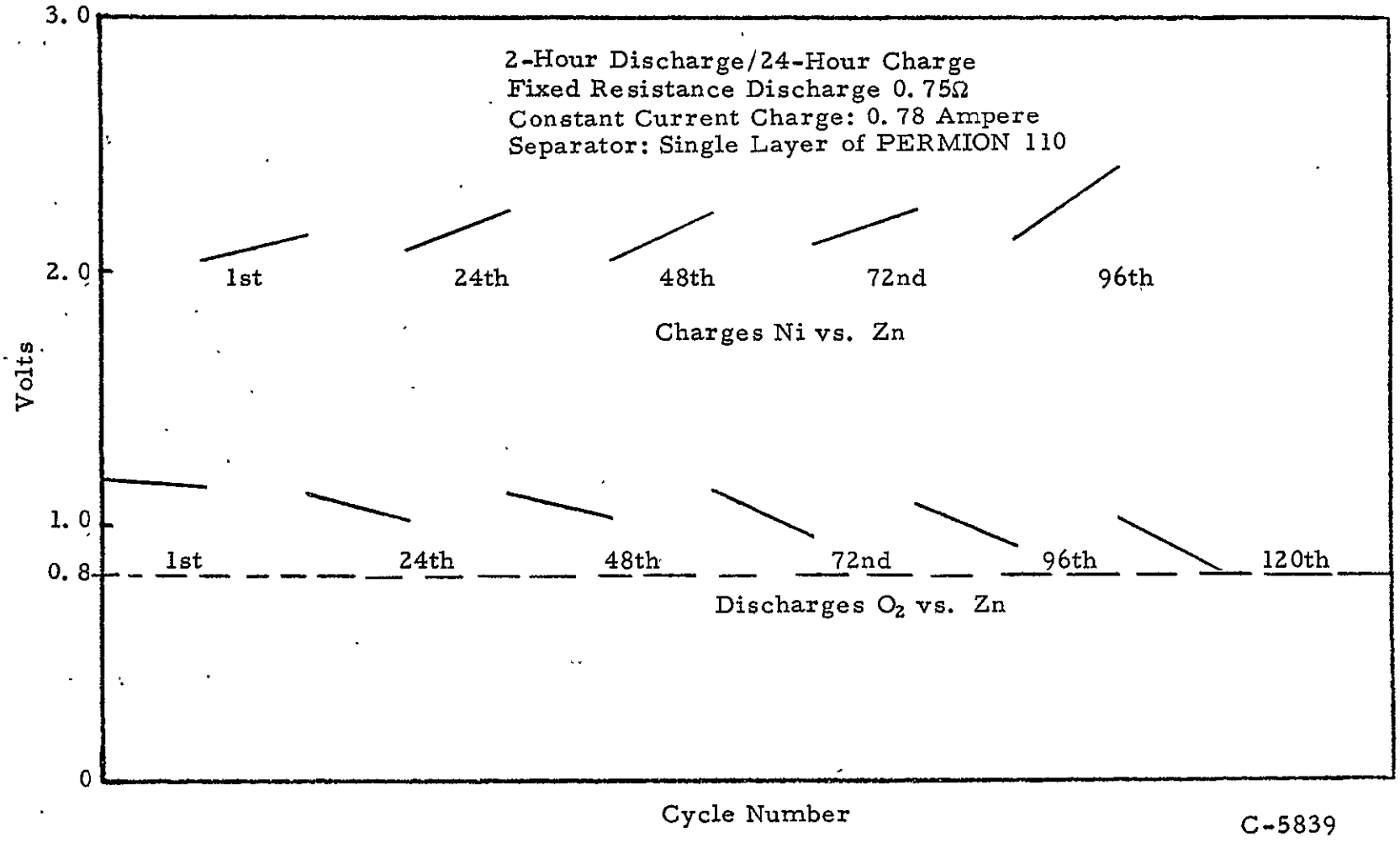

FIGURE 33

PERFORMANCE OF A UNIT CELL EMPLOYING AN AMERICAN CYANAMID "LAB 40" OXYGEN ELECTRODE AND A 20 AMPERE-HOUR ZINC GEL ANODE

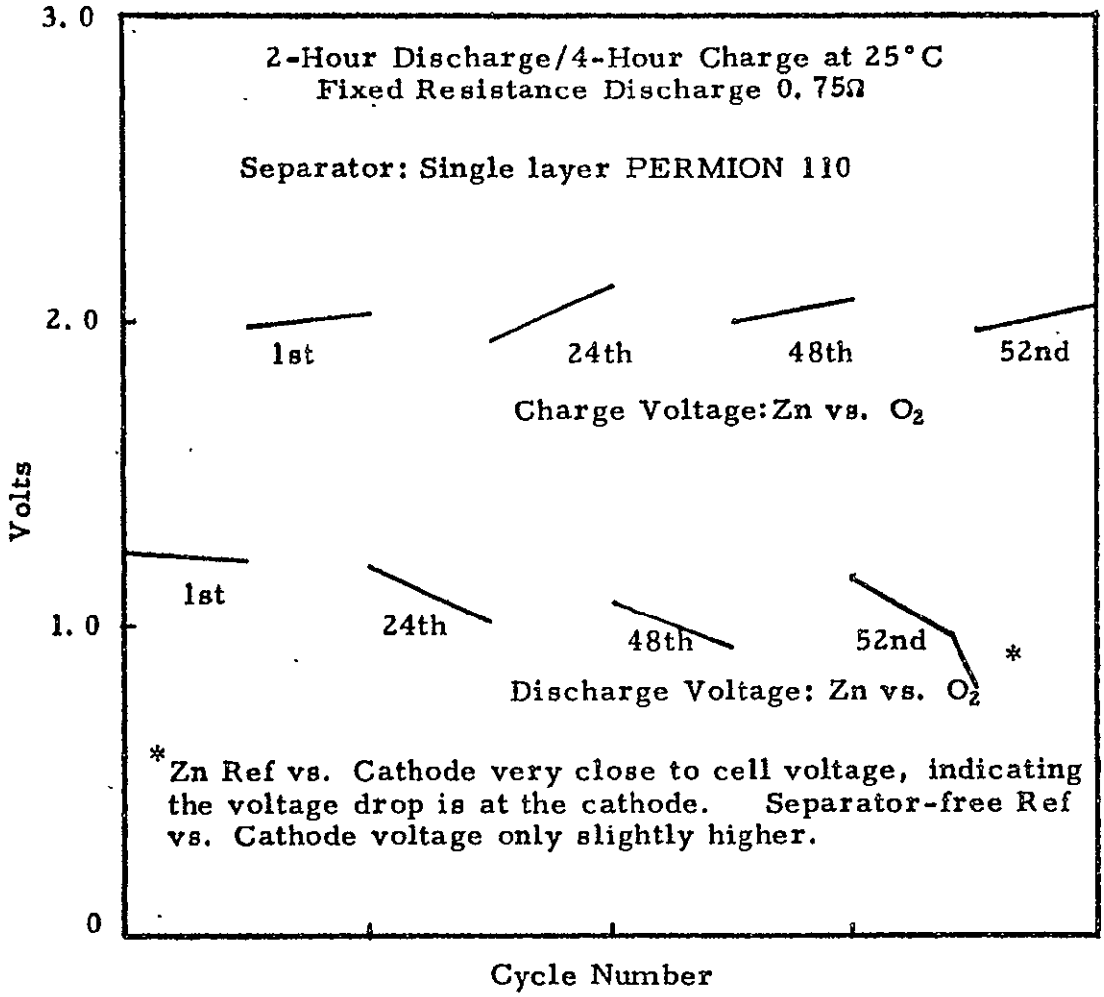

C-5838

FIGURE 34

CYCLING OF AMERICAN CYANAMID LAB-40 ELECTRODE CELL AT 31% ZINC DEPTH

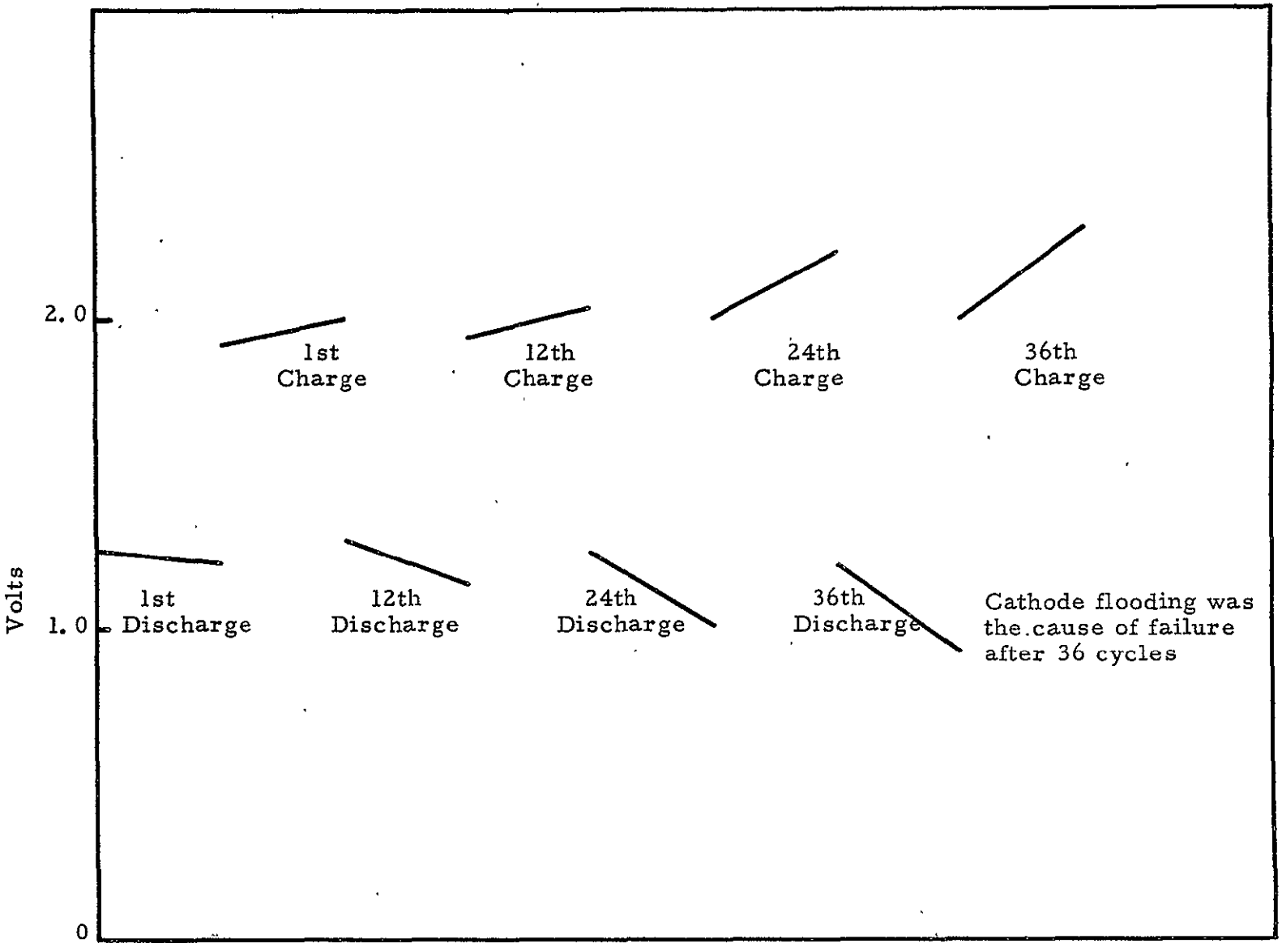

C-4207

FIGURE 35

PERFORMANCE OF A UNIT CELL EMPLOYING AN AMERICAN CYANAMID "LAB 40" OXYGEN ELECTRODE

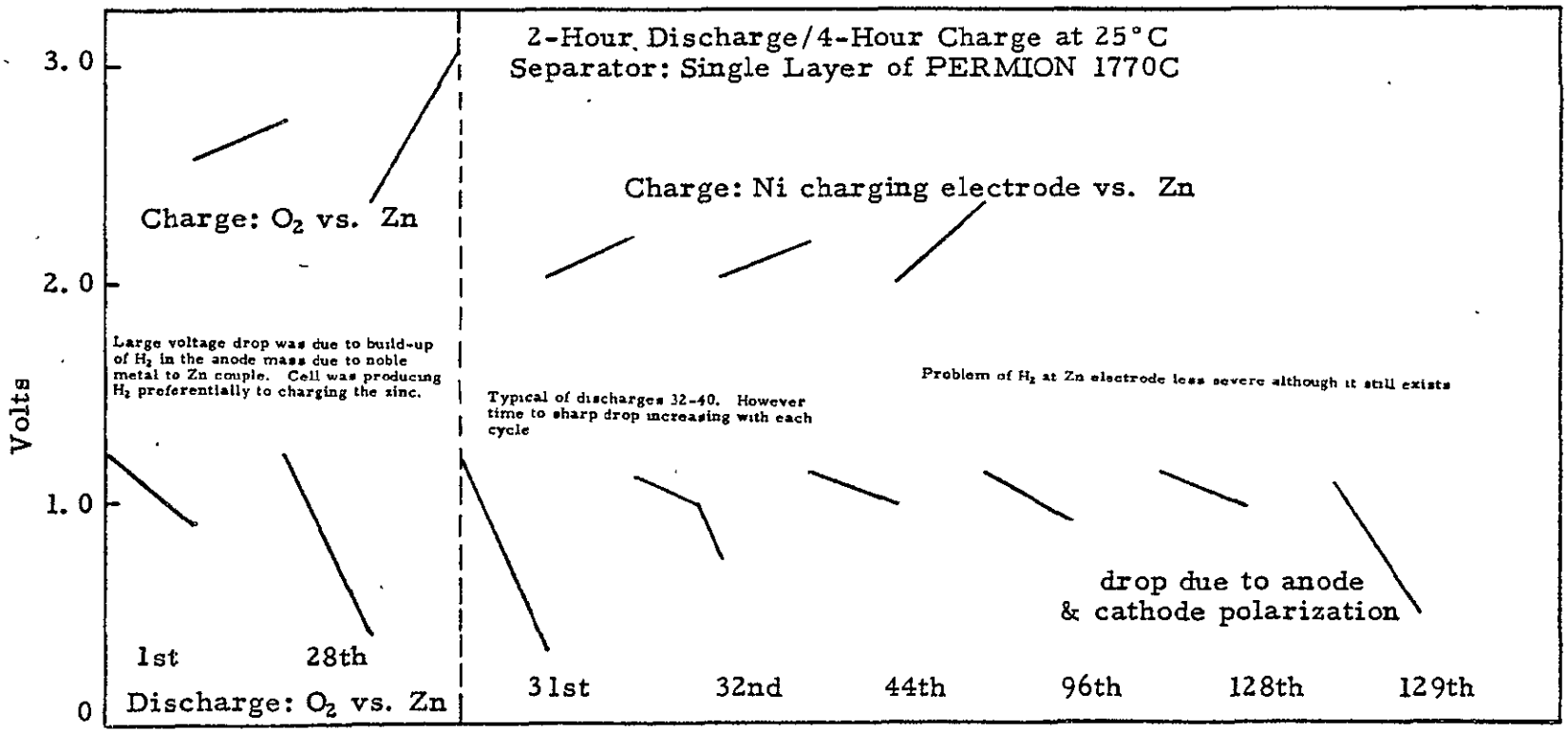

C-5860

FIGURE 36

IR-Free Cathode Polarization - American Cyanamid LAB-40 Vs. Union Carbide T-2

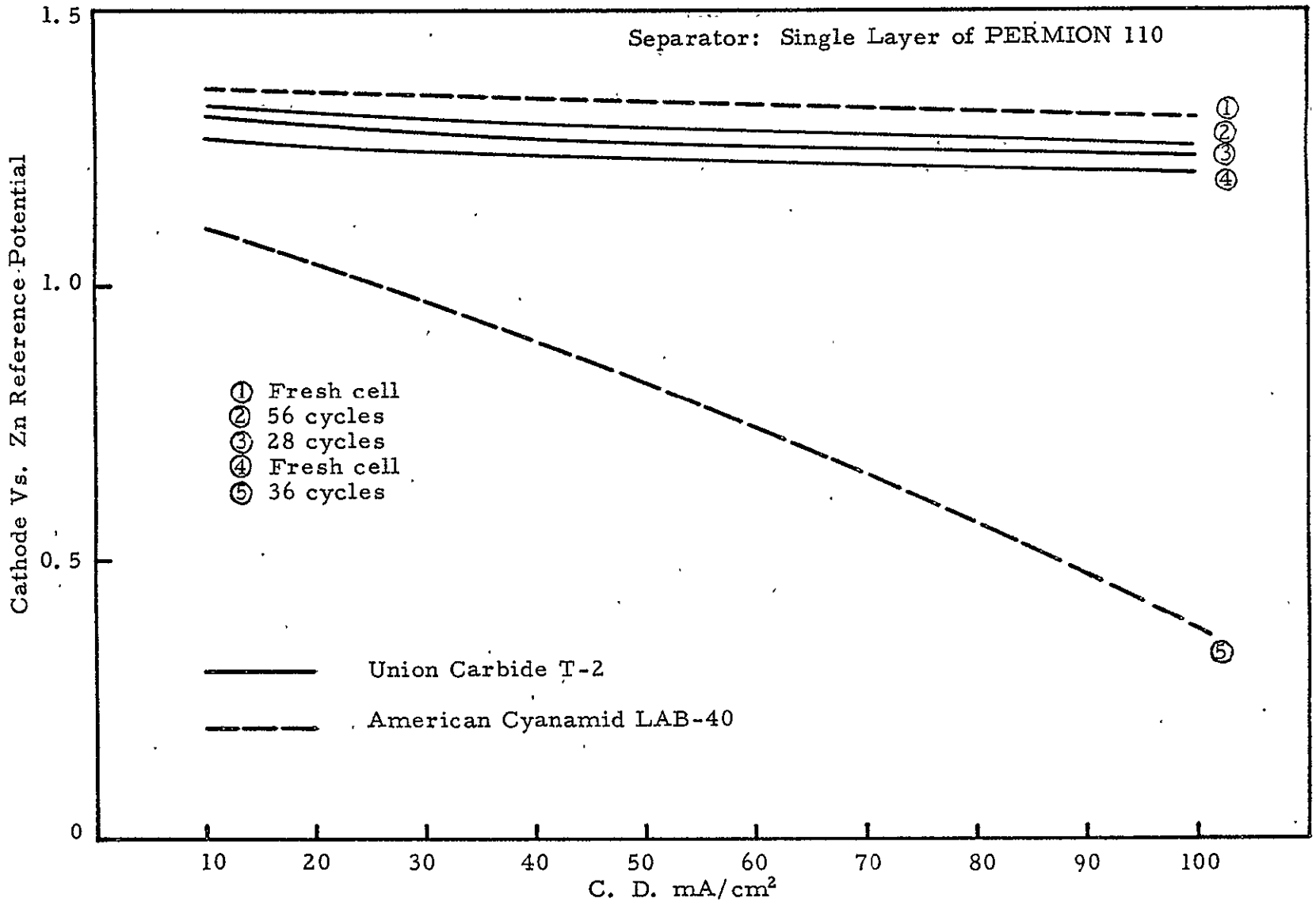

C-4208

FIGURE 37

FORMATION CYCLING OF AN ANODE FABRICATED FROM ZnO FORMULATION DESIGNATED ZnO #19

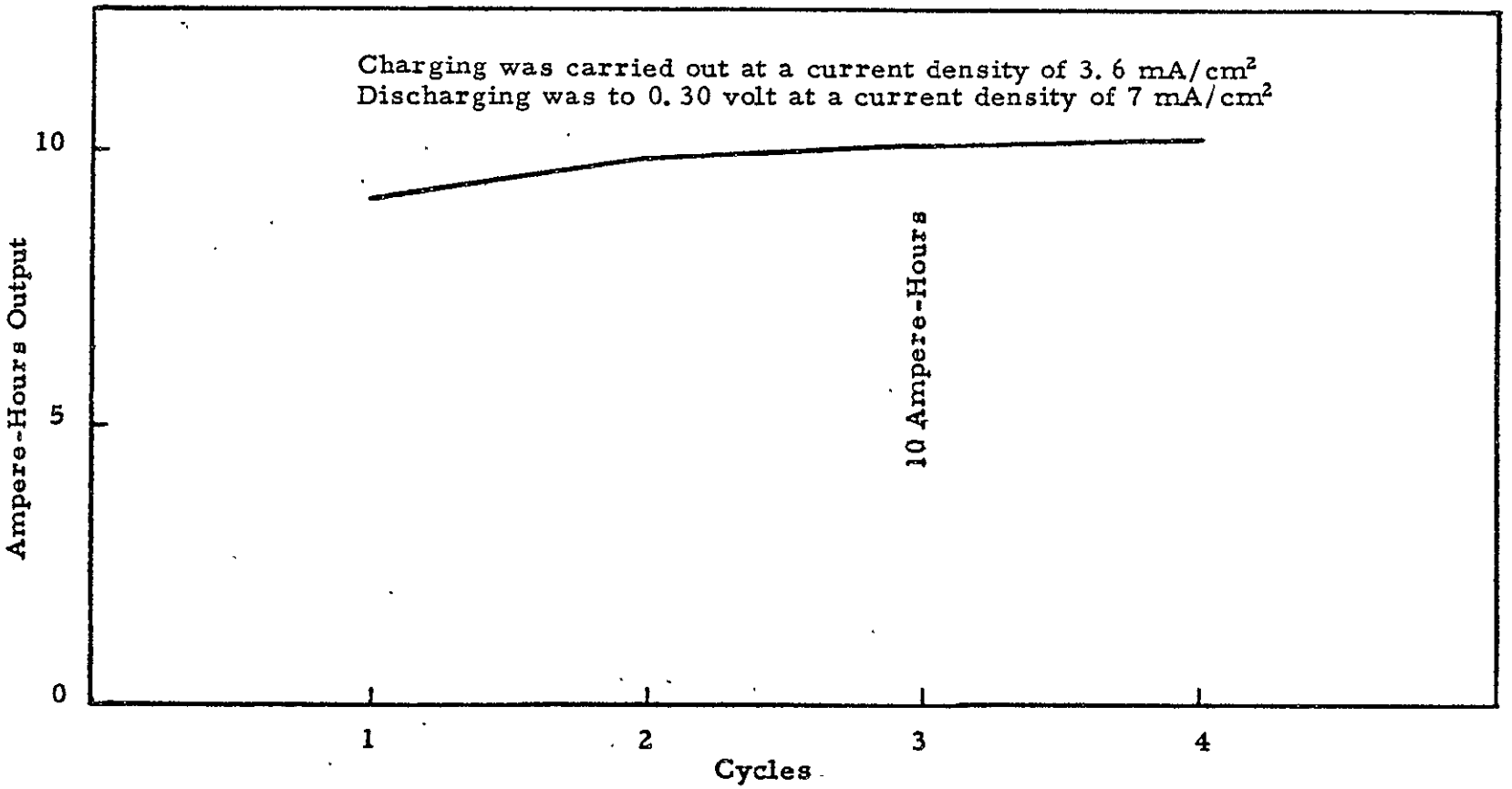

C-5842

FIGURE 38

PERFORMANCE OF A UNIT CELL EMPLOYING A THIN "FIXED-ZONE" OXYGEN ELECTRODE AND A 5 AMPERE-HOUR ZnO-1 ANODE

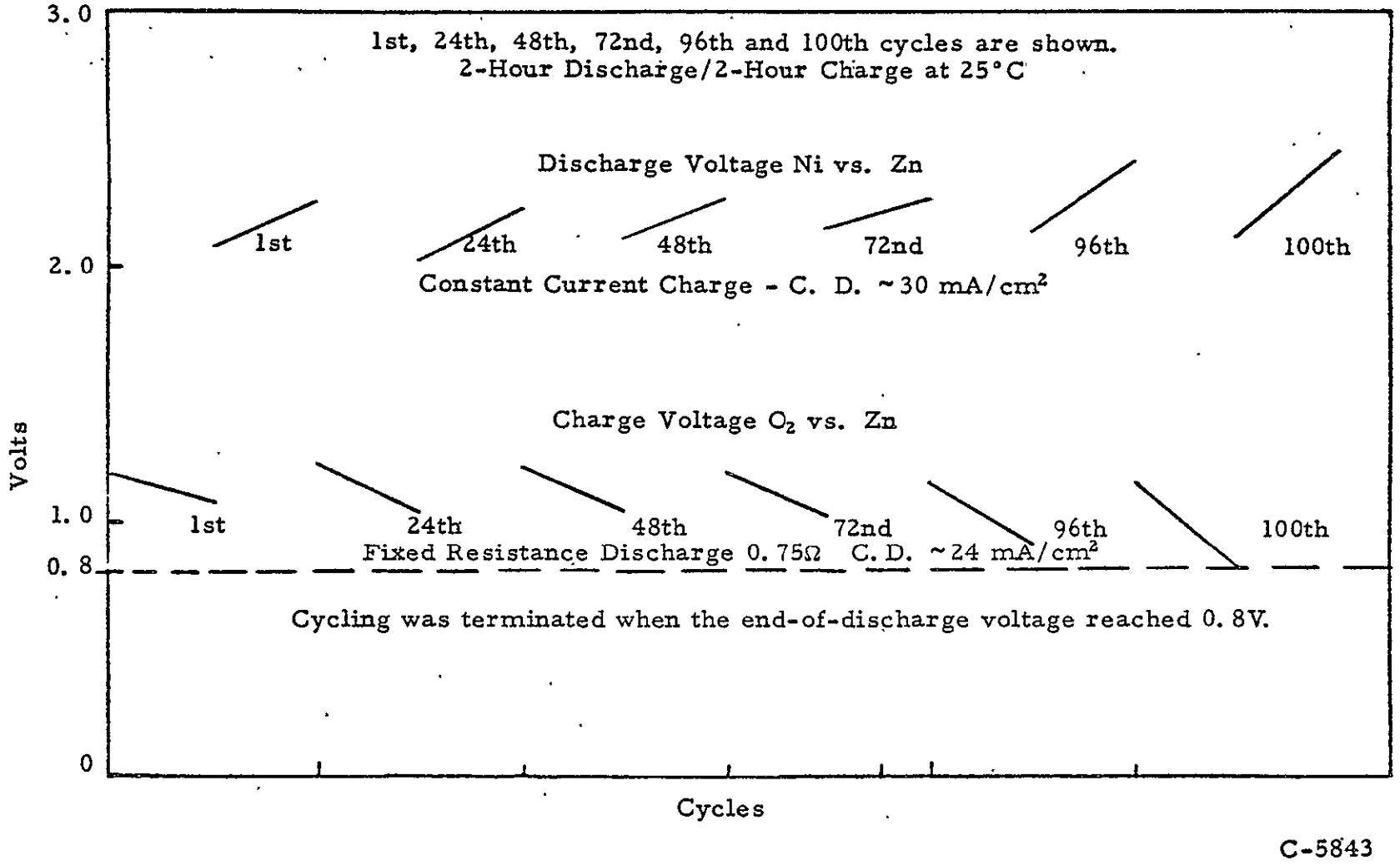

C-5843

FIGURE 39

PERFORMANCE OF A UNIT CELL EMPLOYING A THIN "FIXED-ZONE" OXYGEN ELECTRODE AND A 5-AMPERE-HOUR ZnO#1 ANODE

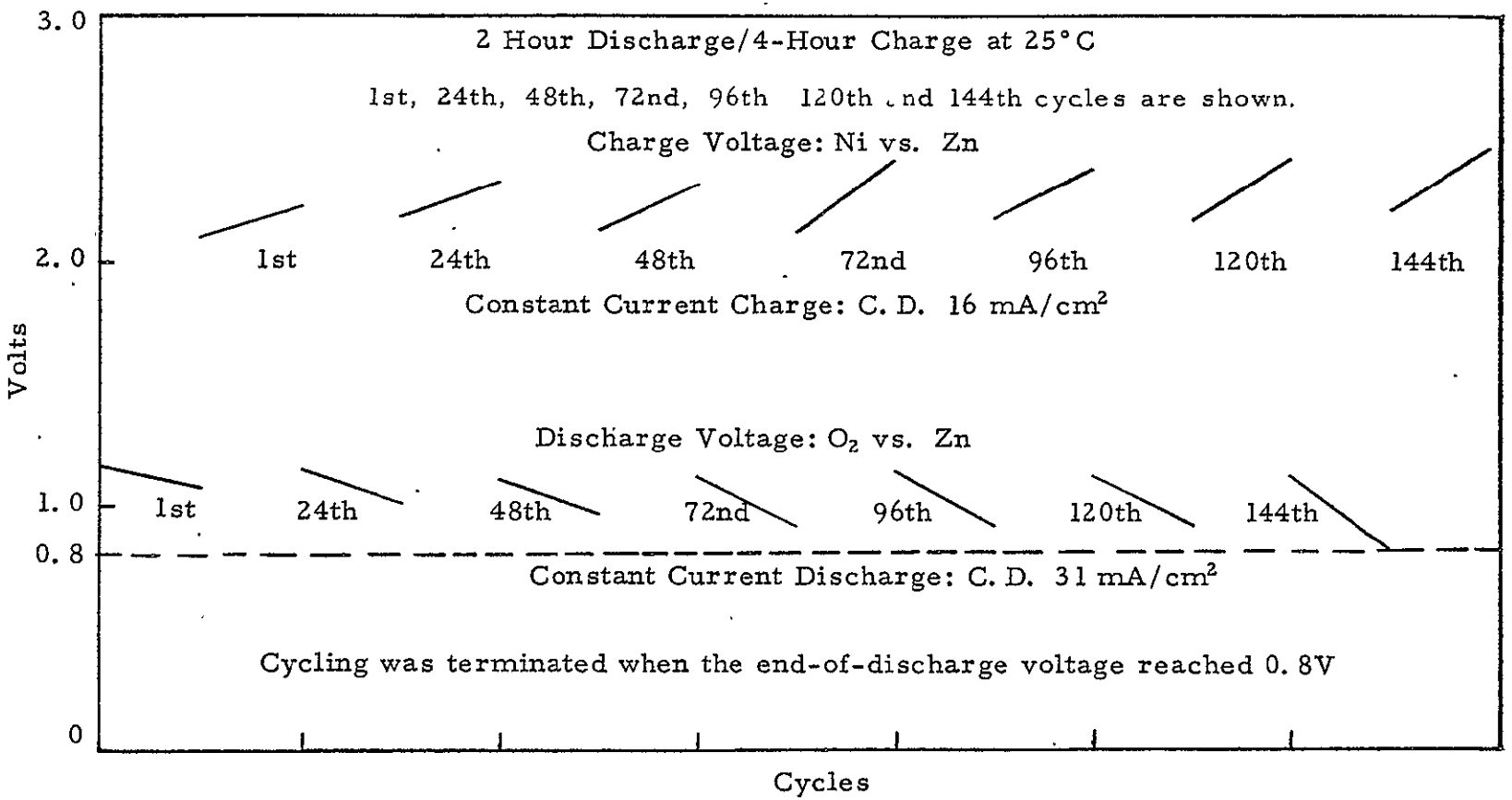

C-5861

FIGURE 40

PERFORMANCE OF A UNIT CELL EMPLOYING A THIN "FIXED-ZONE" OXYGEN ELECTRODE AND A 5-AMPERE-HOUR ZnO#10 ANODE

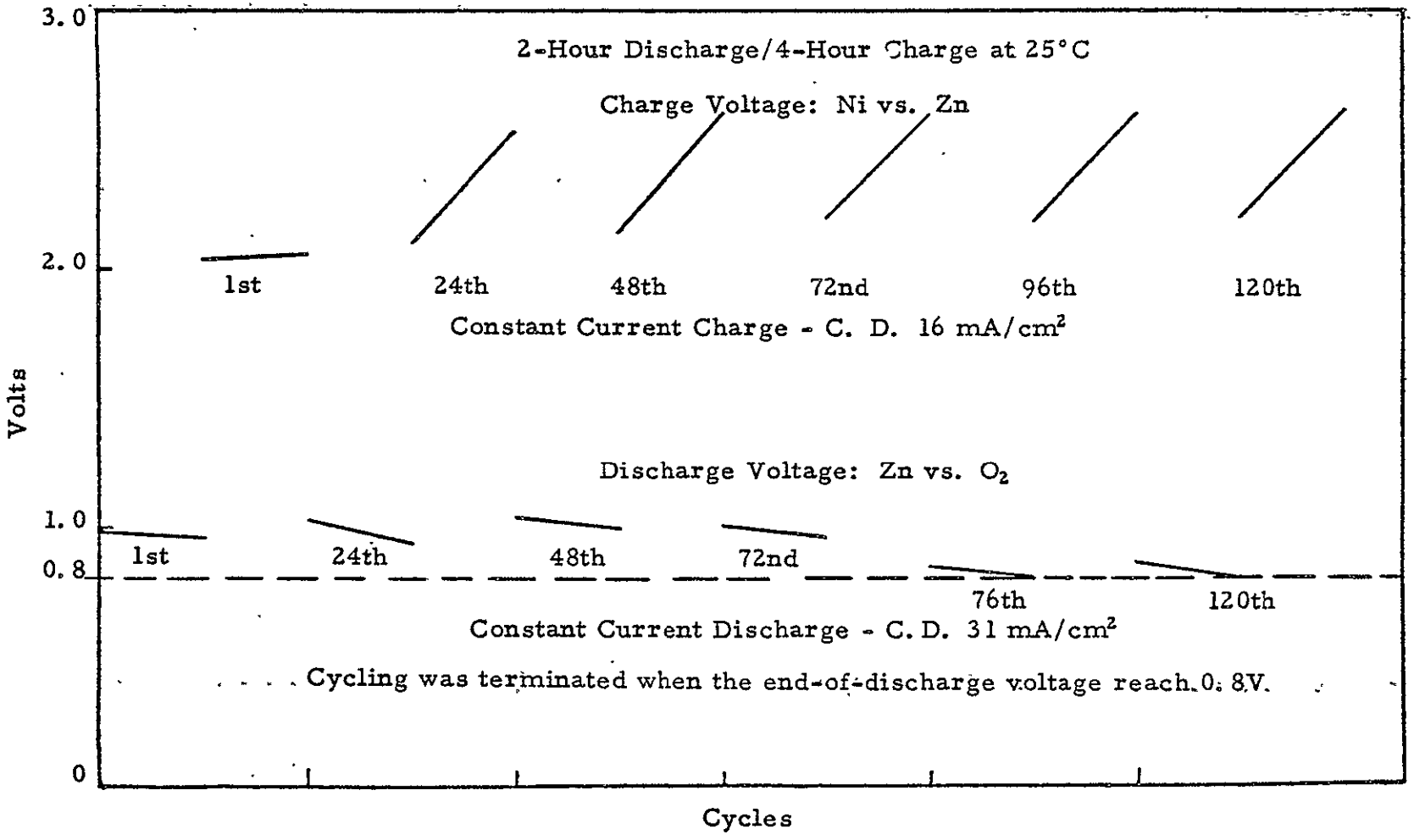

C-5844

FIGURE 41

PERFORMANCE OF A UNIT CELL EMPLOYING A THIN "FIXED-ZONE" OXYGEN ELECTRODE AND A 10-AMPERE-HOUR ZnO#19 ANODE

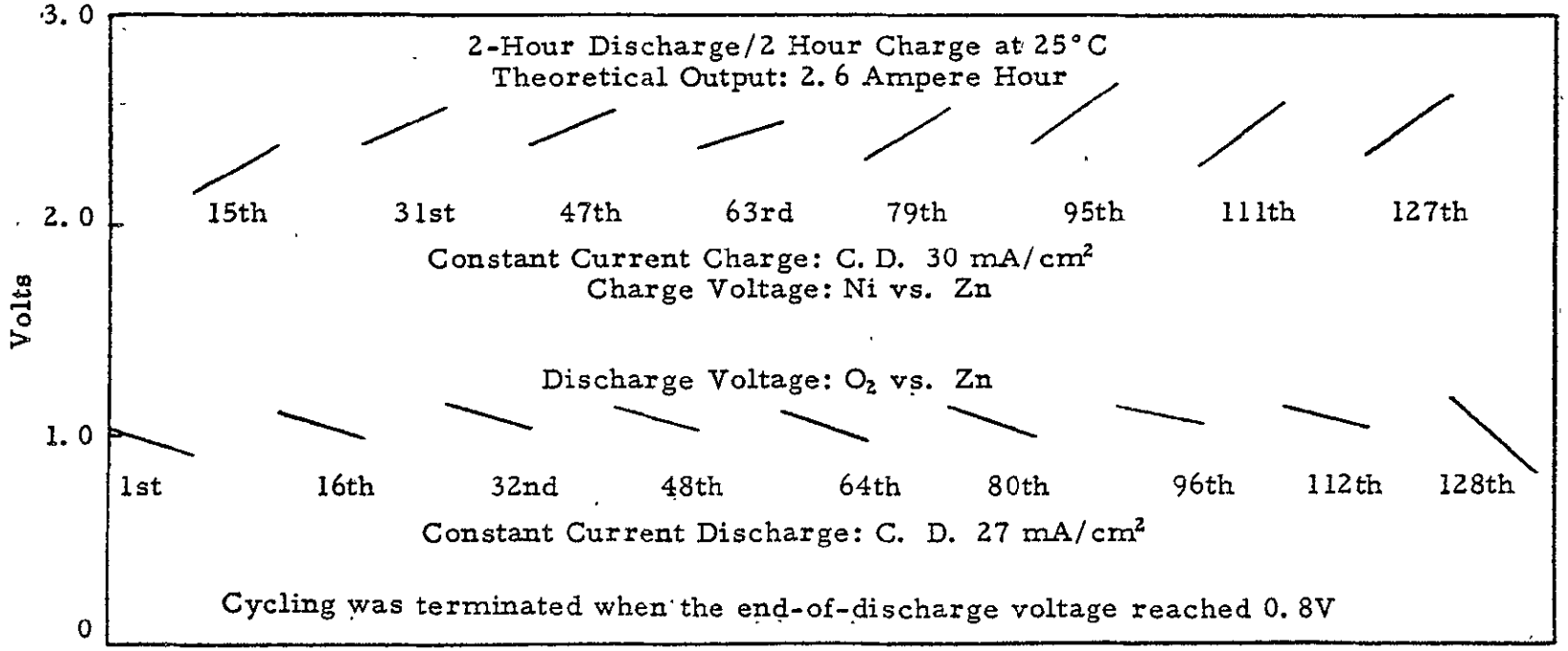

C-5862

FIGURE 42

PERFORMANCE OF A UNIT CELL EMPLOYING A THIN "FIXED-ZONE" OXYGEN ELECTRODE AND A 10-AMPERE-HOUR ZnO#19 ANODE

2-Hour Discharge/4 Hour Charge at 25°C

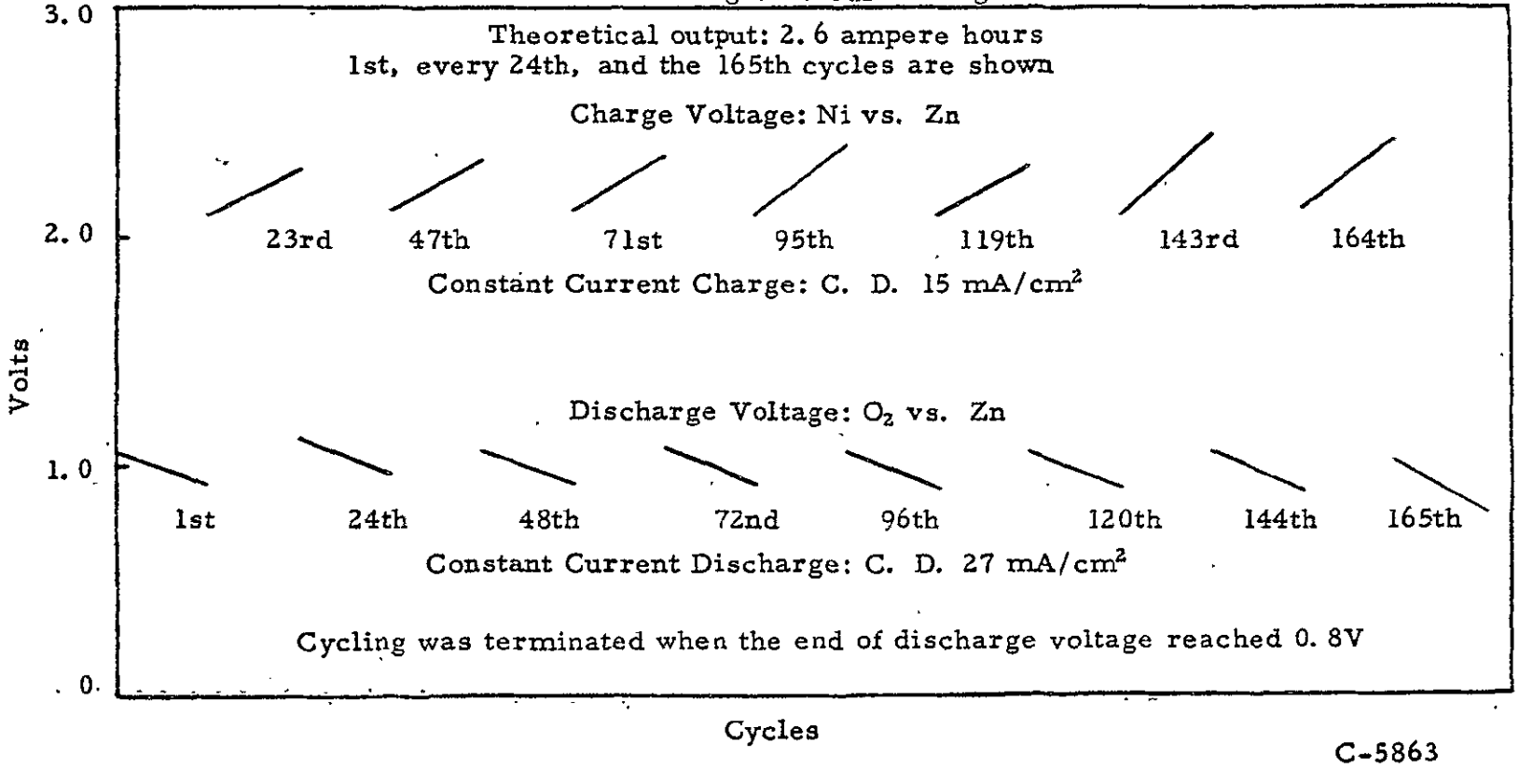

C-5863

FIGURE 43

PERFORMANCE OF A UNIT CELL EMPLOYING A THIN "FIXED-ZONE" OXYGEN ELECTRODE AND A 10 AMPERE-HOUR ZnO#19 ANODE

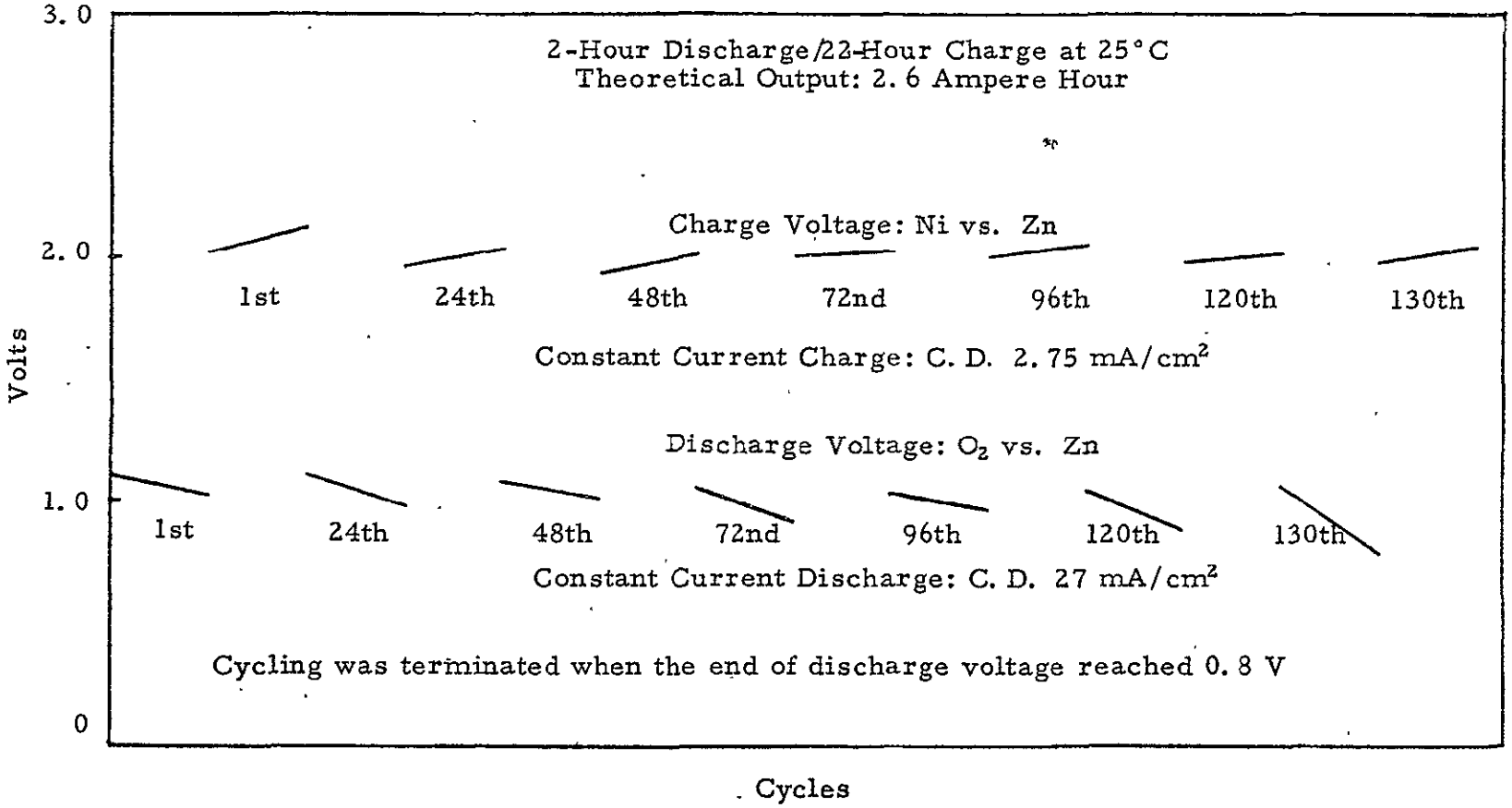

C-5864

FIGURE 44

PERFORMANCE OF A UNIT CELL EMPLOYING A THIN "FIXED-ZONE" OXYGEN ELECTRODE AND A 10-AMPERE-HOUR ZnO#19 ANODE

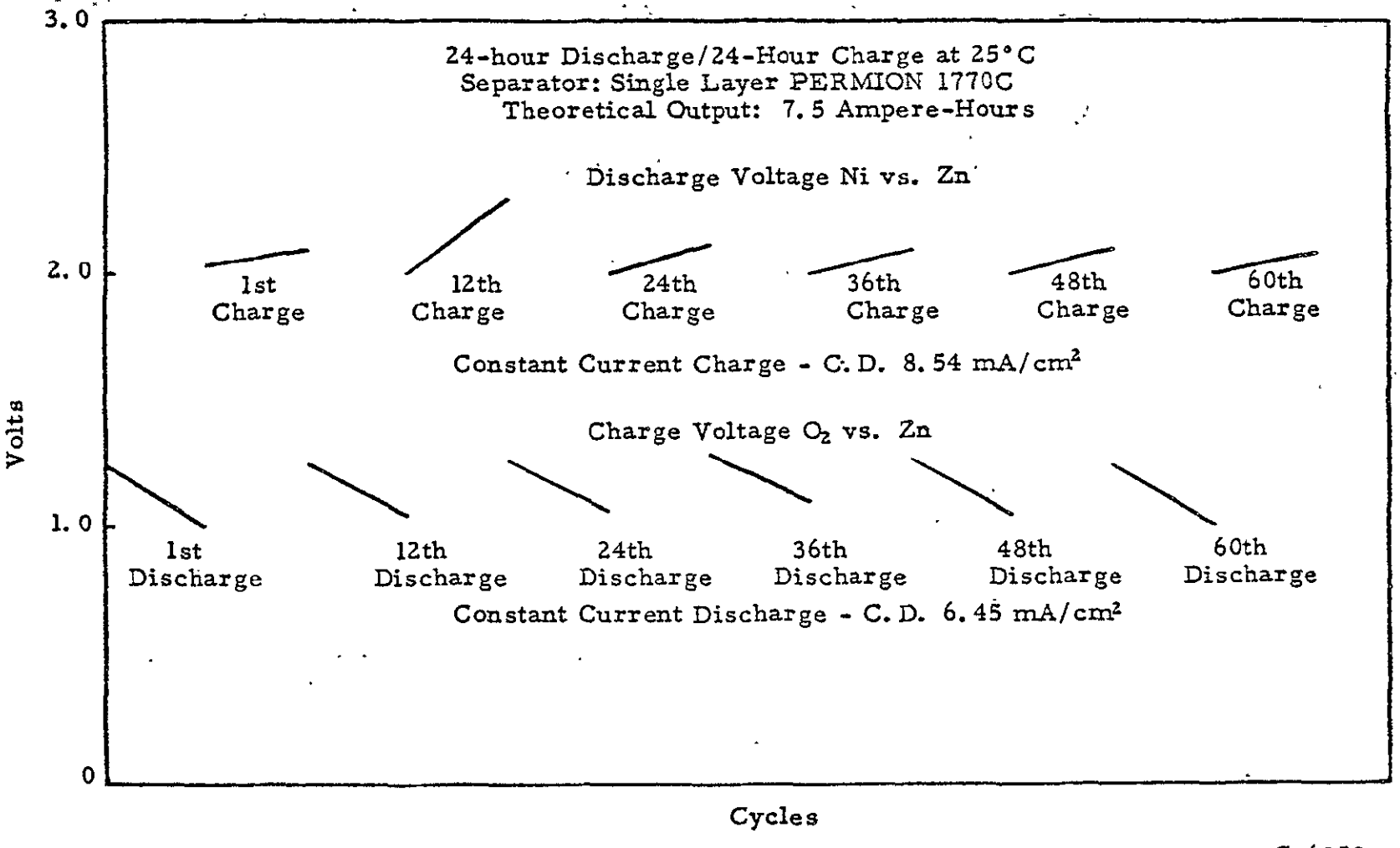

C-6959

FIGURE 45

PERFORMANCE OF A UNIT CELL EMPLOYING A THIN "FIXED-ZONE" OXYGEN ELECTRODE AND A 10-AMPERE-HOUR ZnO#19 ANODE

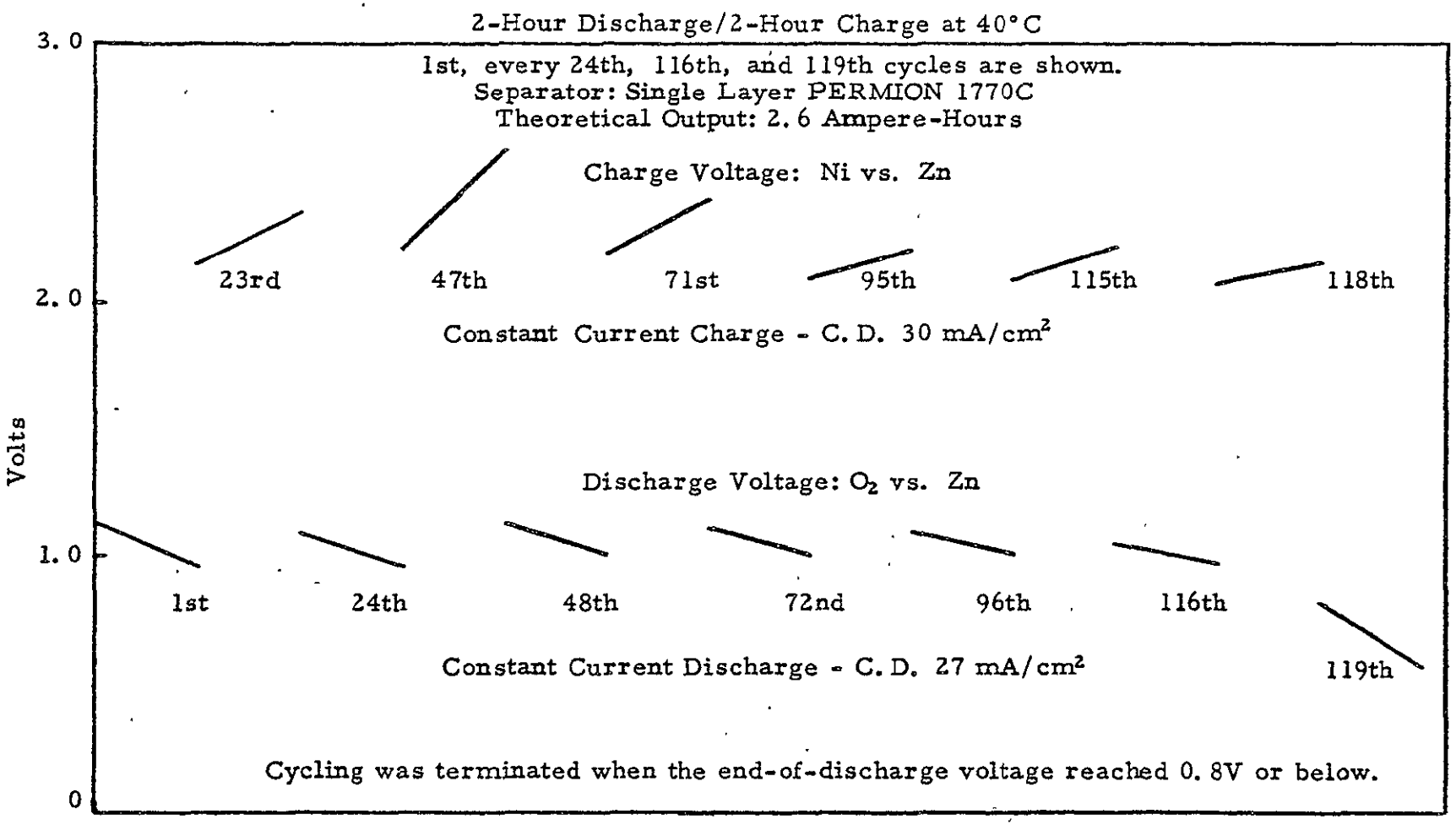

C-5846

FIGURE 46

PERFORMANCE OF A UNIT CELL EMPLOYING A THIN "FIXED-ZONE" OXYGEN ELECTRODE AND A 10 AMPERE-HOUR ZnO-19 ANODE

2-Hour Discharge/4-Hour Charge at 40°C

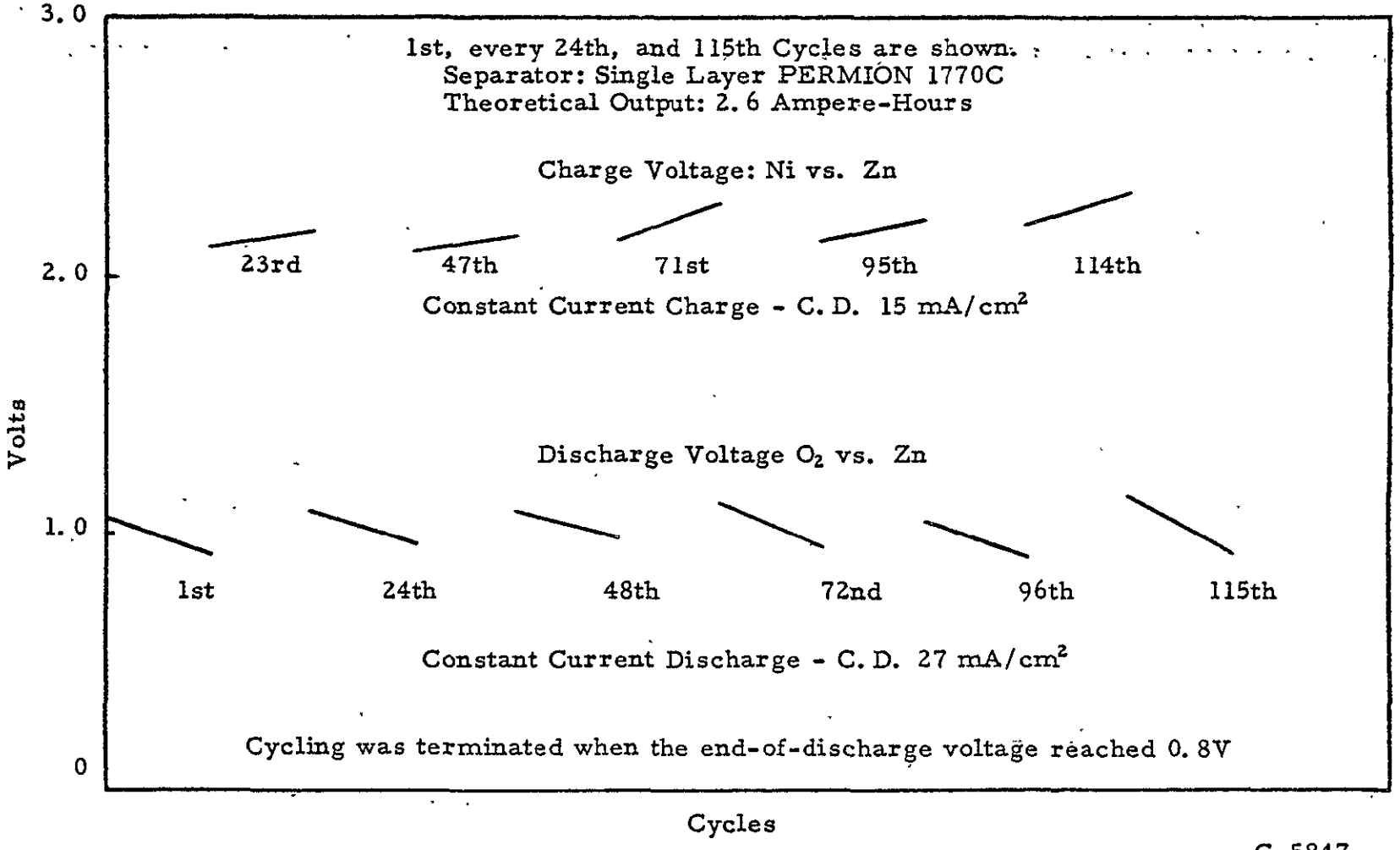

C-5847

FIGURE 47

PERFORMANCE OF A UNIT CELL EMPLOYING A THIN "FIXED-ZONE" OXYGEN ELECTRODE AND A 10-AMPERE-HOUR ZnO#19 ANODE

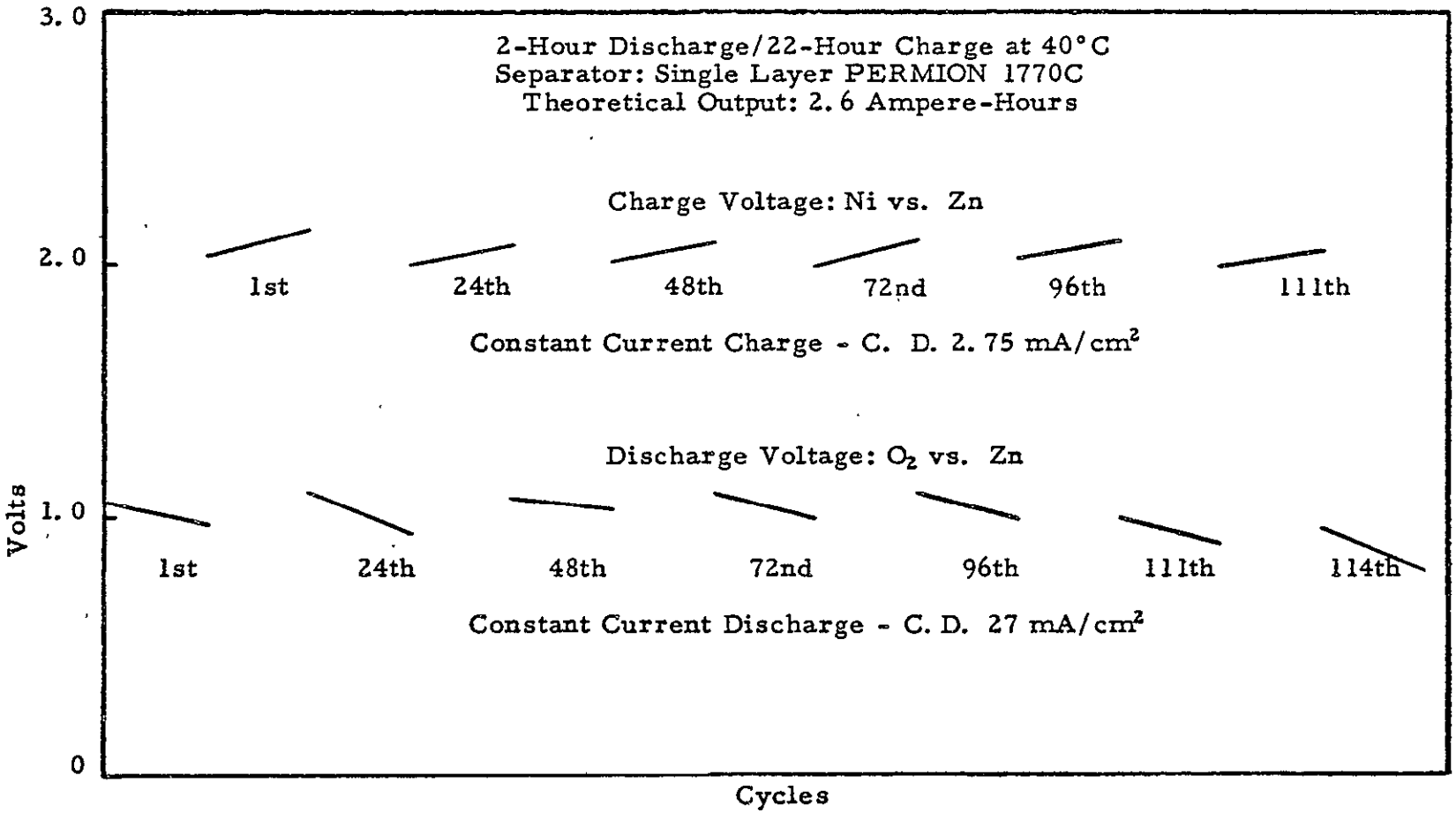

C-5852

FIGURE 48

PERFORMANCE OF A UNIT CELL EMPLOYING A 10-AMPERE-HOUR ZnO#19 ANODE
24-Hour Discharge/24-Hour Charge at 40°C
Theoretical Output: 7.5 Amp. Hours Separator: Single Layer PERMION 1770C

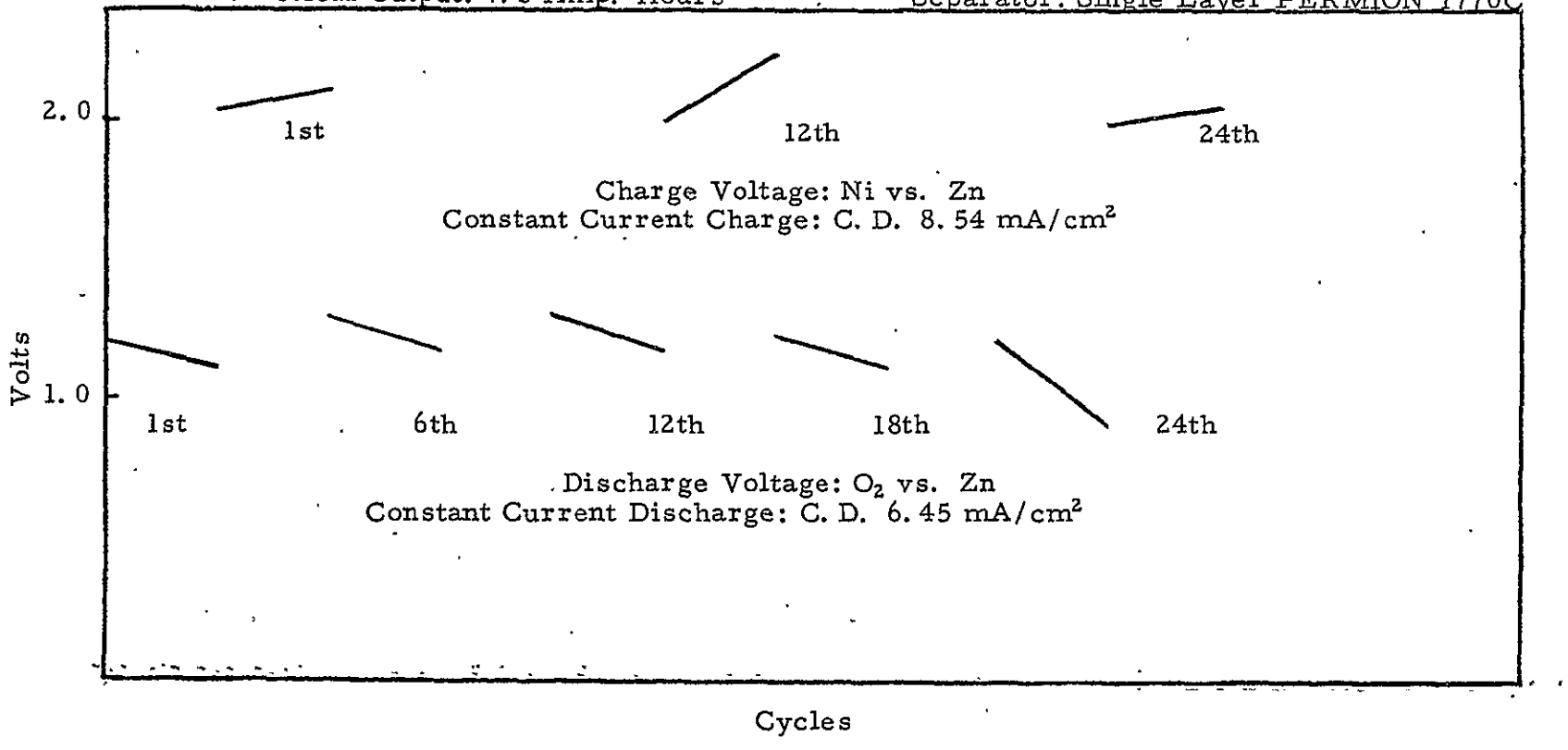

C-5853

FIGURE 49

UNIT CELL EMPLOYING A THIN "FIXED-ZONE" OXYGEN ELECTRODE AND A 10-AMP-HOUR ZnO#19 ANODE

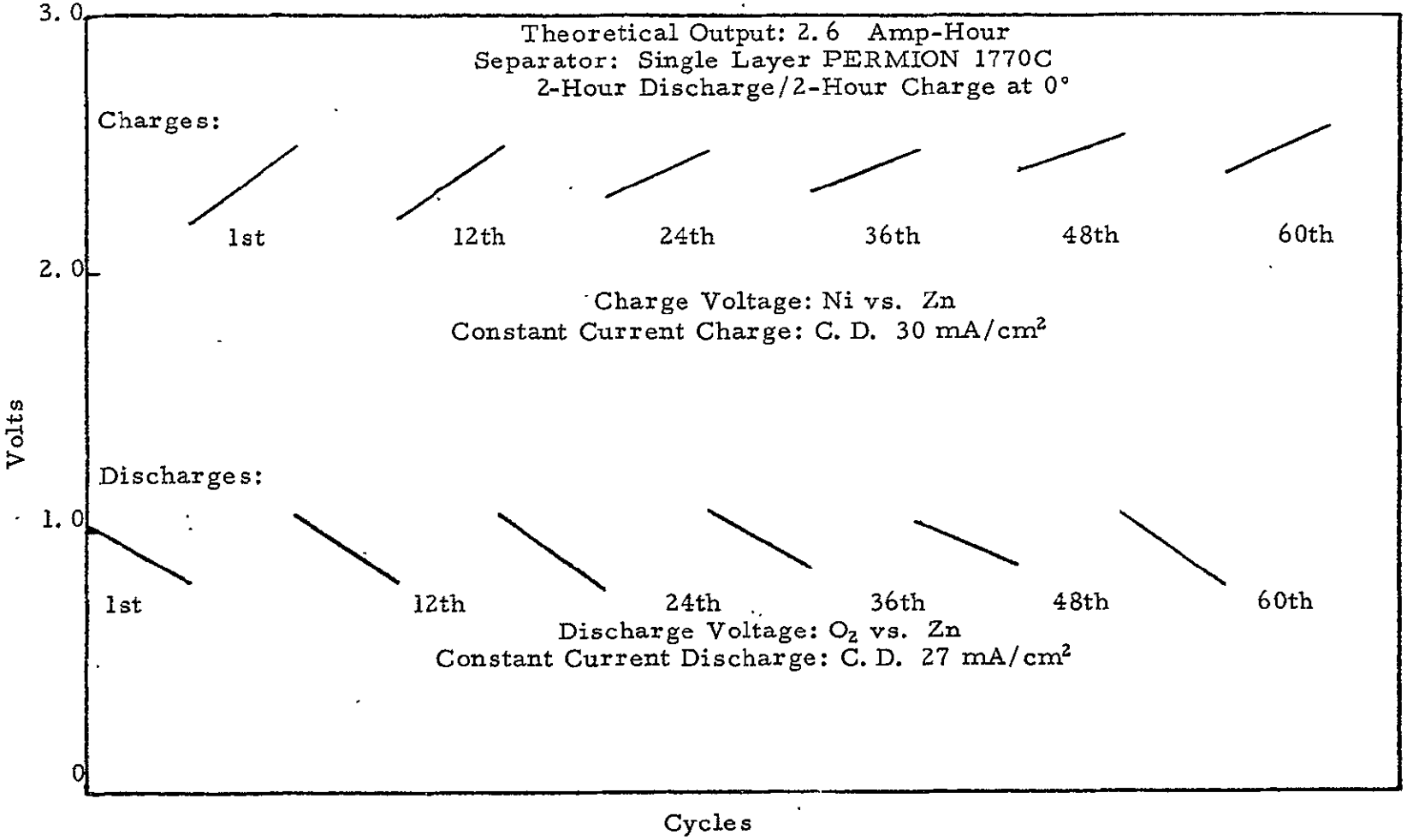

C-5854

FIGURE 50

PERFORMANCE OF A UNIT CELL EMPLOYING A THIN "FIXED-ZONE" OXYGEN ELECTRODE AND A 10 AMPERE-HOUR ZnO-19 ANODE

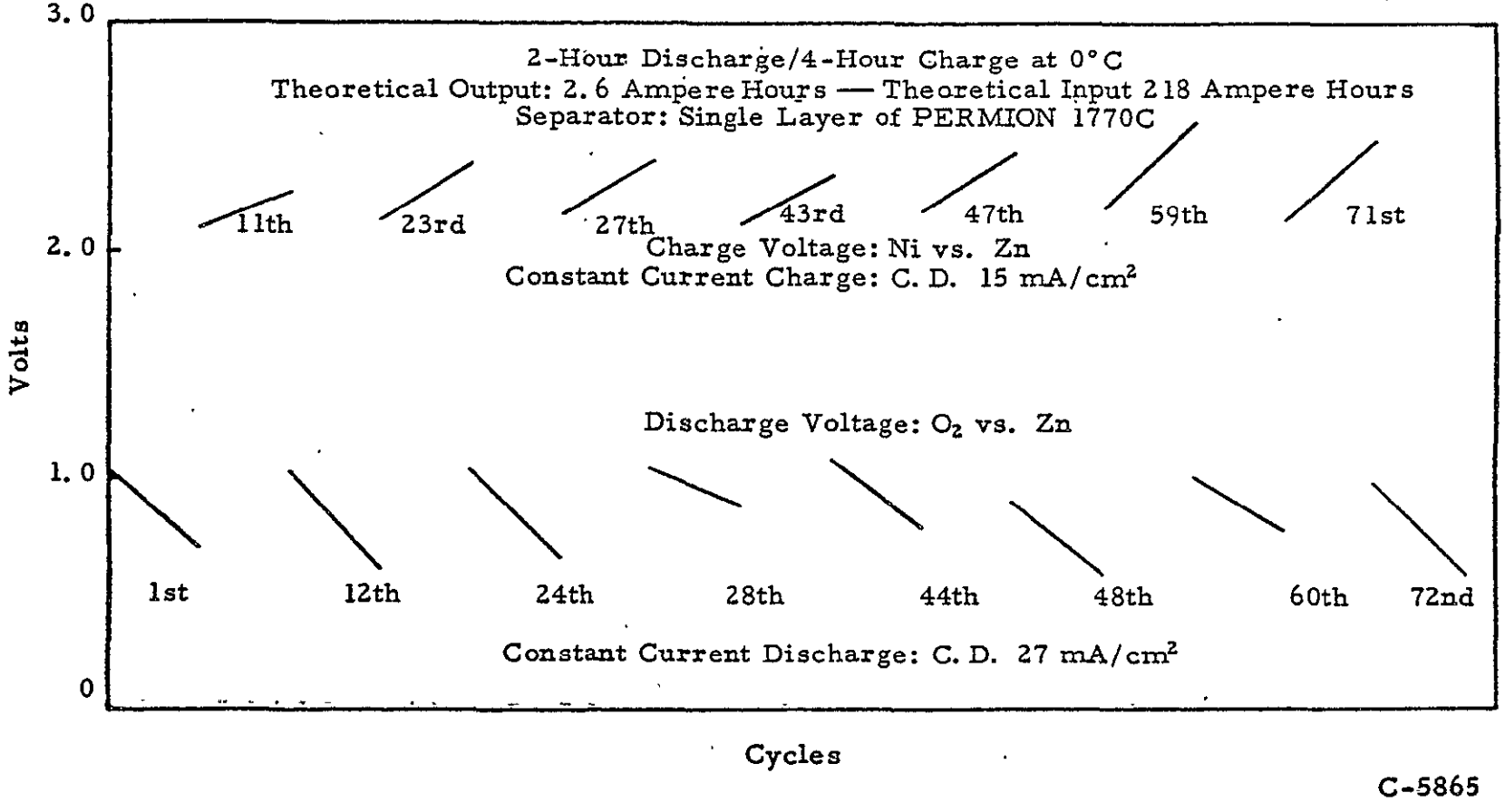

C-5865

FIGURE 51

PERFORMANCE OF A UNIT CELL EMPLOYING A THIN "FIXED-ZONE" OXYGEN ELECTRODE AND A 10-AMPERE-HOUR ZnO#19 ANODE

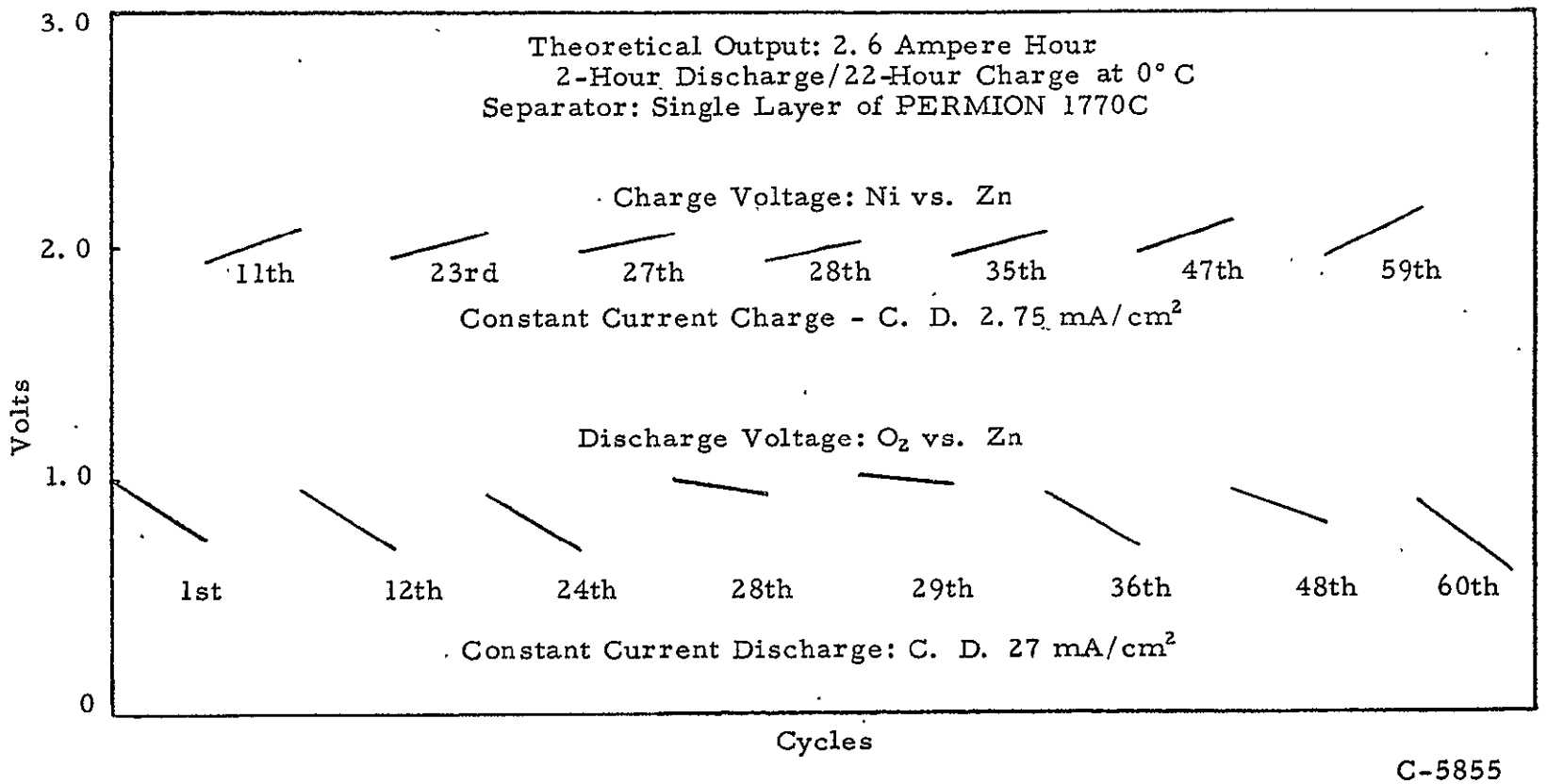

FIGURE 52

PERFORMANCE OF A UNIT CELL EMPLOYING A THIN "FIXED-ZONE" OXYGEN ELECTRODE AND A 10-AMPERE-HOUR ZnO# 19 ANODE

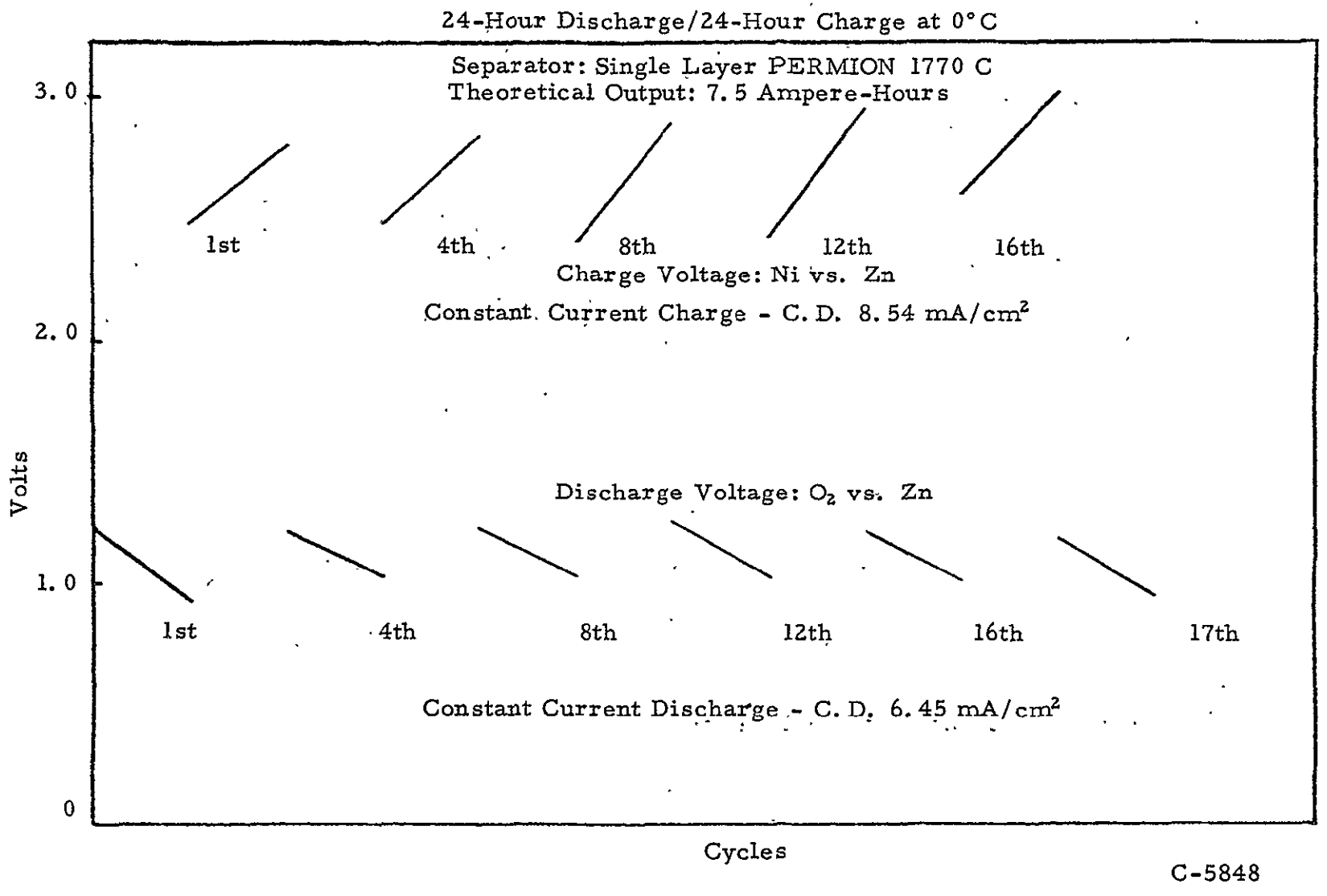

FIGURE 53

DISCHARGE PERFORMANCE OF A UNIT CELL EMPLOYING A THIN "FIXED-ZONE" OXYGEN ELECTRODE AND A 10-AMPERE-HOUR ZnO#19 ANODE CHARGED BY ASYMMETRICAL A-C CHARGE METHOD

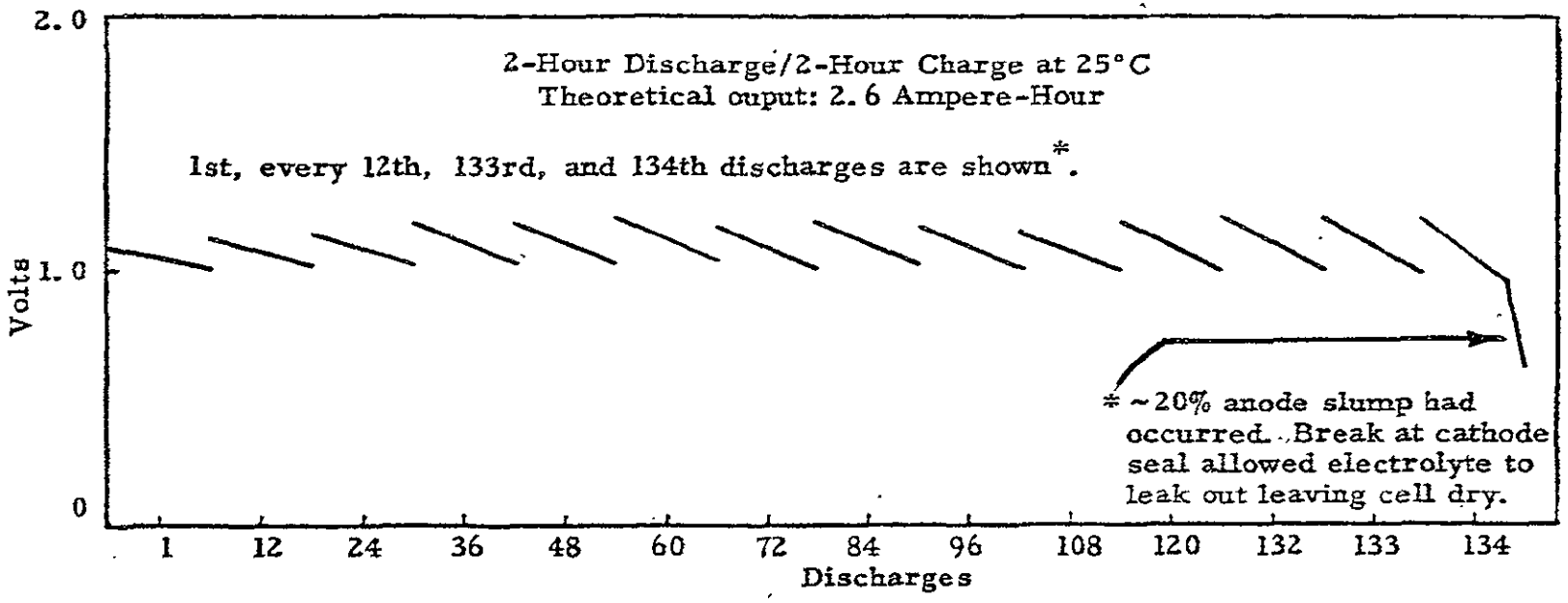

C-5866

FIGURE 54

DISCHARGE PERFORMANCE OF A UNIT CELL EMPLOYING A THIN "FIXED-ZONE" OXYGEN ELECTRODE AND A 10-AMPERE HOUR ZnO#19 ANODE CHARGED BY PERIODIC REVERSED CURRENT METHOD

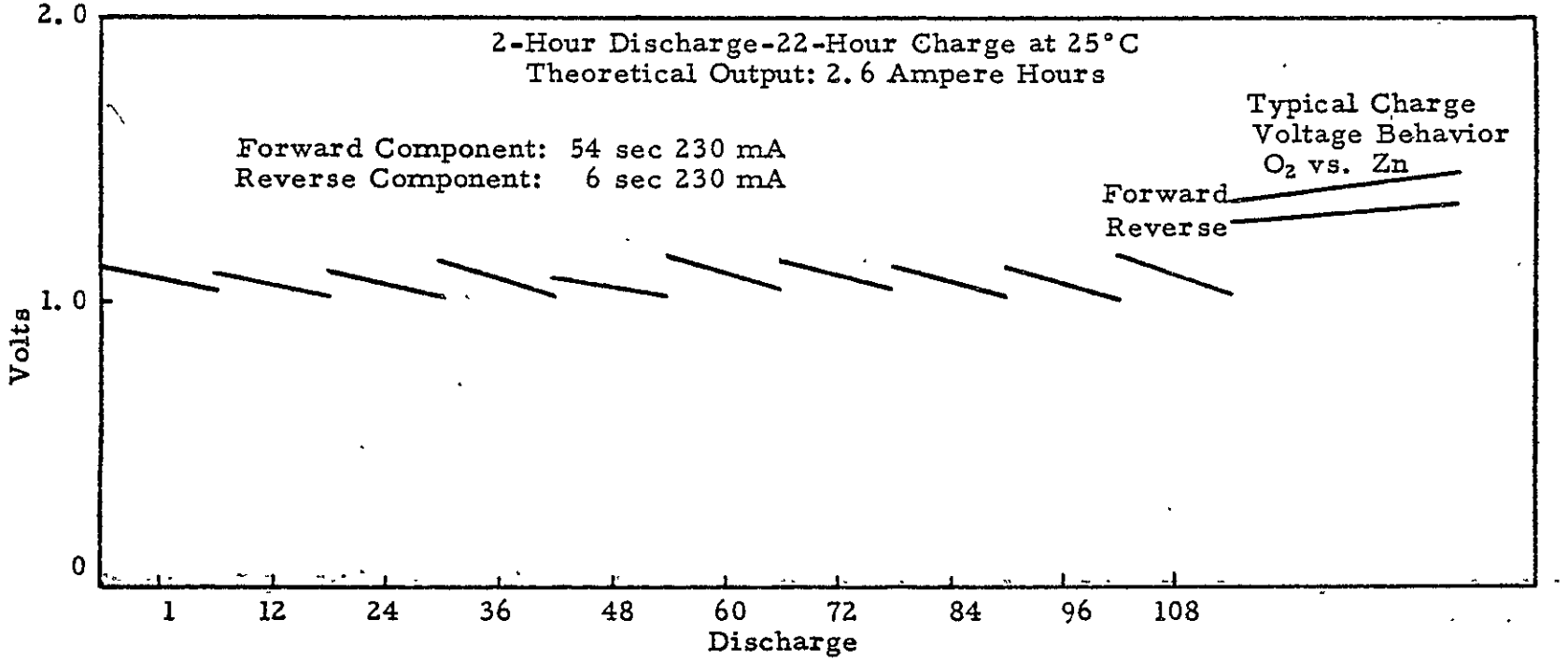

FIGURE 55

PERFORMANCE OF UNIT CELLS EMPLOYING THIN "FIXED-ZONE" OXYGEN ELECTRODES AND 10-AMPERE HOUR ZnO#19 ANODES CHARGED BY PERIODIC OPEN CIRCUIT METHOD

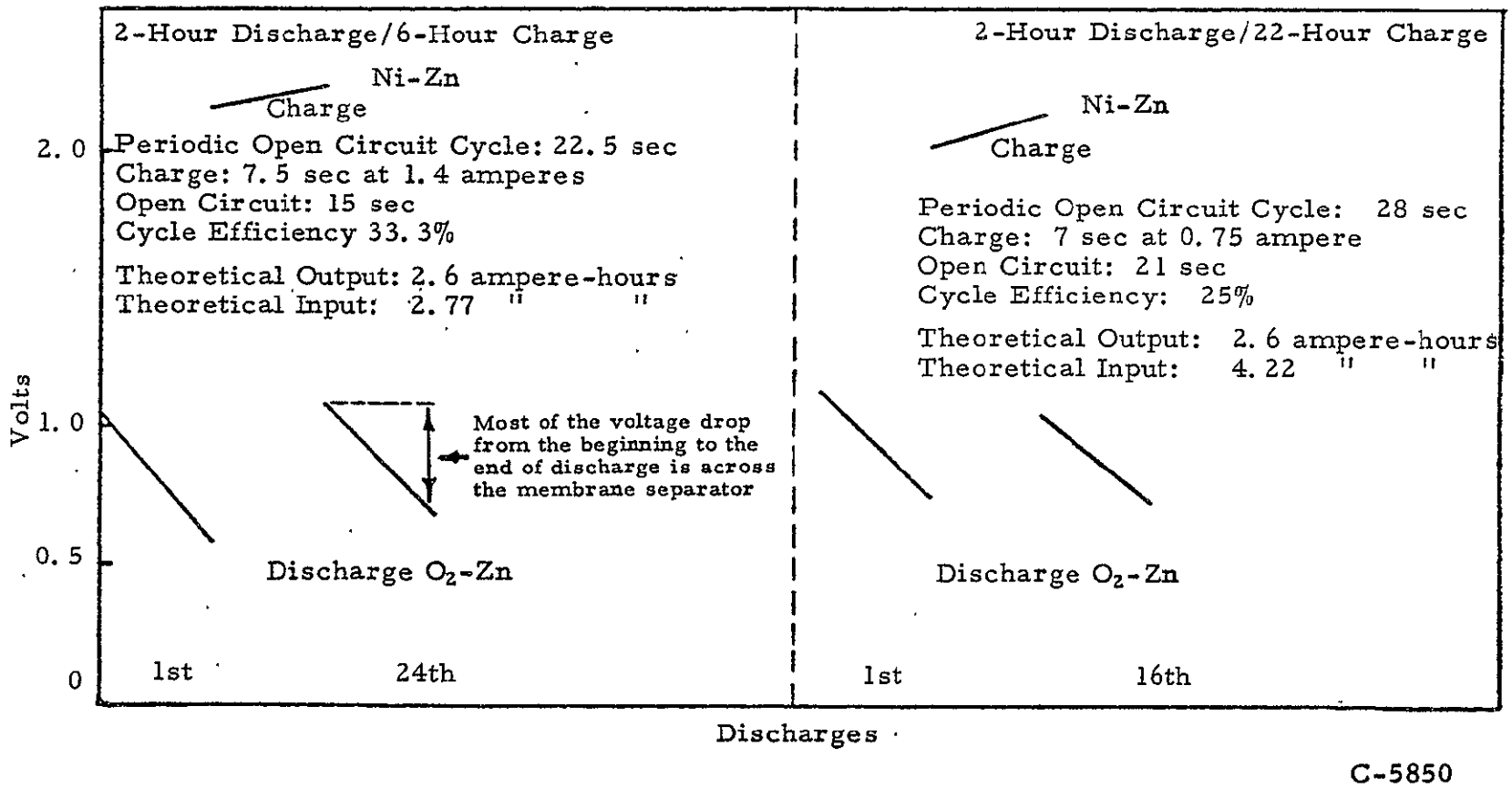

C-5850

FIGURE 56

COMPARISON OF A TYPICAL 2-HOUR DISCHARGE FOLLOWING A 2-HOUR ASYMMETRICAL A-C CHARGING WITH A 2-HOUR DISCHARGE FOLLOWING 2-HOUR CONSTANT CURRENT CHARGING

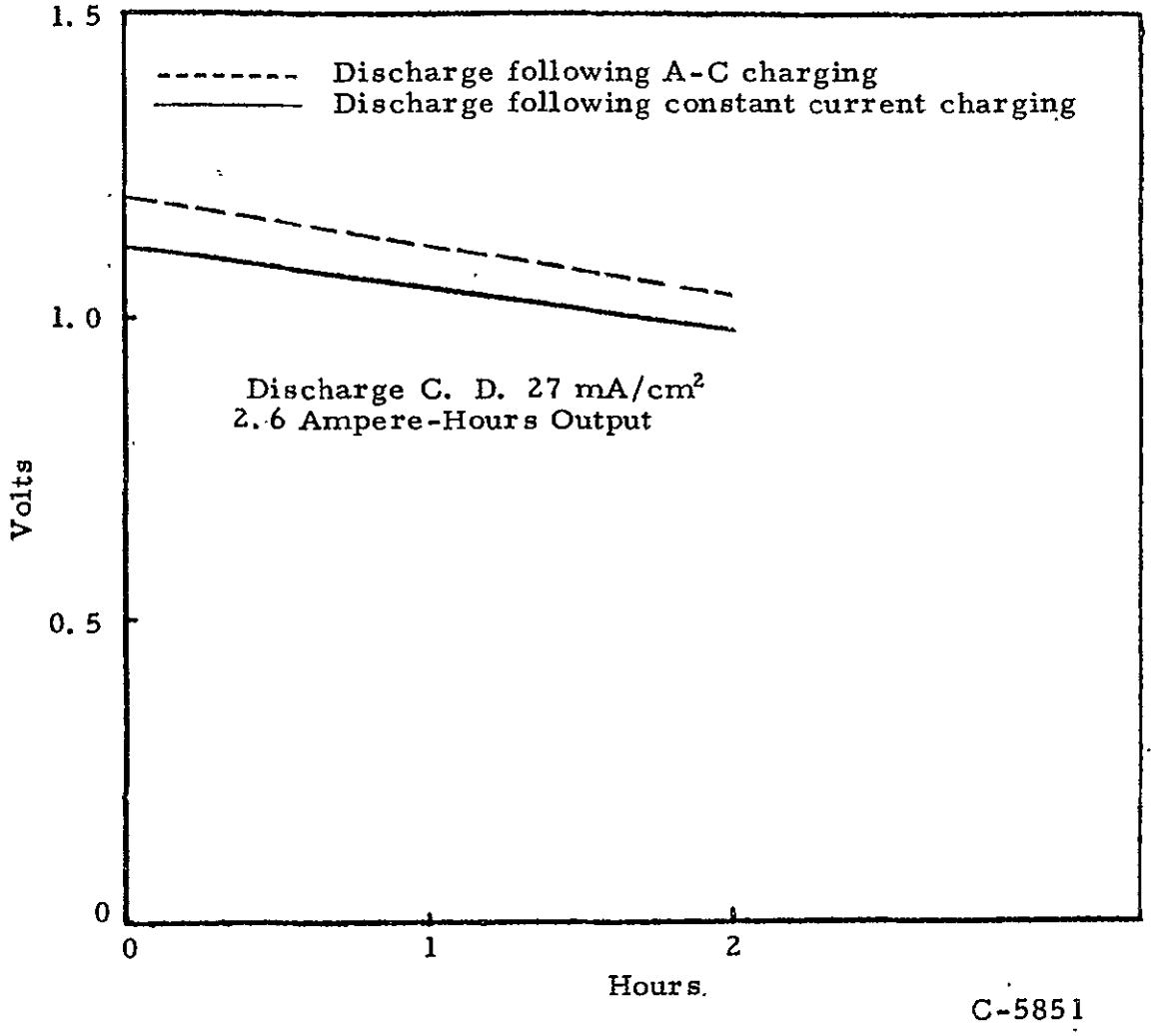

FIGURE 57

COMPARISON OF 2-HOUR DISCHARGE AT 25°C FOLLOWING 22-HOUR PERIODIC REVERSE CHARGING WITH 2-HOUR DISCHARGE FOLLOWING 22-HOUR CONSTANT CURRENT DISCHARGING

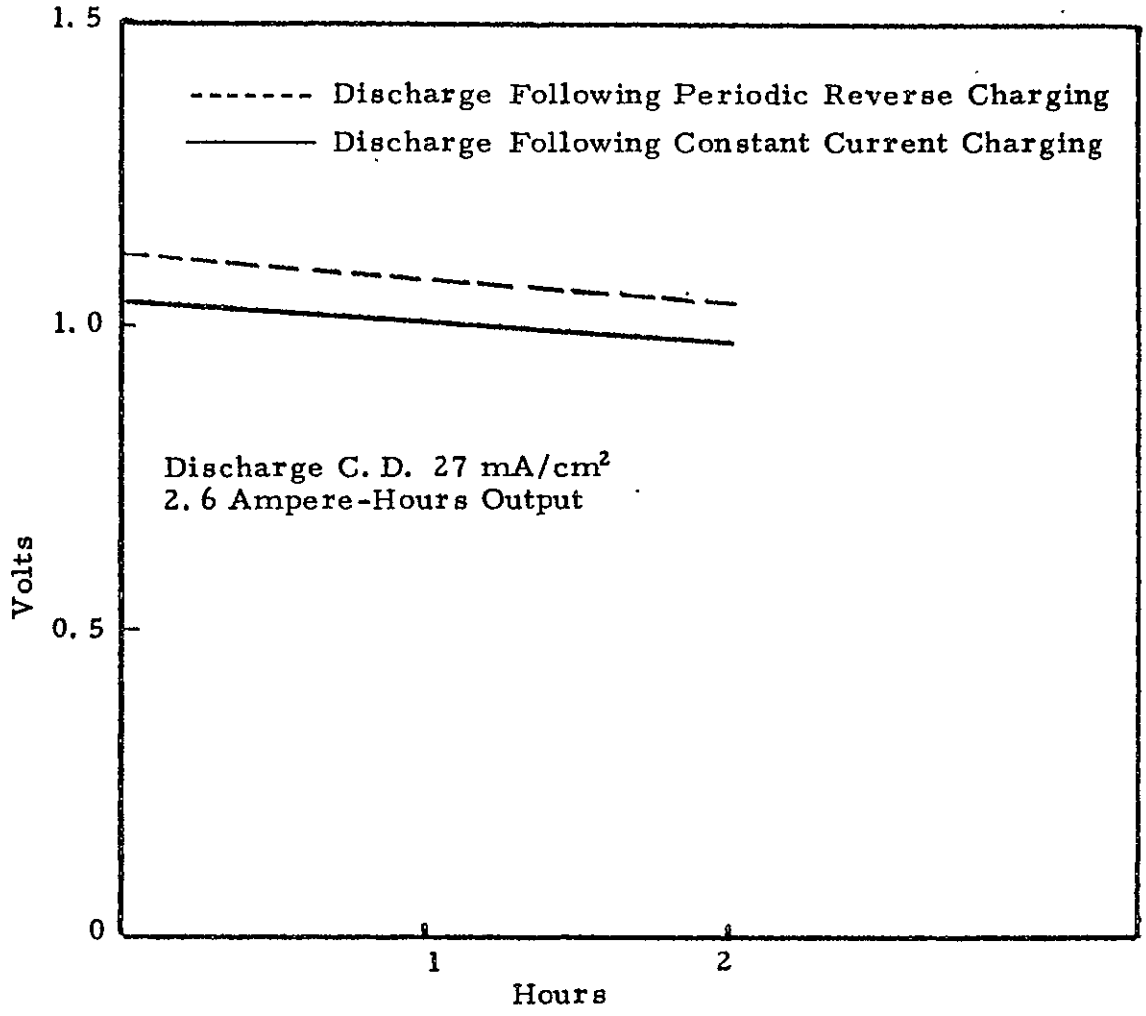

C-5856

J. 6-Volt, 10 Amp-Hr Zinc/Oxygen Rechargeable Battery

1. Design Concept of Battery System

Pursuant to Contract NAS-5-10247, two 6-volt, 10 amp-hr zinc oxygen secondary batteries were built and delivered to NASA. A 2-hour discharge rate and 22-hour charge rate were recommended for these. Appropriate monitoring and safety devices were incorporated in the systems each of which was complete with oxygen containing pressure vessel.

Feasibility studies conducted with unit cells operated at essentially one atmosphere were used in selecting the anodes, membrane separators, cathode materials, etc. Certain compromises were made in the interest of arriving at the most practical battery design for spacecraft use in a zero gravity environment. Thus zinc-oxide type anodes were used in preference to zinc gel anodes even though longer cycle life was obtained in single cells with noncirculating electrolyte from the latter. This was done because of the need to circulate the electrolyte to effect gas-liquid separation if the battery were to be cycled in a zero gravity environment. Electrolyte circulation would have adversely affected the mechanical integrity of the zinc-gel anode because of CMC degradation and subsequent shape change. PERMION 1770C membrane separators were used in both batteries. Union Carbide Corporation "fixed-zone" T-2 oxygen electrodes were used in one of these while American Cyanamid "LAB-40" oxygen electrodes were used in building the second 6-volt, 10 amp-hr battery.

The design concept utilized a common electrolyte which is pumped into and out of each cell through small long channels. These channels result in high resistance conductive paths between cells thereby keeping the parasitic electrical losses to a tolerable level. The effective use of such channels has been demonstrated in fuel cell batteries built and tested at the Parma Technical Center of the Union Carbide Corporation.

2. Construction of Battery System

The proposed system is to operate in a sealed oxygen tank at elevated oxygen pressures. A schematic diagram of the power system is shown in Figure 58. The battery unit with its associated gas/liquid separator-reservoir is contained within the oxygen tank. In operation the reactant oxygen is consumed during discharge. In the charging cycles, oxygen gas is generated within the battery and via the circulating electrolyte is returned to the reactant (oxygen) storage tank for reuse in the next discharge cycle. Circulating the electrolyte by means of a pump removes the generated gas within each cell of the battery. Gas-electrolyte separation would be accomplished in an adjacent compartment by centrifugal action effected by the pump. Hydrogen getters (platinum catalyzed plates) absorb hydrogen gas which may be generated.

FIGURE 58

BLOCK DIAGRAM OF UCC Zn-O_2 BATTERY

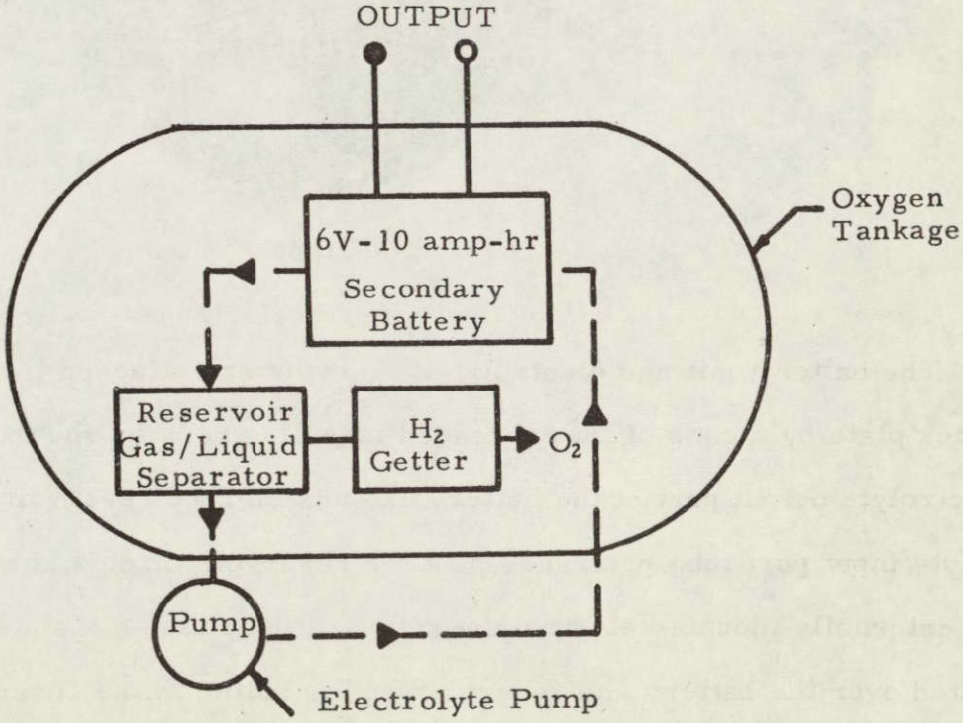

C-4466

The battery construction developed is essentially the same as that proposed in the design study for a 28-volt, 3KWH zinc-oxygen rechargeable battery described in Appendix I. It consists of a compact modular cell which when assembled in a six-cell unit and potted in epoxy resin forms the battery shown in Figure 59.

FIGURE 59

BATTERY UNIT

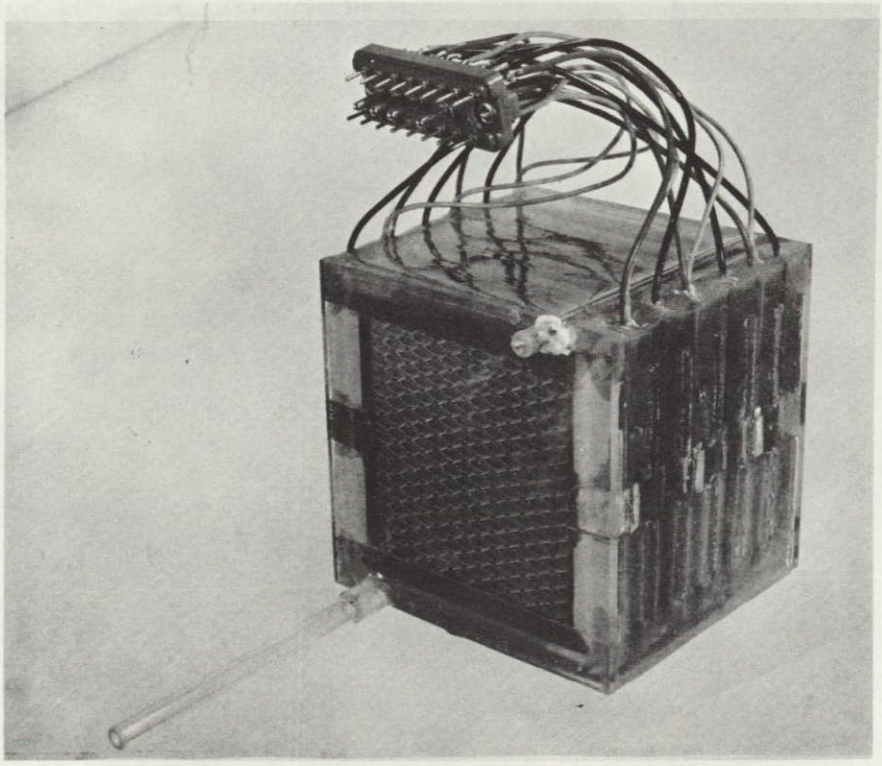

C-4455

The battery unit and electrolyte reservoir are attached to a cover plate and a back plate by means of four threaded mounting rods as shown in Figure 60. The electrolyte output port of the battery extends into the reservoir and the battery electrolyte input port tube protrudes past the reservoir through the cover plate into the externally mounted electrolyte pump. A deep drawn stainless steel case is mounted over the battery and reservoir and is bolted to the cover plate forming the oxygen tankage. The complete rechargeable battery system is shown in Figure 61.

FIGURE 60

SIDE VIEW OF SYSTEM WITH TANKAGE REMOVED

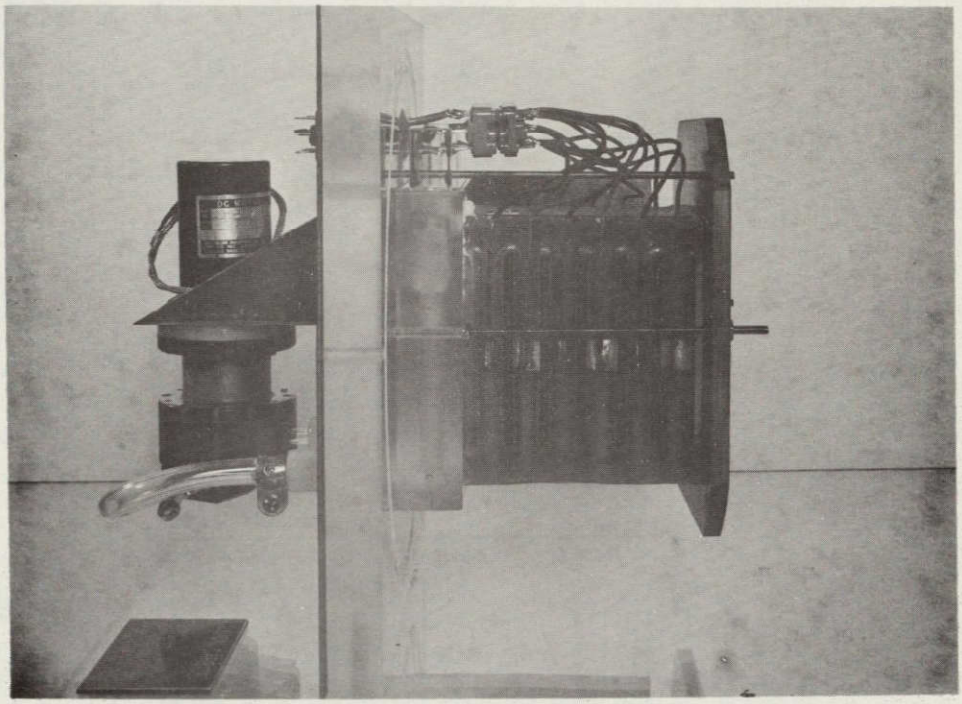

C-4456

FIGURE 61

UNION CARBIDE ZINC-OXYGEN RECHARGEABLE 6-VOLT
10 AMPERE_HOUR BATTERY SYSTEM

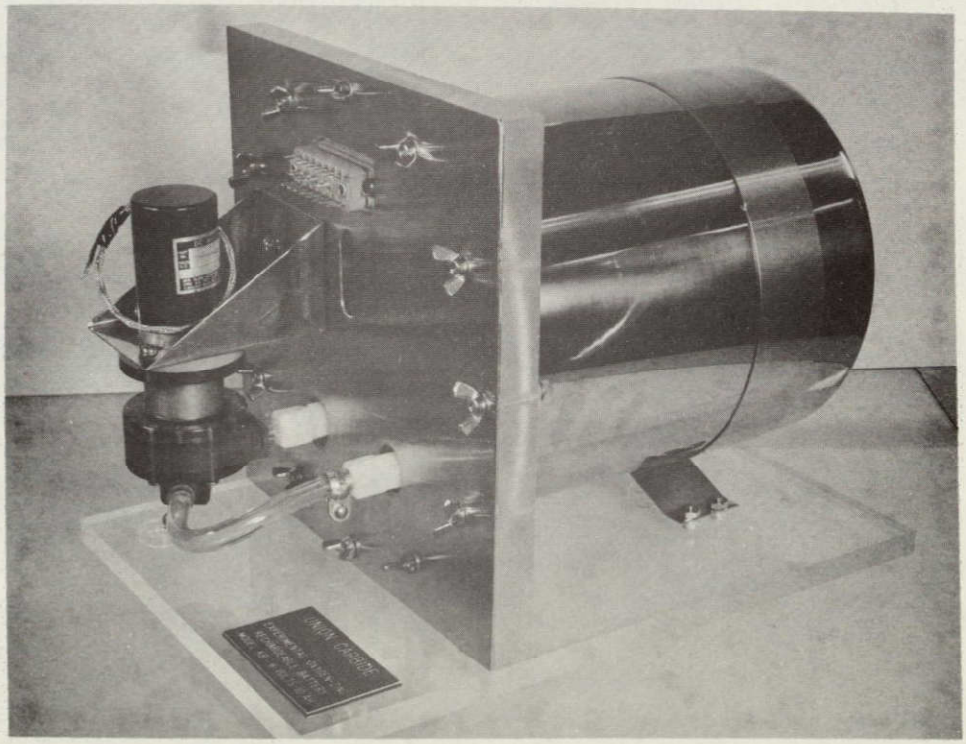

C-4458

a) Modular Cell

The modular construction consists of an anode and two cathode frames which are cemented together to form a dual cathode cell, as shown in Figure 62. Appropriate channels and indentations are incorporated in each frame to form the necessary electrolyte and gas cavities.

FIGURE 62

MODULAR CELL

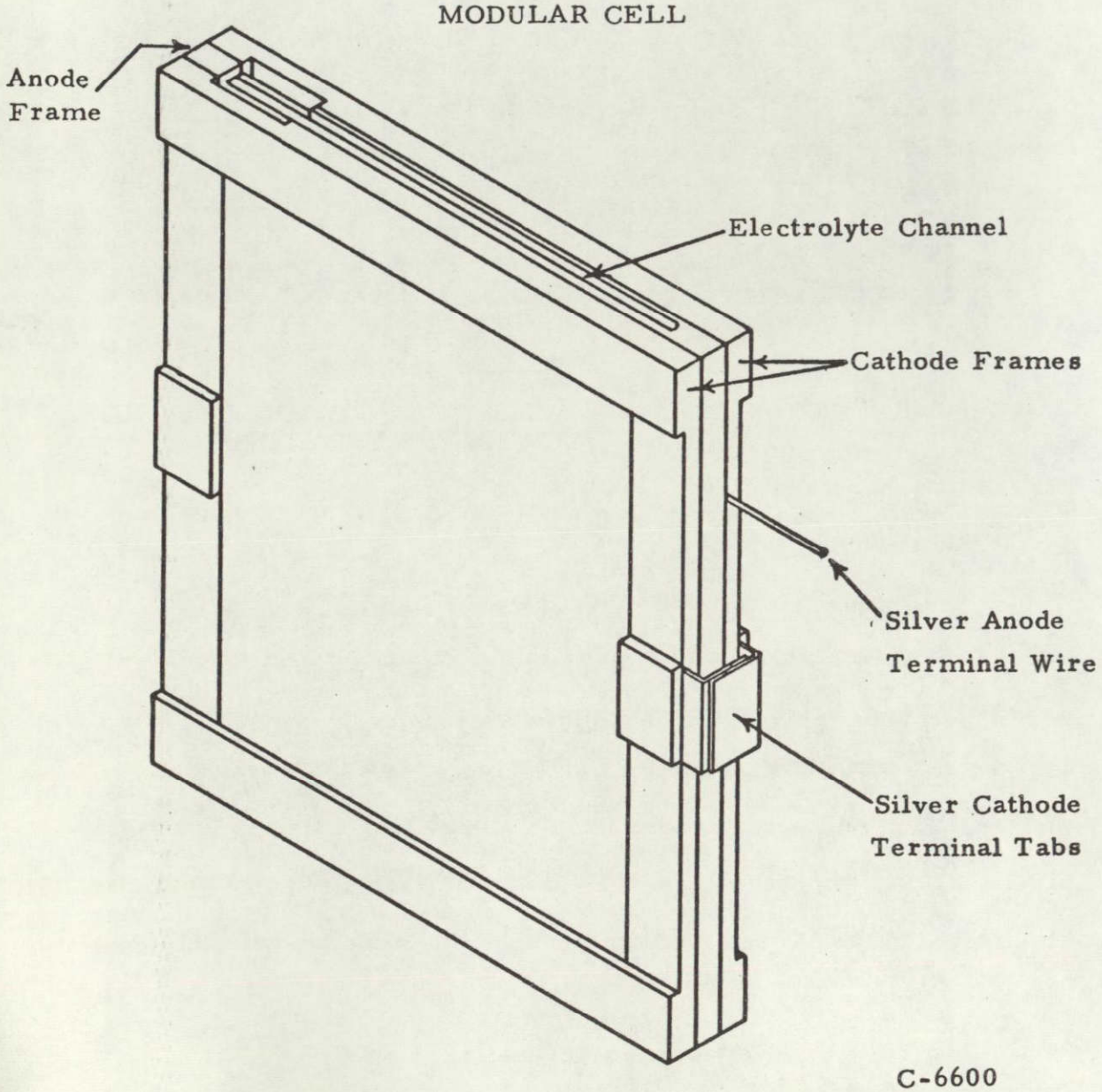

An exploded cross-sectional sketch of the modular cell construction is shown in Figure 63. The molded anode contains 67.7 grams of #ZnO-19 anode mix molded at 500 psi into a perforated silver envelope formed of three spot-welded 3/0 expanded silver grids. The resulting electrode measures 3" x 3" x 0.135". A silver wire (0.032" diameter) spot-welded to the silver envelope serves as the negative terminal lead for the cell.

The cathodes obtained were cut to a 3" x 3" size. A folded 1/4" strip of 5 mil silver sheet, which serves as a current collector, is attached to one edge of the cathode by means of silver epoxy adhesive. Attached to the current collector is a 5 mil by 1/2" wide silver terminal tab. The cathode is cast into an epoxy frame made of three parts Union Carbide 2774 resin and two parts VERSAMID 125 resin. Slots are built into the cathode frame to produce the necessary internal input and output electrolyte ports as well as passages to the exterior to obtain access to the oxygen. The cavity on one side of the cathode frame forms the electrolyte cavity which contains an expanded grid, separator and charging grid, if used. The cavity on the other side serves as the oxygen access passage.

b) Six-Cell Unit

The battery supplied under this contract consists of six (6) cells assembled and potted in epoxy resin. As shown in Figure 64, long electrolyte channels (1/16" diameter x 2-1/4" long) are incorporated in the input and output of each cell to circulate the electrolyte and provide resistive electrical paths between cells to reduce electrolyte leakage currents. The electrolyte ports of each cell are connected in parallel with the input at the bottom of the battery and the output at the top.

Two types of batteries are supplied in this contract. The cells of each battery are constructed essentially in the same manner except for

FIGURE 63

EXPLODED CROSS SECTION OF MODULAR CELL

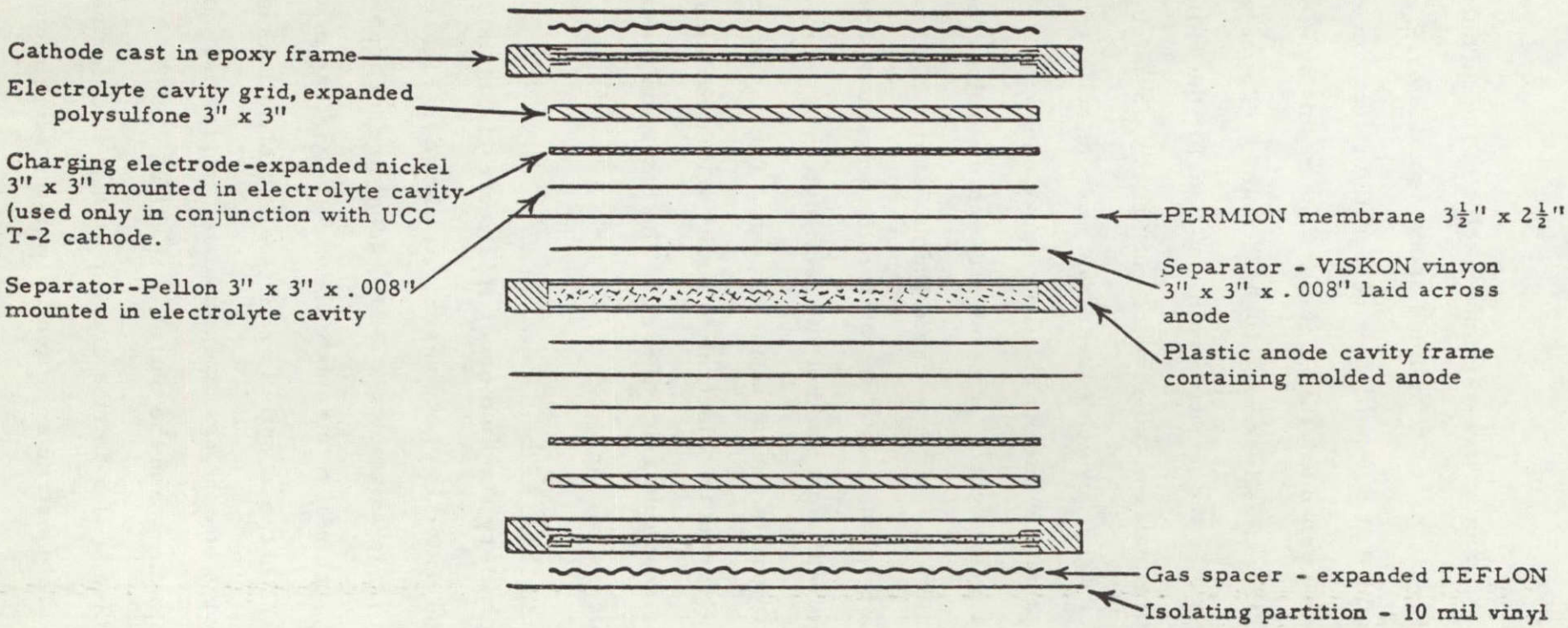

C-6593

FIGURE 64

SIX CELL BATTERY UNIT POTTED IN EPOXY

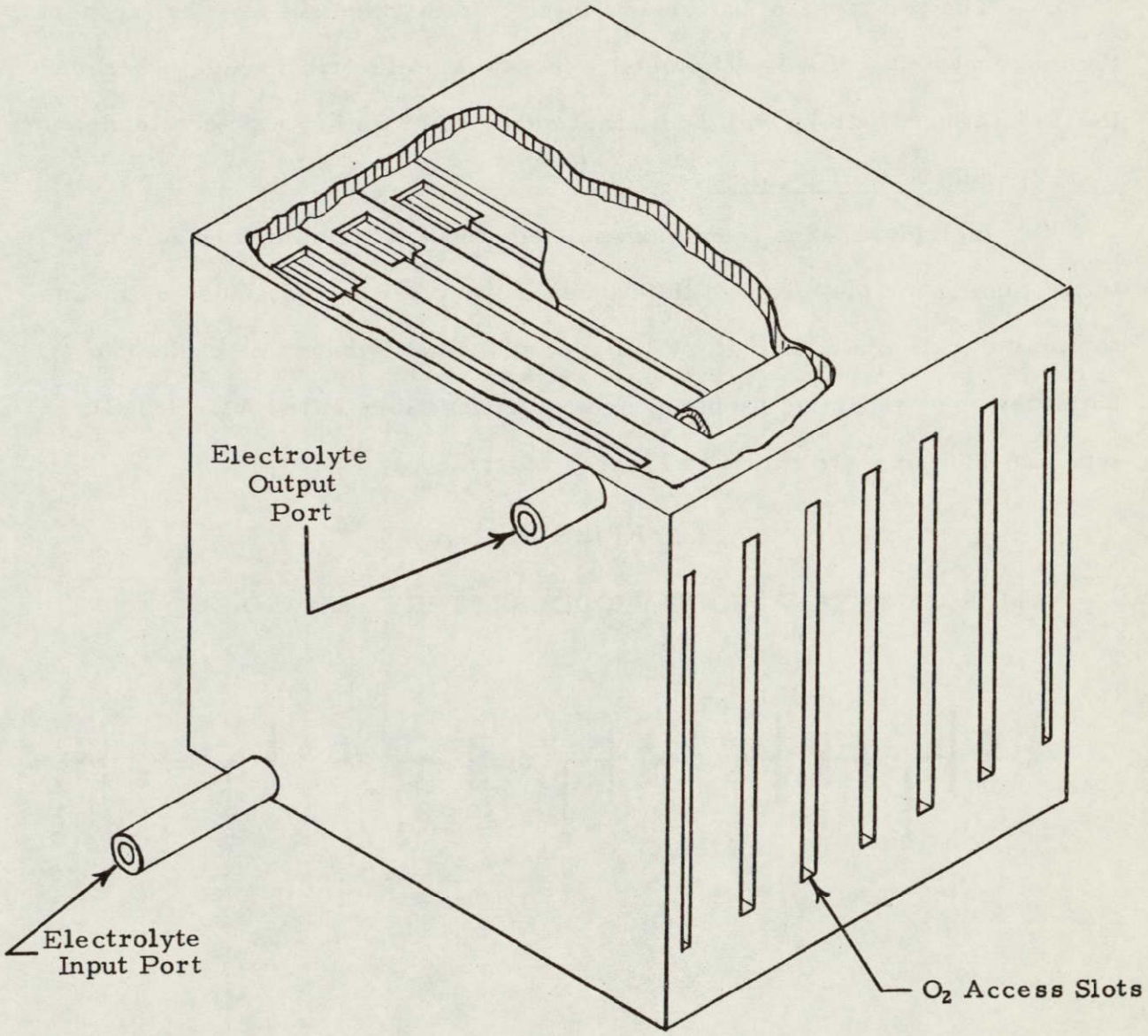

C-6601

the cathode material and the charging electrode. The battery having cells with the Union Carbide T-2 "fixed-zone" cathode material each contain a separate nickel charging electrode. The battery containing cells having American Cyanamid "LAB-40" cathodes utilized the cathode as the charging electrode.

The two types of batteries can also be distinguished by the fact that the one containing "LAB-40" cathodes has twelve electrical leads; whereas, the T-2 cathode battery with additional charging grids has eighteen leads.

c) Electrical Circuitry

Individual leads from each cell electrode are terminated in a plug in the tank cover plate to facilitate inner battery cell connections and means to monitor cell and total battery voltage. Schematic diagrams of the two batteries and respective terminal number connections at the AMPHENOL type 126-806 plug are shown in Figures 65 and 66.

FIGURE 65

(AMERICAN CYANAMID CATHODE) BATTERY TERMINALS

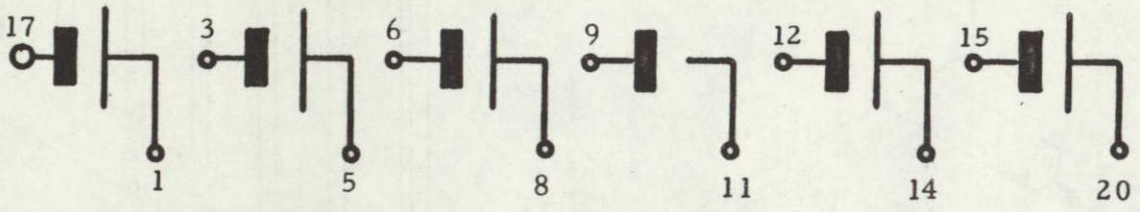

C-4467

FIGURE 66

(UNION CARBIDE CORPORATION T-2 CATHODE) BATTERY TERMINALS

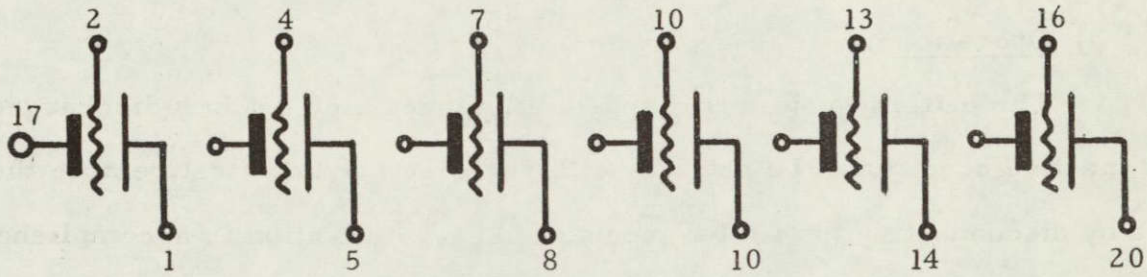

C-4468

d) Reservoir

The reservoir is a block of plastic positioned between the battery and the tank cover. It contains a cavity into which the output electrolyte port of the battery empties. At this point, the gas, which is transported from the interior of the battery in the form of bubbles in the electrolyte, is separated and exhausted into the gas tankage. The reservoir also serves to compensate or adjust for electrolyte volume changes which occur in the battery.

e) Electrolyte Pump

The electrolyte pump is mounted externally on the face of the cover plate by means of a stainless steel bracket. It is mounted outboard to prevent combustion due to the operation of the D. C. (brush) pump motor. The pump operates at tank pressure and is magnetically coupled to but physically isolated from the motor and the external atmosphere.

The pump furnished was designed and used on another project and is much more powerful than necessary for this use. It requires approximately 2.5 volts at 200-250 mA for operation. The pump is rotated at a slow speed and is required to deliver only enough pressure head or electrolyte flow to produce an output of electrolyte from the battery into the reservoir.

f) Tank

The tank is a deep drawn stainless steel container whose bottom is reinforced by a 1/16" welded, circular, stainless steel plate. Four 1/8 NPT ports are installed on the bottom. The open end of the tank has a rolled over lip.

g) Operation

The battery system is shipped fully assembled but in a discharged and inactive condition. To activate (fill with electrolyte), first remove the tank by disconnecting the twelve mounting lugs. Activation is accomplished by injecting 41% KOH + 3-1/2% ZnO by means of a hypodermic syringe into one of the vent holes on the top of the electrolyte reservoir as shown in Figure 67. Electrolyte should be added until the level in the reservoir is at the input tube port from the battery.

FIGURE 67
BATTERY ACTIVATION

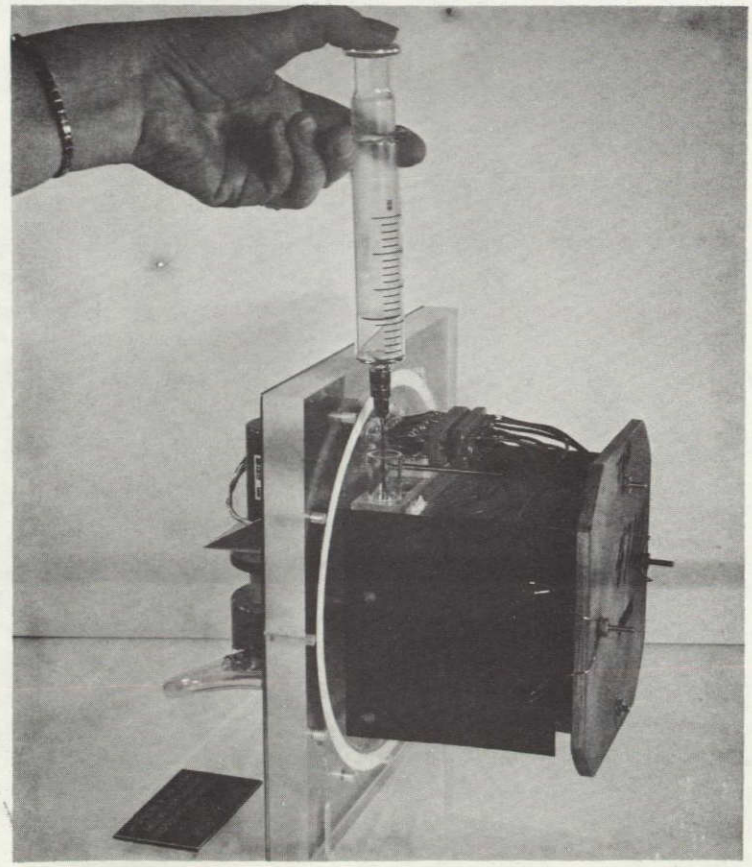

C-4457

h) Socket Connections

The respective cell connections to form the battery are accomplished at the external mating socket connector, AMPHENOL No. 126-807.

In the case of the battery having "fixed-zone" cathodes and an additional charging electrode per cell, a separate socket connection is used, shown in Figure 68 for the charging cycle only.

In the case of the battery having "LAB-40" cathodes, the same socket connections, shown in Figure 69 are used for connecting the cells in series for both charge and discharge cycles.

FIGURE 68

CHARGING SOCKET CONNECTIONS FOR CELLS HAVING CHARGING ELECTRODES

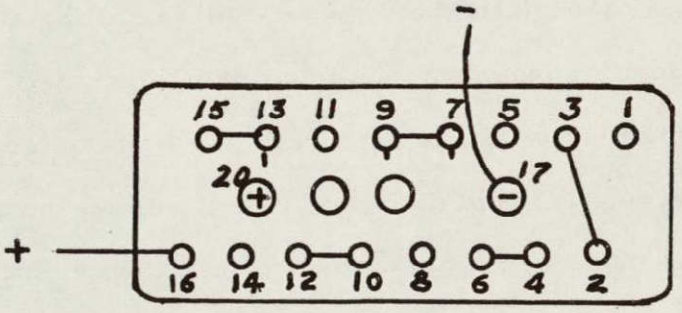

C-4469

FIGURE 69

DISCHARGE SOCKET CONNECTIONS

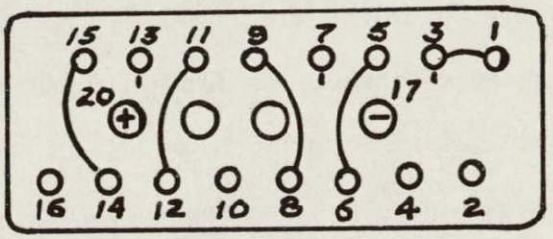

C-4470

3. Testing of Experimental Battery System

Prior unit cell work was conducted with oxygen at essentially one atmosphere pressure. Operation in a closed vessel at elevated oxygen pressures resulted in an increase in cell operating voltage, as well as volumetric electrolyte changes due to compression of inner cell entrapped gas. Since a complete evaluation of the pressurized system would require time and effort far in excess of the commitment of this contract, only the major aspects of such an evaluation were considered. These included (a) the design and construction of a prototype battery suitable for testing, (b) enclosing the battery in a suitable tank, (c) providing a means of pumping electrolyte through the battery, and (d) installing a simplified system for electrically connecting and monitoring each cell. The testing required monitoring the voltage of each cell, the battery temperature, and the tank gas pressure. A rapid decrease in cell voltage indicates cell reversal (of one or more cells) accompanied with the evolution of heat and hydrogen.

For safety reasons, the battery system testing was programmed to evaluate by steps each operating condition in order not to exceed the known safety limits. During the initial discharge cycle, the battery was operated at low tank pressure to determine the feasibility of circulating the electrolyte and the ability of the battery to perform at rated capacity. Subsequent discharge cycles at higher oxygen operating pressures included battery temperature

measurements and extended operating time. The danger of ignition at elevated oxygen pressures plus the possible generation of hydrogen required caution and verification of safe operating conditions.

a) Single Modular Cell Test - (K-1)

This test was conducted to evaluate the feasibility of circulating electrolyte through a cell.

A single cell was constructed (shown in Figure 70) having a "LAB-40" cathode and a zinc oxide type anode. Channels were provided to permit oxygen flow across the face of the cathode, and ports were used to permit electrolyte flow through both inner cavities of the cell.

Electrolyte was circulated through the cell at a slow rate and reused by manually maintaining a electrolyte pressure head at the input port of the cell to produce a flow from the output port. Figure 71 is a chart of the test results showing the voltage level spread for the even discharge and charge cycles. The test was terminated after 51 cycles because of oxygen supply failure over an unattended weekend. Discharging under the conditions of complete depletion of oxygen produces wetting and/or flooding of the cathode which permanently damages the cell.

The test proved the practicability of circulating electrolyte through various chambers of the cell and the collection and transporting of the generated gas external to the cell. Such electrolyte circulation is deemed necessary for the battery to operate in the zero gravity environment of space. Provision of a suitable pump in the electrolyte circulation system would create a synthetic gravitational field for the separation of O_2 from liquid electrolyte during battery charging.

FIGURE 70

PROTOTYPE HALF-CELL K-1

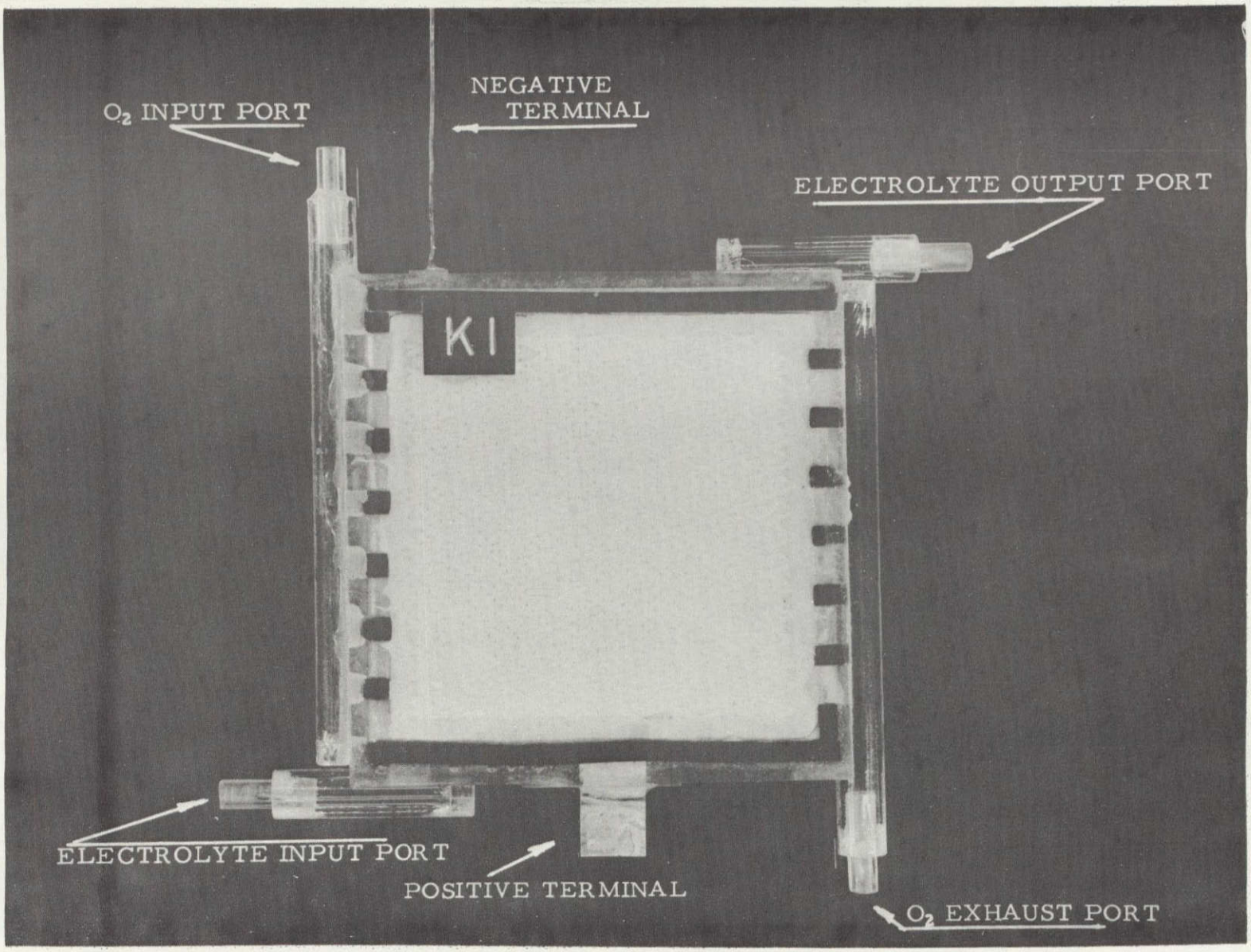

C-5796

FIGURE 71

CELL VOLTAGE VS. CYCLE LIFE
CELL NO. K-1

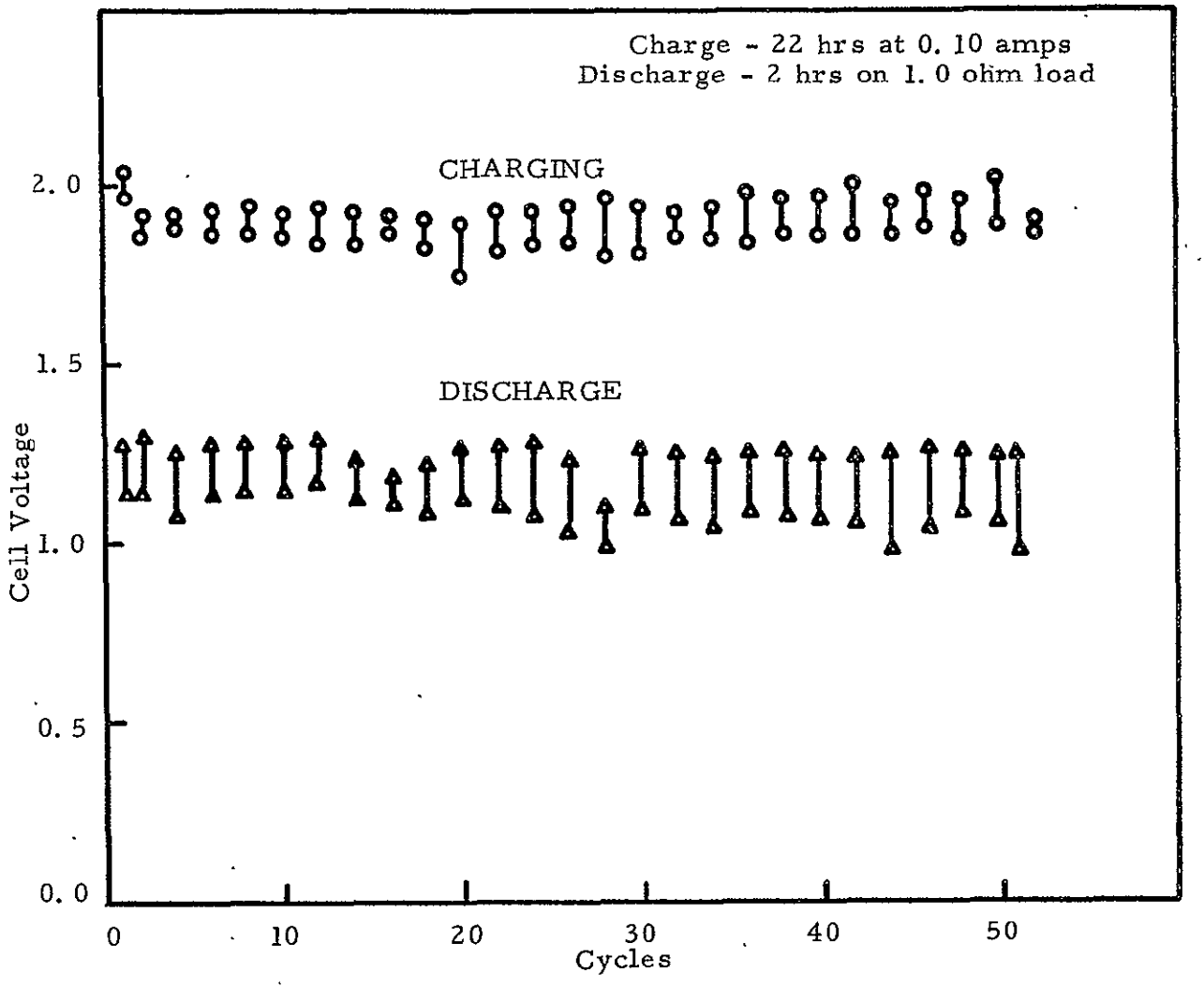

C-6594

b) Battery KB-3

The initial test of the rechargeable battery system was conducted with battery KB-3 which was built with Union Carbide type T-2 cathodes. Due to electrolyte leakage problems, the discharge cycles were conducted with the battery in the tank under manually controlled oxygen conditions, and the charge cycles were performed with the battery outside the tank to allow dissemination of the generated gas into the atmosphere.

Charts of the test data for the first three discharge cycles may be seen in Figure 72. The first discharge cycle proved the feasibility of circulating the electrolyte through both sections of each cell, the collecting of electrolyte and the separation of gas and electrolyte in the reservoir. The battery operated on a 3-ampere load at voltages above six volts.

The second discharge cycle was conducted in the same manner as the first with the battery drain steadily increased in 1-ampere steps to the rated discharge drain of five amperes. This test was terminated due to the rapid decrease in voltage of one cell below 0.8 volt.

The objective of the third discharge cycle was to determine the battery temperature rise and the effect of elevated oxygen tank pressure on the operation of the battery. The battery temperature increased to 132°F on 5-ampere discharge. When the drain was reduced to 3 amperes, the temperature decreased and leveled off at 118°F. The tank was pressurized with oxygen to 12.7 psig with no adverse effects.

In the first three charge cycles, the capacity of the anode was steadily increased by charging to sustain a 3-ampere hour discharge. The fourth discharge cycle is shown in Figure 73. After flushing with oxygen, the system was pressurized with oxygen to 13.4 psi, and after 32 minutes, the tank pressure was

FIGURE 72

ZINC/OXYGEN RECHARGEABLE BATTERY
NO. KB-3

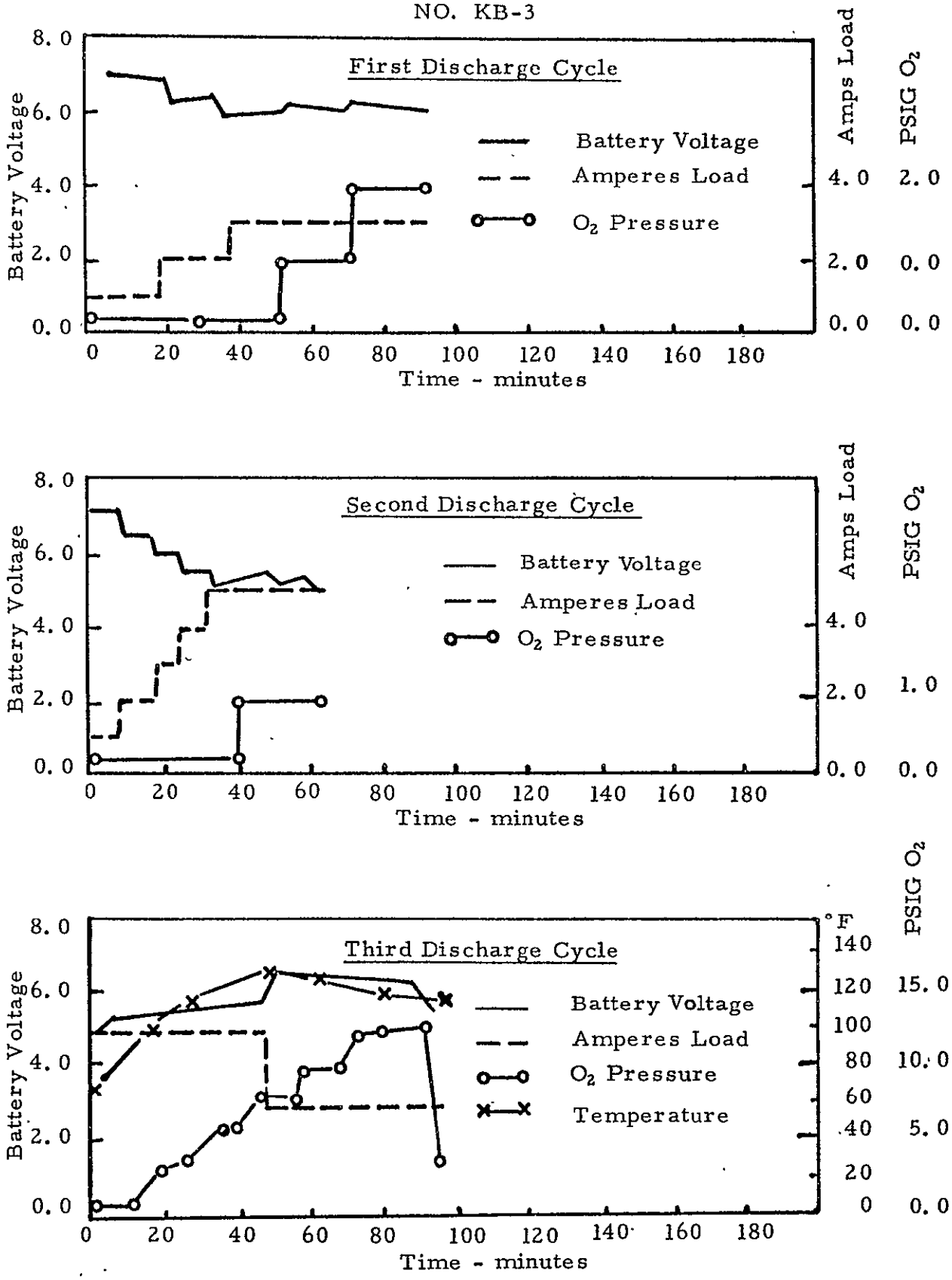

C-6960

FIGURE 73

ZINC/OXYGEN RECHARGEABLE BATTERY
NO. KB-3

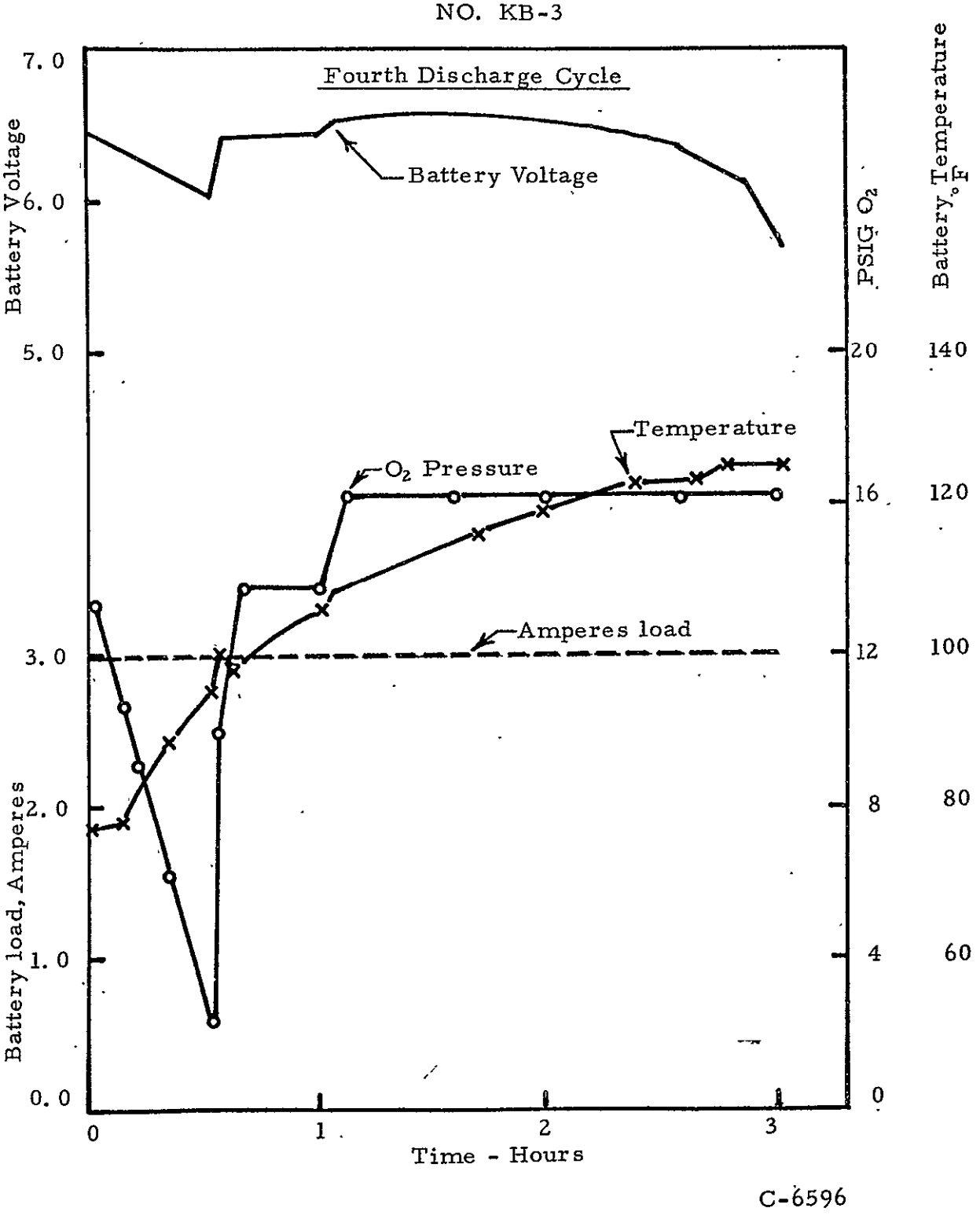

again manually increased with oxygen. While the oxygen consumption, as indicated by the decrease in tank pressure, is greater than the calculated battery oxygen utilization, subsequent analysis of tank gas in later tests indicated the presence of nitrogen in sufficient percentages (16%) to partially account for the difference. On maintaining the current drain at 3 amperes, the battery temperature increased to 125°F which is within a safe operating range and would not dictate the use of a heat exchanger.

c) Battery KB-8

Battery construction improvements eliminated initial battery electrolyte leakage but subsequent problems involving fluctuation of electrolyte levels prevent closed operation on the charge cycle. Due to gas generation, the electrolyte level, as visually noted at the electrolyte reservoir, increases and foaming occurs on the charge cycle. In the discharge cycle, gas tank pressure greatly reduces the electrolyte level to a point of affecting operation.

It was not possible in the limited amount of system testing to effect a balance which would allow continued closed system operation for both the discharge and charge cycles.

The KB-8 battery built with American Cyanamid cathodes ("LAB-40") was discharged across a fixed resistive load of 2.0 ohms. After alternately flushing and pressuring the tankage to 10 psi with oxygen several times to reduce the nitrogen content to a low percentage, the tank was pressurized to 26.4 psi with oxygen and secured. The fixed load was then applied. The chart of the first discharge cycle is shown in Figure 74. Operation was continued for 3.75 hours and was terminated after the rated capacity of 10.0 ampere-hours had been exceeded.

Three discharge cycles (Figures 74, 75, and 76) for the KB-8 battery were obtained before serious blockage of the electrolyte passage occurred during the fourth charge cycle and terminated the test. The blockage was due to the presence of zinc oxide in the parallel electrolyte connecting channels which resulted in an internal gas pressure buildup, eventually forcing gas and electrolyte through the cathode.

During the third charge cycle, gas samples were taken to determine whether hydrogen had been generated. The tank was pressurized and flushed with oxygen, then maintained at 1.0 psi with the battery charging at the 0.5 ampere rate. The tank pressure increased to 4.8 psi after two hours on charge at which time gas sampling indicated 73% oxygen, 26% nitrogen and 1% hydrogen. After increasing the charging rate to 1.0 ampere at a tank pressure of 2.4 psi, a second sample taken after two hours indicated 82% oxygen, 16% nitrogen and 1.5% hydrogen. The presence of hydrogen made it advisable not to pressurize the tank for the 22-hour charging cycle.

NEW TECHNOLOGY

There is one new technological advance which is believed to fall within the scope of this contract to be reported, i.e., the cushioning separator on either side of the Borden C-3 membrane to prevent physical damage to the soft-swelled C-3 membrane. The material employed for this cushioning separator was a nonwoven cellulose mat. Protection of the Borden separator in this manner contributed to the improved cycle life on the two-hour discharge/two-hour charge regime.

FIGURE 74

ZINC/OXYGEN RECHARGEABLE BATTERY
NO. KB-8

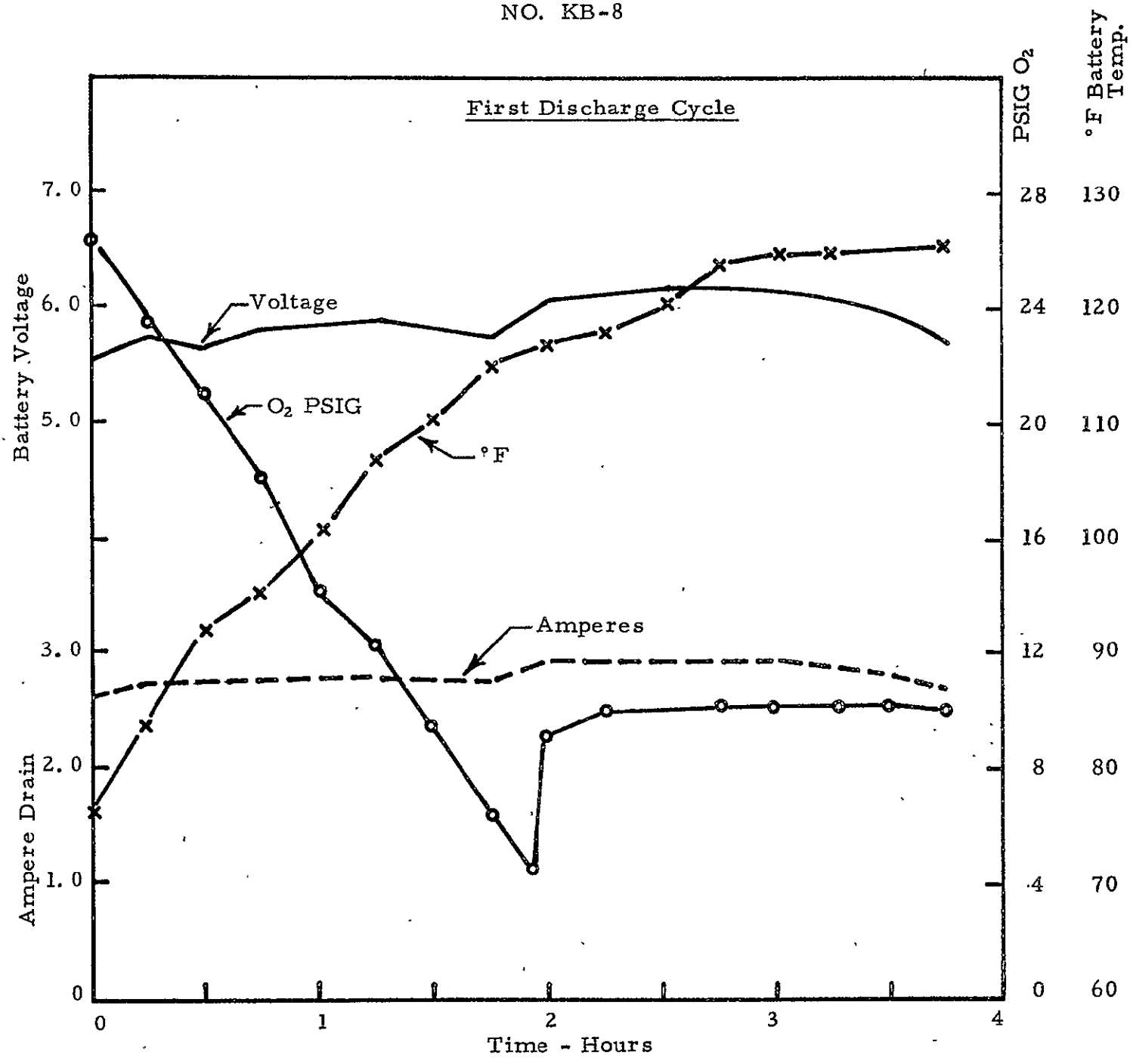

C-6597

FIGURE 75

ZINC/OXYGEN RECHARGEABLE BATTERY
NO. KB-8

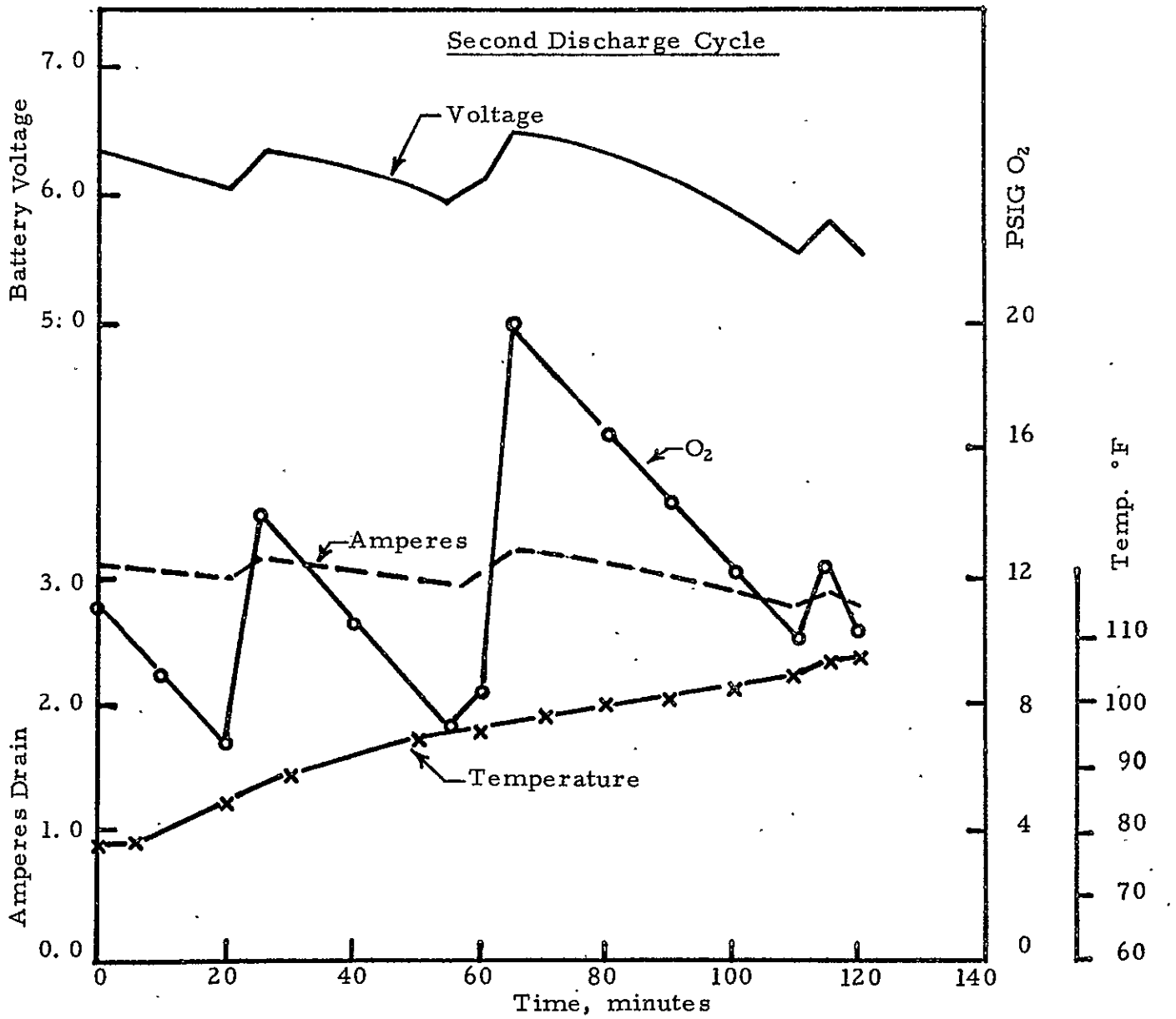

C-6598

FIGURE 76

ZINC/OXYGEN RECHARGEABLE BATTERY
NO. KB-8

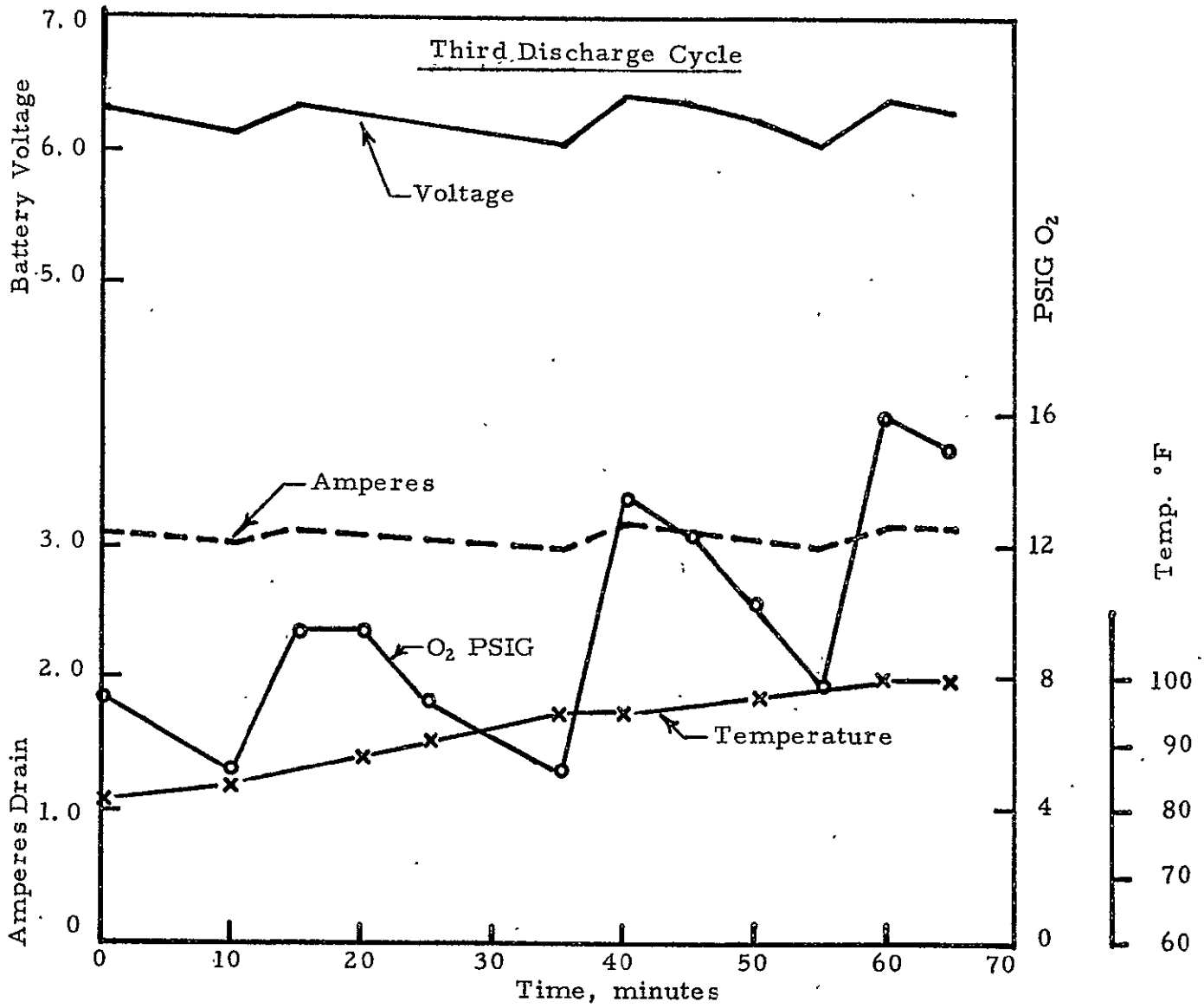

C-6599

CONCLUSIONS AND RECOMMENDATIONS

The zinc-oxygen battery system has been found to be capable of delivering 350 cycles above the 1-volt discharge end-point with zinc powder-carboxymethyl cellulose gel anodes and Union Carbide "fixed-zone" cathodes at 25°C. This cycle life is dependent upon temperature, dropping to 250 cycles at 40°C and 168 cycles at 0°C. Actual depth of zinc discharge is about 15% based upon the weight of the zinc used. A 2-hour discharge/2-hour charge regime was used with constant current charging. Deeper zinc discharge cycling with zinc-gel type anodes results in configurational changes which reduce cycle life. At about 20% depth, for example, the 25°C cycle life of the 2-hour discharge/4-hour charge regime drops to 175 cycles. Cycle life at 0°C and 40°C is further reduced to 100 cycles. Discharge and charge current densities at the 15 and 20% zinc depth are approximately 15 and 20 mA/cm^2.

A separator system consisting of a least one layer of a membrane film, such as Borden C-3 or PERMION 110 or 1770C was found to be mandatory for extended cycle life. Such a film is required to prevent internal cell shorting due to zinc dendrite formation on charge and to separate the oxygen gas on the cathode side of the cell from reaching the zinc electrode and thereby resulting in a chemical short. Obviously this film must be resistant to oxidation. Borden C-3 membrane films were found to perform satisfactorily below current densities of 15 mA/cm^2. At higher current densities a foaming problem was encountered with Borden C-3 films. The use of PERMION 110 or 1770C membrane film circumvented this problem and for this reason the PERMION films are preferred.

The presence of an interconnecting liquid-leveling channel between the electrolyte reservoirs above the positive and negative electrodes of each cell was found necessary in order to compensate for the electroosmotic transport of liquid through the membrane separators with cycling.

Cell charging directly against an American Cyanamid "LAB-40" oxygen electrode was shown to be feasible. Problems encountered, however, include deterioration of the electrode's active layer resulting in polarization and flooding as well as dissolution of the noble metal catalyst into the potassium hydroxide, with subsequent migration to and deposition upon the zinc electrode, resulting in the formation of a hydrogen gassing couple. This was proven by x-ray fluorescent examination of zinc electrodes from such cycled cells.

The zinc-oxygen system employing either zinc-gel or zinc oxide formulated anodes was capable of recharge even from a completely discharged condition.

Cells made with zinc oxide formulated anodes (ZnO#19) discharged at 25°C for 2 hours at current densities of 27 mA/cm^2. These cells delivered 128, 165, and 130 cycles, respectively, when discharge was followed by 2, 4, and 22-hour charges.

Modulated current charging was found to have advantages over constant direct current charging. Configurational zinc anode changes with cycling are significantly retarded when modulated current is used for charging.

Zinc gel-type anodes were found to possess the following advantages over the zinc oxide formulated anodes:

(a) better energy density (1.84 g/AH vs. 1.60 g/AH),

(b) do not require formation charging, and

(c) operate better at 0°C.

Longer cycle life and greater discharge uniformity resulted from the use of Union Carbide "fixed-zone" oxygen cathodes. A nickel charging electrode is needed with this cathode, however, to protect the catalytic carbon layer from oxidation. Resulting cells are therefore of a 3-electrode design.

Data developed from the experimental unit cell work were used as a basis for a paper design study of a 28-volt, 3 KWH rechargeable zinc-oxygen battery. The two-electrode structure, employing American Cyanamid "LAB-40" oxygen cathodes, was selected for this study. An important consideration which led to the selection of the American Cyanamid cathode was the simplicity and weight reduction of the 2-electrode charge-discharge circuit as opposed to that required for cycling a 3-electrode cell system. The energy density of the design battery including tankage and auxiliary equipment is directly related to discharge time and the size of the battery. For a 2-hour discharge, this value is 22 watt-hours per pound. If the discharge time is increased to 8 hours, the energy density rises to 35 watt-hours per pound.

It is recommended that additional work be pursued upon the rechargeable zinc-oxygen system. This recommendation is made in view of the cycle life already attained in the course of this work and the ultimate energy density potential of the system (541 watt-hours/pound).

Specific unit cell work recommended includes:

(a) Concentration upon the development of a highly conductive zinc anode structure susceptible to a minimum of configurational change with cycling.

(b) Emphasis upon low temperature (0°C) performance of the unit cell structure.

(c) Further evaluation of modulated current charging techniques to still further retard configurational change of the zinc anode structure.

(d) Search for an inert separator membrane film that is of lower resistance in the KOH wet condition than those presently used.

(e) As new improved cathodes become available from any source, these should be evaluated in any further work.

It is further recommended that a part of the over-all effort should be with completely enclosed systems complete with tankage and cell auxiliary equipment where the oxygen generated on charge is re-used on discharge.

REFERENCES

1. K. V. Kordesch, "Low Temperature Fuel Cells," Proc. of IEEE, Vol. 51, No. 5, May, 1963.

2. M. B. Clark, W. G. Darland, and K. V. Kordesch, "Thin and Lightweight Electrodes for Fuel Cells," Proc. of 18th Annual Power Sources Conference, Atlantic City, N. J., May 19-21, 1964.

3. M. B. Clark, W. G. Darland, G. E. Evans and K. V. Kordesch, "Thin Fuel Cell Electrodes," Final Report, USAEL, Ft. Monmouth, Contract DA-36-039-AMC-02314(E), Period Ending 31 May 1964, U. S. AECom (AMSEL-RD-PSC), Fort Monmouth, N. J.

4. M. B. Clark, W. G. Darland, and K. V. Kordesch, "Composite Carbon-Metal Electrodes for Fuel Cells," paper presented at the Electrochemical Society Meeting, Washington, D. C., Oct. 13, 1964.

5. K. V. Kordesch, "Fuel Cells with Carbon Electrodes," paper presented at Fuel Cell Conference, Committee for Energy Conversion, Delegation Generale a la Recherche Scientifique et Technique, Paris, Feb. 23-25, 1965.

6. K. V. Kordesch, "Progress of the Carbon Electrode Fuel Cell," paper presented at 19th Annual Power Sources Conference, Atlantic City, N. J., May 18-20, 1965.

7. K. V. Kordesch, "Carbon-Air Electrodes for Low Temperature Fuel Cells," Fuel Cell Symposium, American Chemical Society Meeting, Atlantic City, N. J., September 12-17, 1965.

8. P. R. Rhodes, "Electrochemical Investigation on Graphite Electrodes," Univ. of Ill., Ph. D. Thesis (1965).

9. V. A. Garten, and D. E. Weiss, Revs. Pure and Applied Chem. (Aust.), 7, 70 (1957).

10. V. I. Lygin, N. V. Kovaleva, N. N. Kavtradze, and A. V. Kiselev, Koll. Zh., 22, 234 (1960).

11. J. V. Hallum and H. V. Drushel, J. Phys. Chem., 62, 1502 (1958).

12. J. P. G. Farr, and N. A. Hampson, J. of Electroanalytical Chem., 13, 433 (1967).

13. G. A. Dalin and F. Solomon, "Characteristics of Separators for Alkaline Silver Oxide Zinc Secondary Batteries - Scanning Methods, Chapter 12, 129-141, Ed. by J. E. Cooper and A. Fleischer.

14. A. J. Salkind and J. J. Kelley, "Characteristics of Separators for Alkaline Silver Oxide Zinc Secondary Batteries - Scanning Methods," Chapter 6B, 69-75, Ed. by J. E. Cooper and A. Fleischer.

REFERENCES (CONT'D.)

15. M. Shaw and A. H. Remanick, "Transport Properties of Membranes and their Effect on Alkaline Battery Performance," Extended Abstracts, The Electrochemical Society Meeting, October 6-11, 1968.

16. R. W. Hallows, "Recharging Primary Cells," Wireless World, April 1958, pp. 194-195.

17. D. J. Vargo, "Brief Investigation of an Asymmetrical Alternating-Current Battery-Charging Technique," NASA Report E-3078 (1966).

18. J. McBreen and G. A. Dalin, "The Mechanism of Zinc Shape Change in Secondary Batteries," Extended Abstracts, The Electrochemical Society Meeting, October 9-14, 1966.

APPENDIX

DESIGN STUDY FOR 28-VOLT, 3 KWH ZINC-OXYGEN RECHARGEABLE BATTERY

NASA CONTRACT NAS-5-10247

1.0 SUMMARY

A design study was made of the zinc-oxygen system for the purpose of determining the optimum weight and volume of a 28-volt, 3 KWH secondary metal-oxygen battery for spacecraft has been completed. The design is based on current knowledge derived from feasibility studies conducted under NASA Contract NAS-5-10247. Preliminary engineering layouts indicate the batteries may be contained in spherical tanks with auxiliary mechanisms mounted on three support legs. An overall view of the energy density of such a battery (watt-hours per pound) as a function of hours of discharge is given in Appendix Figure 1.

APPENDIX FIGURE I

ENERGY DENSITY VERSUS HOURS DISCHARGE

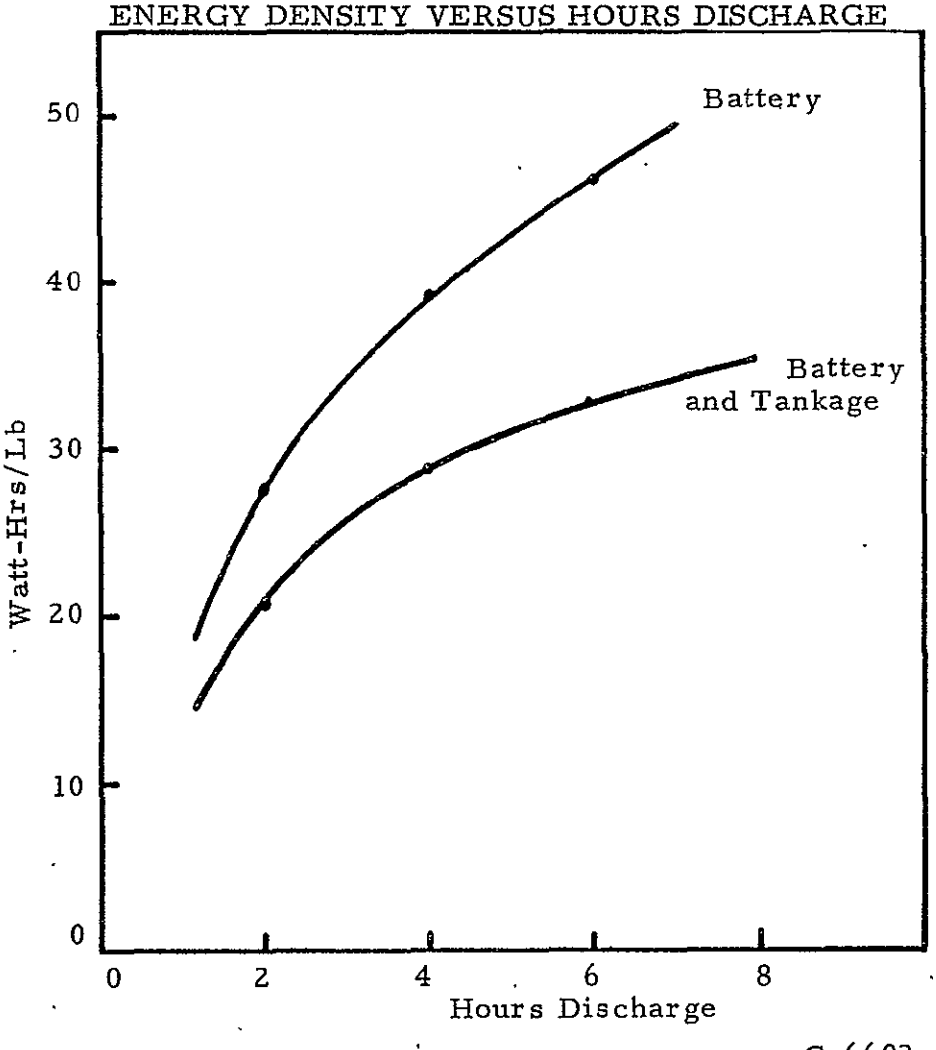

C-6602

2.0 BATTERY DESIGNED FOR 2-HR DISCHARGE/22 HR CHARGE

A battery complete with tankage for the 2-hour discharge and 22-hour charge cycle is estimated to weigh 144 pounds and have an energy density of 20.8 watt-hours/lb. Data showing this are presented in Appendix Table I. The system would be contained in a spherical tank, 21-5/8 inches in diameter, and would have a volumetric energy density of 0.56 watt-hours/in^3. Batteries having the same 3 KWH capacity but designed for longer discharge periods will have appreciably improved energy density values, due to reductions in size made possible by lower current drain requirements. The energy density of a battery designed for 6 hours discharge, for example, would be 32.5 watt-hours/lb.

Battery design is based on the use of "LAB-40" cathode material. This was chosen over the T-2 cathode as an engineering compromise since it simplifies multicell construction by eliminating separate charging electrodes and additional discharge/charge switching gear. The current density of the cell electrodes was limited to 25 mA/cm^2 for this design study while zinc utilization efficiency was limited to 33-1/3%. If the cell efficiency and operating characteristics were improved so that higher current densities could be usefully employed and/or higher anode utilization efficiency could be practically achieved, energy density improvements for this entire system would be additive and could range up to 40-50 watt-hours/lb. This suggests that future work for the achievement of higher energy densities in this zinc/oxygen system might well be concentrated on the zinc electrode.

In the development of power sources for spacecraft applications considerable effort has been supported by the Government and industry to increase the energy density of electrochemical systems in regard to on-board applications.

APPENDIX TABLE I

WEIGHTS AND ENERGY DENSITY SUMMARY
28 VOLT-3 KWH ZINC/OXYGEN RECHARGEABLE BATTERY
(2-hour discharge - 22-hour charge cycle regime)

Cell Components	g/cell	lb/Batt.	Cumulated Totals wt.-lb	Cumulated Totals Watt-hr/lb	Reference
1. Partition Plate	35.2	1.86			Table VII
2. Cathode	520.1	27.46			Sec. 4.3
3. Cathode Collector	23.8	1.26			Table VII
4. PELLON Separator	12.3	0.65			" "
5. PERMION Membrane	3.6	0.19			" "
6. WEBRIL Separator	31.2	1.65			" "
7. VISKON-VINYON Separator	14.9	0.78			" "
8. Anode	580.9	30.67			" "
9. Anode Collector	13.8	0.73			Sec. 4.5
10. Electrolyte	461.2	24.35			Table VII
Total	1 697.0	89.60	89.6	33.4	
Battery Packaging		18.7	108.3	27.7	Sec. 5.2
Oxygen		1.8	110.1	27.2	Sec. 5.3
Tankage		20.3	130.4	23.0	Sec. 6.4
Hardware					
Pump		1.0			Sec. 6.3
Gas/Liquid Sep.		3.5			Sec. 6.2
Reservoir		4.0			
H_2 Getter		1.0			
Misc.-Piping, Fittings, etc.		4.0			
		13.5	143.9	** 20.8	

**Comparable numbers for four and six hours discharge modes are shown in Figure 1.

While the theoretical maximum output for the active materials of the zinc/oxygen system is 490 watt-hours/lb, the reduction of the system to a practical operating rechargeable cell reduces this energy density value. This energy density is further reduced when the cells are packaged into a battery system complete with sustaining hardware. Complete self-sustaining systems with their reactants, tankage and hardware present challenging problems.

3.0 WEIGHTS AND ENERGY DENSITY CALCULATIONS

3.1 Operating Parameters

Feasibility studies conducted under the present contract resulted in the following parameters being used in the design study:

1. A 2-hour-1500 watt (3 KWH) discharge rate.
2. Current density is limited to 25 mA/cm^2-the limiting factor being the anode-membrane separator combination.
3. A 33-1/3% depth of discharge with respect to the anode is the most practical to date.
4. The use of LAB-40 as the cathode electrode eliminates an additional charging electrode and circumvents switching.

3.2 Weights and Density Summary

Appendix Table I presents the weights and density summary for a 2-hour charge/22-hour discharge battery. Reference sections are noted.

3.3 Energy Calculations for Lower Current Drains

Increasing the specified discharge time for the rated 3KWH battery from two to four or six hours, allows reduction of battery size (reduced cross-sectional area by virtue of reduced current requirement for a given current density). This can be seen in Appendix Figure 1.

3.4 Estimated Energy Density Improvements - Improved Design

3.4.1 Higher Current Densities

The present current density operating level of 25 mA/cm^2 is limited by the anode-membrane separator combination. Any improvement resulting in increased electrode current density will reduce the battery size and weight and increase the energy density as shown in Appendix Figure 2.

3.4.2 Increased Depths of Discharge

Zinc anode discharge depth is limited to 33-1/3% in the present design study (based on theoretical zinc available). Any improvement in anode discharge depth will, of course, increase the energy density. An increase to 50% depth, for example, will increase the energy density of the battery package from 27.7 watt-hours/lb to 30.7 watt-hours/lb.

4.0 CELL DESIGN

4.1 Battery and Cell Requirements

Appendix Table II presents a tabulation of the watt-hour and current drain rates for a two, four and six hour discharge cycle for a given 3 KWH battery. As indicated for the maximum energy discharge rate of 1500 watts per hour, a 28-volt battery would have a battery drain of 53.57 amperes.

APPENDIX TABLE II

BATTERY CURRENT DRAINS FOR VARIOUS 24-HOUR CYCLES

Discharge			Charge		
Hrs	Watt/hr	Amp.	Hrs	Watt/hr	Amp.
2	1500	53.57	22	136.4	4.87
4	750	26.78	20	150.0	5.36
6	500	17.85	18	166.6	6.69

APPENDIX FIGURE 2

ENERGY DENSITY VERSUS CURRENT DENSITY

28 Volt, 3 KWH, 2-Hour Discharge
Battery* and Tankage

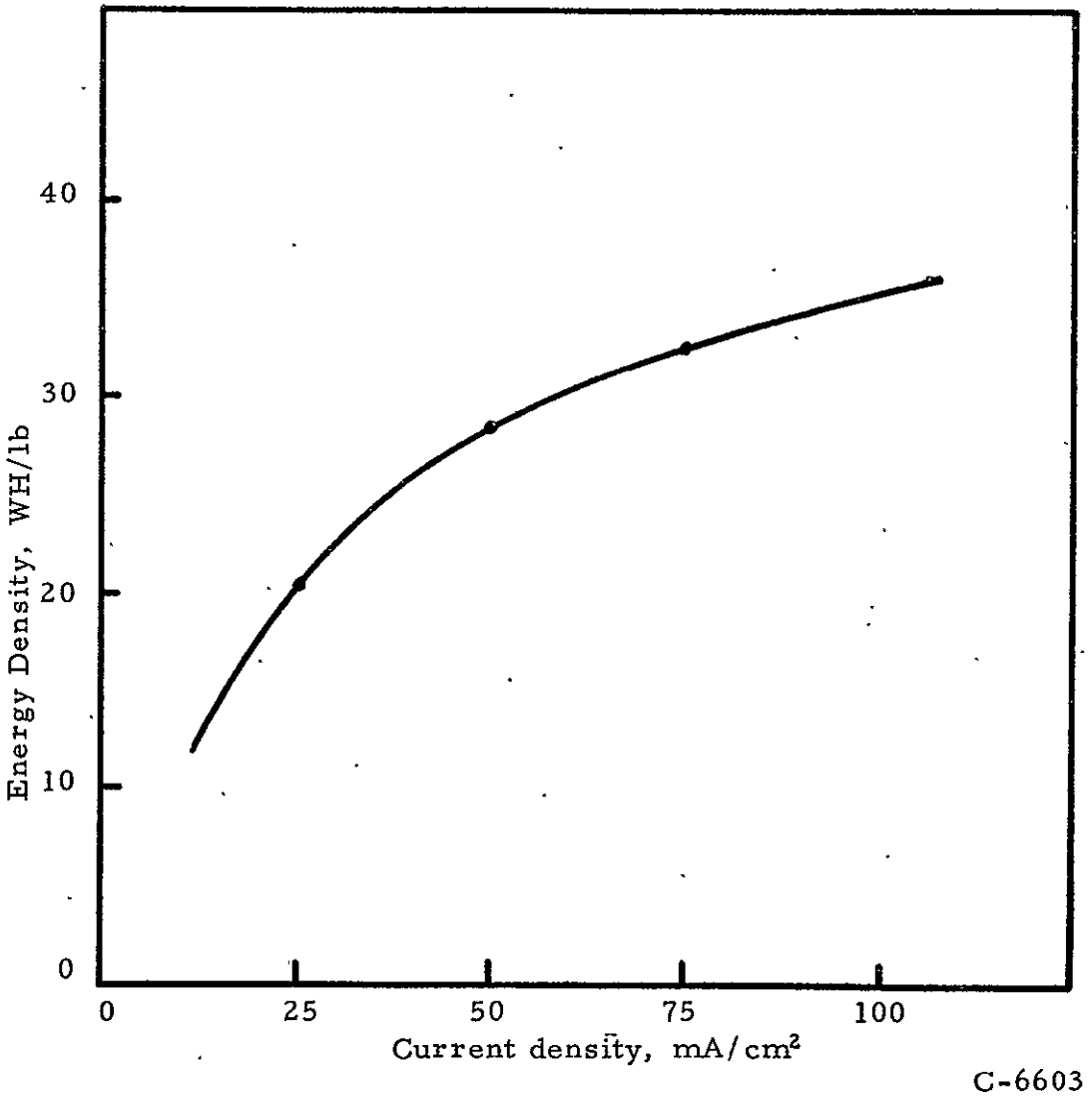

* 33-1/3% anode discharge depth

Appendix Table III shows a tabulation of the number of cells required per battery and ampere-hours capacity per cell based on the current density and the respective cell voltage. The current density and cell voltage are discussed in greater detail in another section

APPENDIX TABLE III

CELL REQUIREMENT FOR 3 KWH-28 VOLT BATTERY

mA/cm^2	Cell Volt.	No. Cells for 28 Volt Batt. Cal.	No.	Watt-hrs	Watt-hrs Per Cell	Amp.hrs Per Cell
25	1.18	23.7	24	3000	125.0	105.93
50	1.12	25.0	25	3000	120.0	107.14

4.2 Cell Construction

Cell design is based upon the feasibility study conducted as part of the present contract and Union Carbide's background in fuel cell, "Air Cell" and rechargeable battery systems. The cell design concept shown in Appendix Figure 3 is based on the utilization of the American Cyanamid LAB-40 oxygen electrode as both a discharge and charge electrode. A PERMION membrane is used to prevent oxide and dendrite shorting. The molded Union Carbide ZnO#1 rechargeable anode was used. A space is provided between the cathodes of each cell and its partition to serve as a channel for oxygen access to the cathodes. Metal collector tabs attached to the respective electrodes enable external electrical connections to be made; parallel connection of the dual cathodes in each cell as well as series connecting of cells in the battery.

APPENDIX FIGURE 3

ZINC-OXYGEN DUAL CATHODE CELL CROSS-SECTION

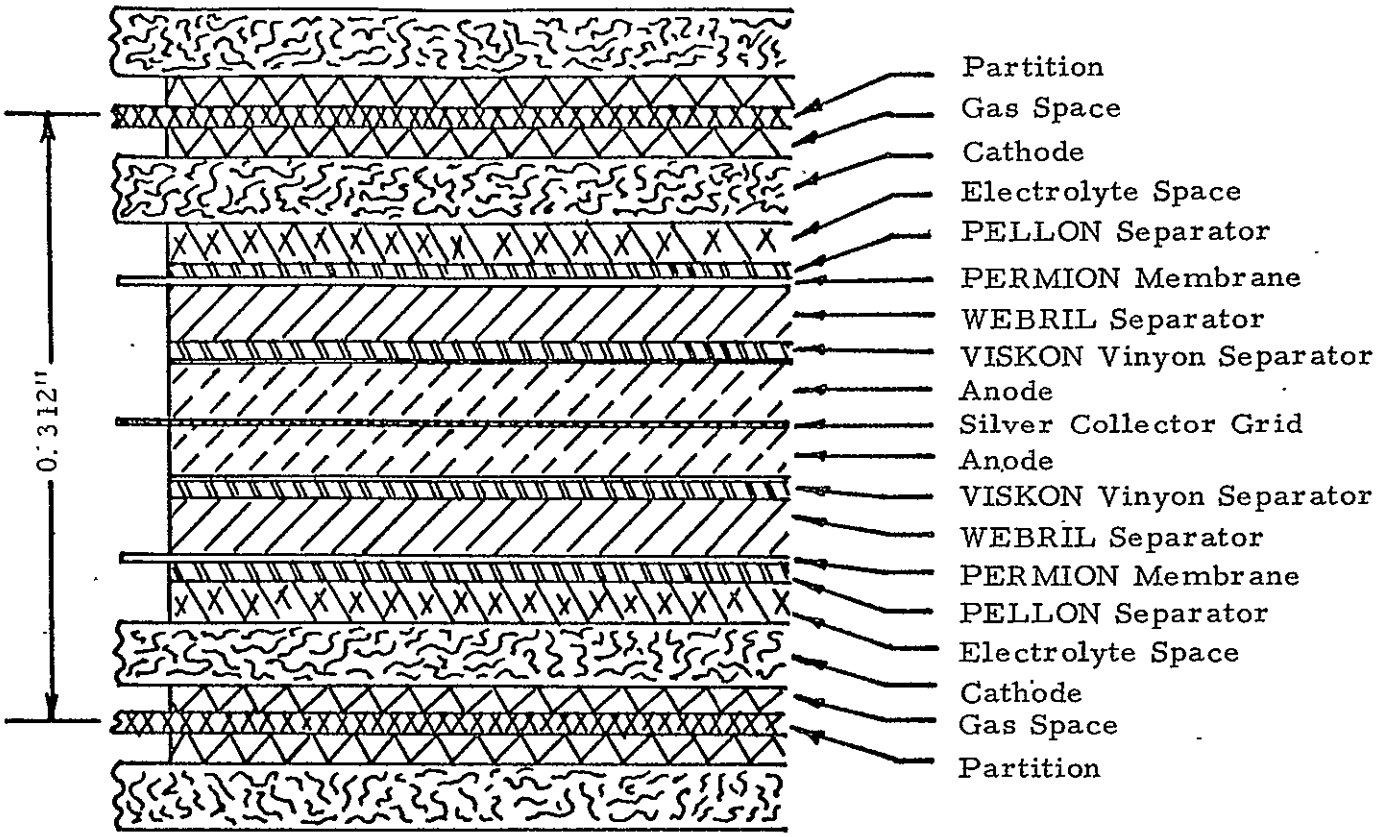

4.3 Cathode

4.3.1 Description

Two types of cathode material have been evaluated. The Union Carbide "fixed-zone" material consisting of an active carbon layer applied to one side of a porous metal backing and the American Cyanamid LAB-40 electrode material. The latter was used in this design study as an engineering compromise. This does not require a separate charging electrode and results in simpler cycling circuitry.

4.3.2 Cathode Area and Size

Feasibility studies to date have indicated a reliable cathode operating current density of 25 mA/cm^2 at a potential of 1.18 volts versus zinc. At this current density the cell requires a cathode area of 332.2 square inches or 18.22

inches per side for a square cell shape factor to produce a cell current of 53.57 amperes, as indicated in Appendix Table II. To reduce the cross-sectional size of the cell, a dual cathode cell construction is proposed and a tabulation of the electrode area and size for various discharge cycles is shown in Appendix Table IV.

APPENDIX TABLE IV

CATHODE AREA AND SIZE PER ELECTRODE FOR DUAL CATHODE CELL

	2-Hr Discharge		4-Hr Discharge		6-Hr Discharge	
mA/cm^2	Area in^2	Per Side in.	Area in^2	Per Side in.	Area in^2	Per Side in.
25	166.10	12.890	83.055	9.113	55.348	7.439
50	83.055	9.113	41.519	6.449	27.674	5.250
75	55.365	7.430	27.679	5.250	18.449	4.280
Amp. Each Side	26.78		13.39		8.92	
Amp. Total	53.57		26.78		17.85	

4.4 Membrane

The membrane which is positioned between the anode and the charging electrode, prevents zinc oxide and dendrite shorting. RAI-1770 C PERMION material has proved very satisfactory for this function.

4.5 Anode

4.5.1 Description

The anode proposed for this battery is the Union Carbide ZnO#1 It is fabricated in a discharged state and requires an initial charge prior to use. The depth of discharge of the anode is 33-1/3% based on the theoretical amount of zinc available.

4.5.2 Anode Calculations

A 15 ampere-hour ZnO#1 anode weighing 27.433 grams (including silver grid envelope) after molding has a volume of 0.5355 cubic inches. The volume to energy density of the ZnO#1 anode is:

$$\frac{0.5355}{15} = 0.03579 \text{ in}^3/\text{AH}.$$

The weight to energy density is:

$$\frac{27.433}{15} = 1.828 \text{ grams/AH}.$$

Using these density values, Appendix Table V presents a tabulation of the required anode volume and weight values per cell for the proposed battery.

APPENDIX TABLE V

CALCULATED ANODE VOLUME AND WEIGHTS PER CELL

	Required Amp-hr/Cell For Depth of Discharge		Volume (in^3) (Amp-hr x 0.0357)		Weight (grams) (Amp-hr x 1.828)	
mA/cm^2	100%*	33⅓%*	100%*	33⅓%*	100%*	33⅓%*
25	105.93	317.82	3.781	11.346	193.64	580.97
50	107.14	321.45	3.824	11.475	195.85	587.61

*Depth of Discharge

Applying anode volume values listed in Appendix Table V and electrode area values (cathode and anode will have the same active areas), anode thickness calculated as follows:

$$\frac{11.346 \text{ in}^3 \text{ (Vol. for 317.82 AH)}}{166.10 \text{ in}^2 \text{ (Electrode Area)}} = \text{0.068 inches anode thickness for two-hour discharge rate}$$

For the increased discharge cycle periods (lower current discharge rates) requiring smaller electrode areas, anode thickness will increase as indicated in Appendix Table VI for a given ampere-hour capacity.

APPENDIX TABLE VI

CALCULATED ANODE THICKNESS

		Anode Thickness - Inches		
mA/cm^2	Anode* Vol. in^3	2-Hour Discharge	4-Hour Discharge	6-Hour Discharge
25	11.346	0.068	0.136	0.205
50	11.475	0.138	0.276	0.414

*33⅓ percent Depth Discharge Anode

4.6 Cell Components - Weights and Volumes

Appendix Table VII is a tabulation of individual cell components as to size, number, volume and weight for the 3 KWH-28 volt battery to operate on a 2-hour discharge/22-hour charge cycle.

5.0 BATTERY DESIGN

5.1 Description

The proposed battery construction would consist of cells, individually assembled as units and stacked to form the battery. At the time of the stack assembly, the individual terminal tabs are connected and core material (to produce electrolyte channels) are positioned prior to potting. The entire battery is potted in a form with epoxy resin.

Gas evolution, particularly on the charge cycle, has posed problems in the feasibility study of the cell system. The study was conducted with cells having separate reservoir chambers for each respective electrolyte cavity on each side of the membrane. Gas evolution has been accompanied with changes in electrolyte levels for each cavity. For a sealed system such as is proposed here, circulating the electrolyte through all cell cavities of the battery will remove gas and compensate for changes of the electrolyte volume. The flow of electrolyte through each cell requires channels in the battery package to evenly distribute and collect the circulating liquid.

Electrolyte leakage current would result from circulating electrolyte; electrically conductive paths exist between cells by virtue of the interconnecting potassium hydroxide streams. Union Carbide has set up a computer program which generates the equivalent network circuit for the stack internal electrolyte loops and using Kirchhoff's law solves the resulting set of simultaneous equations. These calculations show that stack internal resistance is generally negligible and that the effects of load current on leakage may be neglected.

TABLE VII

CELL COMPONENTS - WEIGHTS AND VOLUME - 2 HOUR DISCHARGE

Component	No. Pcs. Per Cell	Thickness Each	Thickness Total	Wt. Gms/in^2	Wt. Gms/in^3	166.10 in^2 Area 12.890 in/side* Volume in^3	166.10 in^2 Area 12.890 in/side* Wt. Gms/Cell	172.66 in^2 Area 13.140 in/side* Volume in^3	172.66 in^2 Area 13.140 in/side* Wt. Gms/Cell	Electrolyte cc	Electrolyte Weight Grams
Partition (1) (Polysulfone)	1	0.010	0.010	0.204	20.41			1.726	35.22		
Gas Space	2	0.015	0.030			4.983					
Cathode (2) (LAB-40)	2	0.032	0.064	1.506				11.050	520.1		
Space (Electrolyte)	2	0.020	0.040		23.112	6.644				108.8	153.6
Separator (4) (PELLON)	2	0.009	0.018	0.037		2.989	12.29			39.7	55.9
Membrane (5) (PERMION)	2	0.004	0.008	0.011		1.329	3.65			17.4	24.5
Separator (6) (WEBRIL)	2	0.027	0.054	0.094		8.969	31.23			117.6	165.8
Separator (7) (VISKON-VINYON)	2	0.010	0.020	0.045		3.322	14.94			43.5	61.4
Anode Collector (9) (Ag - 8.05 in^2 ea.)	1	0.010	---	1.720	172.07	0.080	13.85				
Cathode Collector (3) (Ni - 8.21 in^2 ea.)	2	0.010	---	1.450	145.03	0.164	23.80				
Anode (8)	1	0.068	0.068			11.346	580.97				
						39.826		12.776			
						12.776					
CELL TOTAL			0.312			52.60				327.0	461.2

*Square Shape Factor

5.2 Battery Package Calculations

5.2.1 Cross-Sectional Dimension

Maximum cross-sectional cell component dimension	13.140 inches*
0.500 inch battery case wall	1.000 inch
Battery Case Cross-Sectional Dimension	14.140 inches

5.2.2 End Plates

PANELYTE No. 161, epoxy impregnated glass cloth,
Density - 1.88 grams/cc

2 pieces x $(14.140)^2$ x 0.250 = 99.96 in^3, 6.78 pounds

5.2.3 Length

0.312 inch (unit cell thickness) x 24 cells	7.488 inches
0.250 inch end plates x 2 pieces	.500 inch
Battery Package Length	7.988 inches

5.2.4 Battery Package Volume

Volume = $(14.140)^2$ x 7.988 = 1597.12 in^3

5.2.5 Battery Components Volume and Weight

	Vol.-in^3	Wt.-lbs.
Unit Cell Components (24 cells)	1262.4	89.6
End Plates	99.6	6.8
Total	1362.0	96.4

5.2.6 Epoxy Potting Resin

Battery Package Volume	1597.1 in^3
Battery Components plus End Plates Volume	-1362.0 in^3
Epoxy Resin Volume	235.1 in^3

Epoxy Casting Resin (22.94 g/in^3)

235.1 in^3 x 22.94 g = 5393 g = 11.89 lbs.

5.2.7 Packaging

	Vol.-in^3	Wt.-lbs.
End Plates	99.6	6.8
Epoxy Casting Resin	235.1	11.9
	334.7	18.7

*Ref. Appendix Table VII

5.3 Oxygen Requirements

Table VIII is a tabulation indicating the estimated oxygen requirements for 3 KWH operation based on:

0.2984 g O_2/Amp-hr (theoretical)

$\frac{0.2984}{32}$ x 22.4 (l/mole) = 0.2088 liters/Amp-hr.

It is assumed in the battery design that 10 percent excess oxygen will be required for proper battery operation.

TABLE VIII

OXYGEN REQUIREMENT FOR 3 KWH-28 VOLT BATTERY

mA/cm²	Amp-hr per cell	No. cells	Amp-hr per Batt.	Oxygen		O_2 + 10%		
				Wt-g	Vol-liter	Wt-g	Wt-lbs	Vol-liter
25	105.93	24	2542.3	758.62	530.8	834.48	1.915	583.8
50	107.14	25	2678.5	799.26	559.3	879.18	1.938	615.2

6.0 SYSTEM DESIGN

6.1 Description

The schematic diagram Appendix Figure 4, shows the proposed power system as it would operate from the solar array. By circulating the electrolyte through each cell of the battery, it will be possible to remove the gas generated during the charging cycle. A centrifuge is provided for gas-liquid separation. After the point of gas separation, a getter will be used to remove hydrogen from the O_2 gas prior to its return into the reactant tankage. An electrolyte reservoir/filter is provided in the electrolyte return line to compensate for electrolyte expansion during operation and to filter and adjust for changes in zinc oxide concentration.

APPENDIX FIGURE 4

SCHEMATIC DIAGRAM OF THE PROPOSED POWER SYSTEM

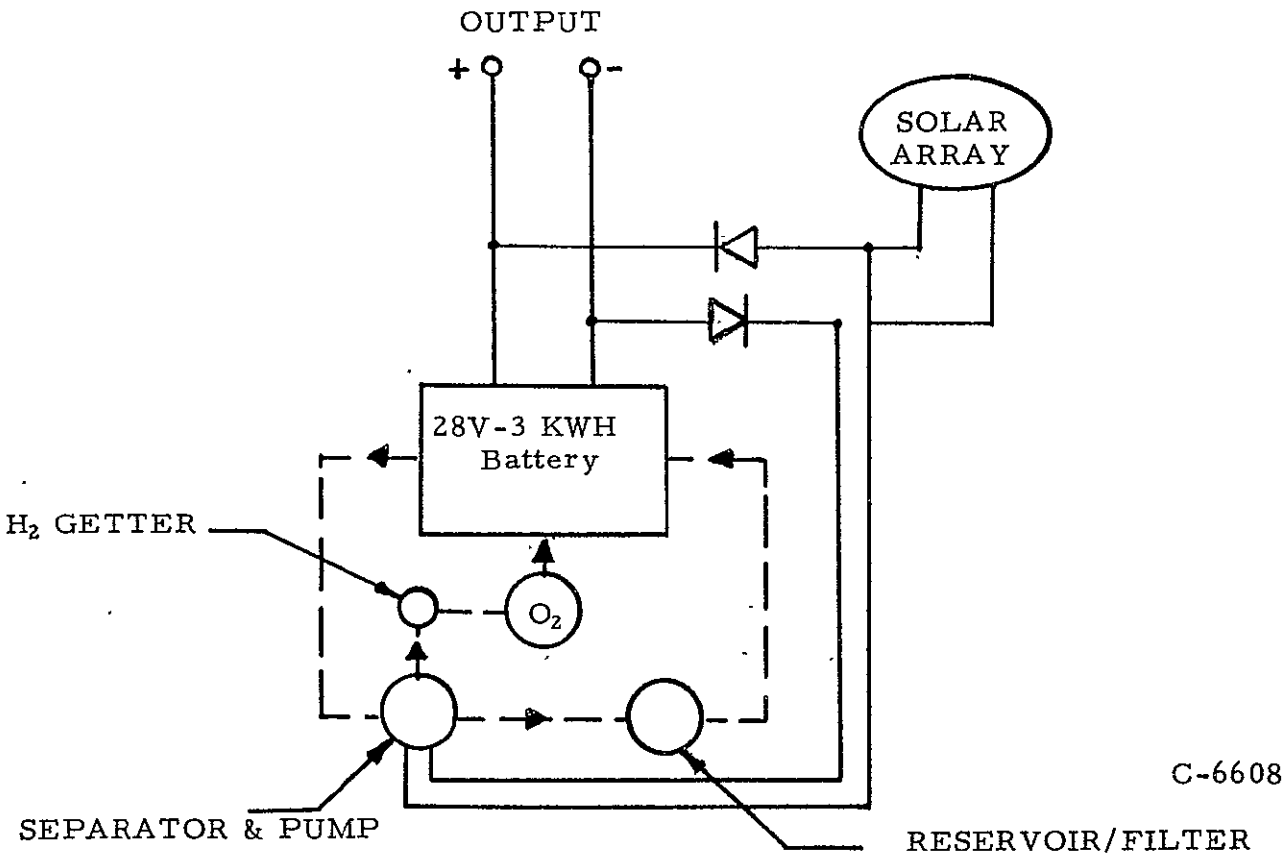

It is also proposed to enclose the battery package within the reactant (oxygen) storage tank to further conserve on space and weight. The electrolyte pump would necessarily be mounted outboard of the tank to lessen the danger of combustion due to the operation of the electrical pump motor.

6.2 Gas-Liquid Separator

Under Contract NAS 3-9430, Union Carbide subcontracted Air Research Manufacturing Co., a division of the Garrett Corp., for an experimental feasibility study of bubble separators. Their work showed positive results with a cyclone-type separator and the proposed design here is based on a similar device.

6.3 Electrolyte Pump

The Fuel Cell Department of the Electronics Division of Union Carbide Corporation has developed small electrolyte pumps which could be applied to this system. The nature of the electric motor operated pump dictates its use outboard of the reactant tankage. The use of an A.C. pump is almost mandatory for any space mission since it is impractical to consider any replacement of brushes in a D.C. motor or operation in a high oxygen partial pressure environment.

It is assumed that spacecraft in which the proposed power system would be employed would have an electric inverter on board and that a small quantity of power could be used to operate an A.C. pump motor.

6.4 Tankage

The system containment vessel is designed for a maximum operating pressure of 150 psi with a safety factor of 3.3 based on yield strength. The material of construction will be 6061-T aluminum alloy having a working stress of 33,000 psi and a material density of 0.1 lb/in^3. All interior tank surfaces to be coated with nickel or suitable plastic to prevent chemical attack by the environment. Using these values, thickness requirements for the vessel have been calculated to be approximately 81 mils. Each flange to be $\frac{1}{2}$ inch thick by one inch in width welded to each spherical half section. Three support legs are $\frac{1}{2}$ inch thick having cutouts to mount hardware and effect reduction of weight. Tankage weight summary as follows:

Spherical tank	=	118.88 in^3
Flange	=	65.29 in^3
Legs	=	19.05 in^3
		203.22 in^3

0.1 lb/in^3 x 203.22 in^3 = 20.3 lbs.

6.4.1 Tankage Structure

A preliminary design of the reactant tankage, containing the battery system, has been developed as shown in the three views of Figure 5. The containment vessel is a half-sectioned sphere, the bottom section having three support legs into which are mounted the electrolyte pump, gas-liquid separator and reservoir-filter. The battery is mounted in the spherical sections and is kept in position by small corner mounts. The two flanged half sections are bolted together to effect pressurization.

FIGURE 5a

TANKAGE STRUCTURE

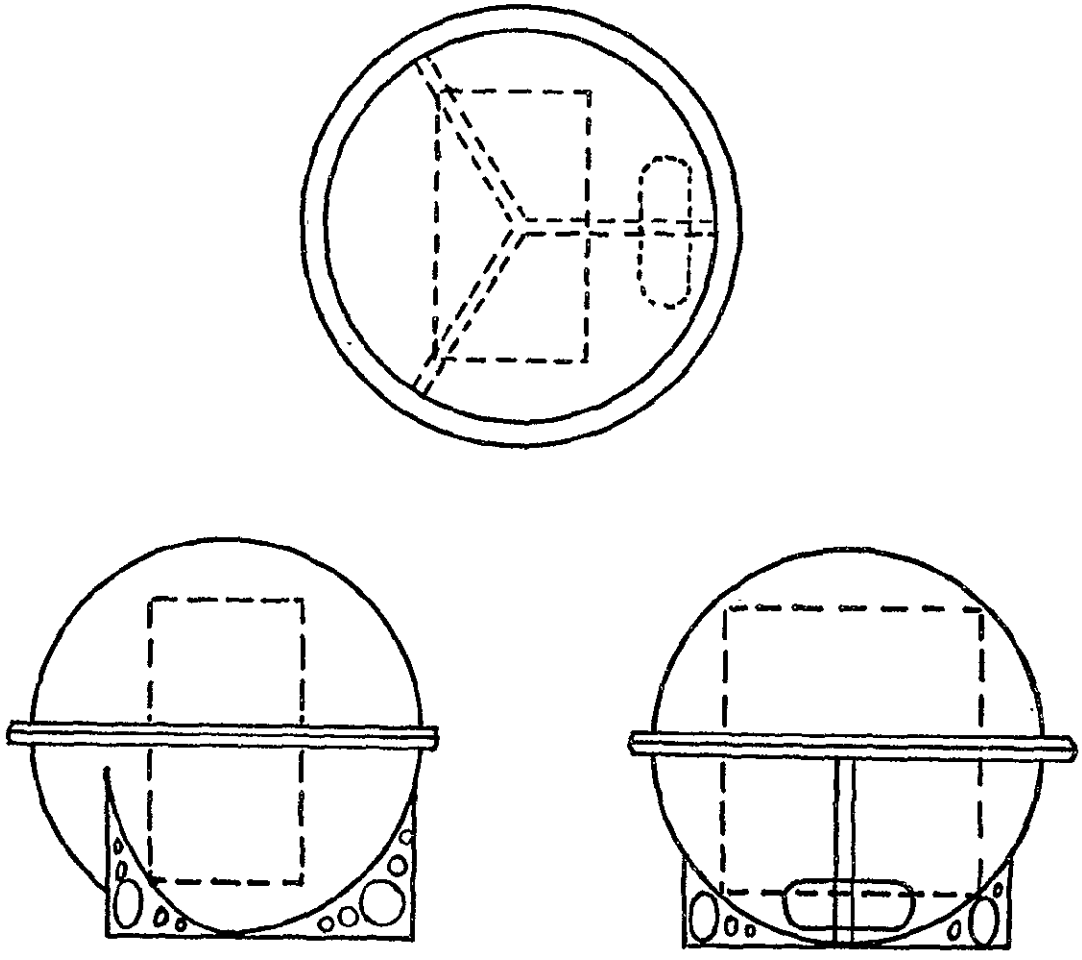

C-4232

6.4.2 Spherical Tank Diameter

Figure 5b

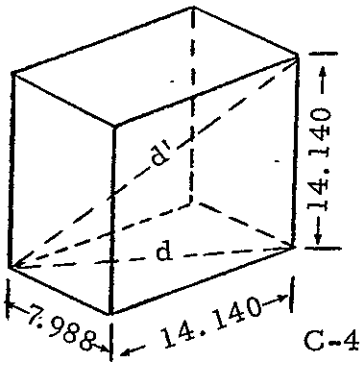

All four corners of the battery to touch I.D. of sphere. The diagonal of the battery rectangle would equal the diameter of the sphere.

$$d' = \sqrt{d^2 + (14.140)^2}$$

$$= \sqrt{(\sqrt{(7.988)^2 + (14.140)^2})^2 + (14.140)^2}$$

d' = 21.533 in. diameter of sphere

6.4.3 Tank Volume

Vol. (I.D.) of Spherical Tank = $4.189\ r^3 = 4.189\ (10.766)^3$

= $5227.20\ in^3$

6.4.4 O_2 Tankage Volume and Calculated Pressure

Vol. (I.D.) of the Spherical Tank	$5227.20\ in^3$
Vol. of Battery	$1597.12\ in^3$
Vol. for O_2 Storage	$3630.08\ in^3$ or 59.49 liters

$$\frac{PV}{V'} = P', \frac{14.7 \times 583.9^*}{59.5} = \frac{8583.3}{59.5} = 144.26 \text{ psi}$$

V = O_2 requirement for operation of STP-liters

V' = Volume of tankage, liters

P = 14.7 psia

P' = O_2 tankage pressure - psia

*Ref. - Section 5.3

6.4.5 Tankage Weight Calculations

6.4.5.1 Material

6061-T Aluminum Alloy

Working Stress = 33,000 psi

Material Density = 0.1 lb/in^3

6.4.5.2 Wall Thickness

$$\frac{Pd}{4S} = \frac{500 \times 21.5}{4 \times 33,000} = \frac{10750}{132000} = 0.081 \text{ in.}$$

6.4.5.3 Wall Volume

$$= 4.189\,(10.847)^3 - 4.189\,(10.766)^3$$

$$= 118.88 \text{ in}^3$$

6.4.5.4 Flange

$\frac{1}{2}$ inch thick - 2 pieces 1.00 inch total

d' (I.D.) = 21.533 + .162 = 21.695

d (O.D.)= 21.533 + 2.0 = 23.533

Flange Volume = $1\,(0.7854\,d^2 - 0.7854\,d'^2)$

$= 1\,(0.7854 \times 23.533^2 - 0.7854 \times 21.695^2)$

$= 65.29 \text{ in}^3$

6.4.5.5 Legs

$$\frac{(21.75)^2 - (21.75)^2(0.7854)}{4} = \text{Area/solid leg}$$

$$\frac{473.06 - 371.54}{4} = \frac{101.52}{4} = 25.38 \text{ in}^2$$

Cutouts 12.68 in^2

12.70 in^2

Figure 6. Support Leg Pattern

Vol/leg = $12.70 \times 0.5 = 6.35 \text{ in}^3$

$\times 3 = 19.05 \text{ in}^3$

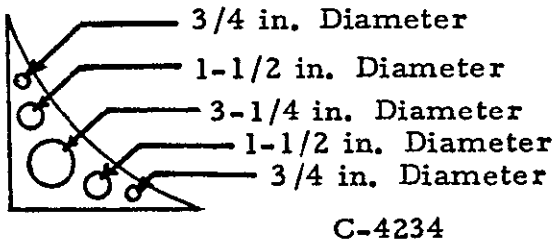

C-4234

OFFICIAL DISTRIBUTION LIST
GODDARD SPACE FLIGHT CENTER
March 4, 1971

National Aeronautics & Space Administration
Scientific and Technical Information Center. Input
P. O. Box 33
College Park, Maryland 20740

Mr. Ernst M. Cohn, Code RPP
National Aeronautics & Space Administration
Washington, D. C. 20546

Dr. A. M. Greg Andrus, Code SCC
National Aeronautics & Space Administration
Washington, D. C. 20546

Dr. E. N. Case, Code UT
National Aeronautics & Space Administration
Washington, D. C. 20546

Mr. Richard Livingston, Code MTG
National Aeronautics & Space Administration
Washington, D. C. 20546

Mr. Jon Rubenzer, M.S. 244-2
Ames Research Center Code PBS
National Aeronautics & Space Administration
Moffett Field, California 94035

Mr. Gerald Halpert, Code 734
Goddard Space Flight Center
National Aeronautics & Space Administration
Greenbelt, Maryland 20771

Mr. Thomas Hennigan, Code 761.2
Goddard Space Flight Center
National Aeronautics & Space Administration
Greenbelt, Maryland 20771

Mr. Joseph Sherfey, Code 734
Goddard Space Flight Center
National Aeronautics & Space Administration
Greenbelt, Maryland 20771

Mr. Louis Wilson, Code 450
Goddard Space Flight Center
National Aeronautics & Space Administration
Greenbelt, Maryland 20771

Mr. Jack E. Zanks, MS 488
Langley Research Center
National Aeronautics & Space Administration
Hampton, Virginia 23365

Mr. John L. Patterson, Code 472
Langley Research Center
National Aeronautics & Space Administration
Hampton, Virginia 23365

Dr. Louis Rosenblum, MS 302-1
Lewis Research Center
National Aeronautics & Space Administration
21000 Brookpark Road
Cleveland, Ohio 44135

Mr. Harvey Schwartz, MS 309-1
Lewis Research Center
National Aeronautics & Space Administration
21000 Brookpark Road
Cleveland, Ohio 44135

Dr. J. Stuart Fordyce, MS 309-1
Lewis Research Center
National Aeronautics & Space Administration
21000 Brookpark Road
Cleveland, Ohio 44135

Mr. Charles B. Graff, S & E-ASTR-EP
George C. Marshall Space Flight Center
National Aeronautics & Space Administration
Huntsville, Alabama 35812

Mr. W. E. Rice, EP5
Manned Spacecraft Center
National Aeronautics & Space Administration
Houston, Texas 77058

Mr. Daniel Runkle, MS 198-220
Jet Propulsion Laboratory
4800 Oak Grove Drive
Pasadena, California 91103

Mr. Sam Bogner
Jet Propulsion Laboratories
4800 Oak Grove Drive
Pasadena, California 91103

Mr. Aiji Uchiyama, MS 198-220
Jet Propulsion Laboratory
4800 Oak Grove Drive
Pasadena, California 91103

Dr. R. Lutwack, MS 198-220
Jet Propulsion Laboratory
4800 Oak Grove Drive
Pasadena, California 91103

Dr. Tom King
Defense Research Establishment
Power Sources Division
Shirley Bay
Ottawa, Ontario, Canada

Dr. Joseph Lackner
Defense Research Establishment
Power Sources Division
Shirley Bay
Ottawa, Ontario, Canada

Dr. M. A. Stott
Telesat Canada
333 River Road
Ottawa, Ontario, Canada

Mr. Nathan Kaplan
Harry Diamond Laboratories
Room 300, Building 92
Connecticut Ave. & Van Ness St, NW
Washington, D. C. 20438

U. S. Army
Electro Technology Laboratory
Energy Conversion Research Division
MERDC
Fort Belvoir, Virginia 22060

Harry Diamond Laboratories
Room 300, Building 92
Connecticut Ave. & Van Ness St., NW
Washington, D. C. 20438

U. S. Army Electronics Command
Attn. AMSEL-KL-P
Fort Monmouth, New Jersey 07703

Mr. Leo A. Spano
Clothing & Organic Materials Division
U. S. Army Natick Laboratories
Arlington, Virginia 22217

Director Power Program
Code 473
Office of Naval Research
Arlington, Virginia 22217

Mr. Harry W. Fox, Code 472
Office of Naval Research
Arlington, Virginia 22217

Dr. J. C. White, Code 6160
Naval Research Laboratory
4555 Overlook Avenue, S.W.
Washington, D. C. 20360

Mr. J. H. Harrison, Code A731
Naval Ship R & D Laboratory
Annapolis, Maryland 21402

Mr. Milton Knight, Air 340C
Naval Air Systems Command
Department of the Navy
Washington, D. C. 20360

Commanding Officer
Naval Ammunition Depot
13022, Mr. D. G. Miley
Crane, Indiana 47522

Mr. Phillip B. Cole, Code 232
Naval Ordnance Laboratory
Silver Spring, Maryland 20910

Mr. C. F. Viglotti, 6157D
Naval Ship Engineering Center
Center Bldg., Prince George Center
Hyattsville, Maryland 20782

Mr. Robert E. Trumbule, STIC
4301 Suitland Road
Suitland, Maryland 20390

Mr. B. B. Rosenbaum, Code 03422
Naval Ship Systems Command
Washington, D. C. 20360

Mr. James E. Cooper, APIP-1
Aero Propulsion Laboratory
Wright-Patterson AFB, Ohio 45433

Mr. Ed Raskind, CREC, Wing F
AF Cambridge Research Laboratory
L. G. Hanscom Field
Bedford, Massachusetts 01731

Mr. Frank J. Mollura, EMRED
Rome Air Development Center
Griffiss AFB, New York 13440

HQ SAMSO
SMTAE/Lt. R. Ballard
Los Angeles Air Force Station
Los Angeles, California 90045

Dr. W. J. Hamer
National Bureau of Standards
Washington, D. C. 20234

Aerospace Corporation
Attn. Library Acquisition GR
P. O . Box 95085
Los Angeles, California 90045

Dr. R. A. Haldeman
American Cyanamid Company
1937 West Main Street
Stamford, Connecticut 06902

Mr. R. A. Knight
AMF Incorporated
689 Hope Street
Stamford, Connecticut 06907

Dr. R. T. Foley
Chemistry Department
American University
Massachusetts & Nebraska Avenues, N.W.
Washington, D. C. 20016

Dr. Frank Swindell
ARTECH, Inc.
2816 Fallfax Drive
Falls Church, Virginia 22042

Dr. H. L. Recht
Atomics International Division
North American Aviation, Inc.
P. O..309
Canoga Park, California 91304

Mr. R. F. Fogle, GF 18
Autonetics Division, NAR
P. O. Box 4181
Anaheim, California 92803

Dr. John McCallum
Battelle Memorial Institute
505 King Avenue
Columbus, Ohio 43201

Mr. B. W. Moss
Bellcomm, Inc.
955 Lenfant Plaza, S. W.
Washington, D. C. 20024

Mr. D. O. Feder
Bell Telephone Labs, Inc.
Murray Hill, New Jersey 07974

Mr. R. L. Beauchamp
Bell Telephone Laboratories
Murray Hill, New Jersey 07940

Dr. Carl Berger
13401 Kootenay Drive
Santa Ana, California 92705

Mr. Sidney Gross
Mail Stop 88-06
The Boeing Company
P. O. Box 3999
Seattle, Washington 98124

Mr. M. E. Wilke, Chief Engineer
Burgess Battery Division
Gould, Inc.
Freeport, Illinois 61032

Dr. Eugene Willihnganz
C & D Batteries
Division of Eltra Corporation
3043 Walton Road
Plymouth Meeting, Pennsylvania 19462

Professor T. P. Dirkse
Calvin College
3175 Burton Street, S.E.
Grand Rapids, Michigan 49506

Mr. F. Tepper
Catalyst Research Corporation
6308 Blair Hill Lane
Baltimore, Maryland 21209

Mr. Robert Strauss
Communications Satellite Corporation
Comsat Laboratories
P. O. Box 115
Clarksburg, Maryland 20734

Dr. L. J. Minnich
G & W. H. Corson, Inc.
Plymouth Meeting, Pennsylvania 19462

The Librarian
Cubic Corporation
9233 Balboa Avenue
San Diego, California 92123

Mr. J. A. Keralla
Delco Remy Division
General Motors Corporation
2401 Columbus Avenue
Anderson, Indiana 46011

Mr. J. M. Williams
Experimental Station, Building 304
Engineering Materials Laboratory
E. I. DuPont De Nemours & Co.
Wilmington, Delaware 19898

Director of Engineering
ESB, Inc.
P. O. Box 11097
Raleigh, North Carolina 27604

Dr. Galen Frysinger
ESB, Inc.
Carl F. Norberg Research Center
19 West College Avenue
Yardley, Pennsylvania 19067

Mr. E. P. Broglio
Eagle-Picher Industries, Inc.
P. O. Box 47, Couples Depart.
Joplin, Missouri 64801

Dr. Morris Eisenberg
Electrochimica Corporation
1140 O'Brien Drive
Menlo Park, California 94025

Mr. R. H. Sparks
Electromite Corporation
2117 South Anne Street
Santa Ana, California 92704

Dr. W. P. Cadogan
Emhart Corporation
Box 1620
Hartford, Connecticut 06102

Dr. H. G. Oswin
Energetics Science, Inc.
4461 Bronx Boulevard
New York, New York 10470

Mr. Martin Klein
Energy Research Corporation
15 Durant Avenue
Bethel, Connecticut 06801

Dr. M. Savitz
Federal City College
425 2nd Street, NW
Washington, D. C.

Dr. Arthur Fleischer
466 South Center Street
Orange, New Jersey 07050

Mr. R. P. Mikkelson
General Dynamics/Convair
Dept. 967-50
San Diego, California 92112

Dr. R. P. Hamlen
Research & Development Center
General Electric Company
P. O. Box 43
Schenectady, New York 12301

Dr. F. Will
General Electric Company
Research & Development Labs
Schenectady, New York 12301

Dr. J. L. Weininger
General Electric Company
Research & Development Labs
Schenectady, New York 12301

Mr. K. L. Hanson
Space Systems, Room M2700
General Electric Company
P. O. Box 8555
Philadelphia, Pennsylvania 19101

Mr. H. Thierfelder
General Electric
Missile & Space Division
Box 8555
Philadelphia, Pennsylvania 19101

Mr. P. R. Voyentzie
Battery Business Section
General Electric Company
P. O. Box 114
Gainsville, Florida 32601

Mr. Guy Rampel
General Electric Corporation
Gainesville, Florida 32601

General Electric Company
Attn. Whitney Library
P. O. Box 8
Schenectady, New York 12301

Mr. David F. Schmidt
General Electric Company
777 - 14th St., N. W.
Washington, D. C. 20005

Mr. John R. Thomas
Globe-Union, Inc.
P. O. Box 591
Milwaukee, Wisconsin 53201

Dr. C. J. Menard
Gould, Inc.
2630 University Ave., S.E.
Minneapolis, Minnesota 55414

Dr. J. E. Oxley
Gould Ionics, Inc.
P. O. Box 1377
Canoga Park, California 91304

Grumman Aerospace Corporation
OAO Proj/S. J. Gaston, Pl 41
Bethpage, Long Island
New York 11714

Battery & Power Sources Division
Gulton Industries
212 Durham Avenue
Metuchen, New Jersey 08840

Mr. Ed Kantner
Gulton Industries
Metuchen, New Jersey 08840

Mr. Paul Cox
Hercules, Inc.
P. O. Box 12145
Research Triangle Park
North Carolina 27709

Dr. P. L. Howard
Centreville, Maryland 21617

Mr. M. E. Ellion
Building 366, MS 524
Hughes Aircraft Corporation
El Segundo, California 90245

Dr. H. T. Francis
IIT Research Institute
10 West 35th Street
Chicago, Illinois 60616

Dr. G. Myron Arcand
Department of Chemistry
Idaho State University
Pocatello, Idaho 83201

Mr. R. Hamilton
Institute for Defense Analyses
400 Army-Navy Drive
Arlington, Virginia 22202

Dr. R. Briceland
Institute for Defense Analyses
400 Army-Navy Drive
Arlington, Virginia 22202

Mr. N. A. Matthews
International Nickel Company
1000 - 16th Street, N. W.
Washington, D. C. 20036

Mr. Richard E. Evans
Applied Physics Laboratory
Johns Hopkins University
8621 Georgia Avenue
Silver Spring, Maryland 20910

Dr. A. Moos
Leesona Moos Laboratories
Lake Success Park, Community D
Great Neck, New York 11021

Dr. Richard A. Wynveen, President
Life Systems, Inc.
23715 Mercantile Road
Cleveland, Ohio 44122

Dr. James D. Birkett
Arthur D. Little, Inc.
Acorn Park
Cambridge, Massachusetts 02140

The Librarian
Livingston Electronic Lab
Honeywell, Inc.
Montgomeryville, Pennsylvania 18936

Mr. Robert E. Corbett
Department 62-25, Building 157
Lockheed Aircraft Corporation
P. O. Box 504
Sunnyvale, California 94088

Mr. R. R. Clune
Mallory Battery Company
So. Broadway & Sunnyside Lane
Tarrytown, New York 10591

Dr. Per Bro
P. R. Mallory & Company, Inc.
Northwest Industrial Park
Burlington, Massachusetts 01801

P. R. Mallory & Company, Inc.
Library
P. O. Box 1115
Indianapolis, Indiana 46206

Mr. Lou Belove
Marathon Battery Company
Kemble Avenue
Cold Spring, New York 10516

William B. Collins, MS.1620
and M. S. Imamura, MS F8845
Martin-Marietta Corporation
P. O. Box 179
Denver, Colorado 80201

Mr. A. D. Tonelli, MS 17 B 22
McDonnell Douglas Astronautics Company
5301 Bolsa Avenue
Huntington Beach, California 92647

Dr. George Moe
McDonnell Douglas Astronautics Company
Headquarters - Space Systems Center
Building 11-3-12 MS 12
5301 Bolsa Avenue
Huntington Beach, California 92647

Dr. John Mauchly
Mauchly Associates Inc.
Commerce & Enterprise
Montgomeryville, Pennsylvania 18936

Rocketdyne Division
North American Rockwell Corporation
Attn. Library
6633 Canoga Avenue
Canoga Park, California 91304

Mr. D. C. Briggs
Power & Control Engineering
Department MS R26
Philco-Ford Corporation
3939 Fabian Way
Palo Alto, California 94303

Mr. Leon Schulman
Portable Power Sources Corporation
166 Pennsylvania Avenue
Mount Vernon, New York 10552

Power Information Center
University City Science Institute
3401 Market Street, Room 2107
Philadelphia, Pennsylvania 19104

Prime Battery Corporation
15600 Cornet Street
Santa Fe Springs, California 90670

Rai Research Corporation
225 Marcus Boulevard
Hauppauge, L. I., New York 11787

Saft Corporation of America
Attn. Mr. D. Verrier
50 Rockefeller Plaza
New York, New York 10020

Mr. A. Mundel
Sonotone Corporation
Saw Mill River Road
Elmsford, New York 10523

Southwest Research Institute
Attn. Library
P. O. Drawer 28510
San Antonio, Texas 78228

Dr. Harvey Seiger
Spectrolab Incorporated.
12484 Gladstone Avenue
Sylmar, California 91342

Dr. Fritz R. Kalhammer
Stanford Research Institute
19722 Jamboree Boulevard
Irvine, California 92664

Dr. J. W. Ross
Texas Instruments, Inc.
34 Forest Street
Attleboro, Massachusetts 02703

Dr. W. R. Scott/M 2/2154
TRW Systems, Inc.
One Space Park
Redondo Beach, California 90278

Dr. Herbert P. Silverman/R-1/2094
TRW Systems, Inc.
One Space Park
Redondo Beach, California 90278

TRW, Inc.
Attn. Librarian TIM 3417
23555 Euclid Avenue
Cleveland, Ohio 44117

Dr. Jose Giner
Tyco Laboratories, Inc.
Bear Hill
Hickory Drive
Waltham, Massachusetts 02154

Dr. Ralph Brodd
Consumer Products Division
Union Carbide Corporation
P. O. Box 6116
Cleveland, Ohio 44101

Union Carbide Corporation
Development Laboratory
P. O. Box 6056
Cleveland, Ohio 44101

Dr. Robert Powers
Consumer Products Division
Union Carbide Corporation
P. O. Box 6116
Cleveland, Ohio 44101

Mr. William Boyd
Utah Research & Development
1820 South Industrial Road
Salt Lake City, Utah 84104

Professor John O'M. Bockris
Electrochemistry Laboratory
University of Pennsylvania
Philadelphia, Pennsylvania 19104

Dr. C. C. Hein, Contract Administrator
Research & Development Center
Westinghouse Electric Corporation
Churchill Borough
Pittsburgh, Pennsylvania 15235

Mr. L. K. White
Whittaker Corporation
3850 Olive Street
Denver, Colorado 80207

Mr. P. Deluca & Mr. Mike Read
Yardney Electric Company
82 Mechanic Street
Pawcatuck, Connecticut 02891

N71-33824

FINAL REPORT. SECONDARY ZINC-OXYGEN CELL FOR SPACECRAFT APPLICATIONS (23 JUNE 1966 - 1 SEPTEMBER 1968)

Union Carbide Corporation
Parma, Ohio

April 1971